

Asphaltene Profiling of Crude and Heavy Fuel Oils to Assist in Forensic Oil Spill Investigations

By

Brenden John Riley

A dissertation submitted in partial fulfilment of the requirements for the degree of

Doctor of Philosophy (Science)

Western Sydney University

School of Science and Health

July 2018

Acknowledgements

I am very grateful for the academic and personal support I have received throughout the duration of this PhD research.

First and foremost, my research would have been impossible without the enduring support of my primary supervisor Dr Val Spikmans. My sincere thanks for the wealth of knowledge that you have shared with me and for your willingness and ongoing commitment to support my research. Your guidance has truly been invaluable, thank you.

I wish to thank my co-supervisors, Prof. Chris Lennard and Stephen Fuller, for their ongoing assistance and readiness to help when required. Thank you both for the knowledge that you have provided and for your contributions to the work presented herein.

I would also like to acknowledge my collaboration with the New South Wales Office of Environment and Heritage, Environmental Protection Science Branch. Thank you for kindly allowing me to conduct research within the laboratory and for providing technical advice and assistance, particularly Stephen Fuller and Anil Gautam.

Thank you to Dr. Richard Wuhler from the Advanced Materials Characterisation Facility at Western Sydney University. I am very grateful for the time and effort both you and your staff invested into this research.

My heartfelt thanks go to Western Sydney University technical staff members Julie Svanberg, Jennie Nelson and Sahar van Dyke. Your technical knowledge, advice, and constant readiness to provide assistance was appreciated immensely.

Thank you also to Assoc. Prof. Paul Wormell for reviewing both of the journal articles which were published as part of this research.

On a personal note, thank you to my family and friends for the continual support provided throughout the duration of this research. Thank you for listening and for motivating me. I would particularly like to thank my peers and good friends Joshua Thompson and Rylee Lam. Thank you both for being there every step of the way, and for always being available when help was required.

Statement of Authentication

The work presented in this dissertation is, to the best of my knowledge and belief, original except as acknowledged in the text. I hereby declare that I have not submitted this material, either in full or in part, for a degree at this institution or any other institution.



...

Publications and Conference Presentations

Publications

Riley BJ, Lennard C, Fuller S, Spikmans V. An FTIR method for the analysis of crude and heavy fuel oil asphaltenes to assist in oil fingerprinting. *Forensic Science International* **2016**; 266: 555-64.

Riley B.J, Lennard C, Fuller S, Spikmans V. Pyrolysis-GC-MS analysis of crude and heavy fuel oil asphaltenes for application in oil fingerprinting. *Environmental Forensics* **2018**; 19: 14-26.

Conference Presentations

The 11th Australian Conference on Vibrational Spectroscopy (ACOVS11) and the 5th Asian Spectroscopy Conference (ASC5), Sydney, Australia, 29th September–2nd October 2015

The Australian and New Zealand Forensic Science Society (ANZFSS) 23rd International Symposium, Auckland, New Zealand, 18th–23rd September 2016

Table of Contents

List of Figures	xi
List of Tables	xv
List of Abbreviations	xvii
Abstract	xix
Chapter 1 - Introduction	1
1.1. Marine Oil Spills	2
1.1.1. Impact of Marine Oil Spills	3
1.1.1.1. Physical Behaviour and Weathering of Oil in Marine Environments.....	4
1.1.1.2. Environmental Impacts	7
1.1.1.3. Social and Economic Impacts	9
1.1.2. Cost of Marine Oil Spills	10
1.1.3. Oil Spill Management in Australia	12
1.2. Crude Oil Refining and Chemical Composition of Oils	13
1.2.1. Crude Oil.....	13
1.2.2. Crude Oil Refining: Processes and Products	14
1.2.3. Chemical Composition of Oil	16
1.2.3.1. Aliphatic Hydrocarbons	18
1.2.3.2. Aromatic Hydrocarbons.....	19
1.2.3.3. Heteroatomic Compounds.....	19
1.2.3.4. Organometallic Compounds	20
1.3. Oil Spill Investigations: Scene Investigation and Sampling	21
1.3.1. Scene Investigations.....	22
1.3.1.1. Oil Spill Detection and Monitoring.....	22
1.3.1.2. Response to Oil Spills	22
1.3.1.3. Paper Trail Investigations	23
1.3.2. Sampling	23
1.3.2.1. Negative Controls	23

1.3.2.2. Spilt Oil.....	24
1.3.2.3. Suspect Oils	25
1.3.2.4. Sample Submission	25
1.4. Oil Spill Investigations: The CEN Method for Oil Fingerprinting as a Foundation for the Development of Asphaltene Profiling Methods	26
1.4.1. Sample Preparation	27
1.4.2. Sample Clean-Up	28
1.4.3. Analytical Controls	28
1.4.4. CEN Analyses	28
1.4.4.1. Tier 1: GC-FID Screening.....	29
1.4.4.2. Tier 2: Oil Spill Identification Using GC-MS.....	30
1.4.5. Oil Fingerprinting Conclusions.....	31
1.4.5.1. Identification	32
1.4.5.2. Inconclusive	32
1.4.5.3. Exclusion.....	32
1.5. Research Rationale: Application of Asphaltenes in Oil Spill Investigations.....	33
1.6. Asphaltenes	34
1.6.1. Molecular Structure of Asphaltenes.....	34
1.6.1.1. Island or Archipelago?	35
1.6.1.2. Heteroatomic Composition	37
1.6.2. Asphaltene Aggregation.....	38
1.6.3. Asphaltene Precipitation	39
1.6.3.1. Precipitation Variables.....	40
1.6.4. Post-Precipitation Processing.....	48
1.6.5. Standardisation of a Forensic Asphaltene Fraction.....	50
1.7. Past and Current Asphaltene Research.....	52
1.7.1. Mainstream Petroleum Chemistry Research.....	52
1.7.2. Research Alluding to the Probative Value of Asphaltenes	53
1.7.2.1. Organic Research.....	55
1.7.2.2. Inorganic Research.....	62
1.8. Scope of Research	63

1.9. Research Aim and Research Questions.....	67
1.10. Research Outcomes.....	70
Chapter 2 - Materials and Methods	71
2.1. Research Samples: Crude and Heavy Fuel Oils.....	71
2.2. Asphaltene Precipitation Method.....	73
2.3. Method Uncertainty.....	74
2.4. Scanning Electron Microscopy	75
2.5. Attenuated Total Reflectance-Fourier Transform Infrared Spectroscopy.....	76
2.5.1. IR Profiling of Asphaltenes.....	76
2.5.2. Visual Comparison of IR Spectra	78
2.5.3. Comparison of Peak Height Ratios.....	78
2.6. Fluorescence Spectroscopy	79
2.6.1. Fluorescence Profiling of Asphaltenes.....	80
2.6.2. Visual Comparison of Fluorescence Spectra	80
2.7. Ultraviolet-Visible Spectroscopy	81
2.8. Evolved Gas Analysis-Mass Spectrometry.....	81
2.8.1. EGA-MS Profiling of Asphaltenes	81
2.8.2. Visual Comparison of Thermograms and Mass Spectra.....	84
2.9. Thermogravimetric Analysis.....	84
2.9.1. TGA-DSC Profiling of Asphaltenes	85
2.9.2. Visual Comparison of Thermograms	86
2.10. Pyrolysis-Gas Chromatography-Mass Spectrometry	86
2.10.1. Py-GC-MS Profiling of Asphaltenes	87
2.11. Isotopic Ratio Mass Spectrometry	88
2.11.1. Isotopic Profiling of Asphaltenes.....	88
2.11.2. Comparison of Carbon Isotope Ratios	90
2.12. Weathering of M. Eastern Crude Oil	91
Chapter 3 - Physical Properties of Oils and Asphaltenes	92
3.1. Colour of Crude and Heavy Fuel Oils.....	92

3.2. Asphaltene Yields	94
3.3. Asphaltene Morphology: Crystalline and Resinous.....	95
3.3.1. Macroscopic Appearance and Malleability.....	96
3.3.2. Microscopic Morphology: Scanning Electron Microscopy	97
3.4. Colour of Asphaltenes.....	99
3.5. Chapter 3 Summary.....	100
Chapter 4 - Spectroscopic Profiling of Asphaltenes	102
4.1. Ultraviolet-Visible Spectroscopy	102
4.1.1. Preliminary UV-Vis Profiling.....	104
4.2. Fluorescence Spectroscopy	105
4.2.1. Excitation Wavelength and Sample Concentration.....	107
4.2.2. Method Uncertainty	108
4.2.3. Visual Comparison of Fluorescence Spectra	110
4.2.4. Overall Evaluation of Fluorescence Profiling.....	115
4.3. Raman Spectroscopy	115
4.4. Attenuated Total Reflectance-Fourier Transform Infrared Spectroscopy.....	116
4.4.1. Method Uncertainty	118
4.4.2. Visual Interpretation of IR Spectra	120
4.4.2.1. IR Spectra and Physical Properties	120
4.4.2.2. Visual Comparison of IR Spectra	121
4.4.2.3. Un-weathered Versus Weathered Asphaltenes	126
4.4.3. Peak Height Ratio Comparisons	126
4.4.4. Comparison of Peak Height Ratios.....	129
4.4.5. Overall Evaluation of IR Profiling.....	133
4.5. Chapter 4 Summary.....	134
Chapter 5 - Thermal Profiling of Asphaltenes.....	136
5.1. EGA-MS.....	136
5.1.1. Method Uncertainty/Comparison of Asphaltene Thermograms	138
5.1.2. Method Uncertainty/Comparison of Asphaltene Mass Spectra	141

5.1.3. Overall Evaluation of EGA-MS Profiling.....	143
5.2. TGA.....	143
5.2.1. Method Uncertainty	144
5.2.2. Comparison of TG Profiles	148
5.2.3. Overall Evaluation of TG Profiling.....	154
5.3. Py-GC-MS.....	155
5.3.1. Interpretation of Py-GC-MS Results.....	156
5.3.1.1. Selection of Representative Asphaltene Pyrolysates	156
5.3.2. Py-GC-MS Optimisation.....	157
5.3.3. Comparison of Oils Using Alkane Profiles.....	159
5.3.4. Comparison of Oils Using Sulfur/Aromatic Profiles	163
5.3.5. Overall Evaluation of Py-GC-MS Profiling.....	170
5.4. Chapter 5 Summary.....	172
Chapter 6 - The Asphaltene Profiling Method.....	174
Chapter 7 - Validation of the Asphaltene Profiling Method - A Blind Study	178
7.1. Asphaltene Profiling Method	179
7.1.1. Asphaltene Precipitation of Replicates and Standards.....	180
7.1.2. Asphaltene Profiles	180
7.1.2.1. Method Uncertainty	181
7.1.2.2. Alkane Pyrograms.....	189
7.1.2.3. Sulfur/Aromatic Pyrograms and IR Spectra	193
7.1.3. Asphaltene Profiling Conclusion	215
7.2. CEN Method Conclusion	216
7.3. Discussion	217
Chapter 8 - Conclusions	226
8.1. Physical Properties	228
8.2. Addressing the Research Questions	229

8.2.1. Research Question 1.....	229
8.2.2. Research Question 2.....	232
8.2.3. Research Question 3.....	232
8.3. Overall Conclusions	234
Chapter 9 - Future Research	236
9.1. Further Investigation of the Variability of Asphaltene Profiles	236
9.1.1. Revision of Asphaltene Pyrograms	237
9.1.2. Statistical Approaches to Asphaltene Profiling.....	237
9.1.3. Variability of Asphaltene Profiles from Different HFOs.....	239
9.2. Further Optimisation of the Asphaltene Precipitation Method	240
9.3. Profiling Additional Chemical Compounds in Asphaltenes	241
9.3.1. Heteroatoms	241
9.3.2. Trace Metals.....	242
9.3.3. Isotopes	242
9.4. Weathering of Asphaltenes	246
9.5. Investigating the Robustness of Asphaltene Methods.....	246
9.6. A Standard for Asphaltene Profiling.....	247
Reference List.....	249
Appendix A - Precursor Oil Fingerprinting Standards	258
Appendix B - Development of An Asphaltene Precipitation Method	259
Appendix C - CEN Oil Fingerprinting: Blind Study.....	267

List of Figures

Figure 1.1: A schematic of the oil refinery process.	15
Figure 1.2: The four major oil fractions: (1) aliphatic hydrocarbons; (2) aromatic hydrocarbons; (3) heteroatomic organic compounds; and (4) organometallic compounds.....	17
Figure 1.3: Examples of vanadium metalloporphyrins found in Venezuelan crude oil.....	20
Figure 1.4: Standard oil sampling methods.....	24
Figure 1.5: Examples of asphaltene island structures.	36
Figure 1.6: Examples of asphaltene archipelago- structures.....	37
Figure 2.1: Visual representation of the asphaltene precipitation method.....	74
Figure 2.2: The Hitachi TM3030 Tabletop Scanning Electron Microscope used for asphaltene imaging.	75
Figure 2.3: The Perkin Elmer Spectrum 400 FTIR/FT-NIR Spectrometer with an ATR attachment used for asphaltene profiling.....	77
Figure 2.4: The Shimadzu RF-5301PC Spectrofluorophotometer used for asphaltene profiling.	80
Figure 2.5: (a) The Shimadzu GC-MS QP2010 Ultra Gas Chromatograph Mass Spectrometer with an online Frontier Laboratories Multi-Shot Pyrolyzer EGA/PY-3030D.....	82
Figure 2.6: A schematic of the Frontier Laboratories Multi-Shot Pyrolyzer (Model EGA/PY-3030D).	83
Figure 2.7: The NETZSCH STA 449C Jupiter Thermos-Balance used for asphaltene profiling.	85
Figure 2.8: The Thermo Fisher Scientific Flash 2000 Organic Elemental Analyzer coupled with a Thermo Fisher Scientific Finnigan Delta-V Isotopic Ratio MS.	89
Figure 3.1: Photographs of oil droplets.....	93
Figure 3.2: SEM micrographs of C ₅ asphaltene particles except M. Eastern (w) and S. Pacific.....	98
Figure 3.3: Asphaltene smears on white paper.	99
Figure 4.1: UV-Vis absorption spectra obtained for asphaltenes from M. Eastern, HFO (u/c) and N. American oils.....	105
Figure 4.2: Fluorescence emission spectra obtained for HFO (u/c) C ₅ asphaltenes	108
Figure 4.3: Fluorescence spectra of replicate asphaltene fractions.....	109
Figure 4.4: Fluorescence spectra observed for HFO (d/c) and M. Eastern asphaltenes.....	111
Figure 4.5: Fluorescence spectra observed for Aust. 1, Aust. 2 and Aust. 3 asphaltenes.	113
Figure 4.6: Fluorescence spectra observed for SE Asian 1 and N. American asphaltenes.	114
Figure 4.7: Fluorescence spectra observed for SE Asian 2 asphaltenes.	115
Figure 4.8: Overlays of Region 1 IR spectra (wavenumber range 650 – 930 cm ⁻¹) for replicates: (a) M. Eastern asphaltenes; and (b) HFO (u/c) asphaltenes.	118

Figure 4.9: Overlays of Region 2 IR spectra (wavenumber range 1260 – 1520 cm ⁻¹) for replicates: (a) M. Eastern asphaltenes; and (b) HFO (u/c) asphaltenes.	119
Figure 4.10: Representative Region 1 IR spectra (wavenumber range 650 – 930 cm ⁻¹).	122
Figure 4.11: Representative Region 2 IR spectra (wavenumber range 1260 – 1520 cm ⁻¹).....	123
Figure 4.12: Region 1 comparison for N. American and HFO (d/c) asphaltenes (N. American = top trace, HFO (d/c) = bottom trace).....	125
Figure 4.13: Representative IR spectra of M. Eastern weathered and un-weathered asphaltenes	126
Figure 5.1: Asphaltene thermograms generated from EGA-MS.....	139
Figure 5.2: MS obtained from asphaltene thermograms using the maxima of Peak 1.....	142
Figure 5.3: TG profiles and DTG profiles of M. Eastern replicate asphaltene fractions	145
Figure 5.4: Irregularities in the DTG baseline of M. Eastern	147
Figure 5.5: TG and DTG profiles for duplicate Aust. 2 asphaltene fractions	151
Figure 5.6: TG and DTG profiles for duplicate SE Asian 1 asphaltene fractions.....	151
Figure 5.7: TG and DTG profiles for duplicate SE Asian 2 asphaltene fractions.....	152
Figure 5.8: TG and DTG profiles for duplicate N. American asphaltene fractions	152
Figure 5.9: TG and DTG profiles for duplicate HFO (u/c) asphaltene fractions	153
Figure 5.10: TG and DTG profiles for duplicate HFO (d/c) asphaltene fractions	153
Figure 5.11: Selected ion pyrograms obtained from HFO (u/c) asphaltenes when analysed at three different pyrolysis temperatures.....	158
Figure 5.12: Two M. Eastern alkane profiles which represent the maximum variance observed between all seven replicate M. Eastern asphaltene fractions.	160
Figure 5.13: Two HFO (u/c) alkane profiles, which represent the maximum variance observed between all seven replicate HFO (u/c) asphaltene fractions.	160
Figure 5.14: The first group of oils classified by alkane profiles	161
Figure 5.15: The second group of oils classified by alkane profiles.....	162
Figure 5.16: The third group of oils classified by alkane profiles	162
Figure 5.17: Two representative sulfur/aromatic profiles for the replicate M. Eastern asphaltenes..	164
Figure 5.18: Two representative sulfur/aromatic profiles for the replicate HFO (u/c) asphaltenes...	164
Figure 5.19: Representative sulfur/aromatic profiles of group 1 asphaltenes	165
Figure 5.20: Representative sulfur/aromatic profiles of group 2 asphaltenes	167
Figure 5.21: Representative sulfur/aromatic profiles of group 3 asphaltenes	169
Figure 5.22: Enlarged BPy and BPE regions for (a) Aust. 1 and (b) Aust. 2.....	169
Figure 5.23: Flow chart indicating the differentiation of the ten studied oils into eight groups based on pyrolysis of asphaltenes.	171

Figure 6.1: A simplified flowchart showing the proposed workflow of asphaltene profiling assisting volatile oil fingerprinting	175
Figure 7.1: Alkane pyrograms of the oil K asphaltene triplicates (K.1, K.2 and K.3) and the re-analysed triplicates (K.1.2, K.2.2, K.3.2).....	182
Figure 7.2: Sulfur/aromatic pyrograms of the oil K asphaltene triplicates (K1, K2 and K3) and the re-analysed triplicates (K.1.2, K.2.2, K.3.2).....	183
Figure 7.3: IR spectra of the oil K asphaltene triplicates (K.1, K.2 and K.3) and the re-analysed triplicates (K.1.2, K.2.2, K.3.2).....	184
Figure 7.4: Alkane pyrograms of the HFO (u/c) asphaltene standard (analysed 3 times during the blind study) and of 2 separate HFO (u/c) asphaltene samples from Chapter 5.....	186
Figure 7.5: Sulfur/aromatic pyrograms of the HFO (u/c) asphaltene standard (analysed 3 times during the blind study) and of 2 separate HFO (u/c) asphaltene samples from Chapter 5.....	187
Figure 7.6: IR spectra of HFO (u/c) asphaltenes. Black line: HFO (u/c) standard analysed during the blind study (analysed 3 times); Blue line: HFO (u/c) IR spectra (mean of 7 replicates)	188
Figure 7.7: C, R, E, Q and S asphaltene alkane pyrograms that were dominated by high-boiling compounds.	190
Figure 7.8: I, G, D, N, P and L asphaltene alkane pyrograms with a sharp, defined cluster of peaks between 32 and 47 min.	191
Figure 7.9: F, K, B, T, U, A, H, O and M asphaltene alkane pyrograms dominated by low-boiling compounds with reduced alkane intensity as RT increased.....	192
Figure 7.10: Sulfur/aromatic pyrogram obtained from oil C asphaltenes.....	194
Figure 7.11: Sulfur/aromatic pyrogram obtained from oil R asphaltenes.....	194
Figure 7.12: Sulfur/aromatic pyrogram and IR spectra from oil E asphaltenes.....	195
Figure 7.13: Sulfur/aromatic pyrogram and IR spectra from oil Q asphaltenes.	195
Figure 7.14: Sulfur/aromatic pyrogram and IR spectra from oil S asphaltenes.....	196
Figure 7.15: Sulfur/aromatic pyrogram and IR spectra from oil I asphaltenes.....	197
Figure 7.16: Sulfur/aromatic pyrogram and IR spectra from oil G asphaltenes.	197
Figure 7.17: Sulfur/aromatic pyrogram and IR spectra from oil L asphaltenes.....	200
Figure 7.18: Sulfur/aromatic pyrogram and IR spectra from oil P asphaltenes.....	201
Figure 7.19: Sulfur/aromatic pyrogram and IR spectra from oil D asphaltenes.	202
Figure 7.20: Sulfur/aromatic pyrogram and IR spectra from oil N asphaltenes.	202
Figure 7.21: Sulfur/aromatic pyrogram and IR spectra from oil F asphaltenes.....	205
Figure 7.22: Sulfur/aromatic pyrogram and IR spectra from oil U asphaltenes.	206
Figure 7.23: Sulfur/aromatic pyrogram and IR spectra from oil A asphaltenes.	207
Figure 7.24: Sulfur/aromatic pyrogram and IR spectra from oil M asphaltenes.....	209
Figure 7.25: Sulfur/aromatic pyrogram and IR spectra from oil K asphaltenes.	209

Figure 7.26: Sulfur/aromatic pyrogram and IR spectra from oil B asphaltenes.....	210
Figure 7.27: Sulfur/aromatic pyrogram and IR spectra from oil T asphaltenes.....	210
Figure 7.28: Sulfur/aromatic pyrogram and IR spectra from oil H asphaltenes.	211
Figure 7.29: Sulfur/aromatic pyrogram and IR spectra from oil O asphaltenes.	211
Figure 9.1: C ¹³ /C ¹² ratios obtained for the asphaltene fractions of crude and heavy fuel oils.....	244

List of Tables

Table 1.1: Past studies and international standards exhibiting the use of various precipitation solvents/solvent-oil-ratios.	41
Table 1.2: An outline of asphaltene research applications in the petroleum industry.	54
Table 2.1: The eleven crude oils and HFOs analysed as part of the method development process.	72
Table 3.1: Visual appearance of the C ₅ asphaltene fraction obtained from crude and heavy fuel oils.	96
Table 4.1: From the 10ppm stock solution, the following dilutions were made in a 4 mL cuvette. These concentrations were approximated assuming 1 drop = 0.1 mL.	107
Table 4.2: RSDs and peak height ratio thresholds calculated for the IR spectra of asphaltenes.	128
Table 4.3: Comparison of peak height ratios between Aust. 1 and Aust. 2 asphaltenes.	130
Table 4.4: Comparison of peak height ratios between N. American and HFO (d/c) asphaltenes.	131
Table 5.1: %RSD calculated from the six replicate M. Eastern asphaltene fractions.	146
Table 5.2: Collated data for DTG peak maxima's of asphaltenes.	149
Table 7.1: Peak height ratios compared between K.1 and K.1.2 asphaltenes.	185
Table 7.2: Peak height ratios compared between K.1 and K.2 asphaltenes.	185
Table 7.3: Peak height ratios compared between I and G asphaltenes.	199
Table 7.4: Peak height ratios compared between G and I.2 asphaltenes.	199
Table 7.5: Peak height ratios compared between I and G.2 asphaltenes.	199
Table 7.6: Peak height ratios compared between G.2 and I.2 asphaltenes.	200
Table 7.7: Peak height ratios compared between D and N asphaltenes.	203
Table 7.8: Peak height ratios compared between D and N.2 asphaltenes.	204
Table 7.9: Peak height ratios compared between D.2 and N asphaltenes.	204
Table 7.10: Peak height ratios compared between D.2 and N.2 asphaltenes.	204
Table 7.11: Peak height ratios compared between A and U asphaltenes.	207
Table 7.12: Peak height ratios compared between A.2 and U asphaltenes.	207
Table 7.13: Peak height ratios compared between A.2 and U asphaltenes.	208
Table 7.14: Peak height ratios compared between A.2 and U.2 asphaltenes.	208
Table 7.15: Peak height ratios compared between B and K.1 asphaltenes.	212
Table 7.16: Peak height ratios compared between K.1 and T asphaltenes.	213
Table 7.17: Peak height ratios compared between B and T asphaltenes.	213
Table 7.18: Peak height ratios compared between H and O asphaltenes.	214

Table 7.19: Peak height ratios compared between H and O.2 asphaltenes.	214
Table 7.20: Peak height ratios compared between H.2 and O asphaltenes.	214
Table 7.21: Peak height ratios compared between H.2 and O.2 asphaltenes.	215
Table 7.22: The blind study conclusion for asphaltene profiling.	216
Table 7.23: The blind study conclusion for the CEN method.	217
Table 7.24: The geographical origin of the oils analysed in this blind study.	218
Table 7.25: The asphaltene profiling conclusion showing the origins of oils.	219
Table 7.26: The CEN conclusion showing the origins of oils.	222
Table 7.27: A comparison of asphaltene profiling and CEN method conclusions derived from the blind study.	223

List of Abbreviations

AAS	Atomic Absorption Spectroscopy
Abs	Absorbance
AMCF	Advanced Materials Characterisation Facility
AMSA	Australian Maritime Safety Authority
API	American Petroleum Institute
ASTM	American Society for Testing and Materials
ATR	Attenuated Total Reflectance
ATR-FTIR	Attenuated Total Reflectance-Fourier Transform Infrared Spectroscopy
Aust. 1	Australian 1 crude oil
Aust. 2	Australian 2 crude oil
Aust. 3	Australian 3 crude oil
Aust. 4	Australian 4 crude oil
BLC	Baseline Corrected
Bpd	Barrels Per Day
C	Carbon
C ₅	<i>n</i> -pentane
C ₆	<i>n</i> -hexane
C ₇	<i>n</i> -heptane
CEN	European Committee for Standardization
cSt	Centistokes
DCM	Dichloromethane
DRs	Diagnostic Ratios
DTG profile	1 st derivative thermogravimetric profile
DWH	Deep Water Horizon
EA	Elemental Analysis
EEZ	Exclusive Economic Zone
EDA	Exploratory Data Analysis
EGA-MS	Evolved Gas Analysis-Mass Spectrometry
EPA	Environment Protection Authority
ETFE	Ethylene tetrafluoroethylene
EV	Exxon Valdez
Fe	Iron
FPD	Flame Photometric Detector
FTIR	Fourier Transform Infrared
GC-FID	Gas Chromatography-Flame Ionisation Detection
GC-IRMS	Gas Chromatography-Isotope Ratio Mass Spectrometry
GC-MS	Gas Chromatography-Mass Spectrometry
GC-PW-plots	Gas Chromatography-Percentage Weathering-plots
H	Hydrogen
HFO (d/c)	Heavy Fuel Oil (diesel cut)
HFO (u/c)	Heavy Fuel Oil (uncut)
HFO/s	Heavy Fuel Oil/s
HPLC	High Performance Liquid Chromatography
IMO	International Maritime Organization
IR	Infrared
ITOPF	The International Tanker Owners Pollution Federation
M. Eastern (w)	Middle Eastern weathered crude oil

M. Eastern 2	Middle Eastern 2 crude oil
M. Eastern	Middle Eastern crude oil
<i>m/z</i>	Mass-to-charge ratio
MS-PW	Mass Spectrometry-Percentage Weathering
N	Nitrogen
N. American	North American crude oil
NATA	National Association for Testing Authorities
Ni	Nickel
NSW	New South Wales
O	Oxygen
OEH	Office of Environment and Heritage
PAH/s	Polycyclic Aromatic Hydrocarbon/s
PCA	Principle Component Analysis
Phy	Phytane
Pri	Pristane
Py-GC	Pyrolysis-Gas Chromatography
Q1	Quartile 1
Q3	Quartile 3
RSD	Relative Standard Deviation
RT	Retention Time
S	Sulfur
SAR/s	Synthetic Aperture Radar/s
SD	Standard Deviation
SE Asian 1	South East Asian 1 crude oil
SE Asian 2	South East Asian 2 crude oil
SE Asian 3	South East Asian 3 crude oil
SEM	Scanning Electron Microscope
SES	State Emergency Service
SPE	Solid Phase Extraction
TGA	Thermogravimetric Analysis
TGA-DSC	Thermogravimetric Analysis-Differential Scanning Calorimetry
THF	Tetrahydrofuran
UAC	Unified Area Command
UCM	Unresolved Complex Mixture
UKN. 1	Unknown crude oil (one of the studied oils)
V	Vanadium
Vol%	Volume percent
Wt%	Weight percent

Abstract

When oil is spilt, investigators compare the chemical profile of the spilt oil with suspected source oils through a process commonly referred to as oil fingerprinting. Oil fingerprints are currently generated exclusively from volatile fractions of oil whilst the non-volatile fraction is discarded. The non-volatile fraction contains asphaltenes, which are defined as the oil fraction that is not soluble in short chain *n*-alkanes. There is sufficient evidence in the literature to suggest that asphaltenes may offer probative information if they were included in oil spill investigations. This PhD research has investigated whether asphaltene profiling methods can in fact provide probative information that warrants their use alongside current oil fingerprinting methods. Asphaltene profiling methods were designed primarily as screening tools for the exclusion of obvious non-related oils prior to conducting conventional oil fingerprinting. A range of spectroscopic and thermal degradation methods were developed and tested using ten different crude and heavy fuel oils. The infrared spectroscopy and pyrolysis-gas chromatography-mass spectrometry methods were found to be the most suitable methods for oil spill investigations. Both methods were probative and capable of differentiating non-related oils, whilst grouping together oils from the same origin. A blind study was also conducted using these two methods. The original sample-set and five additional oils were analysed, and asphaltene profiles were interpreted. The four pairs of duplicated oils that were included in the blind study were correctly grouped together. The majority of non-related oils were differentiated except for two pairs of very closely-related oils which were not differentiated. Taking into account that asphaltene profiling was designed as a screening tool for use only in conjunction with conventional oil fingerprinting, the false inclusion of two pairs of non-related oils was not problematic. Conventional oil fingerprinting successfully differentiated these two pairs of oils following asphaltene profiling.

Chapter 1 - Introduction

There is a high demand on primary energy sources as worldwide energy consumption continues to increase (ExxonMobil 2015). Despite recent growth in renewable energy, oil still remains the leading global primary energy source, ahead of coal, natural gas, nuclear energy, hydro-electricity, and renewable energy sources. Oil, in the form of crude oil, oil sands, shale, or natural gas liquids, can be refined to produce a vast array of oil-derived fuel products with a wide range of energy applications. The diversity of fuel applications and increasing availability of oil-derived fuels has cemented oil at the forefront of global energy demand (BP 2015).

To meet the increasing demand for oil, annual global oil production has increased by ~7,500,000 barrels per day (bpd) over the past decade (one barrel equates to 42 US gallons or 159 litres). Total world production of oil reached 88,673,000 bpd in 2014, with the Middle East accounting for the highest percentage of production throughout the globe (31.7% of this total bpd world production value). The remaining global production is attributed as follows: North America (20.5%), Europe and Eurasia (19.8%), Asia Pacific (9.4%), South and Central America (9.3%) and Africa (9.3%). It is interesting, however, that the highest oil producing regions are not also the highest oil consuming regions. Of the total oil consumed in 2014 (92,086,000 bpd), the Asia Pacific region consumed the most oil at 33.9%. The remaining consumption of oil was accounted for by North America (24.3%), Europe and Eurasia (20.4%), Middle East (9.3%), South and Central America (7.8%) and Africa (4.3%), respectively. The Asia Pacific region, for example, produced only 9.4% of total world oil in 2014 yet the consumption of worldwide oil in this region was 33.9% (BP 2015).

The aforementioned statistics highlight the requirement for an extensive network for global oil trade from producers to consumers. The distribution of oil into consuming regions such as Asia Pacific is evident, so too is the large scale of exports from the highest oil

producing regions such as the Middle East to global consumers (BP 2015). Oil is distributed throughout the world via seaborne transport on marine shipping vessels or via international pipelines (UN 2013, ITOPIF 2016, Speight 2014). In 2012, total worldwide crude oil shipments reached 55,300,000 bpd. Two-thirds of this total was distributed via marine shipping vessels while the remaining was accounted for via pipelines (UN 2013). Given the magnitude of the international oil trade, the occurrence of accidental or intentional oil spills during marine transportation is inevitable.

1.1. Marine Oil Spills

Marine oil spills may occur in a number of different ways. Spills may occur during non-shipping related activities including offshore oil exploration and production, where spills may occur from oil platforms, rigs, or wells. Spills may also occur from oil facilities operating in coastal/estuarine regions, such as refineries, oil terminals, and oil storage facilities. Natural sources, such as natural oil seeps, also contribute significantly to the release of oil into marine environments. Apart from natural seeps, oil spills occurring from marine shipping vessels account for the highest contribution of oil into the environment by a considerable margin (GESAMP 2007).

Incidents that may cause oil spills from seaborne vessels have been categorised by the Australian Maritime Safety Authority (AMSA) as follows: (1) Collision – with another ship; (2) Contact – with an object other than a ship, not the sea floor; (3) Fires/Explosions; (4) Hull Damage; (5) Transfer Spill – loading or unloading; (6) Unauthorised Discharge – deliberate or unintentional; (7) Wrecked/Stranded – damage from the sea floor, which may be sub-categorised as either a drift (un-powered) grounding or a powered grounding; and (8) War Loss. The aforementioned spill types may occur from a range of different shipping vessels,

ranging from small leisure crafts and commercial fishing vessels, through to larger oil tankers and bulk carriers (AMSA 2011).

The International Tanker Owners Pollution Federation (ITOPF) has maintained records of over 10,000 marine oil spills from tankers since 1970. ITOPF have classified marine oil spills into three categories based on the volume of oil spilt: (1) <7 tonnes; (2) between 7–700 tonnes; and (3) >700 tonnes. Although large-scale oil spills (>700 tonnes) dominate the media, the occurrence of large-scale spills has declined rapidly since 1970; only 2 large-scale incidents were recorded in 2015 as opposed to 29 incidents in 1970. The number of small (>7 tonnes) and medium-scale spills (7–700 tonnes) have also declined significantly since 1970; however, both small and medium-scale spills continue to occur more frequently than large-scale spills. Small-scale spills are the most commonly occurring spill category, with 81% of all recorded spills from 1970 to 2015 falling into this category (ITOPF 2016).

Small-scale spills may appear trivial, however, it must be emphasised that these smaller spills are frequently occurring, and the cumulative impact has global reach. Conversely, when a large-scale spill does occur, the impact is often concentrated in one region, which often has considerable impact in the immediate vicinity of the spill, rather than globally (NOAA 2012). Regardless of the scale of oil spills, the impact on the environment is detrimental.

1.1.1. Impact of Marine Oil Spills

Two major oil spill cases have been highlighted herein to demonstrate the extensive impact of marine oil spills. The first case is the Deep Water Horizon (DWH) oil spill, which occurred in the Gulf of Mexico in 2010. The DWH oil rig caused the largest oil spill in US history, when approximately 800 million tonnes (4.4 million barrels) of crude oil leaked from the Macondo well into the Gulf of Mexico (Barron 2012, Griggs 2011). Although the DWH spill was the result of offshore oil production, rather than a spill from a marine shipping

vessel, it adequately demonstrates the impact of marine oil spills. The second case is the Exxon Valdez (EV) oil spill, which occurred in Alaska in 1989. A total of 262,000 barrels of crude oil was spilt from the *Exxon Valdez* shipping vessel into Prince William Sound on the Alaskan coast (Peterson et al. 2003).

Without immediately delving into the elaborate chemistry of oils (which is discussed later), it is important to provide an intrinsic overview of: (1) how oils physically behave in a marine environment; and (2) the weathering processes that may impact oils in marine environments (CEN 2012). These concepts provide essential background information to assist in understanding the impact of oil spills, as well as understanding how the source of an oil spill is determined (also discussed later).

1.1.1.1. Physical Behaviour and Weathering of Oil in Marine Environments

To provide basic context for this research, a brief explanation of weathering effects on oil has been outlined below. Prior to discussion, it should be noted that the investigation of weathering effects on oil was not the primary focus of this PhD research. Oil spill investigators will be quick to note that weathering is a critical factor to consider in oil spill investigations; this has indeed been recognised. This PhD research however, focuses on the development of analytical methods that must first be tested using un-weathered oil as will become evident throughout the remainder of this thesis.

When oil is spilt in seawater, spreading, drifting, emulsification, photo-oxidation, evaporation, dissolution and sedimentation all contribute synergistically to the chemical alteration of oil fingerprints (CEN 2012, Aeppli et al. 2014). Firstly, the physical action of waves will slowly spread oil over the water's surface, forming surface films (ITOPF 2011). As oil spreads, some oil may begin to disperse throughout the water column, forming an emulsion of oil droplets suspended in water (Jernelov 2010, GESAMP 1993, ITOPF 2011).

The density of oil dictates whether oil will float and form surface films, or whether it will sink and disperse. Heavy fuel oils (HFOs) are often of the same density, or greater, than seawater, hence HFOs tend to sink. Crude oils on the other hand, are typically of lower density than seawater, and therefore float (Bornstein et al. 2014, GESAMP 1993). When oil disperses and forms fine droplets in water it becomes more susceptible to both photo-oxidation and biodegradation (GESAMP 1993). Photo-oxidation and biodegradation are the most influential weathering processes that effect oil spills and are described below (Prince and Walters 2007).

Photo-oxidation generally occurs preferentially to biodegradation, and concurrently with evaporation. Photo-oxidation is the molecular breakdown of chemical compounds caused by UV irradiation from sunlight (Jernelov 2010). Photo-oxidation degrades hydrocarbons into oxygenates causing an increase in polarity and propensity for dissolution of oil compounds in water (Payne and Phillips 1985). Generally speaking, PAHs are more susceptible to photo-oxidation than *n*-alkanes (King et al. 2014, Bacosa et al. 2015, Prince et al. 2003). Evaporation affects the lowest boiling compounds in oils, across all compound groups including *n*-alkanes and PAHs. Evaporation results in the removal of low boiling compounds from oil fingerprints which reduces the number of comparable compounds in oils during investigations (CEN 2012).

Biodegradation occurs when micro-organisms break down oil compounds through either aerobic or anaerobic respiration (Prince and Walters 2007, Harayama et al. 1999, Gros et al. 2014). *N*-alkanes are the most susceptible oil compounds to biodegradation, followed by *iso*-alkanes and PAHs which are less susceptible. Biomarkers such as steranes and hopanes are highly susceptible to biodegradation, hence these biomarkers are commonly relied upon for the interpretation of lightly or moderately biodegraded oils (CEN 2012).

Oil droplets are also susceptible to interactions with organic debris in water, which may increase the density of droplets causing them to sink at a quicker rate. Oil droplets that sink to the bottom often accumulate as sediment on the sea floor (ITOPF 2011).

It should be noted that no two oil spills will result in the same degree of oil degradation. In turn, the impact of an oil spill on the marine environment will vary from case to case. To better understand this, consider the different oil types that may be spilt. A light crude oil will behave differently in a marine environment as compared to a HFO due to variances in chemical composition and density (Speight 2014, Jernelov 2010, Bornstein et al. 2014). The ambient conditions surrounding an oil spill also differ from case to case. The swell, wind direction, sunlight, temperature, and available waterborne-bacteria, all influence the severity and rate of oil degradation (Jernelov 2010, GESAMP 1993). Consider two light crude oils of similar chemical composition that have been exposed to very different ambient conditions. The rate of degradation for each of these light oils will vary based on these conditions, not due to differing chemical compositions. Consequently, this will influence how each of the light oils will impact their given environment. Another factor that strongly influences the environmental impact of a spill is the physical location of the incident; a concept discussed below (Jernelov 2010).

It is important to emphasise the reliance on the understanding of weathering processes for the interpretation of oil fingerprints. Light to moderate weathered oils can generally be interpreted quite efficiently based on the analyst's understanding of weathering processes. Heavily weathered oils however, are much more difficult to interpret due to the range of different weathering processes that may have altered oil fingerprints.

1.1.1.2. Environmental Impacts

The EV oil spill was a surface spill of crude oil which occurred in a sheltered waterway during cold ambient conditions. As a result, the EV spill remained on the surface of the water, and within a short time period after the spill (19 days), oil had reached the Alaskan shoreline; the last known volumes of oil reached the shoreline within 2 months of the spill. In contrast, the DWH spill originated from a deep water oil well, where crude oil was spilt into a large body of water with very warm ambient conditions. This meant that oil remained deep in the water column for a longer duration of time before it eventually reached the shoreline (NOAA 2012). These two incidents had very different impacts on the environment as a consequence of the spill location, and also due to the ambient conditions surrounding each spill.

During the DWH incident, dispersants were used within the immediate vicinity of the spill in an attempt to control the flow of oil from the well. This resulted in the formation of fine oil droplets that manifested in the deeper waters surrounding the spill site. When oil forms these fine droplets, small marine organisms are easily contaminated (NOAA 2012, Jenelov 2010). Larger predators are then susceptible to harm if they consume small oil-encrusted organisms, or if they simply inhale the fine oil droplets. Exposure at high enough concentrations will kill larger predators, whilst low level exposure will cause a range of adverse health issues (Jenelov 2010, GESAMP 1993). In the DWH case, deep water organisms, such as invertebrates, squid, fish, sharks and whales, were all at risk of exposure; however, the effects of this spill on these deep water ecosystems has yet to be quantified. The portions of the DWH spill that were not dispersed at the well moved up through the water column towards the surface. As the oil travelled towards the surface, water-soluble oil fractions were dissolved (NOAA 2012). As oil passed throughout the water column, hundreds of mammals were oiled (100 cases recorded by the Unified Area Command (UAC) during the

DWH oil spill) alongside turtles (1000 cases) and birds (10,000 cases) (Barron 2012). The remaining oil that reached the surface was pushed towards the coastline by ocean swells and winds; a portion of this surface film was also targeted with dispersants, hence remained beneath the surface as fine droplets (NOAA 2012). Fisheries and aquatic flora were heavily impacted as the oil moved into the inshore regions of the Gulf. In the end, 1,600 km of coastline were impacted by the DWH oil spill, including the coastlines of Louisiana, Texas, Mississippi, Alabama and Florida. Juvenile sea turtles and birds were also at risk of oil exposure due to beach oiling (Barron 2012). Saltwater marshlands were the worst affected shoreline habitat, although mud flats and mangrove areas were also impacted. The heavy oiling of these ecologically diverse regions meant that not only were marine organisms at risk of oil exposure, so too were terrestrial organisms living and feeding in these habitats (NOAA 2012).

As previously mentioned, the EV spill differed from the DWH spill as it existed predominantly as a surface film. The EV surface film increased the susceptibility of high levels of oil exposure for many birds and marine mammals. Consequently, hundreds of seals, thousands of sea otters, and hundreds of thousands of birds died in the days following the EV spill (Peterson et al. 2003). Surface films also have the potential to impact a larger area of inshore and coastal habitats, including coral reefs, beaches, and estuaries, as well as structures within these habits such as oyster leases, rock platforms, and mangroves (GESAMP 1993, Jernelov 2010). In the end, the EV spill affected approximately 1,990 km of Alaskan coastline, including beaches and rocky shorelines. Algae and benthic invertebrates that resided in coastal habitats died as a result of the oiling, along with many coastal-dwelling birds and mammals. The rate of oil dispersion and degradation in the EV case was shown to slow down over time; oil accumulated in regions with unfavourable conditions for the

breakdown of oil. The persistence of oil led to chronic exposure of numerous marine organisms, causing a multitude of imbalances within local ecosystems (Peterson et al. 2003).

Interestingly, despite the amount of oil spilt by the *Exxon Valdez* being significantly less (~16 times less) than that of the DWH, the EV spill affected more coastline (~300 km more) than the DWH spill. When considering the factors surrounding each of the spills, these statistics become clearer. The EV spill occurred in unfavourable ambient conditions for oil degradation, whereas the DWH spill occurred under relatively favourable conditions. The surface film of oil in the EV case was immediately influenced by swells and winds, whereas the deep water oil spill in the DWH case was not immediately exposed to surface swells and winds. Also, the EV spill occurred in close proximity to the coastline, whereas the DWH spill occurred in a deep sea location (NOAA 2012, Peterson et al. 2003). These two oil spill cases highlight how a range of factors can affect the environmental impact of an oil spill differently, regardless of the quantity of oil spilt (Jernelov 2010).

1.1.1.3. Social and Economic Impacts

The DWH and EV oil spills also had a profound impact on the communities of the affected regions. The study by Gill et al. (2012) observed communities in the Gulf of Mexico affected by the DWH spill, and monitored the impacts that occurred within these communities as a direct result of the DWH spill. The study focused on two communities in Mobile County, Alabama: Bayou La Batre and Dauphin Island. Bayou La Batre is a prominent seafood producing community in Alabama, with a strong dependence on natural resources including fish, oysters and shrimp. The community of Dauphin Island is a beachside tourist destination with recreational attractions including boating and fishing. Gill et al. (2012) compared the acute impacts of the DWH spill on these communities with those

observed in similar research conducted on the Alaskan town of Cordova; a fishing town affected by the EV spill.

Before the EV spill, Cordova relied heavily on natural resources, particularly fish, to maintain a strong foothold in the United States seafood market (it was ranked in the top 10 ports in the United States regarding profit) (Gill et al. 2012). Following the spill however, Cordova fails to rank above 25 on the list. In regards to the DWH spill, approximately 40% of fisheries throughout the entire Gulf of Mexico were closed due to oiling (Barron 2012). The closures were problematic for commercial fisheries, as 33% of the country's (USA's) seafood is sourced from this region (NOAA 2012). In Bayou La Batre, the oiling affected fin-fisherman and oyster farmers, as well as other seafood businesses. In Dauphin Island, the impact of the closures on recreational fishing was problematic, as this affected tourism in area (Gill et al. 2012).

It is clear that the impact of marine oil spills cuts deeper than the environmental destruction commonly depicted in the media. Complex social and economic networks are also impacted as collateral damage to the environmental destruction.

1.1.2. Cost of Marine Oil Spills

When considering the cumulative environmental, social and economic impact of marine oil spills, the perpetrators responsible for oil spills are susceptible to a colossus of financial burdens. Major costs arise from the interruption of coastal industries (i.e., commercial fisheries and tourism), and from the damages to natural resources (i.e., the restoration of reefs) (NOAA 2012). Additional costs may arise from the use of public services in response to an oil spill (i.e., the coastguard helping to contain or clean-up spills), as well as costs associated with damages, or loss of private property (i.e., boats) (GESAMP 1993, NOAA 2012). Government revenues that may be impeded by the occurrence of an oil spill may also

be the liability of the responsible party (i.e., the revenue decrease from ticketed parking meters along affected coastal beaches) (NOAA 2012). This illustrates the importance of identifying the responsible parties for oil spills so that they can be held accountable for associated financial liabilities. In Australia, protective measures are in place to ensure that financial liabilities can be paid in the occurrence of an oil spill (AMSA 2012). All oil tanker owners are required to hold insurance in accordance with the *International Convention on Civil Liability for Oil Pollution Damage 1992* which must be capable of covering oil spill damages up to a limit of AUD (Australian Dollar) \$170 million. Any excess damages exceeding AUD \$170 million are compensated for by the *Convention on the Establishment of an International Fund for Compensation for Oil Pollution*, up to AUD \$1.2 billion (AMSA 2012). All major Australian companies involved in the oil industry must contribute regularly to this fund (AMSA 2012).

Regarding penalties or fines, in Australia, the *Marine Pollution Act 1987* states that the deliberate discharge of oils/oil based mixtures into Australian waters is an offence, and may warrant penalties of up to AUD \$500,000 for natural persons (individuals), and up to AUD \$10 million for corporate bodies. When determining the suitable financial penalty to impose on perpetrators, a number of factors can contribute to the finalised sum. To explain how multiple factors contribute to the financial penalty associated with oil spills, the Laura D'Amato case is highlighted. In 1999, approximately 294,000 litres of Murban crude oil was spilt in Sydney Harbour from the *Laura D' Amato* oil tanker. When the Amato spill occurred, the conditions were in fact very favourable for containing the spill. Whilst conditions were favourable, the final penalty imposed on the offenders was determined with significant consideration to potential damages that could have easily occurred given less favourable conditions. One of the major factors considered was the potential risk of an explosion following the incident, given the highly flammable nature of the Murban crude oil. In

conclusion, the responsible offenders for the Amato spill were charged AUD \$620,000 (Filipowski 2000).

1.1.3. Oil Spill Management in Australia

AMSA regulates the control and prevention of marine pollution, including oil spills, in Australian marine environments. Australian legislation regarding the regulation of marine oil spills has been developed in accordance with the International Maritime Organization (IMO) and its conventions. The control and prevention of marine oil spills in Australian waters is implemented via the *National Plan for Maritime Environmental Emergencies*. This plan has been developed for application within specified geographical boundaries, based on the potential impact of an oil spill incident on Australian welfare. The regions surrounding offshore islands and territories, as well as seas more than 3 nautical miles from the Australian mainland, is defined as the Australian Exclusive Economic Zone (EEZ). Any incident within the EEZ is the responsibility of the Commonwealth government. Internal and coastal waters are identified as being within 3 nautical miles of the Australian mainland. It is the responsibility of Australian state and territory governments to respond to incidents within coastal waters (AMSA 2014).

Regardless of the type of environmental pollution, in New South Wales (NSW), two stages of work are undertaken following incidents. The first stage is the response to an incident, with an aim to prevent further environmental harm (oil response tactics are outlined later in this chapter). The second stage involves the recovery of the affected region, as it is restored to the way it was prior to an incident (NSW EPA 2016).

A range of different agencies may be accountable for the response to an environmental pollution incident; however, this depends on the incident type. For example, in NSW, the State Emergency Service (SES) responds to floods, whilst Fire and Rescue NSW respond to

incidents with hazardous materials on land (NSW EPA 2016). For marine oil spills in NSW, a number of agencies (referred to as ‘combat agencies’) may be required to respond including Transport for NSW, the Port Authority of NSW, or Roads and Maritime Services. The NSW Environment Protection Authority (EPA) may also be required to assist in the response (NSW EPA 2016, Transport for NSW 2015). The role of the NSW EPA is to provide advice on the response plan so that further environmental harm, as well as harm to the public, is minimised. The recovery stage is led by Transport for NSW, whilst the NSW EPA provides technical assistance when required (NSW EPA 2016).

1.2. Crude Oil Refining and Chemical Composition of Oils

Prior to explaining the method for forensic oil spill investigations, an introduction to crude oil (petroleum), petroleum-derived products, and the generic chemical composition of oil is provided below. Knowledge of these fundamental concepts is necessary for understanding the chemical analysis of oils carried out in oil spill investigations; a process known as ‘oil fingerprinting’.

1.2.1. Crude Oil

The term petroleum simply refers to naturally occurring hydrocarbons in sedimentary rock. Hydrocarbons may exist as gas (natural gas), liquid (crude oil) or solid (coal) (Speight 2014). The terms ‘crude oil’ and ‘petroleum’ are therefore analogous; in this thesis, the term crude oil will be used to describe the liquid state of petroleum. Crude oil is the product of geochemical conversion of ancient organic plant and animal matter, deposited and buried beneath the earth’s surface over millions of years. Geochemical conversion occurs as ancient organic remains are exposed to microbial factors, as well as heat generated by the earth’s geothermal gradient (Speight 2014).

1.2.2. Crude Oil Refining: Processes and Products

Crude oil is the raw material from which a multitude of oil-products are derived including light fuel oils, lubricating oils, and HFOs (Speight 2014, CEN 2012). Crude oils and oil-derived products are the subjects of oil fingerprinting. An overview of the oil refining process has been provided below to help better understand the different oil types analysed in oil fingerprinting. A flowchart of the generic oil refining process is provided in Figure. 1.1.

Oil refining is complex, and processes vary considerably depending on: (1) the crude oil feedstock that is supplied to the refinery; and (2) the desired products (Fahim et al. 2010). Regardless of these variables, three general steps form the basis of oil refining:

1. Physical Separation.
2. Catalytic Chemical Conversion.
3. Thermal Chemical Conversion.

Physical separation is the first stage of crude oil refining, and begins with the distillation of oil. Distillation is conducted in two stages: (1) atmospheric distillation; and (2) vacuum distillation. Atmospheric distillation produces a range of products from gases, straight run oils, kerosene, and gas oils (CEN 2012). Vacuum distillation produces two main products: vacuum gas oil and vacuum residue (Fahim et al. 2010). Light fuel oils such as diesel are the products obtained from atmospheric distillation. Lubricating oils are the residue from atmospheric distillation, which may or may not have been vacuum distilled following atmospheric distillation (CEN 2012).

Figure removed: refer to Fahim et al. (2010).

Figure 1.1: A schematic of the oil refinery process. The numerous petroleum products derived from crude oil are depicted; Figure adapted from Fahim et al. (2010).

Catalytic chemical conversion is the second stage of refining, which occurs in numerous ways depending on the distillate fraction that is dealt with. For example, naphtha fractions (C_6 – C_{10}) may be restructured into paraffins and aromatics, for the production of light refinery products such as gasoline. Heavy residues from distillation may also be subject to catalytic conversion in the form of hydrocracking, to form jet fuels, diesel and other fuel oils. Catalytic chemical conversion involves the breakdown of large, heavy residues, to smaller, lighter products in the presence of a catalyst and hydrogen (Fahim et al. 2010).

Heavy distillation residues (particularly vacuum residues) may undergo the third major refinery process: thermal chemical conversion. Thermal conversion is conducted mainly through thermal cracking, which breaks down heavy residues by rejecting carbon. This

process produces coke, and lighter petroleum products such as gas, and gas oils (Fahim et al. 2010).

HFOs are defined as blended products formed from the residues of the various refinery processes outlined above (CEN 2012). HFOs are graded based on their viscosity in centistokes (cSt) at 50°C, and are typically produced in three different grades: HFO30, HFO180, and HFO380. The number in the grade refers to the centistokes of the HFO; the lower the centistoke value the less viscous the oil, and vice versa (Roncoroni et al. 2015).

1.2.3. Chemical Composition of Oil

Oils are complex chemical mixtures composed of hydrocarbons, heteroatomic compounds, and trace metals/organometallic compounds. These compounds can be observed across a very broad boiling range, which may in fact differ between oils sourced from different geographical regions. Boiling ranges differ due to variations in the proportions of low-boiling compounds in relation to high-boiling compounds. To help understand this broad boiling range of compounds, four major groups are defined, as shown in Figure 1.2: (1) aliphatic hydrocarbons; (2) aromatic hydrocarbons; (3) heteroatomic organic compounds; and (4) organometallic compounds (Speight 2014). Each of these groups has been described below.

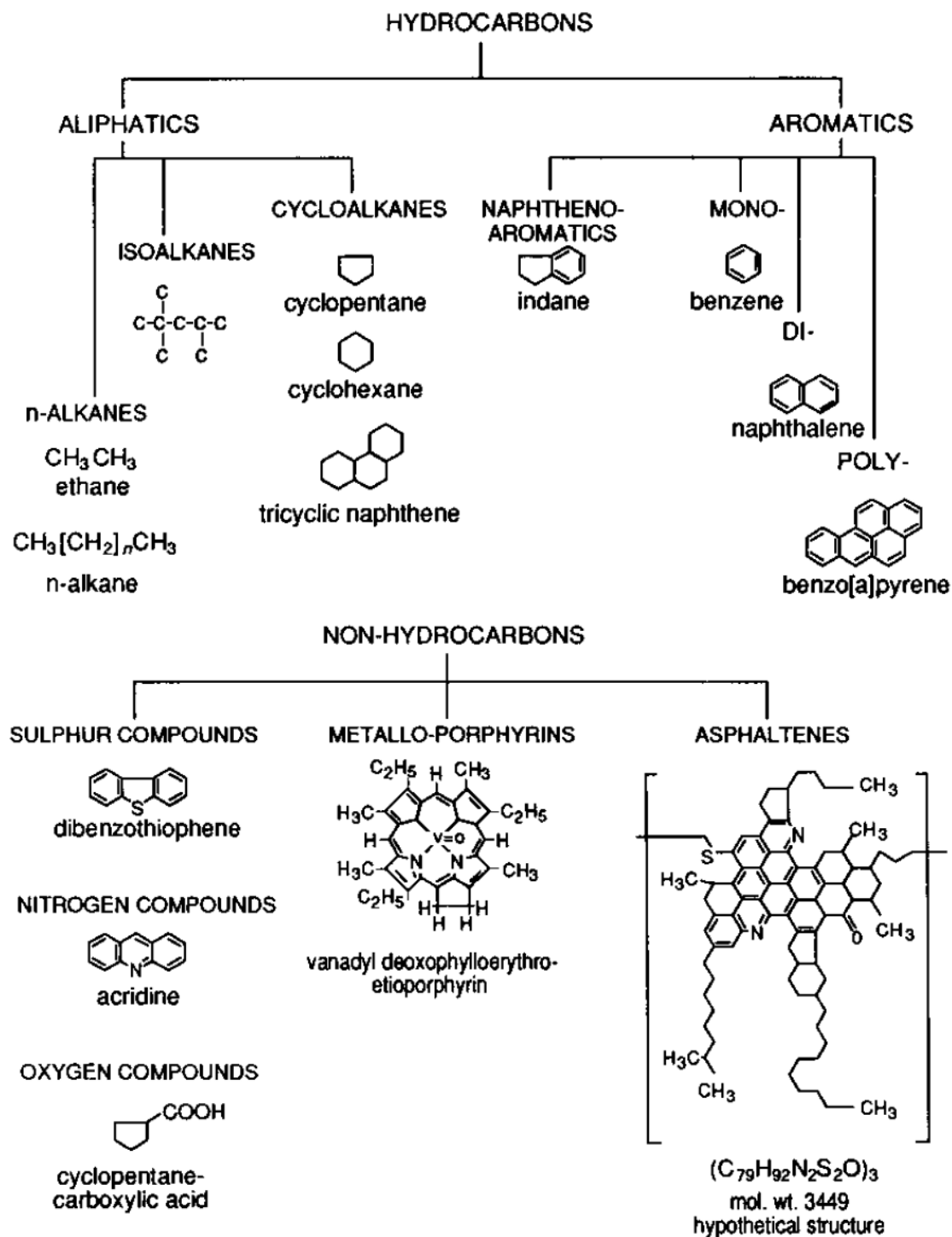


Figure 1.2: The four major oil fractions: (1) aliphatic hydrocarbons; (2) aromatic hydrocarbons; (3) heteroatomic organic compounds; and (4) organometallic compounds. Examples of compounds that may be found in each fraction are shown. Figure adapted from GESAMP (1993).

1.2.3.1. Aliphatic Hydrocarbons

Aliphatics molecules may consist entirely of single bonds (alkanes), or may contain a number of double (alkenes) or triple bonds (alkynes). Aliphatics may also be unbranched (straight-chain), branched (iso-) or cyclic (arranged in a ring without conjugating double bonds), and can vary considerably in size, ranging from C₁₀–C₄₀ (GESAMP 1993, Speight 2014, Wang et al. 2007).

Current oil fingerprinting methods target a range of aliphatic compounds. For example, the isoprenoids pristane and phytane are used for oil comparisons, and also as weathering indicators in oil fingerprinting (CEN 2012). A group of branched cycloalkanes, known as biomarkers, are also of particular importance to oil fingerprinting (Wang et al. 2007). Biomarkers are the carbon backbones of more complex molecules that originate from ancient organisms. Considerable variations between biomarkers in different oils have been recognised; hence, these compounds are useful when comparing oils during spill investigations (Wang et al. 2007, Speight 2014). Hopanes and steranes are biomarkers that are particularly useful in cases where oils are weathered. Hopanes and steranes are relatively large in size (4–5 ring structures ~ C₃₀ in size), and are hence more resistant to weathering than other target compounds (Barakat et al. 1997, Wang et al. 2006 [a]). Smaller biomarkers such as sesquiterpanes and diamondoids have also proven useful for oil fingerprinting, particularly when dealing with lighter fuel oils in which larger biomarkers (hopanes and steranes) are absent (Wang et al. 2006 [a], Wang et al. 2005, Wang et al. 2006 [b]).

Another important group of aliphatics are waxes, which are high molecular weight (300–2500) long straight chain alkanes (C₃₀–C₆₀) and are generally present in crude oils between 1–30 weight percent (wt%) (Ganeeva et al. 2016, Yang and Kilpatrick 2005, Roehner and Hanson 2001). Waxes are not targeted during current oil fingerprinting methods however waxes are important to this PhD research. Waxes have a tendency to co-precipitate

with asphaltenes; the targeted compounds in this research. Wax co-precipitation is discussed later in this chapter.

1.2.3.2. Aromatic Hydrocarbons

Aromatics are hydrocarbon ring structures defined by the presence of conjugating double bonds (McMurry and Simanek 2007). Aromatics in oil range from small mono-aromatic compounds, such as benzene, to larger 2–6 ring polycyclic aromatic hydrocarbons (PAHs) (GESAMP 1993, Speight 2014). Aromatic structures may exist with aliphatic side chains, resulting in a vast array of aromatic isomers that may be present in different oils (McMurry and Simanek 2007, CEN 2012). In regards to oil fingerprinting, PAHs are the most commonly used aromatics for the comparison of oils (Desideri et al. 1985).

1.2.3.3. Heteroatomic Compounds

Heteroatomic compounds are defined by the presence of atoms other than carbon (C) and hydrogen (H), including oxygen (O), sulfur (S) and nitrogen (N). Heteroatomic compounds appear to be present throughout the entire boiling range of oil; however, they are more abundant in the high-boiling fractions, including resins and asphaltenes (Speight 2014). Resins are a broadly defined group of heteroatomic compounds which include naphthenic carboxylic acids, sulfoxides and phenol compounds. Asphaltenes are also a broadly defined group of heteroatomic compounds; however, asphaltenes are much larger than resins (molecular weights ranging from 1000–10,000 for asphaltenes and 700–1000 for resins) (CEN 2012).

Smaller heteroatomic compounds found in the low-boiling range, such as the sulfur-containing compound benzothiophene (BT) (molecular weight = 134 g/mol), are currently targeted in oil fingerprinting (Jacob 1990, CEN 2012). Small heteroatomic compounds such

as BT are volatile, hence can readily be analysed using common oil fingerprinting instrumentation. Resins and asphaltenes however, are not volatile due to their considerably larger size. Of interest here is that, *asphaltenes are not currently used in oil fingerprinting due to the non-volatile nature of these large oil compounds* (CEN 2012, Speight 2014). The importance of this statement is discussed later in this chapter.

1.2.3.4. Organometallic Compounds

Metalloporphyrins are organic compounds found in oil that also contain trace metals such as nickel (Ni), vanadium (V) or iron (Fe). An example of a metalloporphyrin structure has been provided in Figure 1.3.

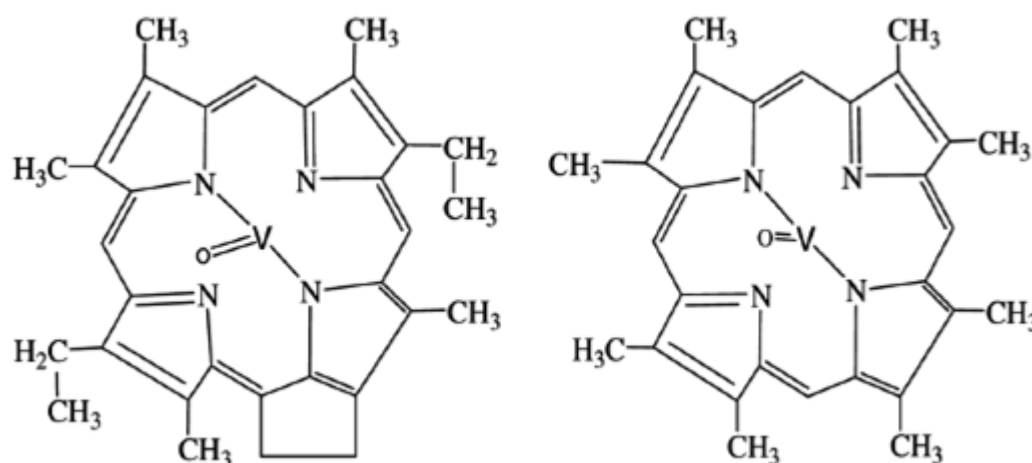


Figure 1.3: Examples of vanadium metalloporphyrins found in Venezuelan crude oil. Figure adapted from Gao et al. (2012).

Ni and V metalloporphyrins are the most commonly occurring organometallic compounds in oils (Gao et al. 2012, Speight 2014). Similar to heteroatomic compounds, metalloporphyrins exist throughout the entire boiling range of oils (Speight 2014). The concentrations of trace metals found in different oils are dependent on the type of oil. Lighter

crude oils tend to have lower trace metal concentrations, whilst heavier oils have higher concentrations (Speight 2014). Crude oils that have high sulfur concentrations, low wax content, and high Ni and V concentrations, are generally of a marine origin. Marine oils typically exhibit higher concentrations of V porphyrins as compared to Ni porphyrins. The reverse can be observed in crude oils of lacustrine (lake) origin. Lacustrine oils commonly have low sulfur concentrations, high wax content, and lower amounts of Ni and V (Makeen et al. 2015, Speight 2014). Organometallic compounds are currently not analysed in oil fingerprinting (Nordtest 2002).

1.3. Oil Spill Investigations: Scene Investigation and Sampling

With a basic knowledge of the chemical composition of oil, the oil spill investigation process may now be discussed. Given the significant impact of marine oil spills, it is paramount that the sources of spills are identified. The source of a spill refers to the location from which the spill originated. Spill sources may include marine shipping vessels, oil rigs, refineries, oil terminals, or oil storage facilities (GESAMP 2007, AMSA 2011). Determining the source of an oil spill may appear like a simple task; however, source determination can be very difficult. For example, consider the Strait of Malacca on Peninsular Malaysia. The Strait of Malacca is a major shipping channel for oil tankers navigating trade routes between the Middle East and far-east Asia. In 2010 alone, 74,000 ships passed through the strait, mostly large oil tankers. With such dense traffic, the occurrence of oil spills is inevitable. As such, 144 oil spills were recorded between the years 2000 and 2005. Identifying the source of oil spills in The Strait of Malacca would be difficult due to the increased number of potential spill sources (shipping vessels) in the region (Zakaria et al. 2017). The role of an oil spill investigator is to identify, with confidence, the true source of an oil spill. Investigations are conducted through a series of processes as described below.

1.3.1. Scene Investigations

1.3.1.1. Oil Spill Detection and Monitoring

In order to investigate an oil spill, the spill must first be detected. Numerous monitoring capabilities are available to provide visual aid for the detection of oil spills at sea. With the use of radar devices, shipping vessels can monitor oceanic regions; however, the area that can be monitored using ships is fairly restrictive. More comprehensive monitoring is achieved through the use of planes and satellites, fitted with synthetic aperture radar/s (SAR/s). SAR is a sensor that transmits microwave energy towards the earth's surface, producing backscatter energy (Fan et al. 2015). This backscatter energy is detected by the SAR sensor, producing an image of the region of interest. If SAR is focused on an oceanic region, the backscatter energy produced from water is very different to the energy produced if oil exists on the water's surface. Oil decreases the backscatter energy deflected back to the sensor; hence it appears as dark regions in SAR images. Water on the other hand, produces a high intensity of backscatter energy; hence, water appears very light in SAR images. This contrast between water and oil is what makes SAR imaging very useful for the monitoring and detection of marine oil spills (Fan et al. 2015).

1.3.1.2. Response to Oil Spills

Once a spill has been detected in Australian waters, a range of combat agencies will respond to the spill. The response strategies used may vary depending on available resources, as well as the severity and the type of the incident. Buoyant booms may be used to physically stop the spread of oil throughout the water. Skimming devices may also be used for the physical removal of oil from the surface of the water. Oil spill control agents are another option for responding to oil spills. For example, dispersants are control agents which chemically break down spilt oil (AMSA 2000, AMSA 2014).

1.3.1.3. Paper Trail Investigations

Once the oil spill is contained, the next step is to identify potential sources, or suspects. Potential sources are identified using an automatic identification system that produces crucial details of shipping vessels located in the vicinity of oil spills. Identified vessels are then treated as suspected sources during the investigation. Although useful for narrowing down suspected sources, identifying vessels in the vicinity of a spill does not conclusively identify the spill source. The latter will be achieved through oil fingerprinting in the laboratory (Desideri et al. 1985, CEN 2012). Before oil fingerprinting can be conducted, oil samples must first be collected. The sampling procedures used in oil spill investigations are outlined below.

1.3.2. Sampling

It is important to have a basic understanding of sampling processes currently used for obtaining oil for fingerprinting. Generally, the sampling practices outlined below yield small amounts of oil for fingerprinting in the laboratory. Asphaltene profiling methods have therefore been developed for small amounts of oil to align with current sampling practices. Three types of oil samples are collected for oil fingerprinting: (1) questioned oil samples from the spill itself, referred to as ‘spilt oil’; (2) known oil samples from suspected spill sources, referred to as ‘suspect oils’; and (3) background samples or ‘negative controls’ (ITOPF 2012).

1.3.2.1. Negative Controls

Negative controls are collected from a region that is representative of the area prior to oil contamination. Topography, chemical composition and physical location (affected by swell, wind, etc.) are all considered when determining the location from which to collect

negative controls (ITOPF 2012). Negative controls help oil spill investigators identify compounds present in the background matrix. Understanding the background matrix can assist in determining the presence of weathering in oils, as well as avoiding the misinterpretation of compounds in spilt oil that may actually be a part of the environment, not the spill sample itself.

1.3.2.2. Spilt Oil

If an oil spill exists as a thick surface slick, oil samples may be collected using glass jars or sorbent pads, as shown in Figure 1.4 (a). In these cases, around 10–20 g of oil is generally obtained for oil fingerprinting. On occasions, the oil spill will exist only as a thin surface film (or sheen), and will require sampling using fine-mesh ethylene tetrafluoroethylene (ETFE) nets (CEN 2012). Thin surface films of oil result in very small amounts of oil being collected and submitted for fingerprinting. All un-used sampling apparatus are also submitted for quality control (ITOPF 2012).

Figure removed: refer to ITOPF (2012).

Figure 1.4: Standard oil sampling methods. (a) Oil spill sampling from the water's surface using a sorbent pad; and (b) scraping oil spill samples from a rocky foreshore. Figure adapted from ITOPF (2012).

Sampling of oil washed up on beaches or on other coastal structures (such as rock platforms, oyster leases or mangroves) often involves collection in a jar if considerable amounts of oil are present. If lesser quantities of oil are available, scrapings of oil from these structures will be collected as shown in Figure 1.4 (b) (GESAMP 1993, Jernelov 2010, ITOPF 2012).

1.3.2.3. Suspect Oils

Suspect oils may be obtained from a range of different potential sources, most often marine shipping vessels. The amount of oil collected from a suspected source is dependent on the collection method used to obtain oil. For example, oils sampled from cargo tanks will require different sampling techniques to oils sampled from bilge tanks; hence the amount of oil obtained for fingerprinting will vary (ITOPF 2012). Oils from cargo tanks are often homogenous and can be sampled from one position in the tank resulting in a relatively small sample of oil. In contrast, bilge tanks are often located beneath the engine, and are designed to collect oil that may accumulate from minor engine leakages. As a result, oil located in bilge tanks (bilge oil) may be a mixture of oils, including HFOs (fuel for vessels) and lubricating oils (used to moderate engine functionality). As a consequence, bilge tanks may require cross-sectional sampling to ensure that the oil sample is representative of the entire depth of the tank. The result may be quite a substantial amount of oil being collected for analysis.

1.3.2.4. Sample Submission

Once the necessary oil samples have been collected, the oils are sent to a forensic environmental laboratory for oil fingerprinting. Oil fingerprinting may be conducted by the same agency that carries out the scene investigation and sampling, or it may be conducted by

a second agency. In NSW, The EPA conducts the scene investigation and sampling, whilst oil fingerprinting is conducted by the NSW Office of Environment and Heritage (OEH).

1.4. Oil Spill Investigations: The CEN Method for Oil Fingerprinting as a Foundation for the Development of Asphaltene Profiling Methods

Chemical variations in oil can be attributed to several factors including the oil type, the geographical origin of the oil, the age of the oil fields from which oils originate, or even as a result of the depth of the oil wells (Speight 2014). These known chemical variations between different oils are the building blocks from which oil fingerprinting was established. Through research and casework, probative chemical compounds have been identified and are used in oil fingerprinting to compare oils and identify the source of oil spills (Desideri et al. 1985, Wang et al. 2006 [a]). Numerous standards have been developed for oil fingerprinting, however the most widely recognised, highly validated, and robust standard is the European Committee for Standardization (CEN) method (CEN 2012). The CEN method was developed by the European Committee for Standardization, in collaboration with an international consortium of oil fingerprinting experts who conduct routine round-robin testing to ensure the robustness of the method. The CEN method allows for greater levels of oil discrimination as compared to other major oil fingerprinting standards such as the Nordtest and the American Society for Testing and Materials (ASTM) methods, which are both considered pre-cursors to the CEN method (Nordtest 2002, ASTM D3328-06 (2013)). For this reason, the CEN method has been considered the most suitable standard for supporting this PhD research. General information regarding both the Nordtest and ASTM methods for oil fingerprinting has been provided in Appendix A to briefly elaborate on the limitations of these methods in comparison to the CEN method.

As highlighted previously, *asphaltenes are not currently used in oil fingerprinting due to the non-volatile nature of these large oil compounds* (CEN 2012, Speight 2014). This PhD aims to explore and evaluate the application of asphaltenes in oil fingerprinting. To produce suitable methods for asphaltene profiling, a foundation was required from which to develop these methods. The principles and practices adhered to in the CEN method have been used as a foundation for the development of asphaltene profiling methods. The CEN method has therefore been influential in ensuring that the developed methods were produced with consideration for casework requirements. The expression of method uncertainty (error) and the comparison of asphaltenes have been conducted to align with the accepted principles and practices applied in the CEN method. The CEN method is too detailed to be described herein, and the reader should refer to the CEN method itself for technical information (CEN 2012). The aspects of the CEN method that were relevant to the development of the asphaltene profiling methods are discussed below.

1.4.1. Sample Preparation

During sample preparation, the aim is to take a single aliquot from each ‘whole oil’ that is large enough to allow for the entire CEN analyses. A single aliquot is taken to minimise sample handling, and to minimise the time taken for sample preparation (Stout and Wang 2016, CEN 2012). Similarly to the CEN method, this research also aimed to obtain single aliquots of asphaltenes that were large enough for asphaltene profiling. Note that the term ‘whole oil’ is used throughout this thesis. The whole oil refers to oil that is unseparated, and therefore contains all oil compounds including aliphatics, aromatics, heteroatomic compounds, and organometallic compounds.

1.4.2. Sample Clean-Up

Sample clean-up in the CEN method is conducted for two reasons: (1) to remove undesirable contaminants that have been extracted along with oil during sample preparation; and (2) to remove non-volatile oil compounds (including asphaltenes) that are incompatible with GC analysis (CEN 2012). The current sample clean-up practice of *discarding asphaltenes prior to oil fingerprinting* has been an influential factor for motivating this PhD research. This PhD has aimed to determine whether or not the currently discarded asphaltenes contain probative information that may be useful in oil spill investigations.

1.4.3. Analytical Controls

The preparation and analysis of duplicate aliquots from a single oil sample allows analysts to gauge variations that may occur during the sample preparation phase. On the other hand, duplicate analyses of a single aliquot will provide insight into the method uncertainty (not the sample preparation). To help decide which oils should have duplicate aliquots taken, rules have been developed which are outlined in the CEN method (CEN 2012).

Although the CEN method specifies only to obtain duplicates under certain circumstances, in this PhD research, duplicate asphaltene aliquots were obtained from every oil sample when possible during the development of asphaltene profiling methods. As a result, more duplicate analyses were conducted than currently required by the CEN method.

1.4.4. CEN Analyses

Analyses in the CEN method is conducted in two separate tiers:

- Tier 1 screening using Gas Chromatography-Flame Ionisation Detection (GC-FID).
- Tier 2 confirmatory analysis using Gas Chromatography-Mass Spectrometry (GC-MS).

1.4.4.1. Tier 1: GC-FID Screening

Tier 1 aims to obtain fast, reliable results that can be used to quickly eliminate non-related oil sources from investigations. Tier 1 involves determining the total hydrocarbon distribution of oils (from C₁₀–C₄₀) and comparing these hydrocarbon distributions between spilt oil and suspect oils. As part of this comparison, the hydrocarbon profiles are compared visually and using Gas Chromatography-Percentage Weathering (GC-PW) plots. GC-PW-plots express the intensities of each alkane peak in the spilt oil as a percentage of each corresponding alkane peak in suspect oils. GC-PW-plots are able to indicate differences between oil samples, either due to weathering or due to actual differences in composition. Isoprenoid ratios of pristane, phytane, *n*-C₁₇ and *n*-C₁₈ are also compared. If obvious visual differences are observed between chromatograms or GC-PW-plots, non-related suspect oils may be eliminated from investigations. It is important that the analyst considers potential weathering of oils whilst conducting the comparison. For example, evaporation will cause the loss of low boiling alkanes; hence the absence of low boiling alkanes may be expected in spilt oil and should be interpreted with care when compared to suspect oils.

It has been suggested in the literature that asphaltenes are less susceptible to weathering than volatile compounds that are currently targeted during oil fingerprinting (Lewan et al. 2014). The investigation of asphaltenes for use in oil spill investigations is therefore warranted as this may alleviate the need for interpreting weathered oils. It is also worth noting that a visual comparison approach akin to the CEN method was utilised for the comparison of asphaltene profiles generated from developed asphaltene profiling methods.

1.4.4.2. Tier 2: Oil Spill Identification Using GC-MS

Tier 2 is designed as the oil spill identification step, as GC-MS is sufficiently sensitive and selective to detect individual oil compounds (CEN 2012).

The comparison during Tier 2 is also performed visually and using PW plots, in this case Mass Spectrometry-Percentage Weathering (MS-PW)-plots. MS-PW-plots function in the exact same manner as GC-PW-plots. A range of PAHs and biomarker compound/compound groups are targeted during Tier 2 comparisons.

Selected ion chromatograms are extracted from the total ion chromatograms of oils using selected mass-to-charge ratios (m/z) which correspond to specific target PAHs and biomarkers. Suspect oils that are different in their PAH and biomarker distributions in comparison to the spilt oil may be excluded from the case.

Again, weathering effects need to be taken into consideration during interpretation. Some weathering effects, such as evaporation, are readily observed in the data, whilst other weathering processes, including biodegradation and photo-oxidation are more complicated to interpret. The complicated nature of interpreting volatile chemical fingerprints from weathered oils further signifies that investigation into asphaltene profiling is worthwhile.

Diagnostic Ratios

To aid in the interpretation of the data, the CEN method incorporates the calculation of diagnostic ratios (CEN 2012). ‘Diagnostic ratios’ or DRs are ratios that have been proven to show authentic variation between oils (Stout and Wang 2008). DRs are calculated using a range of biomarker and PAHs as recommended by the CEN method. DRs may be calculated using either peak heights or areas and are calculated as:

$$DR = \text{Compound A} / \text{Compound B}.$$

An acceptance threshold is calculated by determining the error of the method, and functions as a means of determining if differences observed between DRs in two oils are significant or not (CEN 2012). A difference in just one DR between oils is sufficient to eliminate the suspect source. In contrast, for two oils to be considered from the same source, all DRs must fall within a calculated threshold level, and all other comparisons must support this (i.e., visual comparisons). It is worth emphasising that weathering can be detrimental to the comparison of DRs. Weathering may remove compounds which are required for the calculation of DRs, hence limiting the probative value of oil fingerprinting in such cases. The need to investigate asphaltenes is further reinforced given the potential recalcitrant properties of this currently discarded oil fraction. The concept of using DRs was also applied to asphaltene data in this PhD research.

1.4.5. Oil Fingerprinting Conclusions

At the conclusion of Tier 1 and Tier 2, data is collated to produce oil fingerprints for each of the case oils. The final conclusions of an oil spill investigation are determined from the comparison of oil fingerprints. Four possible conclusions may be derived from the comparison of spilt oil and suspect oils through CEN oil fingerprinting: (1) match; (2) probable match; (3) inconclusive; or (4) non-match (CEN, 2012).

It is important to highlight that the terminology used to describe conclusions in oil fingerprinting differs from accepted terminology in other forensic science disciplines. For instance, the general forensic sciences do not use the term 'probable match'. To better align with the conclusions reported in the majority of forensic science disciplines, conclusions in this PhD have been reported as follows when comparing asphaltene profiles.

1.4.5.1. Identification

Identification - *There is a sufficient amount of information that is the same between two asphaltene profiles. Any differences present between profiles are explainable differences. The oils are from the same origin.*

It is critical to note that whilst some results in this research did support the criteria for identification, it was not possible to definitively confirm the identification. It is not possible at this present time to confirm if two asphaltene fractions are indeed from the exact same origin based on asphaltene profiles. If two asphaltene profiles are the same, the profiles may simply be not specific enough to differentiate the two oils in question. Occasionally in this research, it is stated that two oils were correctly identified as being from the same origin. In such instances however, the origins of oils were known which occurred during method development. During the blind study however, the oil origins were unknown to the analyst. Consequently, if the two compared asphaltene profiles met the criteria for an identification, to be conservative, the result was reported as being **not differentiated from one another**.

1.4.5.2. Inconclusive

Inconclusive - *The available information is the same between two asphaltene profiles; however there is an insufficient amount of information to confirm identification. The asphaltene profiles cannot be excluded either, as there are no unexplainable differences between the two profiles.*

1.4.5.3. Exclusion

Exclusion - *there is a sufficient amount of information available in two asphaltene profiles and unexplainable differences are observed between the two profiles. The oils are differentiated; they are not from the same origin.*

1.5. Research Rationale: Application of Asphaltenes in Oil Spill Investigations

As previously discussed, *asphaltenes are discarded prior to oil fingerprinting.*

Discarding asphaltenes is potentially detrimental for two reasons:

1. An oil fraction that may provide additional information in oil fingerprinting is being overlooked. The literature suggests that asphaltenes are in fact a highly variable oil fraction when compared between oils from different geographical regions (Speight 2014, Gawel et al. 2014). Asphaltenes may therefore provide additional information that could support the currently obtained oil fingerprints based on the volatile fraction.
2. Asphaltenes are believed to be less susceptible to weathering than volatile fractions of oil (Lewan et al. 2014). When presented with heavily weathered oils in investigations, considerable amounts of volatile information may be missing (CEN 2012, ITOF 2011, GESAMP 1993, Jernelov 2010). Furthermore, the interpretation of weathered oils relies more heavily on expert knowledge, which introduces a degree of subjectivity when drawing conclusions. If asphaltenes are more resistant to weathering, the inclusion of asphaltenes in oil fingerprinting may assist with the interpretation of weathered oils during investigations.

The aforementioned points raise some interesting questions. It would be of great benefit to oil fingerprinting if the asphaltene fraction was indeed resistant to weathering, as this would reduce the reliance on expert knowledge for explaining differences attributed to weathering. As methods for asphaltene profiling do not currently exist, it is not possible to test how weathering affects the probative value of asphaltenes. Asphaltene methods must first be developed using un-weathered oils to assess whether asphaltenes provide probative

information that may assist in oil spill investigations. Once asphaltenes are confirmed as a probative oil fraction, weathered oils may be assessed to gauge the effects of weathering on asphaltenes. Prior to discussing the potential application of asphaltenes in oil fingerprinting, it is necessary to provide information on the asphaltene fraction itself, including molecular structure, solubility properties, and past and current applications of asphaltene research. The background information provided on asphaltenes is essential for defining the scope of this PhD research.

1.6. Asphaltenes

As stated previously, the asphaltene fraction is comprised of the heaviest heteroatomic compounds found in oil. Asphaltenes are high molecular weight compounds (1000–10,000), and are non-volatile. The asphaltene fraction is broadly defined and consists of many different molecules, not limited to one specific molecular structure (Leyva et al. 2013, Majumdar et al. 2013, Fossen et al. 2007, Xiong and Geng 2000). The molecular structures of asphaltenes are outlined below, followed by an introduction to asphaltene precipitation. Asphaltene precipitation is the process of solvent-extracting the asphaltene fraction from the remaining oil fractions. Precipitation factors dictate which oil compounds are isolated in asphaltene fractions. As a consequence, asphaltenes are defined based on solubility, rather than molecular structure. Definition by solubility attributes to the vast array of molecules that may be present in asphaltene fractions.

1.6.1. Molecular Structure of Asphaltenes

Although a vast array of molecules may be present in asphaltene fractions, these molecules all have generally accepted molecular components. Asphaltenes generally consist of large aromatic clusters (4–10 rings in size), alkyl chains, and the presence of heteroatoms

(Groenzin and Mullins 2000, Liao et al. 2009, Akbarzadeh et al. 2007). Defining the exact structural arrangement of asphaltenes has been the topic of extensive asphaltene research (Fossen et al. 2007, Mullins 2010, Mullins et al. 2012).

1.6.1.1. Island or Archipelago?

Two theories exist for the structure of asphaltene molecules: the island theory (Sabbah et al. 2011, Mullins 2010) and the archipelago theory (Mullins et al. 2012, Muhammad and Abbott 2013, Peng et al. 1999).

The island theory proposes that each asphaltene molecule is structured with a single centralised aromatic cluster (or PAH ring system), with alkyl chain substituents. The alkyl chains may be branched chain and/or straight chain alkanes (Mullins 2010) (Figure 1.5). Heteroatoms, including sulfur and nitrogen, are also present within these condensed PAH systems.

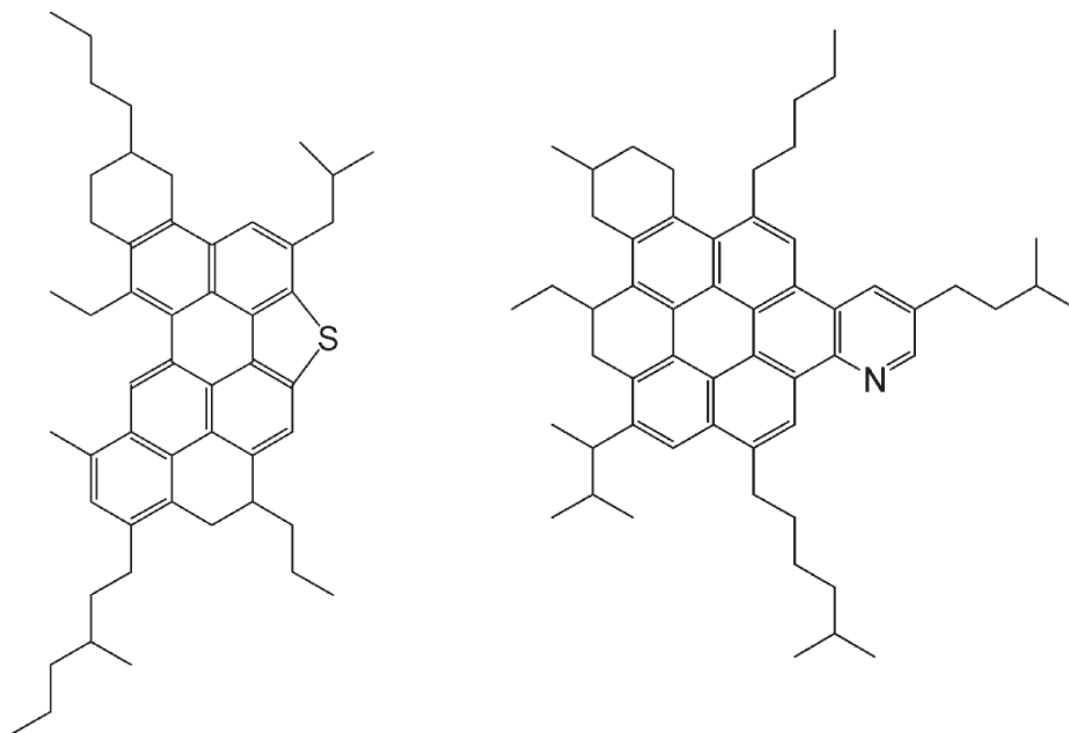


Figure 1.5: Examples of asphaltene island structures. Figure adapted from Mullins (2010).

The archipelago theory suggests that each asphaltene molecule is structured with multiple aromatic clusters, linked together by alkyl-bridges (Mullins et al. 2012) (Figure 1.6). There is sufficient literature in support of both structural theories, whilst some studies have acknowledged the co-existence of both structures (Karimi et al. 2011, Mullins et al. 2012). When considering the forensic comparison of asphaltenes, it is not relevant to conclude which specific structures exist in a given asphaltene sample. If asphaltenes are extracted and analysed in the exact same manner from different oils, any differences observed when comparing asphaltenes can be deemed authentic. Whether differences are attributed to the presence of island or archipelago structures is not relevant. These theories however, may provide reasoning for the observed asphaltene profiles obtained from this research, and certainly may provide important information for the development of asphaltene methods (i.e., thermal degradation techniques that break the alkyl moieties present in both theories).

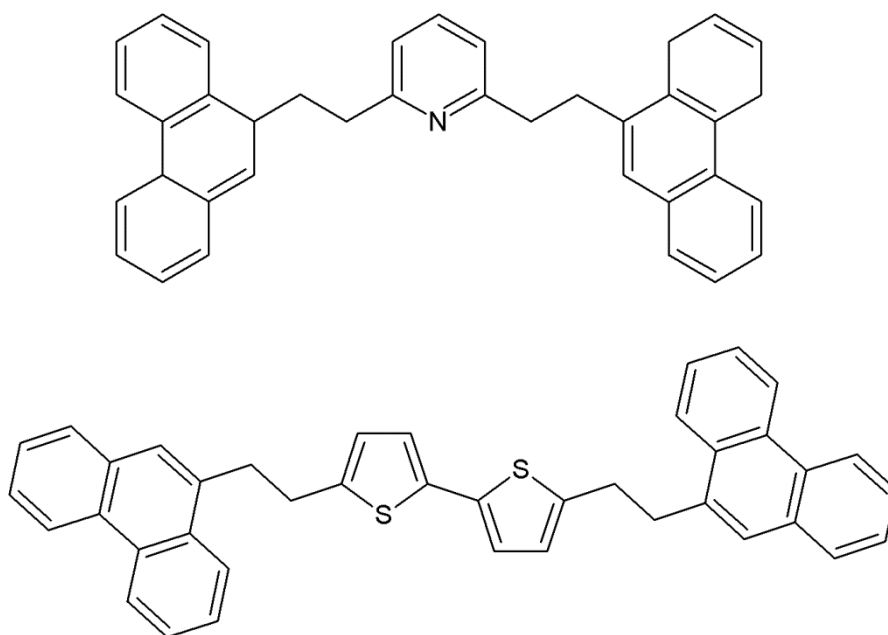


Figure 1.6: Examples of asphaltene archipelago- structures. Figure adapted from Mullins et al. (2012). Molecular structures were produced using ChemSketch Freeware (version 2016 1.1) from Advanced Chemistry Development, Inc. (ACD/Labs).

1.6.1.2. Heteroatomic Composition

The most common heteroatoms observed in asphaltenes are consistent with those observed in whole oil: O, N and S are all present (Fossen et al. 2007). Heteroatoms exist within the aromatic system/s of asphaltene molecules in numerous structural forms depending on the specific heteroatom (GESAMP 1993, Mullins 2010) (Figures 1.2 and 1.6). N can be found in pyrrolic and pyridinic structures, S can be found in thiophene structures, and O may be present in the form of phenols, though much less abundant (Mullins 2010). S can also be found in aliphatic structures such as sulfides, and in sulfoxide structures in which S is double-bonded to O (Pomerantz et al. 2013). Given that asphaltenes possess heteroatoms, asphaltene molecules are polar; specifically the aromatic systems within each molecule (Mullins 2010). Note that the polarity of asphaltene molecules can be altered due to aggregation (described below).

The concentration of heteroatoms in the asphaltene fraction is much higher than the concentration of heteroatoms in whole oil. O content can range from 0.3–4.9%, whilst S content can vary even more, from 0.3–10.3%. N content is also variable, but to a lesser extent, with a range from 0.6–3.3%. The majority of heteroatoms found in oil are native to the asphaltene fraction, more so than the resin fraction. As a result, the isolation of asphaltenes from whole oil will result in a higher concentration of heteroatoms, as compared to the heteroatom concentration measured in whole oil itself (Speight 2014).

1.6.2. Asphaltene Aggregation

Prior to discussing asphaltene precipitation, it is important to mention the aggregation properties of asphaltenes. Whilst asphaltene precipitation causes the macroscopic separation of asphaltene solids from the remaining liquid fractions of oil, asphaltene aggregation involves the formation of nanoscale solids that are suspended in liquid oil (Mullins 2010). Mullins (2010) proposed an aggregation process that consists of three main stages:

1. Island structured asphaltene molecules with polar PAH systems begin to interact with each other via intermolecular attractions.
2. ‘Nanoaggregates’ of around 6–7 asphaltene molecules in size begin to form; this occurs due to the stacking of the PAH systems from each individual molecule. The resultant nanoaggregates are internally aromatic with exposure of combined molecular alkyl chains.
3. ‘Clusters’ are formed from nanoaggregates due to ongoing inter-molecular interactions via the polar PAH systems; typically, clusters are formed from around eight nanoaggregates. The formation of clusters affects the polarity of asphaltene molecules through steric hindrance, as the alkylated exterior of

clusters hinder the interaction of the internally polar PAH systems with other nanoaggregates.

Asphaltene aggregation was an important consideration during this PhD research as sample preparation of asphaltenes in solution has the potential to induce aggregation. It should also be made clear that due to the chemical variability of different oils, asphaltene aggregation does not occur under the same conditions for all oils. For example, if asphaltenes from different oils are dissolving in solvent at the exact same concentration, it is possible that some asphaltenes may aggregate, whilst others may not. As a consequence, differing degrees of aggregation are expected across any given sample-set of oils. Aggregation was therefore carefully considered where preparation of asphaltenes in solution was required.

1.6.3. Asphaltene Precipitation

When excess *n*-alkanes are added to oil, asphaltenes are defined as the insoluble fraction that precipitates out of solution (Trejo et al. 2004). The liquid (or soluble) fraction of oil is known as the ‘maltene fraction’, and consists of aliphatics, aromatics and smaller heteroatomic compounds (such as sulfur-containing compounds and low-boiling resins) (Fossen et al. 2007).

The major problem with this broad definition of asphaltenes is that the chemical composition of asphaltenes varies as precipitation conditions change. From a forensic context, it is not possible to compare asphaltenes as currently defined in the literature, as precipitation conditions differ from study to study, resulting in chemically disparate asphaltene fractions. To apply asphaltenes in oil fingerprinting, it is necessary to standardise the asphaltene precipitation process. This means that the variables which allow for changes in precipitation conditions (precipitation variables) need to be controlled. Controlling

precipitation variables ensures that any differences observed during asphaltene comparison are attributed to the asphaltene sample itself, not variances caused by the precipitation method. A range of precipitation variables that may affect the chemical composition of asphaltenes are highlighted below. The aim is to highlight the significant inconsistencies currently presented in the literature and to reinforce the need for a standardised approach for forensic asphaltene precipitation.

1.6.3.1. Precipitation Variables

A range of solvents and solvent-to-oil ratios used throughout the literature for precipitation (and recommended by a number of international standards) have been collated in Table 1.1. Table 1.1 will be referred to while discussing the disparate nature of solvents and solvent-to-oil ratios currently used for asphaltene precipitation in non-forensic applications.

Precipitation Solvent

As indicated in Table 1.1, a range of different *n*-alkane solvents have been used throughout the literature for obtaining asphaltenes. These include *n*-pentane, *n*-heptane, and to a lesser extent, *n*-hexane. A number of ASTM standards for asphaltene precipitation have also recommended the use of either *n*-pentane (ASTM D893-14 and ASTM D2007-11) or *n*-heptane (ASTM D4124-09 and ASTM D3279-12). Some studies have elected to use a mixture of *n*-alkane solvents for precipitation, such as *n*-heptane/*n*-hexane and *n*-heptane/*n*-pentane mixtures. Throughout this thesis, the following abbreviations will be used to denote this range of *n*-alkanes: *n*-pentane (C_5), *n*-hexane (C_6), *n*-heptane (C_7). These abbreviations correspond to the carbon number of these alkane chains, and are also used to denote the

specific asphaltene fraction of interest (i.e., C₅ asphaltenes, indicating that these asphaltenes were precipitated using *n*-pentane).

Table 1.1: Past studies and international standards exhibiting the use of various precipitation solvents/solvent-oil-ratios. The solvent-to-oil ratios are expressed as volume/weight (v/w). International standards are indicated in bold.

Solvent	Solvent-to-oil ratio (v/w)	Standard Method/ Author
<i>iso</i> -octane	20–60:1	Lewan et al. (2014)
<i>n</i> -heptane	20:1	Tavassoli et al. (2012)
		Ali et al. (2012)
		Barakat et al. (1999)
	40:1	Jahromi et al. (2014)
		Islam et al. (2013)
	50:1	El-Gendy et al. (2013)
		Boukir et al. (1998)
	100:1	ASTM D3279-12 ASTM D4124-09 Oudot and Chaillan (2010)
		Trejo et al. (2004)
	150:1	Silva et al. (2008)
		Liao and Geng (2002)
<i>n</i> -hexane	>40:1	Muhammad and Abbott (2013)
<i>n</i> -pentane	10:1	ASTM D893-14 ASTM D2007-11
	20:1	Pesarini et al. (2010)
	30:1	Podgorski et al. (2013)
	40:1	Peng et al. (1997)
		Adebisi and Thoss (2014)
<i>n</i> -propane	-	Artok et al. (1999)
Petroleum ether (b.p. 30–60°C)	-	Xiong and Geng (2000)
<i>n</i> -heptane/ <i>n</i> -hexane	25:1	Bragado et al. (2001)
	70:1	Wang et al. (2013) *
<i>n</i> -heptane/ <i>n</i> -pentane	40:1	Zhang et al (2014)
	70:1	Wang et al. (2013) *
<i>n</i> -hexane/methanol	-	Zhang et al. (2014)

* indicates the same study.

Table 1.1 also indicates that a range of other solvents (other than C₅, C₆ or C₇) have been employed throughout the literature for the precipitation of asphaltenes; these include toluene, petroleum ether, *iso*-octane and *n*-propane. As stated previously, the chemical composition of asphaltenes varies, as precipitation conditions change. With so many solvents used, it is not surprising that the chemical compositions of precipitated fractions are variable (Fossen et al. 2007, Mullins 2010). It is clear that standardisation of the asphaltene fraction is required prior to application in oil fingerprinting, both from the perspective of obtaining the fraction and chemically defining asphaltenes.

For example, consider the chemical difference in asphaltene fractions obtained when using C₅ and C₇. Oil is to be considered as a continuum. Oil compounds range from the lowest boiling, lowest molecular weight compounds, through to the highest boiling, highest molecular weight compounds. Between the lowest and highest boiling compounds, exists a range of moderate boiling compounds. C₇ very selectively precipitates the highest boiling and heaviest oil compounds; predominantly asphaltene molecules. In comparison, C₅ is not as selective, and tends to not only precipitate asphaltenes, but also a portion of moderate-heavy compounds; typically resins and waxes (Speight 2014). The C₇ fraction therefore contains a higher content of asphaltene molecules and fewer co-precipitates as compared to C₅ (Mullins 2010). Consequently, the chemical composition of C₇ asphaltene fractions will differ from C₅ asphaltene fractions. Furthermore, the natural chemical variability of different oils means that two different oils may simply have different compositions of high-boiling compounds (Speight 2014). In regards to deciding which solvent is most suitable for the precipitation of asphaltenes, this depends on which solvent can produce high enough yields for profiling when provided with small amounts of oil (tested and discussed in Appendix B). It will then be necessary to persist with the most suitable solvent so that the precipitated asphaltenes are comparable to one another.

Solvent-to-Oil Ratio

Another precipitation variable that may influence subsequent asphaltene fractions is the solvent-to-oil ratio; expressed as volume/weight (v/w). As indicated in Table 1.1, a range of different solvent-to-oil ratios have been employed throughout the literature or recommended by international standards; these range from ratios of 10:1 (v/w), through to ratios of 150:1. Whilst the vast majority of studies in the literature make no reference as to why specific solvent-to-oil ratios were used, Ancheyta et al. (2002) investigated the effects of using different solvent-to-oil ratios prior to precipitating the studied asphaltene fractions. Ancheyta et al. (2002) tested the C₅ solvent-to-oil ratio for asphaltene precipitation from a heavy crude oil (Maya crude) and determined that the asphaltene yield (wt%) from the oil was considerably lower at a ratio of 10:1 (10%) than it was at 40:1 (~16–17%). From ratios of 40:1 to 100:1, the wt% plateaued at ~16–17%. It was therefore determined that a 60:1 ratio was ideal for: (1) avoiding errors in asphaltene yield occurring at less than 40:1, taking into consideration that other oils may behave differently; and (2) using as little solvent as possible to avoid additional costs in precipitation research (Ancheyta et al. 2002). Whilst it is very difficult to find data such as this in the literature, the findings by Ancheyta et al. (2002) are a good starting point from which a suitable standard solvent-to-oil ratio may be derived for use in a forensic precipitation method. Other studies such as Trejo et al. (2004) have recognised the finding by Ancheyta et al. (2002), and have also opted for the use of a 60:1 ratio.

Duration of Oil Contact with Solvent

The duration of oil contact with solvent used for asphaltene precipitation is highly disparate throughout the literature (Maqbool et al. 2009, Speight 2014). For example, a contact period of anywhere from 8–10 hrs is widely recommended (Speight 2014); however, Maqbool et al. (2009) challenged these conventional guidelines. The study by Maqbool et al.

(2009) highlighted that the short time frames for which asphaltene precipitation is commonly conducted (between 1–2 days) relies on a misleading assumption that the crude oil/solvent mixtures have reached equilibrium within this time, and that no more separation between asphaltenes and maltenes is possible. Maqbool et al. (2009) studied the percentage precipitation of an Alaskan crude oil over time, using a range of different heptane concentrations at different volume percent (vol%); different vol% of heptane in oil. The results revealed that at low concentrations (46.5–50.0 vol%), asphaltene yields increased very slowly as a function of time – slow continual yield increases were observed over a 100 hour period. The duration of contact had less effect at higher concentrations (55.0–70.0 vol%), as the asphaltene yield reached its maximum within a few hours for 55.0 vol% (or very near to the maximum observed over the 100 hour test period), and within a few minutes for 70.0 vol%. In conclusion, Maqbool et al. (2009) stated that to achieve asphaltene precipitation, the duration for which the oil is in contact with the solvent can vary significantly depending on the concentration of solvent in the solvent/oil mixture. When considering suitable contact duration for oil fingerprinting, the quicker the precipitation process, the better. Oil fingerprinting analysts are often required to provide results within time constraints; hence, an 8–10 hr contact period is far too long. Also, the extremely long times suggested by Maqbool et al. (2009) are even further from what is considered desirable. What is interesting however is that the study by Maqbool et al. (2009) showed that precipitation at higher concentrations (or higher solvent-to-oil ratios) did not require a long duration to achieve maximum precipitation weight. The results observed by Maqbool et al. (2009) support the use of a higher solvent-to-oil of around 60:1 which was also suggested by Ancheyta et al. (2002).

Temperature

The study by Yang et al. (2016) highlighted that although the literature does recognise temperature as an influential precipitation factor, the studied effects of temperature on asphaltene precipitation have contradicted one another. Early research by Mitchell and Speight (1973) concluded that increased temperature resulted in increased asphaltene precipitation from Athabasca bitumen; however, Bjorøy et al. (2012) and Andersen (1994) determined that asphaltene precipitation yields decrease with increasing precipitation temperatures. Furthermore, Maqbool et al. (2011) determined that asphaltene precipitation from crude oil occurred more rapidly at higher temperatures. Whilst these conflicting conclusions may simply be due to differing oil chemistries, it is still necessary to determine a universal precipitation temperature for forensic asphaltene precipitation. Temperature effects were tested and are discussed in Appendix B.

Pressure

Pressure is one variable that is not overly influential during precipitation under laboratory conditions. Pressure however, can influence onset of precipitation during many petroleum industry processes including the field recovery of oils, oil transportation, and oil refining (Yang and Kilpatrick 2005). Similarly to temperature, the effects of pressure on asphaltenes have been intensely studied in petroleum chemistry; however, conclusions derived throughout the literature are still disparate (Bahrami et al. 2015). This is because the vast majority of research dedicated to precipitation pressures is fixated on developing predictive models for very specific industrial processes (Ameli et al. 2016).

Co-Precipitation of Non-Asphaltenic Compounds

Depending on the chemical composition of oil and the precipitation conditions used, moderate to high-boiling compounds such as resins and waxes may co-precipitate alongside higher-boiling asphaltenes (Roehner and Hanson 2001). Along with resins and waxes, trace metals are commonly concentrated in the asphaltene fraction; however the exact co-precipitation mechanism of trace metals is not well understood (Miller et al. 1999, Yakubov et al. 2016).

Whilst the molecular structures of waxes (non-polar aliphatics) are very different to asphaltenes (polar aromatics), wax and asphaltene fractions are both comprised of high molecular weight compounds with poor solubility (Ganeeva et al. 2016). Some studies suggest that the shared solubility properties of waxes and asphaltenes are the cause of wax co-precipitation alongside asphaltenes. The accepted asphaltene precipitation process of adding excess short chain alkanes to oil results in a high proportion of co-precipitated waxes in subsequent asphaltene fractions; neither waxes nor asphaltenes are soluble in short chain alkanes (Thanh et al. 1999, Coto et al. 2011). Other studies have suggested that the mechanism of wax co-precipitation is not attributed to the solubility properties of waxes; instead, wax molecules simply become physically entrained within the molecular structures of asphaltenes, hence co-precipitation occurs (Yang and Kilpatrick 2005). Regardless of which proposed mechanism is correct, it is important to acknowledge that waxes co-precipitate with asphaltenes. It is also important to recognise that the amount of waxes that co-precipitate may vary. As indicated previously, different oils have different wax contents ranging from 1–30 wt% (Ganeeva et al. 2016). Given these variable wax contents, the amount of co-precipitated waxes will be greater in some oils than others (Roehner and Hanson 2001). The amount of co-precipitated wax may also be influenced by changes in precipitation temperature. Individual oils have specific wax precipitation temperatures

(WPT), which are the optimum temperatures at which waxes will precipitate. WPTs vary between different oils (from 0–60°C) depending on the physical properties of oil; as a consequence, temperature will affect wax co-precipitate differently in different oils (Roehner and Hanson 2001, Yang and Kilpatrick 2005).

Resins and asphaltenes are separate oil fractions that are both comprised of heteroatomic compounds. Resin co-precipitation occurs as the solvents used for asphaltene precipitation are not selective to the theoretical molecular weight thresholds defined between resins and asphaltenes. High molecular weight resins are therefore commonly co-precipitated alongside asphaltenes (Speight 2014). The colloidal theory states that asphaltenes exist in oil as solid particles and are stabilised in oil by adsorption of resins to asphaltenes. The adsorbed resins physically separate solid asphaltene particles from one another, hence alleviating the onset of precipitation. When oils are exposed to favourable precipitation conditions, resins desorb from asphaltenes and precipitation occurs (Subramanian 2016). Whilst most resins desorb from asphaltenes, some do not; hence resulting in co-precipitation (Speight 2014).

The types of trace metals found in asphaltenes are analogous with those observed in whole oils: Ni, V and Fe are all present (Fossen et al. 2007, Miller et al. 1999). Unlike whole oils, the concentrations of trace metals are much higher in extracted asphaltene fractions (Speight 2014). Yakubov et al. (2016) analysed 20+ heavy crude oils and concluded that asphaltenes can contain up to 1 wt% of Ni and V (total content). Yakubov et al. (2016) also determined that the concentration range of V in asphaltenes varied significantly across the studied oils (40–1650 ppm), as did the Ni concentrations (9–145 ppm). It is understood that trace metals in asphaltene fractions are either free-existing (not chelated to porphyrins) or are present in metalloporphyrin structures as shown previously in Figure 1.3 (Speight 2014, Gao et al. 2012, Miller et al. 1999). Trace metals are co-extracted alongside asphaltenes during precipitation; however as mentioned, the co-extraction mechanisms are not well understood.

Co-precipitation of non-asphaltenic compounds is of potential benefit to oil fingerprinting as additional chemical variations in the asphaltene fraction may allow for greater discrimination of oils when comparing asphaltenes.

1.6.4. Post-Precipitation Processing

It is common in petroleum studies to conduct post-precipitation processing of asphaltenes. Post-precipitation processes are conducted for two reasons:

1. To 'clean-up' precipitated asphaltenes by removing undesirable co-precipitates prior to analysis.
2. To further separate precipitated asphaltenes into 'sub-fractions', so that sub-fractions can be analysed and studied.

Some examples of post-precipitation processing have been highlighted below. It is important to consider the sheer number of steps involved in some of these processes; additional steps are not ideal when considering the application of asphaltenes in oil fingerprinting. Post-precipitation processing is therefore discussed from a forensic science perspective, with emphasis on why such processes are not suitable for use in forensic asphaltene precipitation methods.

Precipitated asphaltenes are often cleaned-up prior to analysis by solvent washing or rinsing. Jacobs and Filby (1983) precipitated asphaltenes from crude oil by addition of C₅ solvent. Washing was conducted by removing the C₅/maltene solution from the solid precipitated asphaltenes, then adding clean C₅ solvent back onto the asphaltenes. Washing was conducted to dissolve any undesirable, non-asphaltenic compounds that may have been present in the asphaltene fraction following initial precipitation with C₅ solvent. Non-asphaltenic compounds would dissolve into the clean C₅ solvent upon secondary addition;

hence removing undesirable compounds from the asphaltene fraction (Jacobs and Filby 1983).

Solvents are also used for the sub-fractionation of precipitated asphaltenes. Ascanius et al. (2004) precipitated C₇ asphaltenes from seven different crude oils. Solid C₇ asphaltenes were then separated into sub-fractions using N-methyl-2-pyrrolidone (NMP). The asphaltenes were separated into NMP-soluble and NMP-insoluble sub-fractions and analysed using size exclusion chromatography (SEC) to investigate the various molecular weight compounds present in each sub-fraction (Ascanius et al. 2004).

Chromatography has also been used to assist in the sub-fractionation of asphaltenes. After solvent washing (discussed previously), Jacobs and Filby (1983) used a complex sequential elution solvent chromatography (SESC) method to obtain ten different asphaltene sub-fractions for analysis. These sub-fractions were characterised using a series of analytical techniques, and it was found that the early-eluting fractions were smaller asphaltene species with few heteroatoms, whilst the late-eluting fractions were larger, more complex species with extensive heteroatomic content (Jacobs and Filby 1983).

Another common post-precipitation process for asphaltenes is soxhlet extraction. Trejo et al. (2004) used soxhlet extraction to further separate previously precipitated C₇ asphaltenes into three sub-fractions. Soxhlet extraction of asphaltenes was conducted for 4 hrs using a binary solvent at a 2:1 ratio (toluene/C₇). The insoluble solids remaining after extraction were collected as the first sub-fraction. The remaining solvent was evaporated off leaving behind the solids. These solids were added back to the soxhlet extractor, and extracted for another 4 hours using a different solvent ratio of 1:2 (toluene/C₇). The insolubles were collected as sub-fraction 2, whilst the soluble content was collected as sub-fraction 3. These three sub-fractions were then characterised using numerous analytical techniques. Soxhlet extraction has also been used to clean-up asphaltene fractions prior to analysis. Liao et al. (2009) used a

240 hr soxhlet extraction procedure with acetone solvent to clean-up C₇ asphaltenes prior to analysis, by removing soluble co-precipitates. Douda et al. (2008) also used soxhlet extraction to clean-up C₇ asphaltenes, however this time for 40 hr, and using C₇ solvent. Sarmah et al. (2010) and Yakubov et al. (2016) also used soxhlet extraction for the clean-up of asphaltenes, however this time for C₅ and C₆ asphaltenes, respectively. Both extraction processes were conducted using the same precipitation solvent used to obtain the respective asphaltenes (C₅ or C₆), and both extractions were stopped once the extraction solvent became colourless.

Although post-precipitation processes may be useful for mainstream petroleum applications, the vast majority of these processes are not viable in forensic investigations. Firstly, post-precipitation processes are time consuming which is not desirable during forensic casework (Stout and Wang 2016). Secondly, additional sample handling processes introduce unnecessary error in to analysis (CEN 2012). Thirdly, the asphaltene yields obtained from small oil samples (realistic to the sample sizes obtained in casework) are not sufficient to allow for further separation of asphaltenes into sub fractions prior to analysis. Asphaltenes yields are discussed in Chapter 3. Post-precipitation processes were therefore avoided during the development of a suitable forensic precipitation method (Appendix B).

1.6.5. Standardisation of a Forensic Asphaltene Fraction

It is safe to say that the chemical composition of asphaltenes studied throughout the literature is highly variable. The chemical variability of asphaltenes is attributed to three major factors:

1. Oils from different origins have naturally different chemical compositions.
2. Variable asphaltene precipitation conditions are used.
3. Variable post-precipitation processes are used.

These three factors attribute to the analysis of vastly different asphaltene fractions, which have very different chemical compositions. Despite this variability, subsequent fractions are still defined collectively as ‘asphaltenes’. Whilst the chemical composition of oils will always vary in forensic casework, it is possible to limit the variability of asphaltene fractions by standardising precipitation conditions and eliminating post-precipitation processing. Standardising precipitation variables would allow for consistent precipitation of asphaltenes from oils. As a consequence, differences observed when comparing different asphaltene fractions would be authentic. The removal of post-precipitation processes during forensic precipitation would reduce sample handling prior to analysis. An additional bonus would be the minimised time required for precipitation. Overall, the requirements that should be met for the development of an asphaltene method that may assist in oil fingerprinting are:

- Speed and efficiency.
- Repeatability.
- Capability to manage small volumes of oil.
- Asphaltene yields (should be as high yielding as possible).
- Simplicity (limited sample handling).

During my previous Honours research (Riley 2013), a precipitation method was developed in accordance to the aforementioned requirements. The developed method was fast and proved effective for obtaining sufficient asphaltene yields from small oil samples (realistic to case sample sizes). Preliminary repeatability tests were conducted during Honours using infrared (IR) spectroscopy (Riley 2013). IR was used as proof-of-concept that the developed precipitation method was appropriate for use in the development of asphaltene profiling methods in this PhD research. Post-precipitation processes were avoided during the

precipitation method. The asphaltene precipitation method developed during Honours and used in this PhD research is outlined in Appendix B.

1.7. Past and Current Asphaltene Research

This section aims to provide an overview of past and current asphaltene research applications in mainstream petroleum chemistry. This section also emphasises that the application of asphaltenes in oil fingerprinting has not yet been explored. Asphaltene research to date is primarily focused on providing information to the petroleum industry. The latter part of this section will focus specifically on petroleum chemistry research that has alluded to the probative value of asphaltenes. If asphaltenes do provide probative information, this information may be useful in oil spill investigations.

1.7.1. Mainstream Petroleum Chemistry Research

Asphaltene research in the petroleum industry is driven by the need for an improved understanding of asphaltenes to continually improve oil exploration, oil production and oil refining techniques (Sarmah et al. 2013, Al Humaidan et al. 2015, Pillay et al. 2011). A major current trend in asphaltene research has been the study of heavy crude oils (Pillay et al. 2011, Yakubov et al. 2016, Pomerantz et al. 2013). As natural light crude oil stocks are being depleted throughout the world there is an increasing reliance on heavy crude oil feedstocks (Trejo et al. 2004, Sarmah et al. 2013, Akbarzadeh et al. 2004). Heavy crude oils are higher in asphaltenic content, therefore have higher heteroatomic and trace metal contents (Pillay et al. 2011, Yakubov et al. 2016, Pomerantz et al. 2013). Asphaltene-rich feedstocks cause problems during oil production, transportation, and refining, as asphaltene precipitation becomes more prevalent (Trejo et al. 2004, Majumdar et al. 2013). Also, high amounts of heteroatoms and trace metals can negatively affect equipment (i.e., causes corrosion) and

interfere with solvents (i.e., deactivate hydro-treating catalysts during refining) during standard petroleum processes (Gould 1980, Pillay et al. 2011, Ancheyta et al. 2002). To combat the increasing number of problems arising due to the processing of heavier oil feedstocks, it has therefore been necessary to conduct asphaltene research (Trejo et al. 2004, Sarmah et al. 2013). Some studies addressing heavy feedstocks issues are highlighted in Table 1.2. A fundamental approach to combating new and complex problems associated with asphaltenes is to better understand asphaltene structures. Understanding asphaltene structures allows for the application of better refining techniques for high asphaltenic oils, and can also help refineries produce better petroleum products obtained from heavier oils (Coelho et al. 2007, Pillay et al. 2011, Al Humaidan et al. 2015). Some studies of asphaltene structures are highlighted in Table 1.2.

1.7.2. Research Alluding to the Probative Value of Asphaltenes

It is clear that the focus of asphaltene research is primarily in the petroleum industry; this poses a challenge when considering the investigation of a new asphaltene application in forensic science. Some studies have alluded to the potential probative value of asphaltenes which may provide a foundation from which the application of asphaltenes in oil fingerprinting may transcend. This section investigates the literature with the aim to identify studies that allude to the probative value of asphaltenes. Specific components of asphaltenes that may be probative were identified as well as common analytical instrumentation used to analyse asphaltenes. The choice of target components and analytical instrumentation applied in this research not only stems from consultation of the literature, but also from past Honours research (Riley 2013). Some asphaltene components and instrumentation proved promising during Honours therefore a thorough investigation of these promising chemical components and instrumentation was required in this PhD research.

Table 1.2: An outline of asphaltene research applications in the petroleum industry.

Research Field	Authors	Research Objectives and Applications
Petroleum Geochemistry/ Oil Exploration	Ma et al. 2008	The determination of oil source rock is critical in oil exploration for locating potential oil producing regions. The aim of this study was to determine if the analysis of ruthenium ion-catalyzed oxidation asphaltene products could be used for source rock correlations.
Petroleum Geochemistry/ Oil Exploration	Xiong and Geng 2000	Natural biodegradation of oils is problematic for correlating oil to source rock as conventional biomarkers (steranes and hopanes) are affected by weathering and cannot be analysed. This study investigated the use of carbon isotopes from asphaltene pyrolysates for application in oil-source rock correlations of biodegraded oils.
Oil Production	Pomerantz et al. 2013	The gradient of oil in a reservoir is important in oil production. The lighter oil at the top of the reservoir has lower asphaltene concentrations and is the most sought after oil. This study aimed to determine if the molecular composition of asphaltenes also differed across the gradient of an oil well by analysing the sulfur content of asphaltenes.
Oil Refining	Akbarzadeh et al. 2004	Prior to specific heavy oil refining processes, asphaltenes are precipitated and removed, leaving a lower viscous oil fraction that is more suitable for refining. This study aimed to determine a more accurate asphaltene precipitation model to improve purposeful precipitation during these refining processes.
Oil Refining	Al Humaidan et al. 2015	Thermal cracking is a process undertaken during oil refining, to upgrade heavy oil and bitumen to more refined petroleum products. This study aimed to determine the effects of thermal cracking on asphaltene molecules to help oil refiners elucidate the best way of dealing with heavy oil feedstocks.
Oil Refining	Ancheyta et al. 2002	Hydro-treating is a refining process that removes impurities such as heteroatom and trace metals from oils. Heavy oils feedstocks present issues during refining due to high asphaltene compositions; asphaltenes deactivate hydro-treating catalysts. Asphaltenes from crude oils were structurally characterised to help understand how to design more efficient hydro-treating catalysts that are not prone to deactivation.
Oil Refining	Pillay et al. 2011	Oils containing high metal concentrations can be problematic during refining; hence, metals need to be removed. Metalloporphyrins are the primary focus when removing metals in refining however, this study highlights the presence of free existing (non-porphyrin) metals alongside metalloporphyrins. This may change the way oils are treated when removing metals.

Prior to discussion, it must be made clear that analytical methods used in petroleum chemistry (both currently and in the past) cannot simply be transposed to forensic science. Careful considerations must first be made to ensure the suitability of methods for application in oil fingerprinting. Section 1.9 discusses the ideal requirements for a forensic method.

1.7.2.1. Organic Research

Organic Bonds

The use of IR spectroscopy in asphaltene research is extensive, particularly for the identification of asphaltene structures (Gawel et al. 2014, Coelho et al. 2007). IR spectroscopy identifies the vibration of molecular bonds; each bond type (or functional group) is represented by a characteristic vibrational wavenumber (cm^{-1}) (Pavia and Lampman 2001). Characteristic bond vibrations are therefore useful in identifying the structural features of asphaltenes, subsequently helping to improve refinery techniques and geochemical comparisons (Asemani and Rabbani 2015, Gawel et al. 2014, Coelho et al. 2007).

Gawel et al. (2014) studied nine different crude oils as well as their subsequent saturate, aromatic, resin and asphaltene (SARA) fractions using a range of analytical techniques including Fourier Transform Infrared (FTIR) spectroscopy. Gawel et al. (2014) aimed to better understand oil-water emulsions and the oil fractions that may contribute to the occurrence of emulsions. Of all SARA fractions, the asphaltenes were found to be most variable between oils when comparing IR spectra. Although the IR spectra of resins were similar to asphaltenes, the peak intensities and peak widths were more pronounced in the asphaltene spectra. As a result, a greater structural variance was observed in the asphaltene fraction of oil as compared to the saturate and aromatic fractions that are currently targeted in oil fingerprinting. The variances in asphaltenes observed by Gawel et al. (2014) were promising for this PhD research as it showed that asphaltenes are potentially probative with

regards to their structure, and that IR spectroscopy was a suitable technique for obtaining such probative information from asphaltenes (Gawel et al. 2014).

Asemani and Rabbani (2015) used IR spectroscopy to analyse and compare asphaltenes from four different oils. Asemani and Rabbani (2015) used known geochemistry techniques for source correlation (carbon isotopic ratios and GC analyses) to first determine the genetic relationships between the four oils through comparison to source rock. These four oils were then compared to one another using asphaltene IR spectra to determine if the same genetic relationships could be derived as previously observed with known geochemistry techniques. A range of indices that corresponded to IR peaks for aliphatic and aromatic bond types were calculated and used for comparison. In conclusion, the study by Asemani and Rabbani (2015) revealed that the same genetic relationships derived from known geochemistry techniques could also be independently derived through IR analysis of asphaltenes. Although the result only indicated a discrimination power of 50% when using IR spectroscopy, this does indicate that the direct comparison of asphaltenes based on IR spectra can be used to differentiate some oils. This study supports the opinion that IR asphaltene analysis may be probative and could assist in oil fingerprinting. The preliminary results obtained from Honours research also supported the use of IR for asphaltene analysis (Riley 2013). IR asphaltene analysis was therefore investigated during this PhD research.

Thermal Degradation

Pyrolysis has been used extensively for the study of asphaltenes to help understand the molecular structure of asphaltenes as well as to elucidate oil-source rock correlations in geochemical oil exploration (Galarraga et al. 2007, Liao et al. 2009, Sarmah et al. 2013, Doua et al. 2008, Al Humaidan et al. 2015, Makeen et al. 2015). The main advantage of pyrolysis is that it thermally break downs asphaltenes into smaller volatile compounds such

as PAHs which are easier to analyse and are well understood in petroleum chemistry (Speight 2014). As previously explained, volatile compounds are also targeted in the CEN method; therefore, if the same volatiles can be generated from the pyrolysis of asphaltenes, this could prove extremely useful if applied to oil fingerprinting (CEN 2012). Some past studies are highlighted below with particular emphasis on the potentially probative compounds that are generated from asphaltene pyrolysis.

Oil–source rock correlation is a common petroleum geochemistry technique applied during petroleum exploration to identify oil producing regions (Curiale 2008). Chemical information obtained from oils is compared to potential source rock to determine possible genetic relationships (Curiale 2008). Oil-source rock correlation often involves GC analysis and comparison of volatile compounds, akin to current oil fingerprinting practice. Recent advancements in oil-source rock correlations however involve the use of asphaltenes as source correlation tools; some studies are highlighted in Table 1.2 (Ma et al. 2008, Xiong and Geng 2000). Crude oil asphaltenes are believed to be soluble kerogen, and have therefore been identified as a valuable oil fraction for comparison to kerogen source rock (Béhar and Pelet 1985, Liao et al. 2009, Sarmah et al. 2013). The use of asphaltenes for source correlation is of interest to oil fingerprinting, particularly correlations which involve the pyrolysis of asphaltenes.

Galarraga et al. (2007) and Makeen et al. (2015) pyrolysed asphaltenes, and through subsequent GC analysis (Py-GC), successfully correlated questioned oils to known source rocks. Of particular interest were the asphaltene pyrolysates used for correlations. Makeen et al. (2015) successfully correlated oils to source rock using aliphatic, aromatic and sulfur asphaltene pyrolysates. From an oil fingerprinting perspective, the successful application of asphaltene pyrolysis in oil–source rock comparisons is interesting. Instead of obtaining an oil fingerprint that is exclusively representative of volatile oil fractions, an asphaltene fingerprint

(or profile) may also be provided as additional information to assist in oil spill investigations. It is therefore imperative that the applicability of asphaltene pyrolysis in oil fingerprinting is thoroughly investigated.

Oudot and Chaillan (2010) were the first to explore the potential application of asphaltene pyrolysis in oil spill investigations. A heavily weathered oil spill residue originating from the *Amoco-Cadiz* vessel was compared to un-weathered source oil obtained directly from the *Amoco-Cadiz* vessel. Saturate and aromatic fractions were extracted from both the weathered residue and the un-weathered source oil, and analysed using GC-FID. The GC-FID profile of the weathered residue was severely degraded, and was therefore not comparable to the un-weathered source oil. In an attempt to gain useful information from the weathered residue, the asphaltene fraction was precipitated and then pyrolysed at 320°C. The hexane-soluble component of the asphaltene pyrolysates were then extracted and analysed using GC-FID. Oudot and Chaillan (2010) concluded that the GC-FID profile of asphaltene pyrolysates from the weathered residue was similar to the GC-FID profile of the volatile fraction of the source oil. When comparing the two profiles however, there are in fact noticeable differences. For example, the asphaltene pyrolysate profile expressed much higher intensities of C₈–C₁₃ (in relation to the remaining profile) as compared to the volatile profile. Furthermore, and as discussed below, the degree of error associated with comparing two profiles generated from samples which have undergone completely different sample preparations is not suitable for forensic application. Whilst Oudot and Chaillan (2010) have provided preliminary results that demonstrate the potential applicability of asphaltenes in oil spill investigations, there are limitations to the method proposed when considering its application in everyday oil fingerprinting casework. Oudot and Chaillan's method is not time efficient and it required considerable sample preparation prior to analysis, which introduced potential error into the analysis. A new forensic method must be developed that utilises a

pyrolysis unit attached to a GC-MS to reduce sample handling and speed up the analysis. Another limitation to the method proposed by Oudot and Chaillan is the lack of repeatability data which makes it impossible to gauge the associated error of the method. Furthermore, the comparison conducted by Oudot and Chaillan (2010) between the asphaltene pyrolysate GC-FID profile and the volatile GC-FID profile does not account for potential errors associated with sample preparation. Both oil samples were not treated the same prior to analysis; hence there was no accountability for associated variability that may have been introduced during the preparation of both samples. In order to apply asphaltene pyrolysis in oil fingerprinting, it would be preferred to pyrolyse asphaltenes from both the oil spill and potential source oils. The subsequent asphaltene pyrolysates would then be compared to ensure a likewise comparison. The forensic transposition of Pyrolysis-Gas Chromatography-Mass Spectrometry (Py-GC-MS) into oil spill investigations is investigated in this PhD research.

Thermogravimetric analysis (TGA) has also been successfully used to analyse asphaltenes and compare oils based on asphaltenes. Sarmah et al. (2010) compared oils using TGA data obtained from respective asphaltene fractions to gauge the thermal behaviours of asphaltenes. Three asphaltene fractions were obtained, each from different oils. Differences were observed when comparing TG profiles (temperature range of profiles: 80–600°C) obtained from the three asphaltene fractions. Mass losses were observed at different temperatures for the different asphaltene fractions. Furthermore, the total percentage weight loss was also different across the three asphaltene fractions. TGA may also provide probative information that may assist in oil fingerprinting, particularly for the elimination of dissimilar oils based on mass loss differences in asphaltenes. TGA was investigated in Chapter 5.

Heteroatomic Content

Elemental analysis (EA) is perhaps the most commonly applied instrumentation for determining S, O and N compositions in asphaltenes (Leyva et al. 2013, Gawel et al. 2014, Ancheyta et al. 2002). The potential probative value of asphaltene heteroatoms was observed in the three studies below.

Leyva et al. (2013) used EA to determine the S content of asphaltenes extracted from a range of different American Petroleum Institute (API) gravity crude oils. Leyva et al. (2013) concluded that increased S concentrations in asphaltenes were correlated with decreasing API gravity oils; lighter oils had less S than heavier oils. Comparing the S content of asphaltenes could be very useful when considering the analysis of different oil types, such as HFOs and light crude oils that may have very different API gravity.

As well as FTIR analysis, Gawel et al. (2014) also used EA to analyse nine whole oils as well as their respective SARA fractions. The results revealed that the asphaltene fractions of these nine oils varied in O content from 2–14 wt%. N content also varied from 0.5–1.5 wt%, whilst the S content was highly variable from 0.5–10.5 wt% (Gawel et al. 2014). Wt% values of O, N and S content in asphaltenes could provide probative information in oil spill investigations. Wt% values would prove most useful for exclusionary purposes; asphaltenes with different heteroatomic contents may help rapidly exclude non-related oils in oil spill investigations.

Ancheyta et al. (2002) characterised the asphaltene fractions of three different crude oils to aid in the development of suitable hydro-treating catalysts for heavy crude oil refining. S, O and N content were determined using EA along with H and C content, and subsequent ratios (O/C, N/C, S/C) were calculated for comparison. S content varied significantly (3.20–8.25 wt%) whilst minor variations were observed in the O content (0.62–0.97 wt%). N content was not variable (1.32–1.33 wt%). The most variance between asphaltenes was

observed when comparing S/C ratios (0.014–0.038); smaller variations were observed when comparing N/C ratios (0.013–0.014) and O/C ratios (0.005–0.009) (Ancheyta et al. 2002). Heteroatomic ratios of asphaltenes may therefore provide additional probative information in oil spill investigations instead of relying solely on the comparison of the wt% values of asphaltene heteroatoms.

Isotopes

The analysis of asphaltene ^{13}C isotopic ratios has proven applicable in geochemistry for the source correlation of biodegraded oils (Xiong and Geng 2000). Xiong and Geng (2000) focused specifically on the analysis of the ^{13}C values of *n*-alkanes in asphaltene pyrolysates for use in the source correlation of biodegraded oils. The results revealed that the ^{13}C profiles obtained through Gas Chromatography-Isotope Ratio Mass Spectrometry (GC-IRMS) analysis were not significantly different from those obtained for ^{13}C profiles of traditional *n*-alkane markers (non-asphaltenic and prone to weathering) in non-biodegraded oils. In conclusion, asphaltene ^{13}C isotopes may not suffer from weathering effects, and asphaltenes may therefore prove highly probative in cases where heavily weathered oils are encountered.

Asphaltene isotope ratios have also proven useful for determining the source of unknown tar balls found on coastal shorelines (Hartman and Hammond 1980, Macko and Parker 1983). Hartman and Hammond (1980) successfully used a range of isotope ratios to correlate the source of beach tars to a range of natural seepages, as well as to marine vessels which had transported foreign fuels throughout the region of interest. C isotopes specifically, were successful in differentiating seepage oils from foreign oils (Hartman and Hammond 1980). The differentiation of oils based on asphaltene isotopes was achievable due to the very different isotopic ratios of the foreign oils and the natural seepage oils. Isotope ratios of

asphaltenes may be less probative when comparing oils from similar regions; however isotopes should still be investigated for applicability in oil spill investigations.

1.7.2.2. Inorganic Research

Trace Metals (Ni and V)

Yakubov et al. (2016) used Atomic Absorption Spectroscopy (AAS) to compare 20 heavy crude oils using V/ Ni ratios of asphaltenes. All of the studied oils were sourced from a similar geographic region in western Russia. The aim was to determine trends in metal content of the heavy crude oils so that better predictions could be made during the removal of metals in oil refining. V/Ni ratios were calculated for each asphaltene fraction using the V and Ni concentrations determined by AAS. V/Ni ratios were compared between oils to observe trends in metal content (Yakubov et al. 2016). The results revealed significant variations between crude oils when comparing the V/Ni ratios of asphaltenes. V/Ni ratios ranged from 1.1 to 20.9 (Yakubov et al. 2016). Leyva et al. (2013) also used AAS to determine Ni and V content in asphaltene fractions from a range of crude oils. Leyva et al. (2013) specifically analysed five crude oils of different API gravity and compared the asphaltene properties of these oils including the metal content. Leyva et al. (2013) concluded that heavier crude oils with lower API gravity contained higher concentrations of Ni and V as opposed to lighter crude oils with higher API gravity.

In the two aforementioned studies, the analysis of Ni and V content in asphaltenes proved to be potentially probative. The Ni and V content of asphaltenes was capable of differentiating oils from one another (Yakubov et al. 2016, Leyva et al. 2013). If applied to oil fingerprinting, the Ni and V content of asphaltenes could prove useful for exclusionary purposes, as well as for providing information that may be used in collaboration with other results to support the identification of oil.

1.8. Scope of Research

This section discusses the numerous avenues available for research in the application of asphaltenes in oil fingerprinting, and identifies the specific avenue that this PhD research has taken. The application of asphaltenes in oil fingerprinting was a new endeavour for both asphaltene and oil fingerprinting research. As a consequence, there was a substantial range of research avenues that may have been explored during this PhD research.

The first consideration was the standardisation of an asphaltene precipitation method that was suitable for oil fingerprinting. In order to thoroughly optimise an asphaltene precipitation method, a dedicated research project would have been required. Each precipitation variable would need to be critically tested to determine the most optimum conditions for forensic precipitation. A forensic precipitation method was developed during Honours research on the basis of preliminary testing of precipitation variables and general consultation of the literature (Appendix B). The precipitation method proved fit for oil fingerprinting during Honours, and adhered to the requirements of a forensic method (Riley 2013). As a result, the precipitation method developed during Honours was again used in this PhD research for obtaining asphaltenes for analysis. Although the developed precipitation method could be applied operationally as it exists, further optimisation may be beneficial to ensure that the fastest, and highest yielding method is available for casework application. The main priority however, when delving into this new field, was to critically assess whether or not asphaltenes offer probative information that may assist in oil spill investigations. It would not have been logical to invest a dedicated research effort into the development of a flawless precipitation method before first proving that asphaltenes do offer probative information. Further optimisation of the precipitation method has therefore been reserved for future work pending the outcomes of this research.

To determine the suitability of asphaltenes for oil fingerprinting, it was essential to test a range of analytical instrumentation that had shown promise based on past non-forensic research. Asphaltenes contain an abundance of potentially probative information which may be obtained through the analysis of organic bonds, thermal degradation properties, heteroatomic content, isotopes, and trace metal content. To ensure that the scope of this research fell within the desired time-frame, only the organic components of asphaltenes were targeted and tested, specifically the organic bonds and the thermal degradation of asphaltene organics. A number of methods were developed for a range of spectroscopic and thermal degradation instrumentation that had previously shown promise in non-forensic asphaltene research. As only a portion of the chemical composition of asphaltenes was investigated, future research will be necessary to investigate the heteroatomic, trace metal and isotopic contents of asphaltenes for application in oil fingerprinting. It is worth emphasising that although isotopes are organic components of asphaltenes, the analysis of isotopes was not a primary focus in this research. It is known that without the collaboration of secondary techniques, isotopic analysis is largely limited to exclusionary purposes in environmental forensic investigations (Philp 2015). Whilst this may be the case, there are still many different avenues to explore when considering the isotopic analysis of asphaltenes including the isotopic analysis of a range of elemental isotopes (C, N, O, S). The analysis of bulk asphaltene isotopes may also be assessed against the analysis of individual asphaltene compounds. A dedicated research project would be required to produce adequate data to determine the applicability of asphaltene isotopes in oil spill investigations. Preliminary bulk carbon isotopic ratio data was obtained out of interest during this research and supports an avenue for future isotopic research. The bulk carbon isotope analysis of asphaltenes is discussed in Chapter 9.

Another very important aspect to consider was the weathering of oils. Oil fingerprinting experts will be quick to note that the validity of any method designed for oil fingerprinting will rely on the ability of the method to analyse both un-weathered and weathered oils. Whilst it is acknowledged that weathering must be studied, asphaltenes from un-weathered oils must first be analysed to determine whether asphaltenes are in fact probative. By analysing un-weathered oils, there can be certainty in any differences observed when comparing asphaltenes, as differences will not be attributed to the weathering of asphaltenes. The differences can be attributed to chemical variations in asphaltenes themselves. Once suitable asphaltene profiling methods are developed, a range of asphaltenes from both weathered and un-weathered oils will then be required to gauge the suitability of methods for use in casework where weathered oils may be encountered. It is proposed in the literature that asphaltenes may exhibit a degree of resistance to weathering; asphaltenes may still weather but they are expected to weather much less than currently targeted oil fingerprinting volatiles (Lewan et al. 2014, Xiong and Geng 2000). This is an interesting incentive for future research as the ability to analyse and compare compounds that are more weathering-resistant would alleviate many problems associated with the interpretation of results from weathered oils.

It is also worth noting that, if the currently proposed hypothesis for asphaltenes being weathering resistant is disproved, asphaltene profiling will still be valuable to oil spill investigations. Asphaltene profiles will provide additional information to investigators that is currently not available regardless of the effects of weathering. In this PhD research, a single weathered oil sample was provided to obtain preliminary information on the performance of weathered asphaltenes when compared to un-weathered asphaltenes using developed asphaltene profiling methods.

The number of oils used for asphaltene precipitation and profiling was also a major consideration for the scope of this research. It was not possible to analyse asphaltenes from

hundreds of different oils, without first having developed the methods to do so. The development of proof-of-concept methods was therefore conducted using a relatively small sample-set of eleven oils from a broad range of different geographical regions. Spilt oil is not compared to all other oils in the world during casework, only to a limited number of suspect oils. Method development has therefore been conducted with the expectation that further optimisation will occur as the number of oils analysed increases over time. Consequently, new information provided by an increased number of oils will be used to adjust and optimise the developed methods as required. This approach is very similar to the CEN method in which constant amendments are made as further knowledge becomes available through research and casework experience. It is worth mentioning that during the blind study (Chapter 7), five additional oils that had not been analysed during method development were added to help test the reliability of asphaltene profile interpretation. It is also important to mention that the overall number of oils available for method development and the blind study was hindered due to the fact that crude oils are very difficult to obtain. However, for proof-of-concept, eleven oil samples were considered sufficient.

In summary, the scope of this PhD research is outlined as follows. An existing asphaltene precipitation method that has proved sufficient through preliminary testing was used to obtain asphaltenes from eleven un-weathered oils. The eleven oils were obtained from a range of different geographical regions, hence exhibited a range of different chemical compositions. This relatively small sample size of oils was considered sufficient for the development of proof-of-concept asphaltene profiling methods. Future profiling of asphaltenes from additional oils would be considered pending the results of this research. Asphaltenes were also precipitated from a single weathered oil sample for preliminary comparison. Numerous proof-of-concept methods were developed for the profiling of asphaltenes. The aim of developing these profiling methods was to determine if probative

information could be obtained from the asphaltene fraction of oil. Each of the developed methods was also compared to one another to determine which method provided the most probative information.

1.9. Research Aim and Research Questions

The aim of this research was to *determine if asphaltene profiling methods could be developed to provide probative information that may assist in oil spill investigations.*

It is important to emphasise that this research did not aim to calculate the discrimination power of the developed asphaltene profiling methods. Much larger sample sizes would be required to do so. Instead, asphaltene profiles obtained from each of the developed methods were compared to determine which methods offer the most probative information. It must also be emphasised that the information provided from asphaltene profiles is intended to assist in oil spill investigations, not to replace current oil fingerprinting practices. Asphaltenes have been studied herein to provide additional information to investigations from an oil fraction that is currently discarded.

In order to address the research aim, the following research questions needed to be answered:

1. *Does each asphaltene profiling method meet the requirements for a forensic method?*
2. *Which asphaltene profiling methods are most suitable for oil spill investigations?*
3. *Do the asphaltene profiling methods provide results which allow for reliable interpretation?*

To address Research Question 1, it is important to understand some basic requirements of forensic methods in general. Ideally, forensic methods should be:

- Readily available and cost-effective.
- Widely accepted in the scientific community.
- Non-destructive.
- Robust, and ideally fast.
- Capable of producing repeatable information.
- Capable of producing probative information.

(CEN 2012, ITOPF 2012)

When specifically referring to forensic methods for asphaltene profiling, it is important that the following requirements are met where possible. Forensic asphaltene profiling methods should be:

- Capable of analysing small sample sizes.
- Capable of analysing asphaltenes with little to no sample preparation (to avoid destruction or alteration of asphaltenes prior to analysis).

(CEN 2012)

The ability of each asphaltene profiling method to address the aforementioned requirements was both evaluated and discussed in Chapters 4 and 5. Some of the aforementioned requirements, such as the availability and cost of instrumentation, were discussed prior to the discussions of method development. By consulting the literature, as well as practicing environmental forensic laboratories such as the NSW OEH, it was possible to select instrumentation which best aligned with some of the specified requirements above. Other requirements however could not be gauged until methods were developed and tested.

For example, for some instrumentation, the ability to analyse small samples of asphaltenes could not be gauged until methods were created and results were interpreted. The development of each method was therefore dictated to best align with the requirements specified above.

Research Question 2 was addressed by comparing each of the developed asphaltene profiling methods to one another. Asphaltene profiling methods were compared based on the ability of each method to address the forensic requirements specified in Research Question 1. For example, two methods may both be readily available, cost effective, and non-destructive, however the repeatability and probative value of information produced from each method may differ. The suitability of each method was therefore gauged by determining which of the developed methods best addressed Research Question 1. The suitability of asphaltene profiling methods in relation to one another was also discussed throughout Chapters 4 and 5.

Research Question 3 was investigated in Chapters 6 and 7. To determine if the results from asphaltene profiling methods could be interpreted reliably, it was necessary to conduct a blind study. The blind study would involve profiling asphaltenes from a range of oils where the origin of the oils was unknown to the analyst. The removal of information regarding the origin of oils would remove bias associated with the interpretation of results. The origin of the oils would then be revealed at the conclusion of the blind study so that the reliability of interpreting asphaltene profiles could be accurately assessed. If the analyst could correctly differentiate oils from different origins whilst not knowing the origin of the oils, the interpretation of asphaltene profiles could be considered reliable. Furthermore, if the analyst could correctly identify two oils of common origin, this would also confirm the reliability of interpreting asphaltene profiles.

1.10. Research Outcomes

Given the magnitude of the global oil industry, and the inevitable occurrence of oil spills throughout the world, this research will have both national and international relevance (NOAA 2012). At the conclusion, this research aims to:

- Successfully develop asphaltene methods that provide probative information.
- Provide the environmental forensic science industry with knowledge and tested methods that allow for the consideration of asphaltene application in oil spill investigations. This research was conducted in collaboration with oil fingerprinting experts from the NSW OEH, Environmental Protection Science Branch which allowed for the direct exchange of information to industry.
- Provide a foundation for future research in this new field of asphaltene and oil fingerprinting research.

Chapter 2 - Materials and Methods

As described in Chapter 1, the forensic application of asphaltene profiling relies on suitable profiling methods being developed in conjunction with the standardisation of the asphaltene precipitation conditions. The development of the precipitation method and profiling method are interlinked and one cannot be developed without the other. This chapter details the asphaltene precipitation method used in this research. The asphaltene profiling methods developed during this research are also outlined herein.

2.1. Research Samples: Crude and Heavy Fuel Oils

Eleven oils were obtained for the development of asphaltene profiling methods. Eight of the oils were un-weathered crude oils from different geographical origins including Australia, South East Asia, North America and the Middle East. One of the oils was a weathered sub-sample of the Middle Eastern crude oil which was known to have undergone both evaporative and photo-oxidative weathering. The weathering process for the Middle Eastern crude oil is described in Section 2.12. The two remaining oils were HFOs. Both HFOs were the exact same oil but of different grade: one HFO was grade 380 (an uncut grade), whilst the other was grade 180 (cut with diesel). The geographical origin of the HFOs was unknown but was likely a blend of crude oils from numerous regions. It is also worth noting that two Australian crude oils (Australian 1 and Australian 2) were sourced from the same oil field; however, the Australian 1 oil was collected approximately 10 years prior to the Australian 2 oil. The details of all eleven oils are provided in Table 2.1. Throughout this thesis, each of the studied oils will be referred to by their corresponding abbreviations, as listed in Table 2.1.

Table 2.1: The eleven crude oils and HFOs analysed as part of the method development process. The geographical origin of each of the oils has been provided where possible.

Type of Oil	Geographical Region	Oil Abbreviation
Crude Oil	Middle Eastern	M. Eastern
	South Pacific	S. Pacific
	South East Asian 1	SE Asian 1
	South East Asian 2	SE Asian 2
	North American	N. American
	Australian 1	Aust. 1
	Australian 2 (same oil field as Australian 1)	Aust. 2
	Australian 3	Aust. 3
HFO 180 grade (cut with diesel)	Unknown	HFO (d/c)
HFO 380 grade (uncut)	Unknown	HFO (u/c)
Weathered Crude Oil	Middle Eastern - weathered (same crude oil as above)	M. Eastern (w)

Five additional oils were obtained after the development of the asphaltene methods. The details of these five oils were unknown at the time of analysis as they were analysed as part of a blind study (Chapter 7, Appendix C). The origins of these five oils are revealed in Chapter 7 following the discussion of the blind study results. In total, 16 different oils were therefore analysed for the development and testing of asphaltene profiling methods.

Although the geographical origin of spilt oil does not need to be determined in oil fingerprinting, the geographical origin of oils has been provided out of interest. The aim of oil fingerprinting is to determine if oil collected from an oil spill is the same or different to oil collected from suspected sources. If the geographical origin of oil happens to be identified as a part of the oil fingerprinting process then this information should be provided. This is especially true if oils from specific origins are known to possess unique chemical markers; for example, the C₃₀ oleanane hopanes found only in Nigerian crude oils (CEN 2012).

Some oils used in this research are from completely different geographical regions, whilst others are from very similar regions (Table 2.1). The geographical origins of the studied oils are provided primarily as general information to the reader to help gauge the probative value of asphaltene profiling methods. Although it was not the aim of this research

to determine the geographical origin of the studied oils, it will become apparent throughout the following chapters of this thesis that some of the developed methods can potentially provide this information.

2.2. Asphaltene Precipitation Method

As stated previously, the asphaltene precipitation method used in this research was developed during past Honours research (Riley 2013). The method development process employed in this earlier research is explained in Appendix B. It is acknowledged that the development of the precipitation method was not conducted as part of this PhD research; however, it is necessary to provide information regarding the method development process so that the reader can understand why certain precipitation parameters were adhered to for obtaining asphaltenes.

Asphaltene fractions were precipitated from oils using excess reagent grade C_5 at a 60:1 v/w ratio (solvent in mL: oil in g) at room temperature. The C_5 solvent was gently agitated as oils were added drop wise over a period of 20 min (Figure 2.1 (a)). The C_5 /oil mixtures were left to sit for 1 h at room temperature followed by centrifuging at 3000 rpm for 5 min using a Hettich Zentrifugen D- 7200 (*Hettich, Germany*). Asphaltene solids that adhered to the side of the centrifuge tubes (Figure 2.1 (b)) were separated from C_5 and oven dried at 105°C (Figure 2.1 (c)). C_5 asphaltenes were collected after oven drying and were stored in glass vials in a -20°C freezer prior to analysis. C_5 asphaltenes were used for the development of all asphaltene profiling methods. C_5 asphaltenes have therefore simply been referred to as ‘asphaltenes’ throughout the remainder of this thesis (apart from Appendix B).

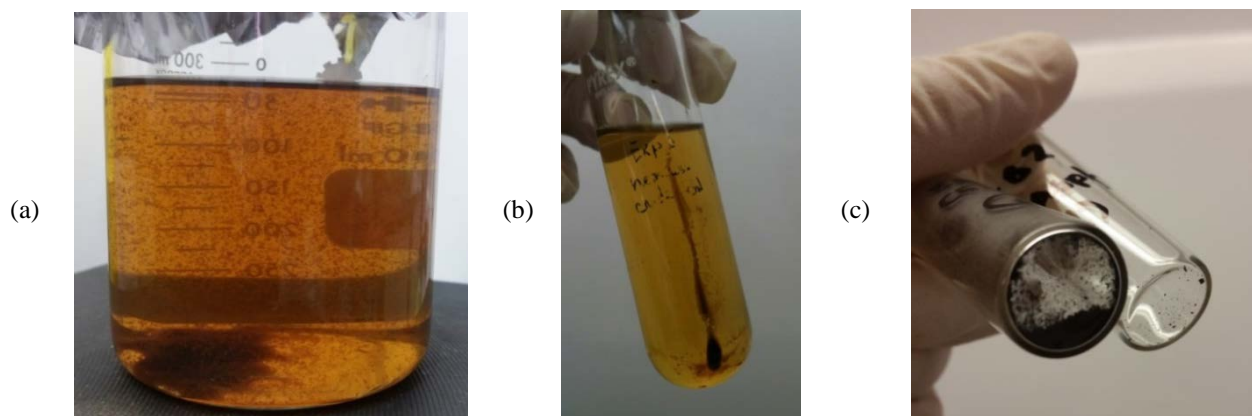


Figure 2.1: Visual representation of the asphaltene precipitation method: (a) precipitation occurring after addition of oil to excess C_5 solvent; (b) physical separation of asphaltenes from maltenes after centrifuging; and (c) solid asphaltenes after oven drying, ready for analysis.

2.3. Method Uncertainty

Throughout this research, asphaltenes were precipitated in replicate aliquots from single oil samples. For the majority of asphaltene methods, seven asphaltene aliquots were precipitated from both the HFO (u/c) and M. Eastern crude oil samples as a measure of method uncertainty. It is standard practice to analyse seven replicates from a single representative sample as a measure of method uncertainty. The use of replicates for measuring method uncertainty is defined in the *'Guidelines for the Validation and Verification of Quantitative and Qualitative Test Methods'* published October 2013 by the National Association for Testing Authorities (NATA); the national accreditation body for forensic laboratories in Australia (NATA 2013). For the remaining oils, asphaltenes were precipitated in duplicate; two aliquots from each of the oils. The analysis of duplicate aliquots provided a method to monitor the consistency of results across all asphaltenes, not just for the HFO (u/c) and M. Eastern asphaltenes. Duplicates also acted as an internal quality control during forensic comparisons – duplicates were treated as separate samples which should be indistinguishable from one another throughout the comparison. Asphaltenes were only precipitated once from the M. Eastern (w) oil due to the limited amount of oil available.

Chapters 3, 4, 5 and 7 provide further information on the number of replicates that were extracted and analysed for each of the oils.

2.4. Scanning Electron Microscopy

A Hitachi TM3030 Tabletop Scanning Electron Microscope (SEM) (*Hitachi, Japan*) was used to observe the microscopic morphologies of asphaltenes (Figure 2.2). A 12 mm conductive carbon tab (*ProSciTech, Australia*) was attached to a sample stage of similar diameter; solid, un-coated asphaltene particles were then placed on the carbon tab ready for imaging. Asphaltene particles were located via manual searching using Hitachi Tabletop Software (TM3030) in ‘Compo’ Image Mode. Representative particles were chosen for imaging.

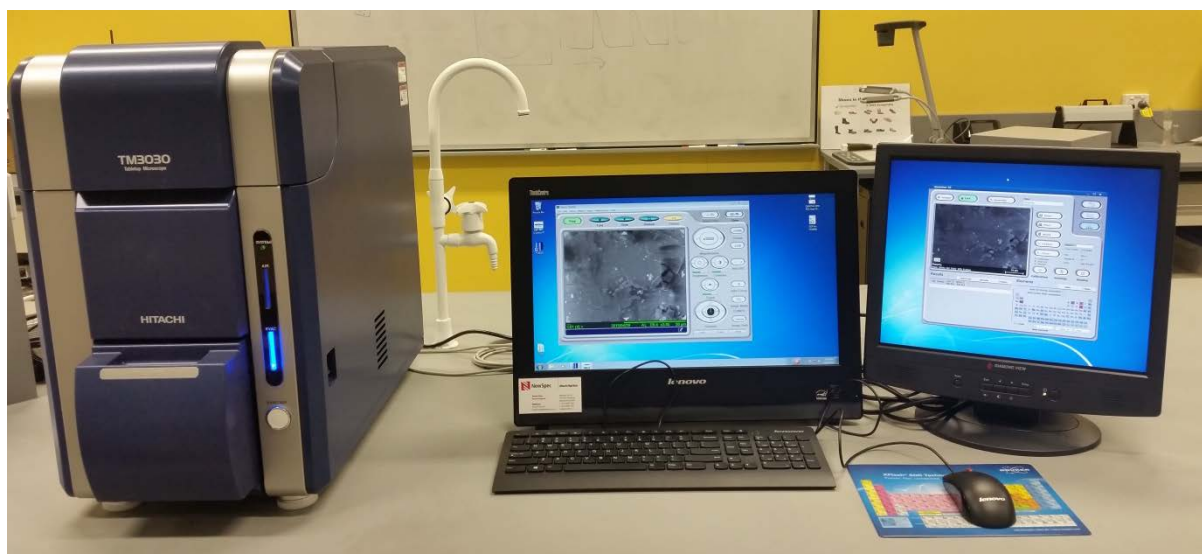


Figure 2.2: The Hitachi TM3030 Tabletop Scanning Electron Microscope used for asphaltene imaging.

Micrographs were obtained using a backscatter detector. Asphaltenes from each of the oils were imaged at 250x magnification, using an accelerating voltage of 15 kV and a working distance of 10.00 – 10.70 mm (depending on the specific sample analysed). 15kV

was used to allow for the option of both imaging and basic elemental analysis. The micrographs obtained from imaging are discussed in Chapter 3. Some basic elemental analysis was also conducted out of interest; however, this information did not prove useful and is not further discussed.

2.5. Attenuated Total Reflectance-Fourier Transform Infrared Spectroscopy

The Attenuated Total Reflectance-Fourier Transform Infrared Spectroscopy (ATR-FTIR) method developed for the analysis and comparison of asphaltenes is detailed below. For simplicity, the ATR-FTIR method will be referred to hereafter as the IR method.

2.5.1. IR Profiling of Asphaltenes

Asphaltenes were analysed on a Perkin Elmer Spectrum 400 FTIR/FT-NIR Spectrometer (*Perkin Elmer, Australia*), using an Attenuated Total Reflectance (ATR) attachment with a germanium crystal (Figure 2.3). A Perkin Elmer Infrared Spectrophotometer Polystyrene Calibration Film (*Perkin Elmer, USA*) was used as a reference material to ensure that the instrument was performing properly prior to analysis. A background spectrum was also collected and assessed prior to the analysis of each asphaltene sample.

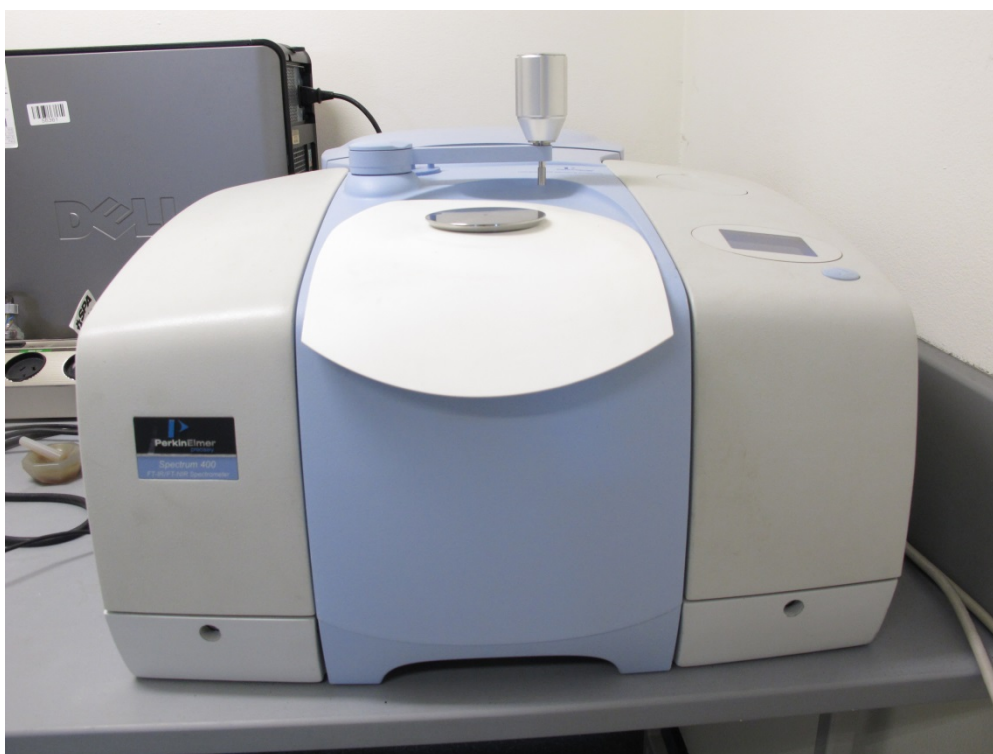


Figure 2.3: The Perkin Elmer Spectrum 400 FTIR/FT-NIR Spectrometer with an ATR attachment used for asphaltene profiling.

Asphaltene solids were analysed directly after oven drying. As determined during Honours, it is recommended that ~2.2–2.5 mg of asphaltenes are provided for successful IR analysis (Appendix B, Riley 2013). It is important to note however, that this amount is provided simply as a guideline. Depending on the malleability of asphaltenes, it is possible to analyse asphaltenes weighing <2 mg. Solid, crystalline asphaltenes were ground using a mortar and pestle to obtain sufficient contact with the crystal. Resinous asphaltenes did not require grinding. The distinction between crystalline and resinous asphaltenes is discussed in Chapter 3. IR spectra were obtained in transmission mode (%T) with a scan range of 4000–650 cm^{-1} and a resolution of 1 cm^{-1} . Prior to analysis, all spectra were baseline corrected (BLC) and normalised using Perkin Elmer Spectrum software, version 6.3.4 (*Perkin Elmer, Australia*). IR spectra were not ATR-corrected prior to comparison. ATR-correction is only

necessary if spectra generated using an ATR attachment are compared to spectra that were generated without an ATR attachment. All IR spectra in this research were obtained using an ATR attachment; hence ATR-correction was not required.

2.5.2. Visual Comparison of IR Spectra

As discussed in Chapter 1, the visual comparison of chromatograms in CEN oil fingerprinting involves comparing chromatograms from spilt oil to chromatograms from suspect oils (CEN 2012). If a spilt oil chromatogram visually overlays with a suspect oil chromatogram, these two oils cannot be differentiated (CEN 2012, Christensen and Tomasi, 2007). In this research, the visual comparison of asphaltene IR spectra was conducted using the same principles abided by in the CEN method. Two specific regions of the IR spectra were chosen for visual comparison: Region 1 ($650\text{--}930\text{ cm}^{-1}$) and Region 2 ($1260\text{--}1520\text{ cm}^{-1}$). The rationale for using these two regions is discussed in Chapter 4 along with the results of visually comparing Regions 1 and 2.

2.5.3. Comparison of Peak Height Ratios

For the calculation of peak height ratios, spectra were converted to absorbance. Peak height ratios were calculated from the IR spectra of asphaltenes. The comparison of peak height ratios between asphaltenes was analogous to the manner in which the CEN method compares DRs generated from GC-MS data (CEN 2012). In short, an acceptance or threshold level was determined for peak height ratios based on the repeatability data obtained from the seven replicate HFO (u/c) and M. Eastern asphaltenes. The aim was to set one threshold value that could be used for all peak height ratio comparisons, rather than to set specific acceptance levels for each ratio separately. The calculated threshold level is discussed in Chapter 4. Asphaltene duplicates were used as an internal quality control check of the

calculated threshold level (also discussed in Chapter 4). The process of comparing peak height ratios is outlined by considering the comparison of two separate asphaltene samples. Two asphaltene samples that need to be compared are analysed and the peak height ratios are calculated for each sample separately. The mean value and absolute difference of the two asphaltene samples are then determined for each peak height ratio. The relative difference is calculated by expressing the absolute difference as a percentage of the mean. The relative difference is then compared to the calculated threshold level. If the relative difference is higher than the threshold, the peak height ratios of the two asphaltene samples are considered different, and vice versa. Therefore, if all peak height ratios used for comparison fall within the threshold level, the asphaltenes (and subsequently the oils too) cannot be differentiated. If only one peak height ratio is higher than the threshold, the two asphaltene samples are considered to have different origins. The calculation and comparison of all peak height ratios is discussed in Chapter 4.

2.6. Fluorescence Spectroscopy

The fluorescence profiling method required optimisation of three parameters: (1) determining the most suitable solvent for dissolving C₅ asphaltenes prior to fluorescence analysis; (2) determining the optimum excitation wavelength through consultation of the literature; and (3) determining the optimum sample concentration for analysis. Chapter 4 has been reserved for a detailed discussion of how the optimum parameters for fluorescence profiling of asphaltenes were determined. The final fluorescence profiling method used for the analysis and comparison of asphaltenes in Chapter 4 is outlined below.

2.6.1. Fluorescence Profiling of Asphaltenes

Asphaltene solutions were prepared to a concentration of 10 ppm and then diluted to approximately 2.5 ppm in High Performance Liquid Chromatography (HPLC) grade tetrahydrofuran (THF). The asphaltene/THF solution was analysed in fluorescence emission mode using a Shimadzu RF-5301PC Spectrofluorophotometer (*Shimadzu, Australia*) (Figure 2.4), with an excitation wavelength of 275 nm and an emission range of 285–540 nm. The 275 nm excitation wavelength was chosen to align with the excitation wavelengths commonly used for the fluorescence analysis of asphaltenes in the petroleum industry (Mullins 2010). The 285–540 nm emission range was chosen to avoid overlap with the 275 nm excitation band and to cut out resonance beyond 540 nm. Both excitation and emission slit widths were 5 nm, and the sample interval was set to 1 nm. Fluorescence parameters were controlled using Shimadzu RFPC Fluorescence Spectroscopy Software for RF-5301PC (Version 2.04) (*Shimadzu, Australia*).

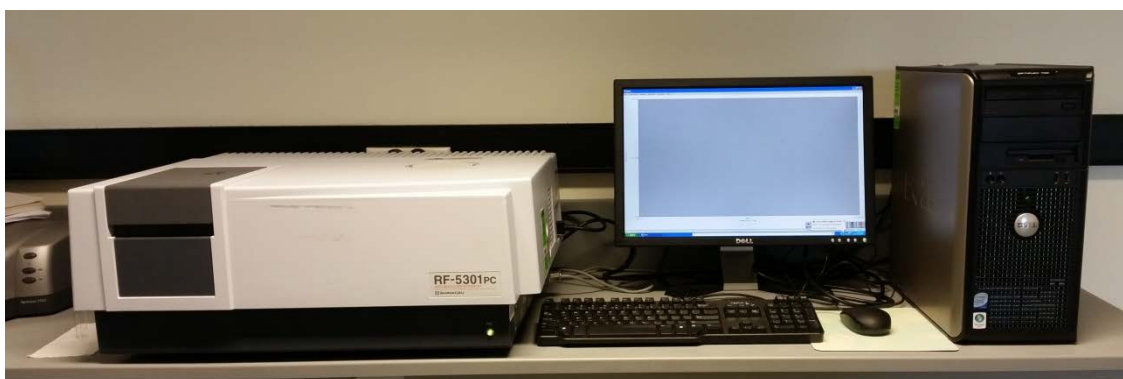


Figure 2.4: The Shimadzu RF-5301PC Spectrofluorophotometer used for asphaltene profiling.

2.6.2. Visual Comparison of Fluorescence Spectra

Fluorescence data was transferred to Microsoft Excel (2010) and each asphaltene fluorescence spectra was normalised to 390 nm. For visual comparison, the data was expressed in a scatter plot generated using Microsoft Excel (2010). Fluorescence spectra of

asphaltenes were compared by assessing the maximum emission wavelength of each asphaltene sample, as well as the overall shape of the spectra. The comparison of asphaltene fluorescence spectra is discussed in Chapter 4.

2.7. Ultraviolet-Visible Spectroscopy

A UV-2600 Ultraviolet-visible (UV-Vis) Spectrophotometer (*Shimadzu, Australia*) was used to measure the absorption of UV-Vis radiation in C₅ asphaltenes. UV-Vis absorption spectra were obtained in single scan mode (from 800–200 nm) with a sampling interval of 2 nm. C₅ asphaltenes were prepared to a concentration of 10 ppm in HPLC grade THF for analysis. The spectrophotometer employed in this research was a double beam system which allowed for the reference cuvette (filled with THF) and sample cuvette (filled with asphaltene/THF solution) to be exposed to the same source of radiation.

2.8. Evolved Gas Analysis-Mass Spectrometry

Evolved Gas Analysis-Mass Spectrometry (EGA-MS) parameters used in this study for the analysis of asphaltenes were chosen based on the EGA-MS technical note provided by Frontier Laboratories (2012) for the analysis and comparison of natural and synthetic fibres. This technical note uses the same Frontier Laboratories Multi-Shot Pyrolyzer available for this research (as specified below).

2.8.1. EGA-MS Profiling of Apshaltenes

Solid asphaltenes were analysed using a Shimadzu GC-MS QP2010 Ultra Gas Chromatograph Mass Spectrometer (*Shimadzu, Australia*) equipped with an online Frontier Laboratories Multi-Shot Pyrolyzer EGA/PY-3030D (*Frontier Laboratories, Japan*) (Figures 2.5 and 2.6).

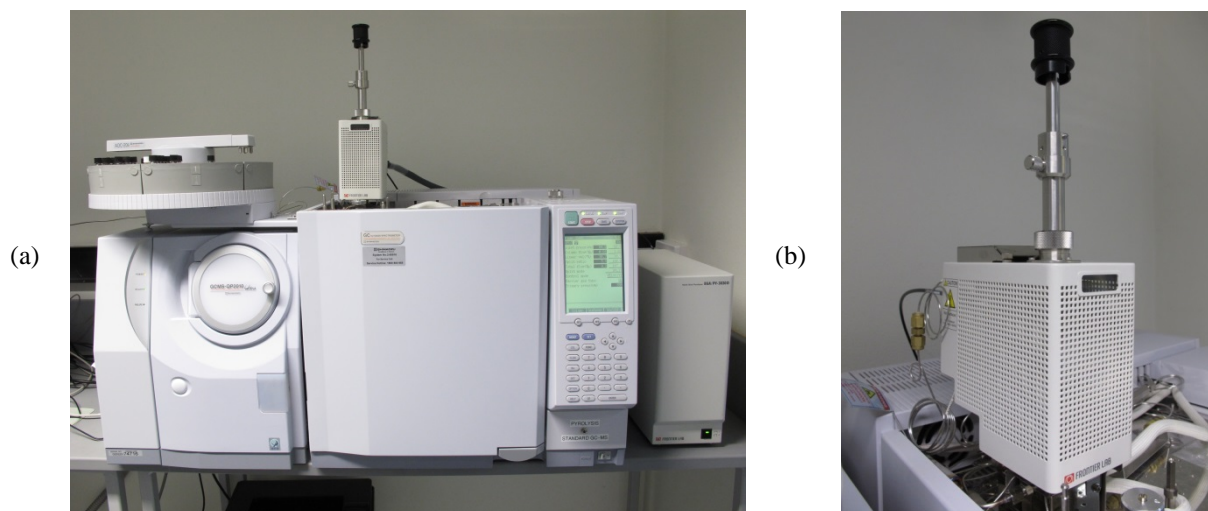


Figure 2.5: (a) The Shimadzu GC-MS QP2010 Ultra Gas Chromatograph Mass Spectrometer with an online Frontier Laboratories Multi-Shot Pyrolyzer EGA/PY-3030D; and (b) the Frontier Laboratories Multi-Shot Pyrolyzer EGA/PY-3030D loaded with an asphaltene sample (the sample is positioned outside the furnace).

Prior to the analysis of asphaltenes, a blank (no sample loaded) was analysed to ensure no carry-over occurred between analyses. Approximately 100–500 μg of solid asphaltenes were added to a 50 μL Disposable Eco-Cup (*Frontier Laboratories, Japan*) and attached to an Eco-Stick SF (*Frontier Laboratories, Japan*). The Eco-stick was then inserted in the Double Shot Sampler, which was attached to the pyrolysis unit in the sample cup standby position (with the sample cup loaded above the furnace, not inside the furnace). When MS analysis was initiated, the sample cup was released from the Double Shot Sampler and dropped into the furnace for the duration of the analyses. Evolved gas analysis was conducted from 100–1000°C at 20°C/min with acquisition ceasing immediately upon reaching 1000°C. The interface temperature between the pyrolysis unit and the GC injector port began at 200°C at the start of acquisition and remained 100°C above the furnace temperature until reaching and holding at 300°C. The pyrolysis furnace temperature and the interface temperature were set using the EGA/PY-3030D Control software (Ver.1.60) (*Frontier Laboratories, Japan*).

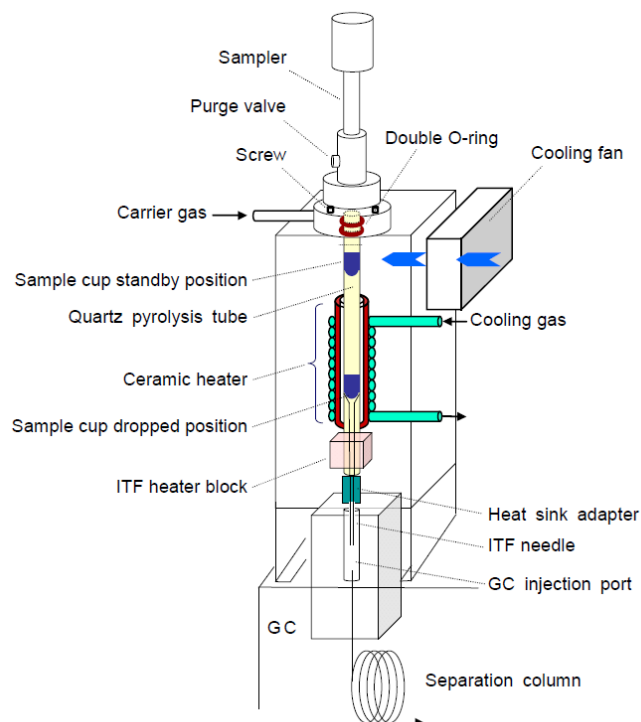


Figure 2.6: A schematic of the Frontier Laboratories Multi-Shot Pyrolyzer (Model EGA/PY-3030D). The sample cup standby position allows the sample to remain outside of the furnace (ceramic heater) until analysis commences, at which time the sample cup is dropped into the furnace (EGA-MS) or lowered into the furnace (Py-GC-MS). Figure sourced from the Multi-Shot Pyrolyzer Model EGA/PY-3030D Operation Manual (Ver. 1.21).

The GC-MS was controlled using GCMS Real Time Analysis Software (Shimadzu GCMSsolution Version 4.20) (Shimadzu, Australia). It should be noted that although GC separation is bypassed during EGA-MS (pyrolysates flow directly from the pyrolysis unit to the MS), GC parameters were still maintained to ensure the uninterrupted flow of pyrolysates to the MS. The GC injector was set to 300°C with a 100:1 split ratio. An Ultra Alloy EGA capillary tube (2.5 m length, 0.15 mm ID) with a deactivated hollow metal stationary phase was used (Frontier Laboratories, Japan). Helium gas was used as the mobile phase, with a column flow rate of 0.84 mL/min. The GC oven temperature program was set to a constant 300°C for the duration of analyses. The transfer line temperature (from GC to MS) was also 300°C. The MS ion source temperature was 250°C, with electron impact set to 70 eV for ionisation. Full scan analysis was conducted from m/z 35 to m/z 550. GC-MS Post Analysis

Software (Shimadzu GCMSsolution Version 4.20) (*Shimadzu, Australia*) was used to extract selected ion profiles.

2.8.2. Visual Comparison of Thermograms and Mass Spectra

The Frontier Laboratories (2012) technical note compares forensic samples visually based on: (1) the shape of thermograms; and (2) the average mass spectra calculated for each thermogram peak. A similar approach was adopted in this research for the forensic comparison of asphaltene thermograms and mass spectra. Prior to comparison the x-axis values were converted to temperature instead of retention time (RT) (as expressed by data extracted from GC-MS Post Analysis Software). The temperature axis was calculated in Microsoft Excel (2010) using the temperature rate outlined above for acquisition (100–1000°C/min). Asphaltene thermograms were compared visually to one another along with the comparison of average mass spectra calculated for each thermogram peak. The comparison of asphaltene thermograms and average mass spectra is discussed in Chapter 5.

2.9. Thermogravimetric Analysis

Thermogravimetric Analysis (TGA) was conducted at the Western Sydney University Advanced Materials Characterisation Facility (AMCF). The analytical method below was proposed on the basis of previous work conducted by the AMCF on similar compounds using the same instrument (R. Wuhler 2016, personal communication, 26 April). As a result, method optimisation was not required.

2.9.1. TGA-DSC Profiling of Asphaltenes

Solid asphaltenes were analysed using a NETZSCH STA 449C Jupiter thermos-balance (NETZSCH, Australia) in Thermogravimetric Analysis - Differential Scanning Calorimetry (TGA-DSC) mode (Figure 2.7).



Figure 2.7: The NETZSCH STA 449C Jupiter Thermos-Balance used for asphaltene profiling.

DSC analysis was conducted simultaneously with TGA; however the DSC profiles did not provide probative information, hence are not further discussed. The calibration range of the instrument balance was between 0.001–5000 mg; hence, small samples could be analysed. To be consistent, all asphaltene samples analysed were weighed as close to 1 mg as possible. Asphaltenes were weighed in aluminium pans and placed on the sample carrier next to the reference pan (an empty aluminium pan). The temperature program used for analysis was 20–590°C/10°C per min. The temperature program was kept below 600°C due to the high S content of some asphaltenes in the sample-set. There is a potential for adverse S

reactions when exceeding 600°C, which can damage the instrument detector. Asphaltenes were analysed in an inert atmosphere, using nitrogen at 100 mL/min, and argon as a protective gas at 25 mL/min. Proteus Software (version 6.1) was used to control instrument parameters.

2.9.2. Visual Comparison of Thermograms

NETZSCH Proteus Thermal Analysis software (version 6.1) was used to calculate mass changes in asphaltene thermograms observed throughout the analytical temperature range. The mass change values were calculated using 1st derivative thermograms (DTG profiles) which indicate the rate of mass change and help identify stages of mass change in thermograms. The comparison of asphaltene thermograms is discussed in Chapter 5.

2.10. Pyrolysis-Gas Chromatography-Mass Spectrometry

Given that the Py-GC-MS analysis of asphaltenes has not previously been explored for application in oil fingerprinting, it was decided that the GC-MS parameters would remain as consistent as possible with the technical guidelines for Tier 2 CEN analysis. The use of similar GC-MS parameters (between Py-GC-MS and Tier 2 of the CEN method) allows for the seamless addition of Py-GC-MS of asphaltenes in oil fingerprinting. Minimal changes are required to the operating conditions of GC-MS when switching from asphaltene pyrolysis to CEN analysis. The CEN technical report provides extensive details on how to optimise and determine the most appropriate GC-MS parameters. This is outside the scope of this research and not further discussed. The reader is referred to the CEN technical report for further information (CEN, 2012).

In regards to the furnace temperature used for asphaltene pyrolysis, 750°C was deemed most suitable after testing a range of flash pyrolysis temperatures by pyrolysing HFO asphaltenes (discussed in Chapter 5).

2.10.1. Py-GC-MS Profiling of Asphaltenes

Solid asphaltenes were analysed using a Shimadzu GC-MS QP2010 Ultra Gas Chromatograph Mass Spectrometer (*Shimadzu, Australia*) equipped with an online Frontier Laboratories Multi-Shot Pyrolyzer EGA/PY-3030D (*Frontier Laboratories, Japan*). Prior to the analysis of asphaltenes, a blank (a 50 µL disposable Eco-Cup (*Frontier Laboratories, Japan*) without sample) was analysed to ensure no carry-over occurred between analyses. Approximately 1 mg of asphaltenes was added to sample cup and attached to an Eco-Stick DF (*Frontier Laboratories, Japan*). The Eco-stick was then inserted in the Double Shot Sampler, which was attached to the pyrolysis unit in the sample cup standby position (with the sample cup loaded above the furnace, not inside the furnace). When GC-MS analysis was initiated, the sample cup was lowered into the furnace. Flash pyrolysis was conducted for 1 min at a furnace temperature of 750°C. After 1 min, the sample cup was raised back out of the furnace for the remainder of the analysis to prevent carry-over. The interface temperature between the pyrolysis unit and the GC injector port was 300°C. The pyrolysis furnace temperature and the interface temperature were set using the EGA/PY-3030D Control software (Ver.1.60) (*Frontier Laboratories, Japan*).

The GC-MS was controlled using GCMS Real Time Analysis Software (Shimadzu GCMSsolution Version 4.20) (*Shimadzu, Australia*). The GC injector was set to 300°C with a 100:1 split ratio. A Restek Rtx®-5MS column (30 m length, 0.25 mm ID, 0.25 µm film thickness) with a Crossbond® 5% diphenyl, 95% dimethyl polysiloxane stationary phase was used. Helium gas was used as the mobile phase, with a column flow rate of 1.03 mL/min. The

GC oven temperature program was set as follows: 42°C for 0.95 min, then 5.52°C/min to 325°C (10 min hold time at the end). The interface temperature (from GC to MS) was 300°C. The MS ion source temperature was 250°C, with electron impact set to 70 eV for ionisation. Full scan analysis was conducted from m/z 35 to m/z 550. GC-MS Post Analysis Software (Shimadzu GCMSsolution Version 4.20) (*Shimadzu, Australia*) was used to extract selected ion profiles.

Pyrolysates (compounds generated from pyrolysis) were identified in pyrograms by comparing RTs with CEN RTs for target compounds and also by using the software mass spectrum database, Shimadzu Mass Spectrum NIST library (NIST 2011, Release 1.00) (*Shimadzu, Australia*). The specific target pyrolysates used for the comparison of asphaltene pyrograms are discussed in Chapter 5. A principally visual approach was adopted for comparing pyrograms in line with common forensic practice (Zellner and Quarino 2009, Palus et al. 2008, Sarkissian et al. 2004).

2.11. Isotopic Ratio Mass Spectrometry

IRMS analysis of asphaltenes was conducted in a NATA accredited laboratory (*Environmental Forensics, Office of Environment and Heritage, Australia*) using a NATA accredited analytical method for IRMS analysis. Optimisation was not required for the IRMS method.

2.11.1. Isotopic Profiling of Asphaltenes

A Thermo Fisher Scientific Flash 2000 Organic Elemental Analyzer (*Thermo Fisher Scientific, Germany*) coupled to a Thermo Fisher Scientific Finnigan Delta-V Isotopic Ratio MS (*Thermo Fisher Scientific, Germany*) was used for the bulk analysis of solid asphaltenes

for the determination of carbon C^{13}/C^{12} isotope ratios (Figure 2.8). Isodat 3.0 Software (version 3.0) was used to control instrumental parameters.

Thermo Fisher Scientific
Finnigan Delta-V
Isotopic Ratio MS
(employed in this
research)

*Gas chromatograph (not
employed in this
research)*

*Elemental analyzer for H
and O (not employed in
this research)*

Thermo Fisher Scientific
Flash 2000 Organic
Elemental Analyzer
(employed in this
research)



Figure 2.8: The Thermo Fisher Scientific Flash 2000 Organic Elemental Analyzer coupled with a Thermo Fisher Scientific Finnigan Delta-V Isotopic Ratio MS.

Blanks (CO_2 zero methods) and CO_2 linearity tests were conducted prior to asphaltene analysis. Linearity tests were conducted at various intensities between the 2–12 mV calibration range of the instrument. The instrument was deemed suitable for analysis once the standard deviation (SD) was below 0.1 (between 0.04–0.08) across the intensity range (2 mV, 4 mV, 6 mV, 8 mV, 10 mV and 12 mV). By doing this, there was certainty that the C^{13}/C^{12} ratios obtained did not differ with samples of different intensities. As long as the intensity of each sample fell within the calibration range of the instrument (2–12 mV), the SD would be less than 0.1 between compared measurements. For example: the SD between two samples at

intensities of 3000 mV and 6000 mV would be less than 0.1. Cyclohexanone dinitrophenylhydrazone standard (*Thermo Fisher Scientific, United Kingdom*) was used to condition the oxidizing tube in the EA prior to analysis.

Approximately 50 µg of solid asphaltenes from each of the oils were wrapped in tin capsules (*Thermo Fisher Scientific, United Kingdom*). Estimations were based off the weights of initial asphaltene samples added to the first few cups. Weighing of asphaltenes was quickly deemed too tedious and weights were simply estimated to fall within the calibration range of the instrument. The tin capsules were then placed into the EA auto-injector for analysis. NBS 22 Oil, No. 443 (*International Atomic Energy Agency, Austria*) was analysed every tenth sample as a quality control check.

2.11.2. Comparison of Carbon Isotope Ratios

The C^{13}/C^{12} isotope ratios of asphaltenes as obtained from IRMS were transferred to Microsoft Excel 2010 for processing. Quartile 1 (Q1), the median, quartile 3 (Q3), the minimum, and the maximum were calculated for replicate asphaltenes to produce box-and-whisker plots (Tukey, 1977). For duplicates, the minimum and maximum values were plotted to show the absolute difference between duplicates. A combined chart was generated showing the box-and-whisker plots and the absolute differences between duplicates. The resulting chart was used to gauge the variations between carbon isotopic ratios of asphaltenes obtained from different oils. The comparison of asphaltene carbon isotope ratios is discussed in Chapter 8. It should be highlighted that isotope profiling was conducted purely out of interest to provide preliminary results as a foundation for future research.

2.12. Weathering of M. Eastern Crude Oil

The weathering of the M. Eastern crude oil was performed by Stephen Fuller of the NSW OEH. A sub-sample of the weathered M. Eastern oil was kindly provided for the extraction and analysis of asphaltenes. Asphaltenes from the M. Eastern (w) oil were used for preliminary comparison to un-weathered oils and to gauge the performance of the asphaltene profiling methods.

The M. Eastern crude oil was weathered as follows. A sub-sample of the M. Eastern crude oil was placed in a watch glass over deionised water. The oil formed a thin layer approximately 200 μm thick on top of the water and completely covered the water layer. The setup was placed outside with full sun exposure over an Australian summer for 5 months. Whenever the water layer visibly diminished due to evaporation, the water was topped up to maintain the same volume for the duration of the experiment. The weathered oil sample was analysed by Stephen Fuller using the CEN method (results not shown) and evaporative and photo-oxidation weathering effects were found to have taken place. No sign of biodegradation was present.

Chapter 3 - Physical Properties of Oils and Asphaltenes

Basic physical properties of the studied oils and their respective asphaltene fractions were observed and are discussed herein. Whilst physical properties are certainly interesting, these properties are not relied upon for confirming the source of oil spills. Instead, this chapter aims to highlight the trends observed in physical properties that were shown to complement asphaltene chemical profiles. Although this chapter does not directly address Research Questions 1 and 2, the physical properties can be used to support analytical profiling methods and are therefore still relevant in addressing the Research Questions.

3.1. Colour of Crude and Heavy Fuel Oils

The colour of crude oil is dependent on chemical composition (Yang 2017). A range of different oil colours may therefore be observed as a result of chemical variations between different oils (Yang 2017). Crude oils may be black, dark brown, light brown, brownish yellow, yellow, dark green or light red in colour, to list a few (Yang 2017, Ryder 2004). HFOs are always very dark in colour (dark brown to black) due to their high asphaltene content (Roncoroni et al. 2015).

Of the eleven studied oils, the colours of ten oils (all except M. Eastern (w)) were observed prior to asphaltene precipitation. Although oil colour was visually observed in the laboratory, photographs were also taken to represent the colours of oils (Figure 3.1). Photographs were taken as follows:

1. Oils were removed from the freezer and defrosted. Once defrosted, oils were then stirred to homogenise;
2. One drop of each of the oils was placed on a white non-porous surface (white laminated paper);

3. Oil drops were photographed; and
4. All oils were photographed under the same lighting conditions using identical camera and flash settings. Photographs were not altered/colour corrected prior to addition to the thesis.

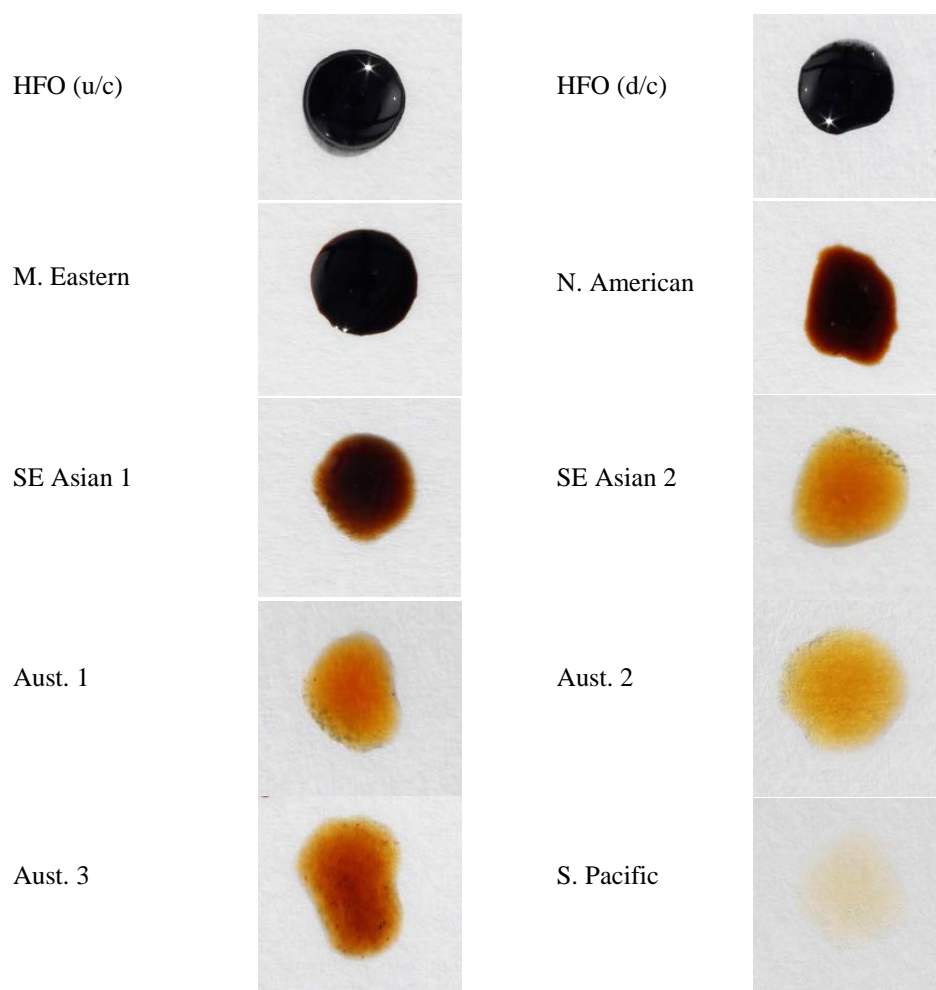


Figure 3.1: Photographs of oil droplets showing the colour of the studied oils (except for M. Eastern (w) oil). One drop of each of the oils was placed on white laminated paper, and photographed using the exact same camera and flash settings.

Notable colour differences were observed between the studied oils. As observed in Figure 3.1, the HFO (d/c), HFO (u/c) and M. Eastern oils were black in colour, whilst the N. American, SE Asian 1, SE Asian 2, Aust. 1, Aust. 2, Aust. 3 and S. Pacific oils were brown. Of all of the brown coloured oils, the N. American and SE Asian 1 were the darkest, whilst

the S. Pacific oil was the lightest. Although the observed colour differences were quite obvious, these observations were still subjective in nature. Consequently, colour differences should not be relied upon as forensic evidence in oil spill investigations. Colour differences do however correlate with other physical properties.

3.2. Asphaltene Yields

Sufficient C₅ asphaltene yields for profiling were precipitated from ten of the eleven studied oils; the S. Pacific oil did not yield sufficient asphaltenes for profiling. As a consequence, S. Pacific oil was readily differentiated from the other studied oils prior to asphaltene profiling.

The aim of asphaltene precipitation in this research was to obtain sufficient asphaltene yields for the development of asphaltene profiling methods and also to obtain chemically repeatable asphaltene fractions. Whilst asphaltene yields were indeed sufficient for method development and profiles were chemically repeatable, the amount of asphaltenes yielded varied upon repetition. Accurate and repeatable precipitation yields were not attainable due to the processes adhered to during precipitation. Firstly, speed was a priority for the separation of maltenes from asphaltenes. The liquid maltene fraction was pipetted from the solid asphaltenes after centrifugation; hence leaving behind solid asphaltenes adhered to the centrifuge tube. The removal of suspended asphaltenes in the maltene fraction was inevitable during this process which ultimately introduced error in the final product yields between precipitations. Furthermore, once asphaltenes were dry, the solid asphaltenes were physically scraped from the inside of the centrifuge tubes and collected in vials for analysis. It was not possible to physically collect all of the precipitated asphaltenes by scraping. Whilst more accurate yields could have been achieved by dissolving asphaltenes into collection vials and evaporating off the solvent to leave behind solid asphaltenes, this was not a time efficient

process hence was not pursued. It was also undesirable to dissolve asphaltenes after precipitation as this may induce aggregation; hence chemical alteration prior to analysis. As a consequence of these precipitation processes it was not possible to obtain repeatable and accurate yield weights which were suitable for use as forensic evidence. Asphaltene yields are therefore not reported in this thesis. In order to use yields as part of the forensic comparison for asphaltene profiles, the asphaltene precipitation method will need to be optimised to obtain very accurate asphaltene yields whilst still being time efficient. Additional research will be required if accurate asphaltene yields are desired.

Whilst comparison based on yields was not possible, it is interesting to note that in general, black-coloured oils yielded higher amounts of asphaltenes than the lighter, brown-coloured oils. For example, the black-coloured M. Eastern oil was considerably higher yielding (percentage yield of 4–5%) than the remaining crude oils which were brown in colour, such as the Aust. 1 oil (<0.5%). If these observations are repeatable, it may be possible for investigators to gauge whether oils are high or low yielding prior to asphaltene precipitation. In order to confirm if these observations are repeatable, future research will be required using a larger sample-set of oils.

3.3. Asphaltene Morphology: Crystalline and Resinous

Asphaltenes from ten of the studied oils were separated into two distinct groups on the basis of morphology: crystalline and resinous asphaltenes. Morphology observations were based on three asphaltene characteristics: (1) the macroscopic appearance of asphaltenes; (2) the malleability (or structural behaviour) of asphaltenes; and (3) the microscopic appearance of asphaltenes. These three characteristics are discussed below for the asphaltene fractions precipitated from the eleven studied oils.

3.3.1. Macroscopic Appearance and Malleability

Visual appearance was first observed at a macroscopic level in the laboratory whilst malleability was observed by physically exerting pressure on solid asphaltenes using a metal spatula. It is known that the physical consistency of asphaltene solids can be best described as having a tendency to fracture or crumble when pressure is exerted upon them (Sarmah et al. 2013, Speight 2014). Table 3.1 shows the crystalline/resinous classification of asphaltenes.

Table 3.1: Visual appearance of the C₅ asphaltene fraction obtained from crude and heavy fuel oils. The S. Pacific crude oil did not provide a C₅ asphaltene yield.

Crude oil or HFO	Morphology of C ₅ -asphaltenes
Aust. 1	Resinous, waxy
Aust. 2	Resinous, waxy
SE Asian 1	Resinous, rubbery
SE Asian 2	Resinous, rubbery
Aust. 3	Mixture of crystalline and resinous, waxy
N. American	Crystalline
M. Eastern	Crystalline
M. Eastern (w)	Crystalline
HFO (d/c)	Crystalline
HFO (u/c)	Crystalline
S. Pacific	N/A

Crystalline asphaltenes were defined by their shiny, crystalline appearance, and their tendency to fracture when physical pressure was applied upon them. HFO (u/c), HFO (d/c), M. Eastern, M. Eastern (w) and N. American asphaltenes exhibited crystalline properties. On the contrary, resinous asphaltenes were defined by their matte (non-shiny) appearance, and soft, malleable texture. Some resinous asphaltenes exhibited a very soft, waxy consistency (Aust. 1, Aust. 2), whilst others exhibited a harder, rubbery consistency (SE Asian 1 and SE Asian 2). Asphaltenes obtained from the Aust. 3 oil were different from the other oils investigated as they appeared to be a mixture of both resinous and crystalline material.

3.3.2. Microscopic Morphology: Scanning Electron Microscopy

Solid asphaltene particles were imaged using a Hitachi TM3030 Tabletop SEM with the aim of confirming the distinction made between crystalline and resinous asphaltenes above. Representative SEM micrographs of asphaltenes from each of the studied oils are presented in Figure 3.2. M. Eastern (w) and S. Pacific asphaltenes were not imaged due to limited sample availability. The distinction between crystalline asphaltenes and resinous/waxy asphaltenes was confirmed on a microscopic scale as observed in the SEM micrographs. HFO (d/c), HFO (u/c), and M. Eastern asphaltenes exhibited sharp, fractured edges, and consisted of particles of varying sizes. Fracturing of asphaltenes was less pronounced in the remaining micrographs of resinous asphaltenes. Interestingly, the N. American asphaltenes do not appear to be sharply fractured in the represented micrograph despite showing crystalline characteristics when observed macroscopically (black and shiny in appearance). The micrograph for the Aust. 3 asphaltenes also depicts a more resinous composition however macroscopically Aust. 3 asphaltenes appear to be a crystalline/resinous mixture. The resinous component of the Aust. 3 asphaltenes is likely more dominant than the crystalline component.

It is acknowledged that the crystalline/resinous classification of asphaltenes is highly subjective hence it should be reinforced that such classifications are not to be used as stand-alone forensic evidence. It is important however, to provide these physical observations in this thesis as this information can help explain the chemical differences observed between asphaltenes from different oils. Resinous and crystalline distinctions based on chemical analysis are discussed throughout the remaining thesis chapters.

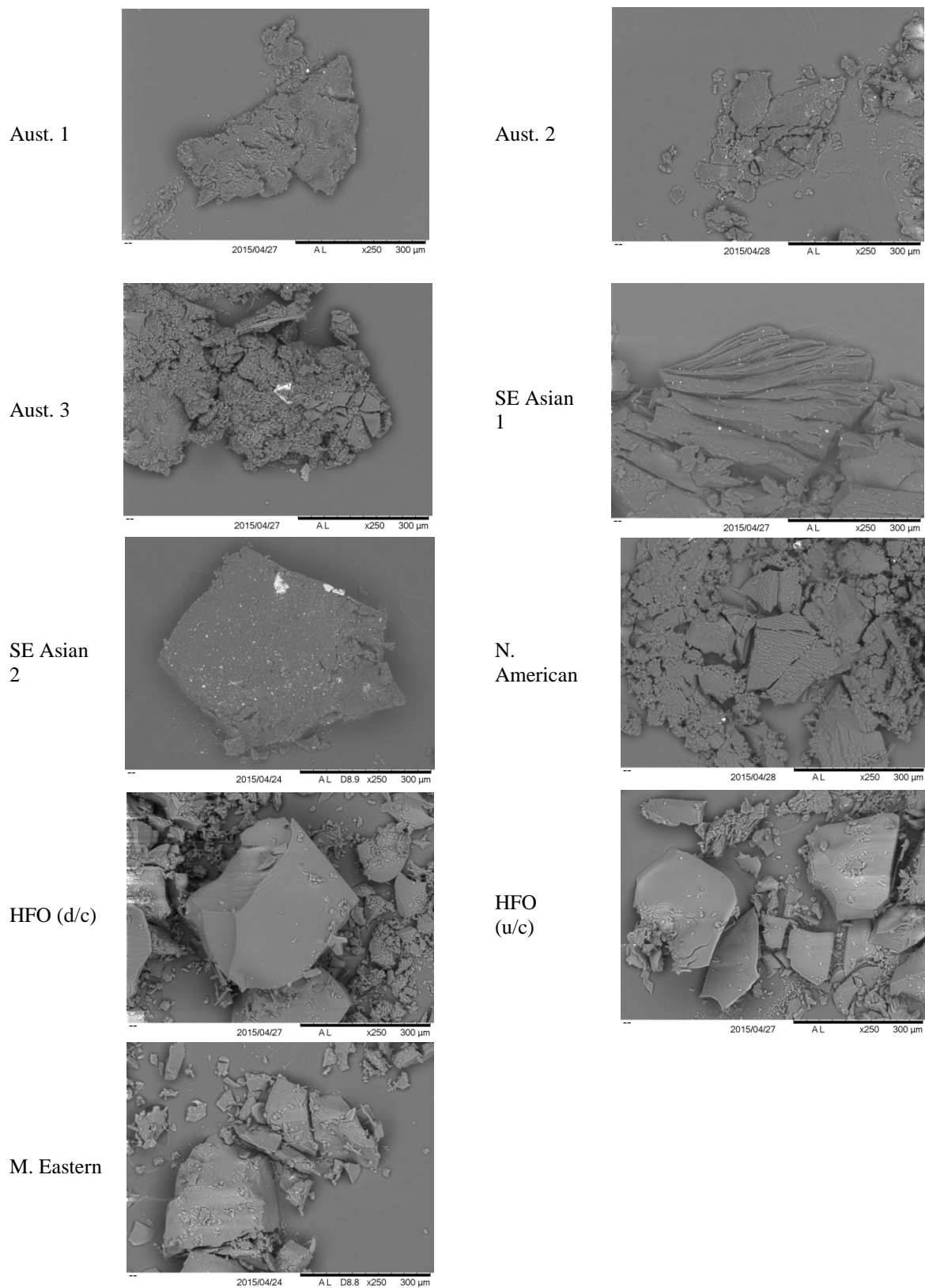


Figure 3.2: SEM micrographs of C₅ asphaltene particles except M. Eastern (w) and S. Pacific.

3.4. Colour of Asphaltenes

Asphaltenes are either black or brown in colour which is dependent on chemical composition (Oyekunle, 2006). The colour of asphaltenes may therefore provide information regarding potential chemical variations between different asphaltenes. In this research, both black and brown coloured asphaltenes were observed. Asphaltenes from the studied oils were smeared as thin layers to provide for better colour representation than the thicker solid particles obtained directly from precipitation. HFO (u/c), HFO (d/c), M. Eastern, M. Eastern (w) and N. American asphaltenes produced black smears, whilst, Aust. 1, Aust. 2, Aust. 3, SE Asian 1 and SE Asian 2 asphaltenes produced dark-brown smears. A photograph of the asphaltene smears is provided in Figure 3.3.

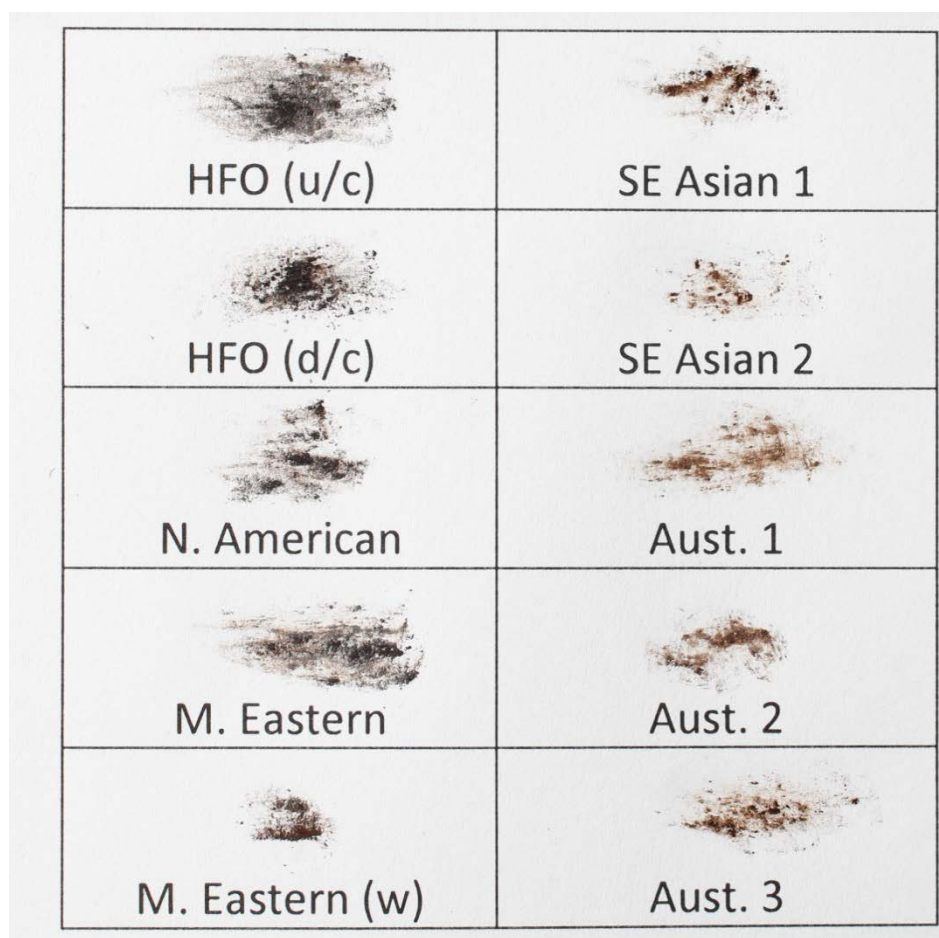


Figure 3.3: Asphaltene smears on white paper.

Although highly subjective, the observed colour differences of asphaltenes from different oils support the afore-mentioned groupings of asphaltenes into crystalline and resinous asphaltenes. Black coloured asphaltene smears corresponded to crystalline asphaltenes (HFO (u/c), HFO (d/c), M. Eastern, M. Eastern (w) and N. American asphaltenes) whilst brown coloured asphaltene smears corresponded to resinous asphaltenes (Aust. 1, Aust. 2, SE Asian 1 and SE Asian 2 asphaltenes) or resinous dominant mixtures such as Aust. 3. The observed colour difference between asphaltenes from different oils supported the decision to pursue Ultraviolet-Visible (UV-Vis) spectroscopic analysis of asphaltenes (as discussed in Chapter 4). Spectroscopic analysis in the visible light spectrum would provide an objective measure of asphaltene colour which may provide probative information given the visual colour differences observed in the smears. It is also interesting to note that the colour of whole oils was correlated with the colour of subsequent asphaltene fractions.

3.5. Chapter 3 Summary

Although the physical properties of oils and asphaltenes should not be relied on solely for determining the source of oil spills, it is still interesting to note the distinct differences observed between the studied oils. The observed differences suggest that the chemical compositions of the oils are different and so too are the chemical compositions of their respective asphaltene fractions. Chemical profiling of asphaltenes is therefore likely to provide probative information that may assist in oil spill investigations.

The physical properties of asphaltenes, in particular their morphologies, can be linked to the asphaltene profiles generated throughout this research. This will become clearer throughout the following chapters as resinous and crystalline classifications are discussed alongside asphaltene profiles.

As mentioned, the S. Pacific crude oil did not yield sufficient asphaltenes for analysis, therefore the S. Pacific oil was readily differentiated from the other studied oils prior to analysis. It should be noted that the failure of lighter oils to yield asphaltenes may be a limitation of asphaltene profiling; if multiple oils in a case do not provide an asphaltene yield, existing oil fingerprinting methods are the only viable option for analysis. The failure of some oils to yield asphaltenes reinforces why the application of asphaltene profiling in oil fingerprinting has been designed as a complementary tool for use alongside current oil fingerprinting practices; not as a stand-alone approach.

Chapter 4 - Spectroscopic Profiling of Asphaltenes

The aim of this chapter was to address both Research Questions 1 and 2. To address Research Question 1, each of the spectroscopic asphaltene profiling methods was evaluated against the forensic requirements specified in Chapter 1. To address Research Question 2, each of the asphaltene profiling methods was compared to one another to determine which spectroscopic method was most suitable for oil spill investigations. Comparisons were based on the ability of each method to address the forensic requirements specified for Research Question 1. Asphaltene profiling methods were developed for four commonly available spectroscopic techniques: UV-Vis, Raman, fluorescence, and IR spectrophotometers.

4.1. Ultraviolet-Visible Spectroscopy

UV-Vis spectroscopy measures the absorbance (Abs) of a sample across the ultraviolet and visible light spectrum (200–800 nm). Samples are exposed to radiation from a Deuterium lamp for the UV region, and from a tungsten-halogen lamp for the visible region (Perkampus 1992). UV-Vis spectroscopy is an accepted and peer-reviewed analytical technique for the analysis of asphaltenes, as evident in many past research applications (Evdokimov and Losev 2011, Ostlund et al. 2003, Ghosh et al. 2007). UV-Vis spectrophotometers are also readily available, cost-effective and fast.

Asphaltene aggregation studies often employ UV-Vis spectrophotometers. For instance, Ghosh et al. (2007) explored the aggregation of coal-derived asphaltenes at various concentrations using both UV-Vis and fluorescence spectroscopy. Asphaltenes were dissolved in benzene, toluene and carbon tetrachloride at various concentrations, and were analysed to produce UV-Vis absorption spectra between 600–400 nm. The resulting spectra were quite similar in overall shape between all three solvents, showing a slow, gradual increase in Abs from 600–400 nm. The study by Ghosh et al. (2007) only analysed

asphaltenes from a single coal sample; hence it was not possible to determine the probative value of UV-Vis spectroscopy from this study as no comparisons were made between different asphaltenes. Following on from the previous chapter however, it would be expected that differences in the UV-Vis spectra for the studied asphaltenes would be observed, as visual colour differences were noted.

The major limitation of UV-Vis spectroscopy is the need to dissolve solids (such as asphaltenes) prior to analysis. The dissolution of asphaltenes is problematic due to the tendency of asphaltenes to aggregate in solution. In toluene, asphaltenes have been shown to begin molecular interactions at concentrations ~ 60 mg/L, in which dimer aggregates are observed (Oh and Deo 2007). Dimer aggregation is followed by tetramer aggregation (interaction between two dimers) at ~ 100 mg/L, and finally the formation of nanoaggregates at ~ 150 mg/L (Oh and Deo 2007). Although these aggregation thresholds are a good guideline, the inherent chemical variability of the asphaltene fraction will cause varied aggregation properties between different asphaltenes (i.e., two asphaltene fractions from two different oils may have very different aggregation concentrations). Furthermore, many factors such as time, temperature and pressure can influence aggregation of asphaltenes whilst in solution. The ability of asphaltenes to aggregate in solution makes the dissolution of asphaltenes prior to analysis less appealing. To be conservative and to ensure that the possibility of asphaltene aggregation was minimised, asphaltenes were diluted to a concentration of 10 ppm for analysis. To take further precautionary measures, asphaltene solutions were analysed immediately after preparation.

Prior to analysis it was necessary to determine the most suitable solvent for dissolving asphaltenes; dichloromethane (DCM), toluene and THF were tested (all solvents were HPLC grade). As stated in Appendix B, asphaltenes did not dissolve readily in all of the tested solvents. Some asphaltenes readily dissolved, whilst others did not. Those that did not

dissolve were subject to sonication until the suspended solids were dissolved. Sonication allowed for the dissolution of further asphaltenes; however despite 1 hr of sonication, some asphaltenes still did not dissolve. Failure of asphaltenes to dissolve was not sample specific; for example, some of the replicate M. Eastern asphaltenes did dissolve whilst others did not. These observations may be explained by variable sizes of asphaltene particles between precipitated fractions. Of the tested HPLC grade solvents, THF performed the best and readily dissolved more asphaltenes than DCM or toluene. Asphaltenes were therefore dissolved in THF and prepared to a concentration of 10 ppm for UV-Vis profiling. At this concentration the samples were brown in colour.

4.1.1. Preliminary UV-Vis Profiling

It was necessary to test the probative value of the developed UV-Vis spectroscopy method for asphaltene profiling. To do so, preliminary UV-Vis profiling was conducted on asphaltenes precipitated from three different oils: M. Eastern, HFO (u/c) and N. American. UV-Vis absorption spectra for the M. Eastern, HFO (u/c) and N. American asphaltenes showed very similar profiles to those observe in the literature for coal-derived asphaltenes, with slow gradual increases in Abs from 600–400 nm (Figure 4.1, Ghosh et al. 2007).

The spectral region between 600–400 nm was very similar between M. Eastern, HFO (u/c) and N. American asphaltenes. Between 400–250 nm, the three different asphaltene fractions show a more steady increase in Abs which was followed by a rapid rise in Abs in the UV region of the spectra (250–200 nm). Blank analysis of THF solvent revealed that the observed peak was to some extent caused by the THF solvent itself, not the asphaltenes. A stronger UV-Vis signal intensity might be obtained at higher asphaltene concentrations, but this is not viable with the potential for aggregation.

In light of the preliminary UV-Vis profiling conducted herein, UV-Vis spectroscopy did not meet the basic requirements of a forensic method. As a consequence, UV-Vis profiling was not further investigated.

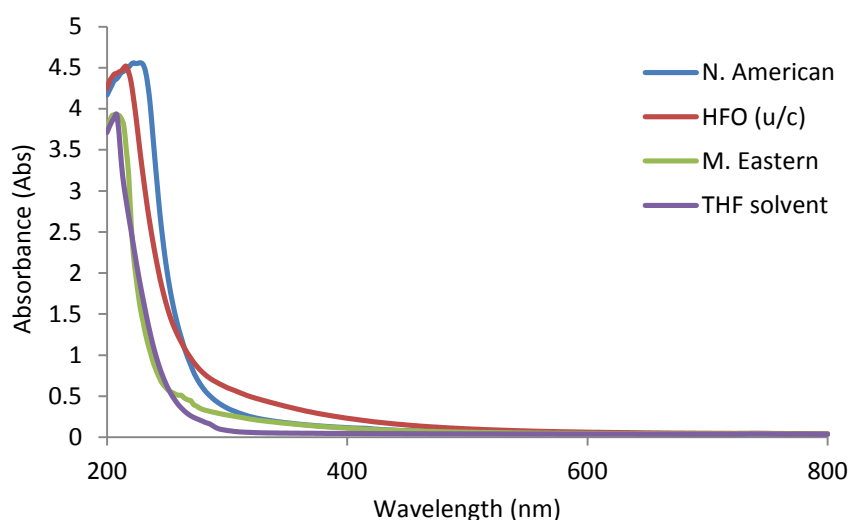


Figure 4.1: UV-Vis absorption spectra obtained for asphaltenes from M. Eastern, HFO (u/c) and N. American oils. The overlap with the THF solvent peak at 220–250 nm should be noted.

4.2. Fluorescence Spectroscopy

Fluorescence spectroscopy involves irradiating samples with a light source which causes electrons to excite from ground state energy to an excited state of energy. As electrons fall back down to the ground state, energy is emitted in the form of fluorescence. Fluorescence spectrophotometers detect fluorescence as absorbance (Bourdet and Eadington 2012). Aromatics are the key fluorescence targets in petroleum as the electrons which form π bonds (C=C) in these molecules readily fluoresce (Ryder 2004, Mullins 2010, Bourdet and Eadington 2012, McMurray and Simanek 2007). The specific wavelengths at which aromatics fluoresce are largely governed by the sizes of aromatic structures (i.e., how many aromatic rings are joined together in a molecule). In general, the smaller the aromatic structure the lower the excitation wavelength. Conversely, the larger the aromatic structure

the higher the excitation wavelength (Mullins 2010). For example, benzene structures (1 aromatic ring) typically emit around 280 nm at an excitation of 265 nm, whilst pentacene structures (5 aromatic rings) emit around 590 nm at an excitation of 580 nm (Mullins 2010). Mullins (2010) showed that at a range of excitation wavelengths (265 nm, 290 nm, and 340 nm), asphaltene fluorescence emission was observed between 350–550 nm. The observations by Mullins (2010) suggests that asphaltenes with different PAH content would have different fluorescence emission wavelengths. It was therefore necessary to investigate fluorescence spectroscopy to determine if the studied asphaltenes had different aromatic compositions and subsequently, different fluorescence emission spectra.

Fluorescence spectrophotometers are readily available and cost effective instruments that are capable of rapid analysis. The major limitation to fluorescence spectroscopy is the need to dissolve asphaltenes prior to fluorescence profiling. The dissolution of asphaltenes for fluorescence profiling was analogous to the preparation used for UV-Vis, Asphaltenes were prepared in THF to a concentration of 10 ppm and analysed immediately to minimise the likelihood of asphaltene aggregation. Reagent grade THF and HPLC grade THF were assessed to determine the optimum THF grade for fluorescence profiling of asphaltenes. Whilst there was no apparent difference in the ability of each THF grade to dissolve asphaltenes, reagent grade was found to fluoresce considerably more than HPLC grade. The more expensive HPLC grade alternative was therefore required to minimise solvent interference during fluorescence profiling. The dissolution of asphaltenes prior to profiling was considered a destructive approach because the molecular properties of asphaltenes are capable of changing whilst in solution due to aggregation. The dissolved asphaltene fractions were hence considered destroyed samples; re-precipitation of asphaltenes was not conducted following fluorescence profiling.

4.2.1. Excitation Wavelength and Sample Concentration

It was known from the literature that fluorescence emission of asphaltenes was best observed at smaller excitation wavelengths (between 265 and 340 nm) to allow for the detection of a broader range of aromatics as opposed to higher excitation wavelengths (Mullins 2010). After preliminary testing, an excitation wavelength of 275 nm was chosen to investigate the distribution of PAH systems (>2 rings in size) in asphaltene fractions.

Firstly, the optimum sample concentration was determined. HFO (u/c) asphaltenes were precipitated and a 10 ppm stock solution of asphaltenes in THF was prepared. A range of solutions of varying concentrations were then created by diluting from the 10 ppm stock solution (Table 4.1). This range of solutions was then analysed to determine the optimum concentration of asphaltenes for fluorescence profiling.

Table 4.1: From the 10ppm stock solution, the following dilutions were made in a 4 mL cuvette. These concentrations were approximated assuming 1 drop = 0.1 mL.

Approximate Concentration of Diluted Solution	Dilution Method
0.1 ppm	10 ppm stock solution was added to the cuvette and pipetted back out. The cuvette was then filled with THF.
0.8 ppm	3 drops of 10 ppm stock solution was added to the cuvette and then filled with THF.
1.4 ppm	6 drops of 10 ppm stock solution was added to the cuvette and then filled with THF.
2.5 ppm	10 drops of 10 ppm stock solution was added to the cuvette and then filled with THF.
5 ppm	20 drops of 10 ppm stock solution was added to the cuvette and then filled with THF.
10 ppm	10 ppm stock solution was added undiluted into the cuvette.

The resulting fluorescence spectra obtained for these concentrations are presented in Figure 4.2. The spectrum obtained for the 10 ppm concentration has not been presented as the detector was overloaded. It should also be noted that HPLC grade THF was observed to fluoresce at 300 nm; hence fluorescence spectra presented below are shown from 315 nm to 540 nm to remove the solvent peak. The results demonstrate that concentrations of approximately 2.5–5 ppm were most suitable for the fluorescence profiling of asphaltenes, as these concentrations allowed for greater detail and resolution in the resulting spectra. The final concentration chosen for the analysis and comparison of asphaltenes was approximately 2.5 ppm.

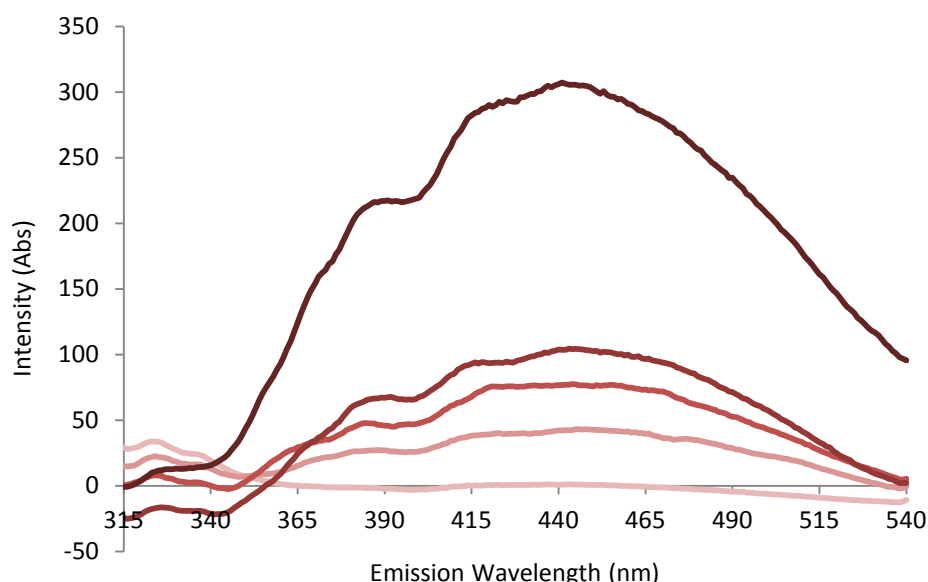


Figure 4.2: Fluorescence emission spectra obtained for HFO (u/c) C₅ asphaltenes at five different approximated concentrations: ~ 0.1 ppm, ~ 0.8 ppm, ~ 1.4 ppm, ~ 2.5 ppm and ~ 5 ppm (from lightest line to darkest line). These spectra are not normalised.

4.2.2. Method Uncertainty

To gauge method uncertainty, fluorescence spectra were obtained from replicate asphaltenes. Seven replicate asphaltene extracts were precipitated from both M. Eastern and HFO (u/c) oils. Figure 4.3 shows the repeatability of replicate fluorescence spectra which were normalised to 390 nm for comparison.

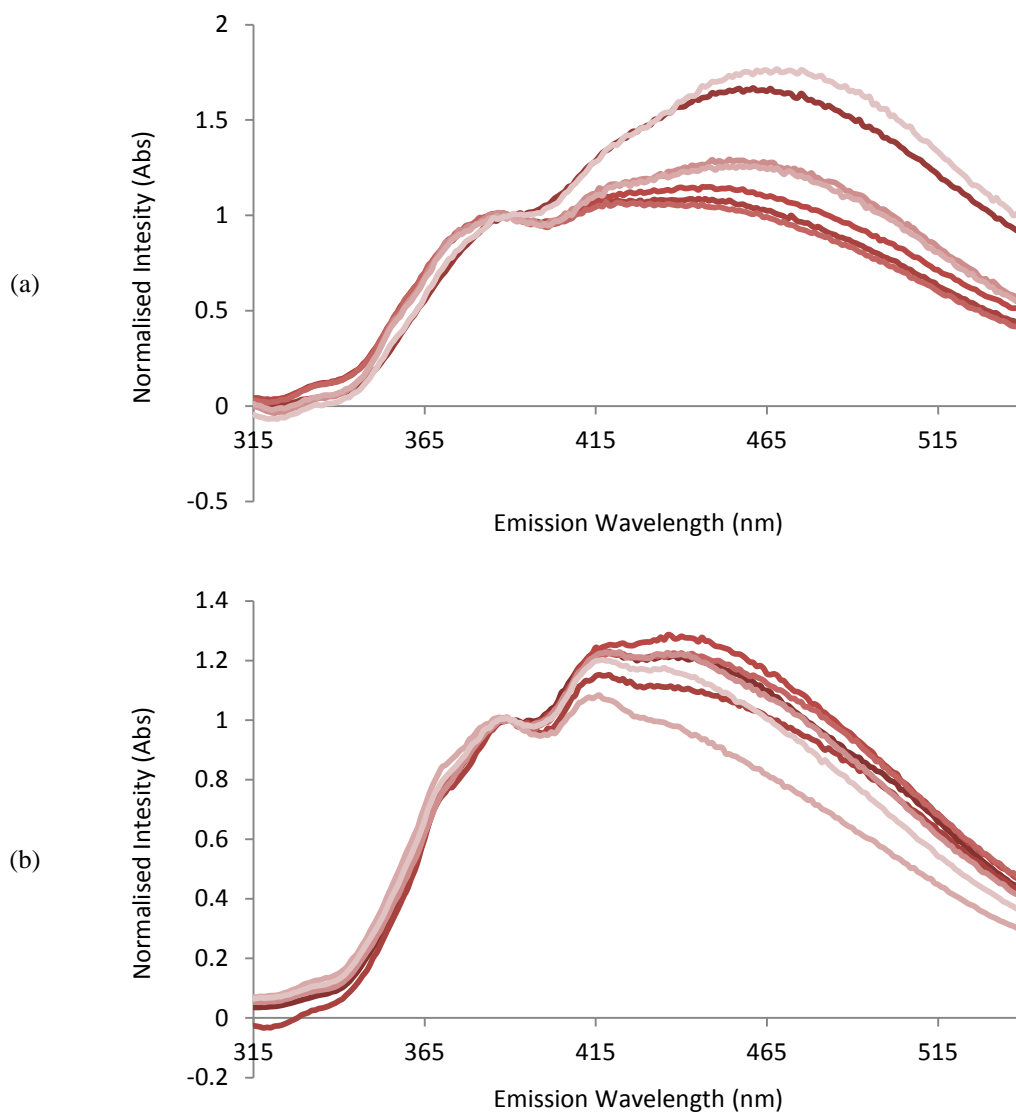


Figure 4.3: Fluorescence spectra of replicate asphaltene fractions(a) M. Eastern; and (b) HFO (u/c).

The maximum emission wavelength observed for the M. Eastern replicates was consistently between 465–475 nm, whilst the emission maximum for HFO (u/c) replicates was consistently between 420–435 nm. The HFO (u/c) replicates had more consistent profile shapes than the M. Eastern replicates. Two of the M. Eastern spectra had a higher intensity around the emission maximum than the remaining five M. Eastern replicate spectra. The two variable M. Eastern spectra also showed a slight red shift (towards 540 nm) in comparison to the remaining replicate spectra. Due to the minor variability observed in the M. Eastern replicate spectra, it was decided that the comparison of asphaltene fluorescence spectra would

be conducted conservatively. Only very obvious differences would be relied upon as probative information for comparing asphaltenes from different oils.

4.2.3. Visual Comparison of Fluorescence Spectra

Asphaltenes were precipitated in duplicate from a further seven oils for fluorescence profiling and subsequent comparison. Duplicate asphaltenes were precipitated from HFO (d/c), N. American, SE Asian 1, SE Asian 2, Aust. 1, Aust. 2 and Aust. 3 oils. The M. Eastern and HFO (u/c) replicates were also included in the comparison; a total of nine oils were therefore used for comparison.

If fluorescence spectra of asphaltenes were observed to have similar maximum emission wavelengths and profile shapes, these asphaltenes were not be differentiated from one another; hence the corresponding oils were not differentiated. Conversely, if fluorescence spectra of asphaltenes showed different maximum emission wavelengths and profile shapes, these asphaltenes were deemed different; hence corresponding oils were differentiated. Although asphaltenes from different oils may share the same maximum emission wavelength, the profile shape may still differ as observed below. All spectra were normalised to the signal intensity at 390 nm prior to comparison.

The nine oils were differentiated into five different groups. The first group included HFO (d/c) and M. Eastern oils. The fluorescence spectra of M. Eastern and HFO (d/c) asphaltenes exhibited the same maximum emission wavelength of 455–465 nm (Figure 4.4).

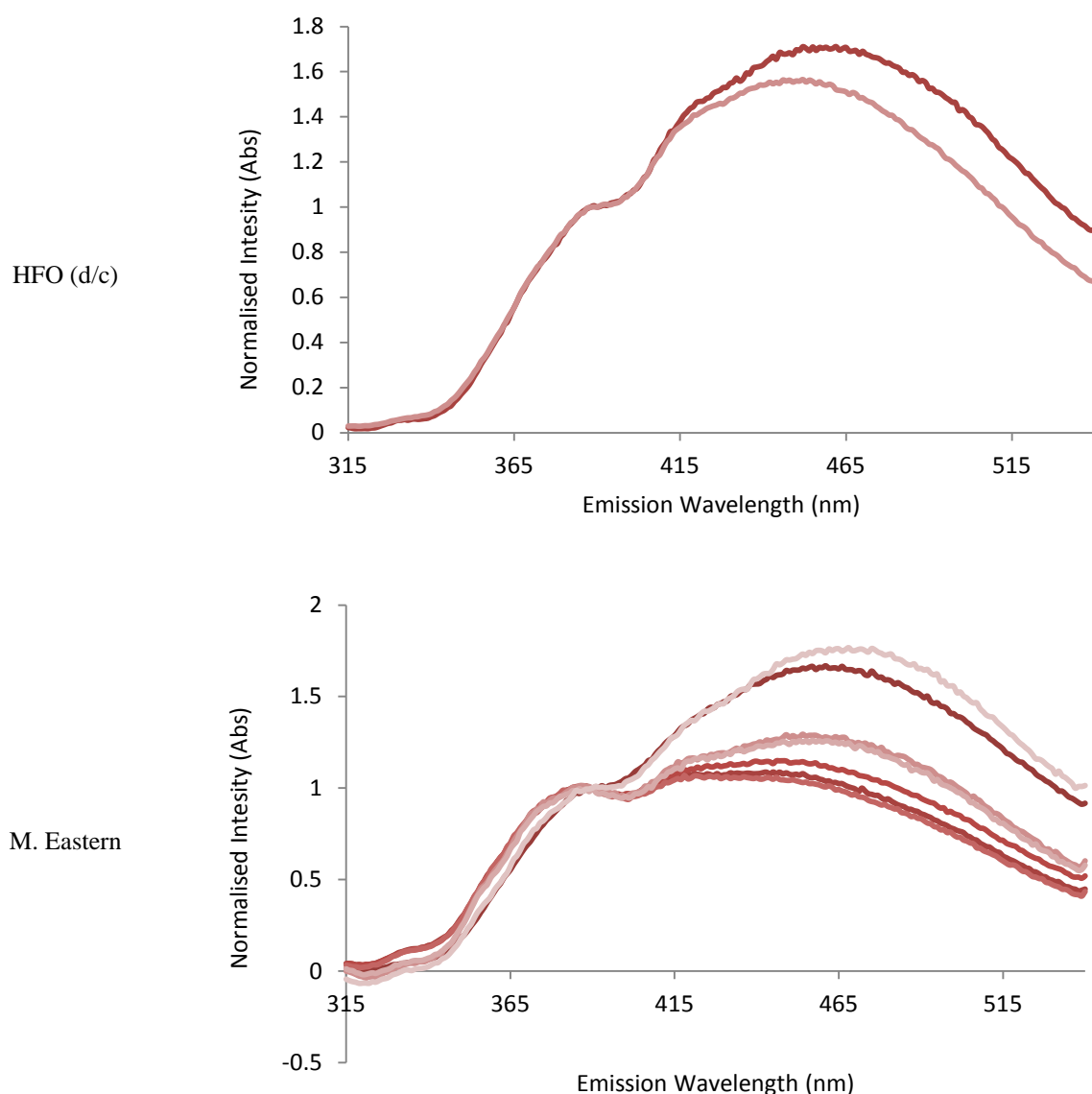


Figure 4.4: Fluorescence spectra observed for HFO (d/c) and M. Eastern asphaltenes.

The 455–465 nm maximum was unique to the M. Eastern and HFO (d/c) asphaltenes. M. Eastern and HFO (d/c) spectra also shared a very similar profile shape to one another as both indicated a shift towards red wavelengths (red shift). This red shift is characteristic of asphaltenes containing larger aromatic ring structures (Mullins 2010). M. Eastern and HFO (d/c) asphaltene profiles were most similar to the second group, HFO (u/c) asphaltenes (Figure 4.3). The difference however, was that the fluorescence spectra of HFO (u/c) asphaltenes showed consistently lower maximum emission peaks between 420–440 nm as

opposed to 455–465 nm as observed for M. Eastern and HFO (d/c) asphaltenes (Figures 4.3 and 4.4).

The differences observed between the first two groups were very interesting as HFOs of different grades were differentiated on the basis of fluorescence spectra of asphaltenes. As discussed later in this chapter, the two studied HFO grades could not be differentiated from one another using the developed IR method. Whilst interesting, further testing with additional HFOs of varying grades would be required to confirm these initial observations, but only if fluorescence profiling proves to be the most suitable method for oil spill investigations.

The third group consisted of the three Australian asphaltene fractions from the Aust. 1, Aust. 2 and Aust. 3 oils which all had very similar fluorescence spectra. The maximum emission wavelength of the Australian asphaltenes was 370 nm (Figure 4.5).

The asphaltenes from the fourth group (SE Asian 1 and N. American) also exhibited a maximum emission wavelength of 370 nm (Figure 4.6); however there was a distinct difference in profile shapes between the Australian asphaltenes and the SE Asian 1 and N. American asphaltenes. The spectra of the Australian asphaltenes exhibited a prominent peak at 370 nm, whilst the spectra for the SE Asian 1 and N. American asphaltenes exhibited a flat plateau across the spectral region between 370–385 nm.

The SE Asian 2 asphaltenes were differentiated from all other asphaltenes as the fifth group. SE Asian 2 asphaltenes were easily identified due to the steep rise in the spectra from 310–355 nm, a plateau in the maximum emission wavelength/s between 355–365 nm, followed by a steep decline in intensity after 365 nm (Figure 4.7).

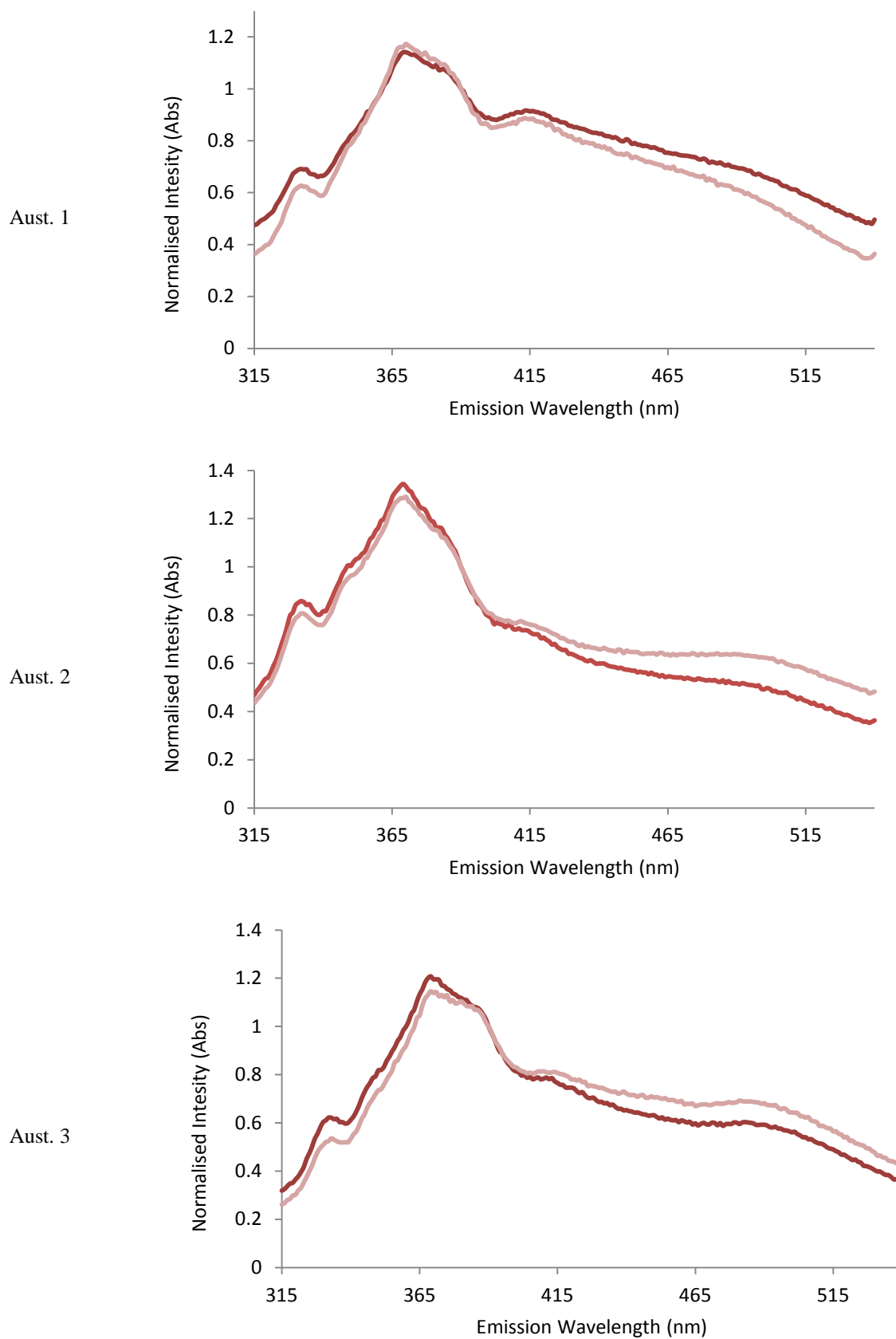


Figure 4.5: Fluorescence spectra observed for Aust. 1, Aust. 2 and Aust. 3 asphaltenes.

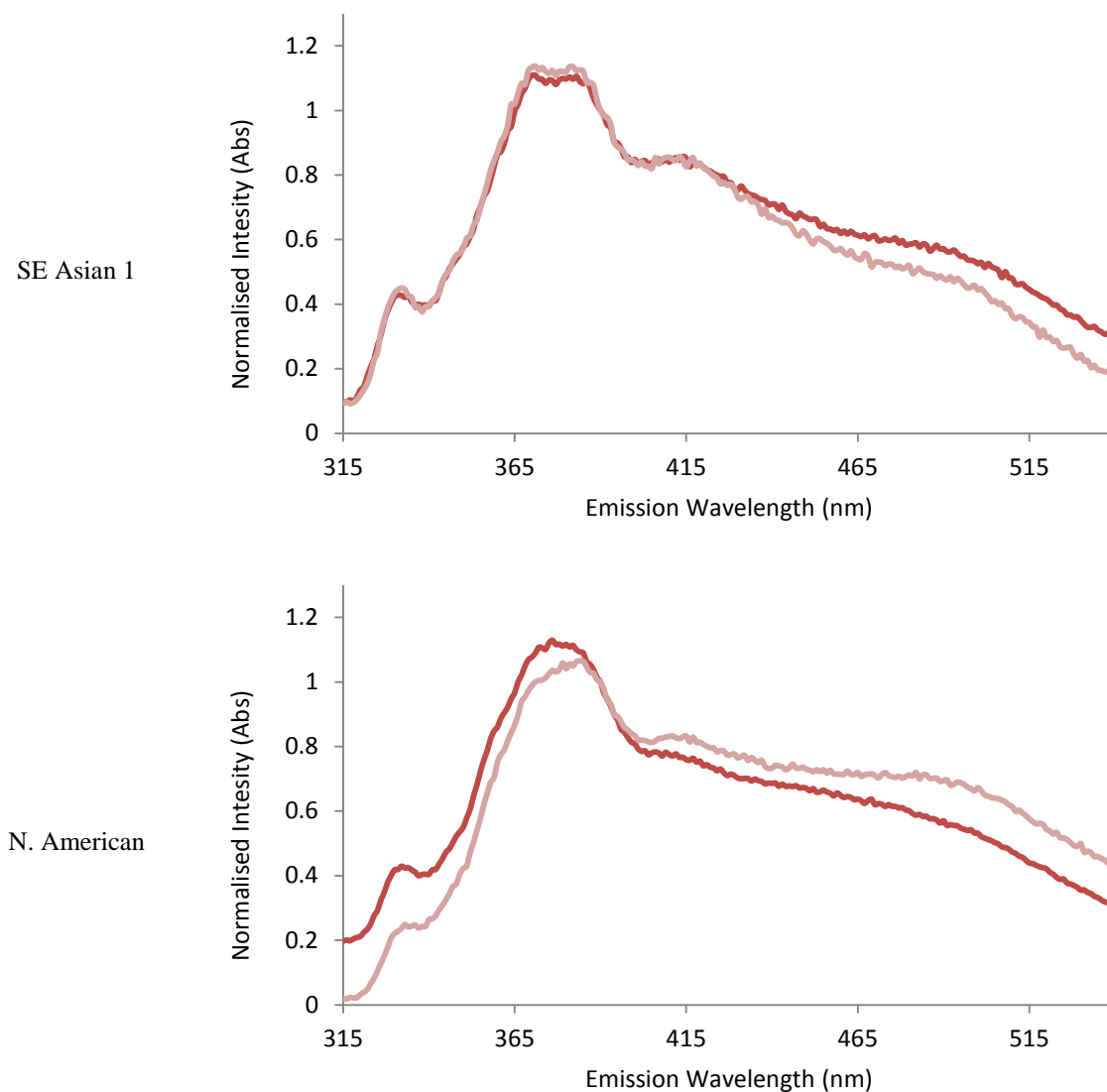


Figure 4.6: Fluorescence spectra observed for SE Asian 1 and N. American asphaltenes.

Overall, a blue shift (a shift towards blue wavelengths) was observed in the fluorescence spectra of the Aust. 1, Aust. 2, Aust. 3, SE Asian 1, N. American and SE Asian 2 asphaltenes which indicates the presence of smaller aromatic structures in these specific asphaltene fractions (Mullins 2010).

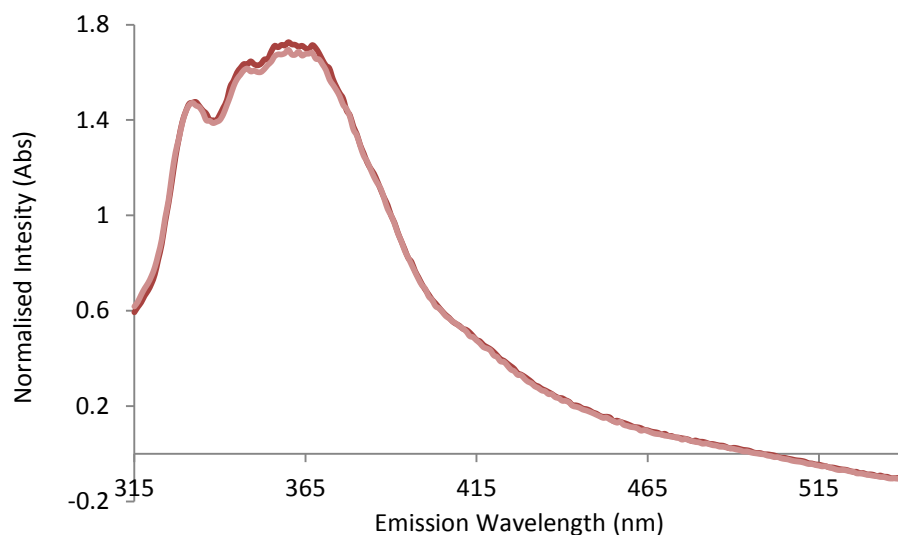


Figure 4.7: Fluorescence spectra observed for SE Asian 2 asphaltenes.

4.2.4. Overall Evaluation of Fluorescence Profiling

Fluorescence profiling of asphaltenes successfully differentiated nine different oils into five distinct groups. Whilst fluorescence profiling offered probative information for the exclusion of oils, the sample handling associated with the fluorescence profiling method was not ideal; asphaltenes had to be dissolved prior to analysis. Dissolving asphaltenes may result in aggregation and the chemical alteration of asphaltenes prior to analysis. It was therefore necessary to investigate other spectroscopic techniques that allow for rapid solid state analysis of asphaltenes in order to better align with the ideal requirements of a forensic method.

4.3. Raman Spectroscopy

Raman spectroscopy involves irradiating a sample with a laser (either using UV, Vis, or NIR wavelengths) and observing the scattering of light (Raman scattering) that may be caused due to interaction of the laser with molecules (Smith and Dent 2005). Raman spectroscopy has been applied to the analysis of petroleum and a range of petroleum-derived

products to obtain structural information from these complex mixtures (Ascanius et al. 2004). Raman spectroscopy was appealing for application in this research as asphaltenes could be analysed in a solid state. Raman spectroscopy however, was limited in its application as compounds that fluoresce may be destroyed by short wavelength (UV) lasers during analysis (Ascanius et al. 2004). Whilst it was known that asphaltenes fluoresce, precautions were taken to determine if Raman spectra could be obtained from the studied asphaltenes without fluorescent interference.

M. Eastern and HFO (u/c) asphaltenes were used to gauge the suitability of Raman spectroscopy for the analysis of asphaltenes. In order to reduce asphaltene fluorescence, a number of basic parameters were controlled. Firstly, an excitation laser with a long wavelength (785 nm) was used for analysis. Longer wavelengths, such as 785 nm as opposed to 514 nm, reduce electronic absorption, in turn reducing fluorescence (Smith and Dent 2005). The integration was also reduced from 10 seconds to 1 second. By shortening the duration for which asphaltenes were exposed to the 785 nm excitation laser, the likelihood of fluorescence was reduced. Despite controlling these two parameters, both M. Eastern and HFO (u/c) asphaltenes fluoresced during analysis and were ultimately destroyed. As a longer wavelength laser was not available at the time of analysis, it was decided to pursue other spectroscopic techniques. A 1064 nm laser may be considered for application in future work when available.

4.4. Attenuated Total Reflectance-Fourier Transform Infrared Spectroscopy

IR spectroscopy irradiates samples with IR radiation which causes characteristic vibrations of molecular bonds; each bond type (or functional group) is represented by a characteristic vibrational IR wavenumber (cm^{-1}) (Pavia and Lampman 2001). As discussed in

Chapter 1, IR vibrations have proven useful in the petroleum industry for identifying the structural features of asphaltenes (Gawel et al. 2014, Asemani and Rabbani 2015). For example, Gawel et al. (2014) showed that of all SARA oil fractions, the asphaltene fraction had the most variable IR spectra when compared between oils from different origins. Additionally, Asemani and Rabbani (2015) showed that the calculation of geochemical IR indices could be used to successfully differentiate a small sample-set of asphaltenes from one another. Overall, IR spectroscopy is a well-established technique which is accepted in petroleum science for the characterisation of asphaltene structures. Preliminary results from past Honours research suggested that the IR spectra of asphaltenes might offer probative information when comparing asphaltenes from different oils (Riley 2013). IR spectroscopy also proved to meet the practical requirements of oil fingerprinting. IR spectroscopy is non-destructive and commonly available in forensic laboratories. Minimal sample is required for IR analysis and little to no sample preparation is required following precipitation, with solid state analysis being possible. IR spectroscopy also offers high sample throughput which allows for fast screening of asphaltenes. The probative value of IR asphaltene profiling is explored below. To gauge the probative value of IR spectra, asphaltenes from eleven different oils (including a weathered oil sample) were precipitated for analysis: S. Pacific, Aust. 1, Aust. 2, Aust. 3, SE Asian 1, SE Asian 2, N. American, HFO (d/c), HFO (u/c), M. Eastern, and M. Eastern (w). Asphaltenes from the S. Pacific oil were not analysed however, due to insufficient asphaltene yield. As a result, asphaltenes from ten oils were analysed and compared using IR spectroscopy. *The results presented herein have been published (Riley et al. 2016).*

4.4.1. Method Uncertainty

For the comparison of FTIR spectra for C₅ asphaltene fractions, some variability is expected, given the sample preparation (asphaltene precipitation) required. Since asphaltenes are a solubility fraction where precipitation is highly dependent on solvent-to-oil ratio, temperature, time and chemical composition of the oil itself, the asphaltene spectra are not expected to necessarily provide a point for point overlay (Podgorski et al. 2013, Edmonds et al. 1999, Tojima et al. 1998).

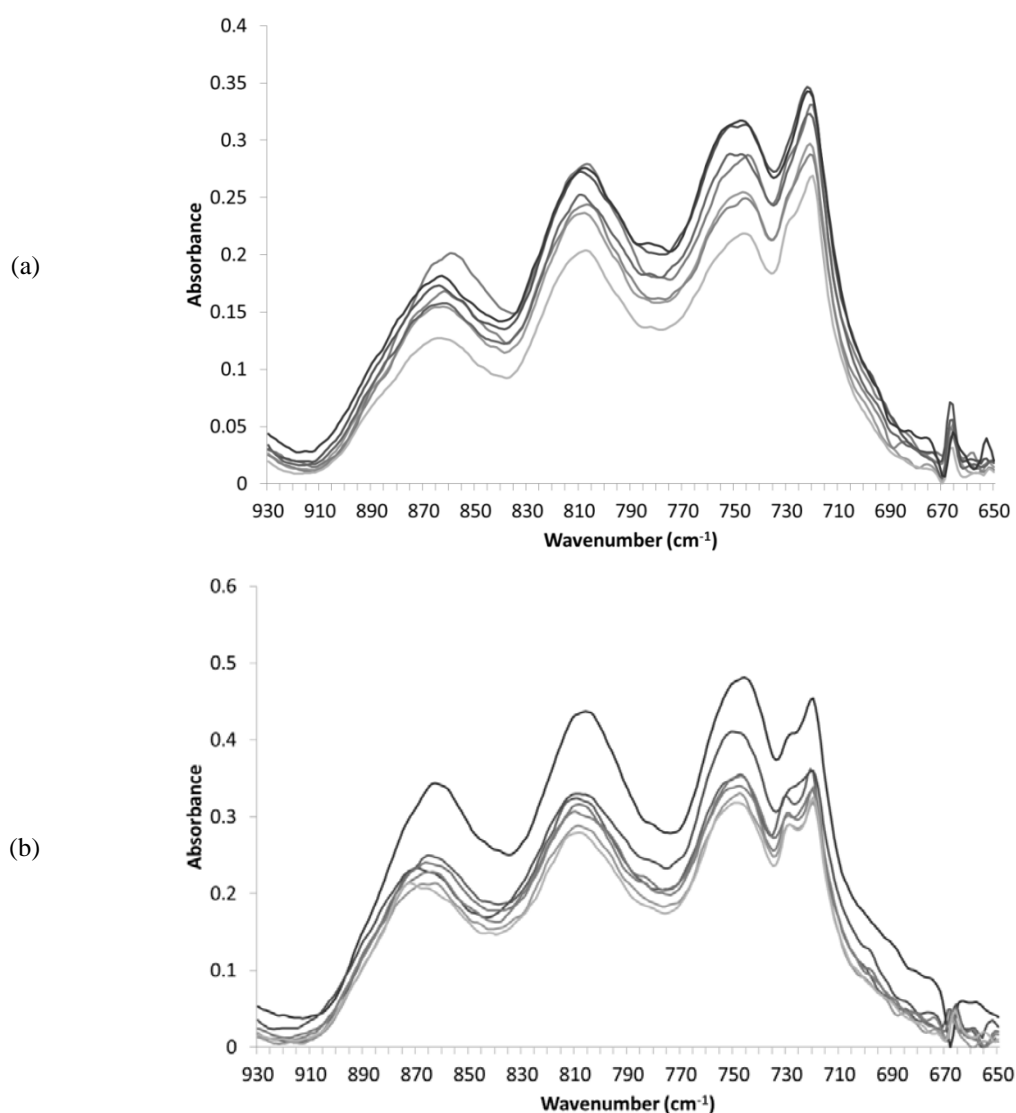


Figure 4.8: Overlays of Region 1 IR spectra (wavenumber range 650 – 930 cm⁻¹) for replicates: (a) M. Eastern asphaltenes; and (b) HFO (u/c) asphaltenes.

To account for potential variability in asphaltene spectra, the asphaltenes for the M. Eastern crude oil and the HFO (u/c) were each extracted 7 times and their FTIR spectra compared to determine the method repeatability (Figures 4.8 and 4.9). The asphaltene fractions of all other oils were extracted in duplicate (with the exception of Aust. 2). Overlays of IR spectra from replicate asphaltenes were visually compared to ensure that any characteristics that were used for comparison with different oils were repeatable (Figures 4.8 and 4.9).

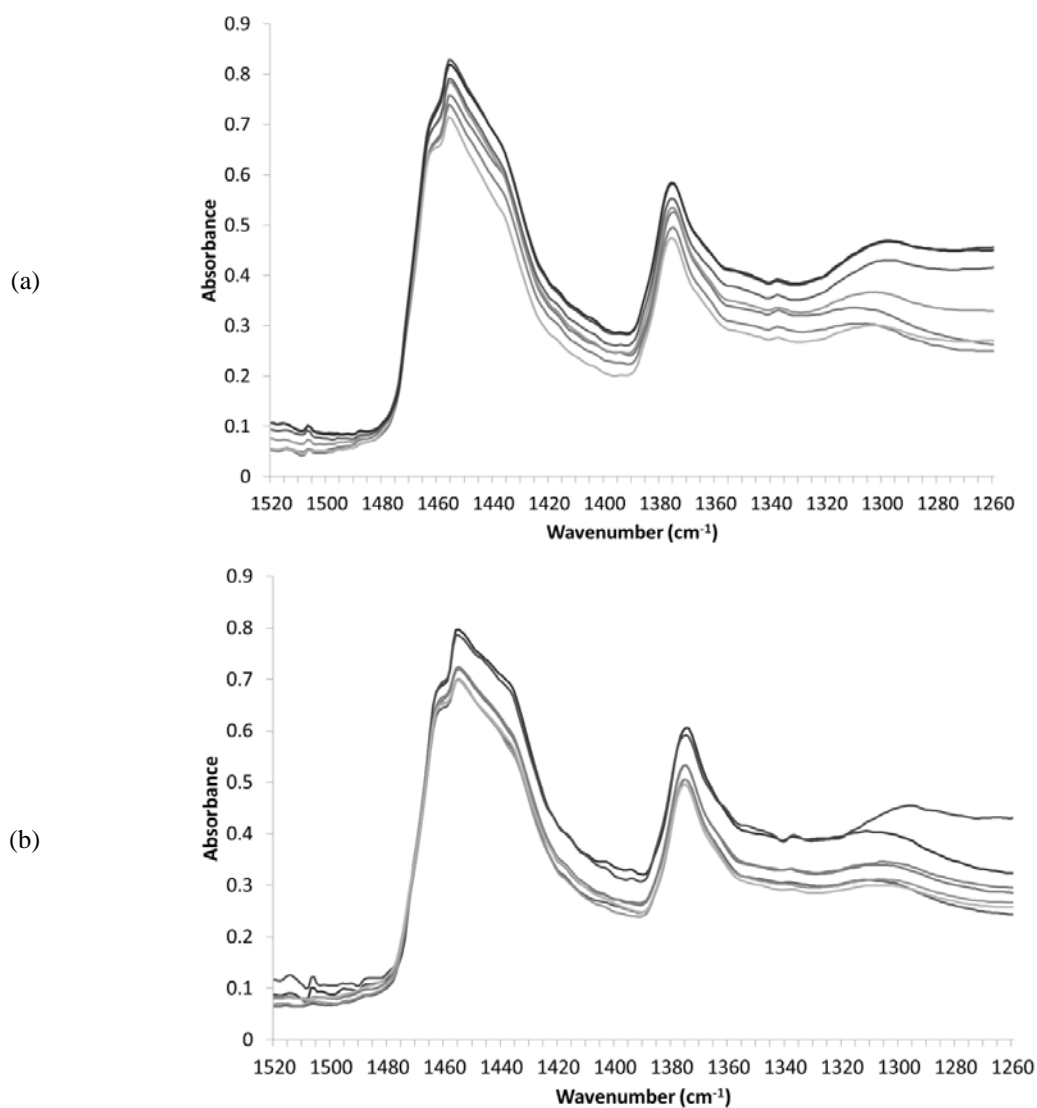


Figure 4.9: Overlays of Region 2 IR spectra (wavenumber range 1260 – 1520 cm⁻¹) for replicates: (a) M. Eastern asphaltenes; and (b) HFO (u/c) asphaltenes.

4.4.2. Visual Interpretation of IR Spectra

As mentioned in Chapter 2, Region 1 (650–930 cm^{-1}) and Region 2 (1260–1520 cm^{-1}) of the IR spectra were used for the comparison of asphaltenes. Regions 1 and 2 were chosen based on two principles: (1) Regions 1 and 2 are known regions of the IR spectra that do not weather for whole oils (as per ASTM D3414-98); and (2) Regions 1 and 2 were most probative when comparing asphaltenes. Region 1 corresponded to aromatic C–H out-of-plane bending modes, whilst Region 2 corresponded to a range of alkane C–H₂ and C–H₃ bending modes (Coelho et al. 2007, Pavia and Lampman 2001). Although the identification of IR vibrational modes corresponding to all peaks observed would be interesting, it was not required for the purpose of oil fingerprinting. Representative spectra for asphaltenes from each of the oils are provided in Figures 4.10 (Region 1) and 4.11 (Region 2), respectively, and discussed below.

4.4.2.1. IR Spectra and Physical Properties

Overall, the IR profiles of asphaltenes aligned with the physical properties of asphaltenes (specifically the visual appearance of asphaltenes) as discussed in Chapter 2. Asphaltenes with crystalline morphologies (M. Eastern, N. American and HFOs) shared similar IR spectra to one another. Asphaltenes with resinous morphologies also had similar IR spectra to one another (Aust. 1, Aust. 2, Aust. 3, SE Asian 1 and SE Asian 2); however consistent differences were observed between IR spectra of the crystalline and resinous asphaltenes. Resinous asphaltenes displayed a sharp double peak between 710–730 cm^{-1} in the IR spectra, but these peaks were either absent from the spectra for the crystalline asphaltenes or less apparent (see Figure 4.10 (g) and (h)). The peak around 1457 cm^{-1} was sharper and has a more clearly apparent doublet structure for the resinous asphaltenes than for the crystalline asphaltenes; the 1457 cm^{-1} peak was broader and wider for crystalline

asphaltenes. The Aust. 3 fraction consisted of a mixture of crystalline and resinous C5 material, and this was also reflected in the FTIR results. Aust. 3 asphaltenes were precipitated from the oil four times and each asphaltene fraction was analysed in duplicate. Two distinctive spectra for Aust. 3 were observed as shown in Figures 4.10 and 4.11. One Aust. 3 spectrum was similar in appearance to spectra obtained for resinous asphaltenes, whilst the other spectrum was similar in appearance to spectra obtained for crystalline asphaltenes. It seems that the Aust. 3 oil is highly sensitive to asphaltene precipitation conditions; further research will be needed to determine exactly which conditions are causing the variations observed in the asphaltene content.

4.4.2.2. Visual Comparison of IR Spectra

Figures 4.10 (Region 1) and 4.11 (Region 2) are presented and discussed herein. Region 1 and Region 2 of the IR spectra of asphaltenes were overlaid to reveal some obvious visual differences.

When comparing the IR spectra of resinous asphaltenes, SE Asian 1 was distinctly different from the other resinous asphaltenes for Region 1, but in particular Region 2. SE Asian 1 asphaltenes were very distinct due to the presence of sharp double peaks around $710\text{--}730\text{ cm}^{-1}$ and $1460\text{--}1475\text{ cm}^{-1}$. SE Asian 2 asphaltenes were also easily identified based on Regions 1 and 2. Although the Region 1 spectrum for SE Asian 2 is visually similar to SE Asian 1, Region 2 was distinctly different to SE Asian 1. Region 2 of the spectrum for SE Asian 2 asphaltenes was also different to the other resinous asphaltenes. SE Asian 2 asphaltenes generated the only IR spectra which displayed shoulders on either side of the peak at 1377 cm^{-1} .

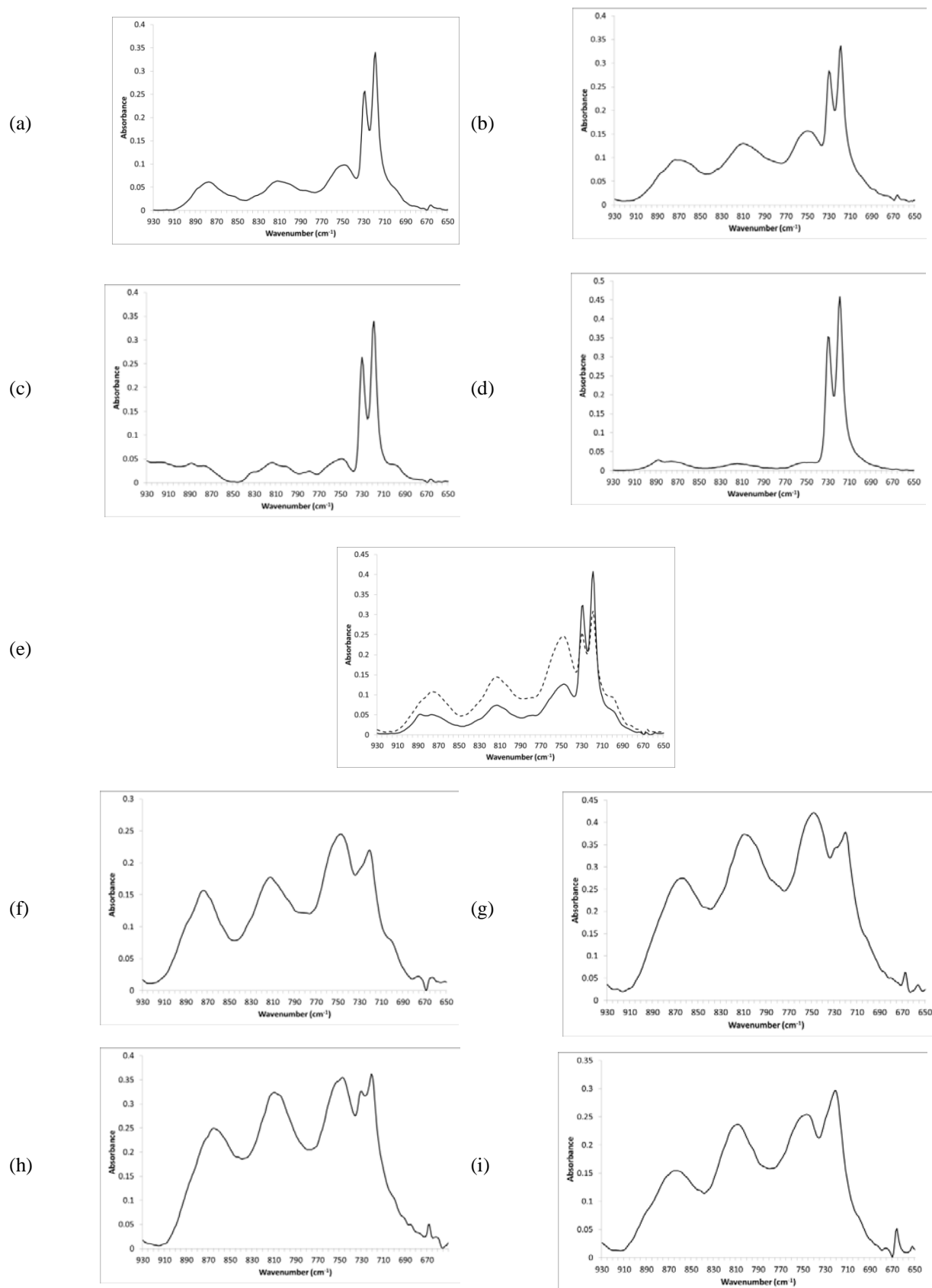


Figure 4.10: Representative Region 1 IR spectra (wavenumber range 650 – 930 cm⁻¹). The asphaltenes presented include (a) Aust. 1, (b) Aust. 2, (c) SE Asian 2, (d) SE Asian 1, (e) Aust. 3 (solid line = resinous, dotted = crystalline), (f) N. American, (g) HFO (d/c), (h) HFO (u/c) and (i) M. Eastern.

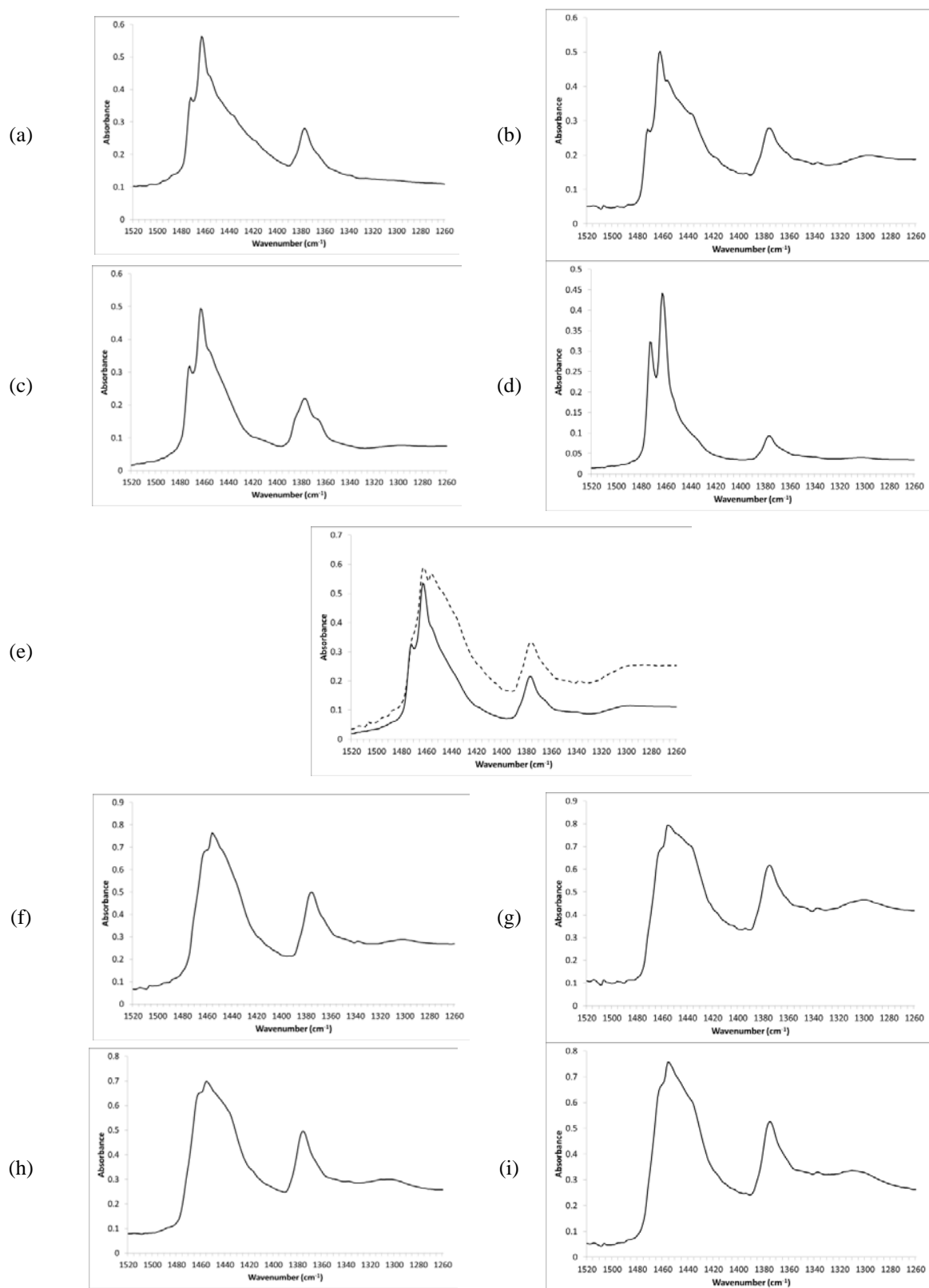


Figure 4.11: Representative Region 2 IR spectra (wavenumber range 1260 – 1520 cm^{-1}). The asphaltenes presented include (a) Aust. 1, (b) Aust. 2, (c) SE Asian 2, (d) SE Asian 1, (e) Aust. 3 (solid line = resinous, dotted = crystalline), (f) N. American, (g) HFO (d/c), (h) HFO (u/c) and (i) M. Eastern.

Despite variability in the IR spectra of duplicate Aust. 3 asphaltenes, Aust. 3 asphaltenes were still differentiated from all other asphaltenes independent of whether the resinous or crystalline spectrum was observed. The resinous Aust. 3 spectrum was most similar to that of Aust. 1 and Aust. 2, although not identical. The Aust. 3 spectrum displayed a double peak between 870–900 cm^{-1} which was absent from Aust. 1 and Aust. 2 spectra. Aust. 3 also has a strong shoulder at 701 cm^{-1} which was barely visible in the Aust. 1 spectra and not visible in the Aust. 2 spectra. Region 2 was similar in appearance for Aust. 3 when compared to both Aust. 1 and Aust. 2, although overlaying the spectra demonstrated a difference in the slope between 1400–1460 cm^{-1} ; the slope observed in the Aust. 3 spectrum was steeper (overlay not shown). The crystalline Aust. 3 spectrum was very specific. Region 1 was similar to the other Australian asphaltenes although the peaks between 740–930 cm^{-1} were significantly higher in the Aust. 3 spectrum. A double peak was observed around 1460 cm^{-1} in Region 2 for Aust. 3, which was not observed in any of the other oils analysed. It was likely that the crystalline spectrum for Aust. 3 was based on a combination of resinous and crystalline material, however this was the most crystalline spectrum obtained for Aust. 3.

Aust. 1 and Aust. 2 asphaltenes were more difficult to differentiate from one another. The spectra were similar in appearance, although the peaks between 730–930 cm^{-1} were relatively lower in absorbance for Aust. 1 compared to Aust. 2, when observing these peaks relative to the peaks between 710–730 cm^{-1} . The use of peak height ratio calculations was beneficial in this instance and will be discussed below. In the spectrum for Region 2, in particular between 1400 and 1480 cm^{-1} , the shoulder peaks are more prominent for Aust. 2 compared to Aust. 1. Although the differences between Aust. 1 and Aust. 2 seem minor, these differences were consistent when observing the replicate asphaltene fractions.

The differentiation of crystalline asphaltenes was mainly based on Region 1 of the IR spectra. The HFO (u/c) spectrum was different in Region 1 based on the double peak present

at $710\text{--}730\text{ cm}^{-1}$ which was not observed in Region 1 for the remaining asphaltenes. M. Eastern asphaltenes were identified by the high ratio of the peak at 719 cm^{-1} compared to the other peaks in the Region 1. When comparing the N. American and HFO (d/c) asphaltenes, the broad peak at 1460 cm^{-1} in Region 2 shows a shoulder around 1440 cm^{-1} for HFO (d/c) which was much less apparent for N. American asphaltenes. Although the Region 1 spectra of HFO (d/c) and N. American asphaltenes seem similar in appearance, overlaying these two spectra (Figure 4.12) showed clear differences between the two asphaltene fractions. The spectrum for N. American asphaltenes exhibited a peak at 876 cm^{-1} whilst the spectrum for HFO (d/c) asphaltenes exhibited a peak at 867 cm^{-1} .

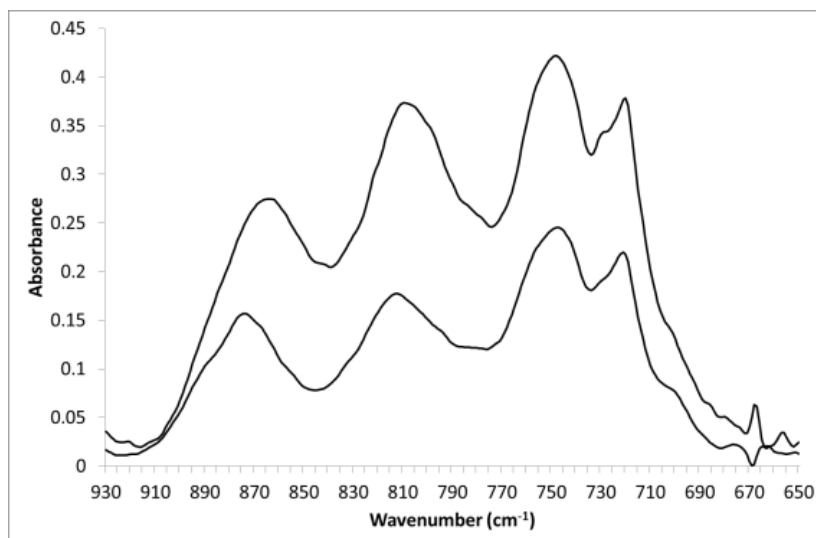


Figure 4.12: Region 1 comparison for N. American and HFO (d/c) asphaltenes (N. American = top trace, HFO (d/c) = bottom trace).

Based on the visual comparison of IR spectra of asphaltenes, seven oils (SE Asian 1, SE Asian 2, Aust. 3, HFO (u/c), HFO (d/c), N. American and M. Eastern) were clearly differentiated from all other oils. Aust. 1 and Aust. 2 were visually differentiated based on minor variations; however it was recommended to conduct peak height ratio analysis to confirm these findings.

4.4.2.3. Un-weathered Versus Weathered Asphaltenes

The IR spectra of the M. Eastern and M. Eastern (w) asphaltenes are shown in Figure 4.13. Despite five months of weathering, the IR spectra of M. Eastern and M. Eastern (w) asphaltenes were very similar in appearance. The main differences between spectra were observed between 870 and 930 cm^{-1} in Region 1 and between 1260 and 1310 cm^{-1} in Region 2. In these identified spectral regions, the spectrum for the M. Eastern (w) asphaltenes showed a higher absorbance as compared to the spectrum for the M. Eastern asphaltenes. An additional band structure around 880 cm^{-1} was also observed in the M. Eastern (w) asphaltenes which was not observed in the M. Eastern asphaltenes. It is known that weathering effects are present in whole oil IR spectra between 900 and 1300 cm^{-1} (refer to ASTM D 3414_98). It was therefore reasonable to infer that the observed differences between IR spectra were due to weathering (Robustillo et al. 2012).

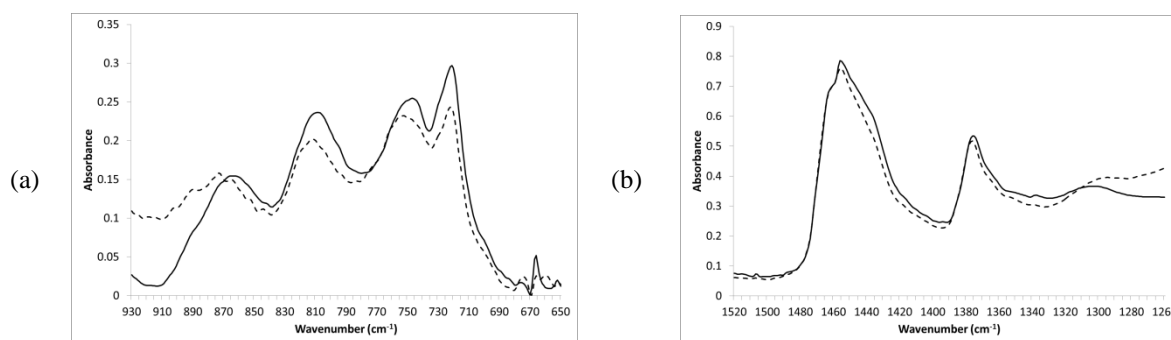


Figure 4.13: Representative IR spectra of M. Eastern weathered and un-weathered asphaltenes (M. Eastern weathered = dotted line, un-weathered = solid line): (a) Region 1 (650–930 cm^{-1}) and (b) Region 2 (1260–1520 cm^{-1}).

4.4.3. Peak Height Ratio Comparisons

The approach to comparing the FTIR peak height ratios between samples to determine if two samples have the same FTIR spectra was analogous to the manner in which the CEN method uses diagnostic ratios from GC analyses (CEN 2012). In short, an acceptance or

threshold level is determined for peak height ratios based on repeatability data. The aim was to set one threshold value that can be used for all peak height ratio comparisons, rather than to set specific acceptance levels for each ratio separately. Two samples that need to be compared are analysed and the peak height ratios are calculated for each sample separately. The mean value of the two samples is then determined for each peak height ratio, as is the absolute difference between the peak height ratios from both samples. The relative difference is calculated by expressing the absolute difference as a percentage of the mean of the two peak height ratios. This relative difference is then compared to the threshold level. If the relative difference is higher than the threshold, the peak height ratios of the two samples are considered different, and vice versa. Therefore, if all peak height ratios used for comparison fall within the threshold levels, the oils cannot be differentiated and the oils require further analysis using the CEN method. If only one peak height ratio is higher than the threshold, the two samples are considered to have different origins.

In order to determine an acceptable threshold level for the comparison of peak height ratios, it was necessary to determine the repeatability of the peak height ratios. It was observed that individual IR spectra for any single asphaltene fraction did not contain the collective number of peaks that were identified in the IR spectra across all of the studied asphaltenes. Ideally, one asphaltene standard could be developed that contains all of the distinctive IR peaks for a wide range of oil types. However, as a standard of this kind is not currently available, the seven replicate M. Eastern and HFO (u/c) asphaltenes were analysed to determine the repeatability of the peak height ratios. Universal threshold levels were then set from repeatability data. M. Eastern and HFO (u/c) oils were chosen for replicate asphaltene precipitation based on the sufficient asphaltene yields obtained from these two oils. Table 4.2 shows the RSD values obtained for the peak height ratios of replicate M. Eastern and HFO (u/c) asphaltenes.

Table 4.2: RSDs and peak height ratio thresholds calculated for the IR spectra of asphaltenes. Calculations were based on replicate asphaltene fractions obtained from M. Eastern and HFO (u/c) oils.

Peak height ratio	M. Eastern		HFO (u/c)	
	RSD (%) n=7	Threshold (2.8 * RSD) (%)	RSD (%) n=7	Threshold (2.8 * RSD) (%)
1463/1377	4.5	13	5.1	14
1457/1377	2.7	8	2.6	7
1437/1377	1.6	5	1.6	4
1368/1377	2.3	6	2.1	6
867/719	7.2	20	5.5	15
809/719	3.8	11	3.8	11
748/719	5.2	15	5.6	16
729/719	Not present	Not present	1.5	4

As observed in Table 4.2, the RSDs calculated for the peak height ratios were above 5%, which is the default RSD limit used in the CEN method (CEN, 2012). Given that the C5 asphaltene fractions are solubility classes, the higher RSDs were to be expected. The threshold used for deciding whether compared asphaltenes were from the same origin, was based on a 95% confidence level, and was calculated by multiplying the RSD values by 2.8 in the same manner performed in the CEN method (CEN 2012). As indicated in Table 4.2, the threshold levels calculated from the peak height ratios of replicate asphaltene fractions are at or below and RSD of 20%. Based on replicate results, a threshold level of 20% was set for the comparison of asphaltenes using peak height ratios. It may be necessary to adjust this threshold level over time when more replicates and other oils have been analysed. The duplicate asphaltene fractions obtained from the remaining oils were also analysed as an internal quality control check of the threshold level. Asphaltene fractions that were known to be from the same oil needed to fall within the 20% threshold.

4.4.4. Comparison of Peak Height Ratios

Pairwise comparisons of asphaltenes were conducted using peak height ratios. The mean values of the M. Eastern and HFO (d/c) replicates were calculated and used for comparison to the other oils. For all other oils the duplicate asphaltene fractions were compared to each other and to the asphaltene fractions from the other oils, with the exceptions of Aust. 2 and M. Eastern (w), which were only compared to other asphaltenes due to the absence of a duplicate sample. Examples of pairwise comparisons are shown in Tables 4.3 and 4.4 for two resinous asphaltenes (Aust. 1 versus Aust. 2) and two crystalline asphaltenes (N. American versus HFO (d/c)), respectively.

As discussed above, the C₅ asphaltene fractions of Aust. 1 and Aust. 2 were hard to differentiate using visual examination alone. The results in Table 4.3 demonstrate that, although some peak height ratios of asphaltenes were considered the same, five peak height ratios were found to be significantly different. Even though Aust. 1 and Aust. 2 oils were from a similar geographical region, the oils were still correctly classified as being from different origins. The results for the comparison of the duplicate Aust. 1 asphaltenes are also shown in Table 4.3. In this case, all peak height ratios were within the 20% threshold and the duplicates were correctly classified as being from the same source.

N. American and HFO (d/c) asphaltenes were differentiated based on ratio comparisons due to substantial differences observed between four of the compared ratios. Each of the four differences were attributed to the presence of a peak or shoulder in one asphaltene spectrum and an absence of the same peak or shoulder in the other asphaltene spectrum. The results of duplicate comparisons are also shown for both N. American (Table 4.4(b)) and HFO (d/c) (Table 4.4(c)). In both sets of duplicates, all peak height ratios fell below the 20% threshold hence these duplicates were correctly classified as originating from the same source.

Table 4.3: Comparison of peak height ratios between Aust. 1 and Aust. 2 asphaltenes: (a), and comparison of peak height ratio data for duplicate Aust. 1 asphaltene fractions (b). If the relative difference for a single peak height ratio is greater than the threshold of 20%, the peak height ratio is classified as ‘different’; vice versa, the peak height ratio is classified as ‘not different’. A relative difference of 200 is obtained when a peak or shoulder is observed in one IR spectrum, which is not present in the other IR spectrum.

(a)	Ratio	Peak height ratios		Mean	Absolute difference	Relative difference (%)	Conclusion
		Aust. 1	Aust. 2				
	1472/1377	1.34	1.00	1.17	0.34	29	Different
	1463/1377	2.01	1.80	1.90	0.21	11	Not different
	1457/1377	1.58	1.50	1.54	0.08	5	Not different
	1437/1377	1.14	1.15	1.15	0.01	1	Not different
	1368/1377	0.75	0.83	0.79	0.08	10	Not different
	888/719	0.14	0.19	0.17	0.05	32	Different
	877/719	0.18	0.27	0.23	0.09	40	Different
	814/719	0.18	0.38	0.28	0.19	69	Different
	748/719	0.29	0.46	0.38	0.17	46	Different
	729/719	0.75	0.83	0.79	0.07	9	Not different

(b)	Ratio	Peak height ratios		Mean	Absolute difference	Relative difference (%)	Conclusion
		Aust. 1	Aust. 1 duplicate				
	1472/1377	1.34	1.33	1.33	0.00	0	Not different
	1463/1377	2.01	2.01	2.01	0.00	0	Not different
	1457/1377	1.58	1.61	1.60	0.02	1	Not different
	1437/1377	1.14	1.14	1.14	0.00	0	Not different
	1368/1377	0.75	0.73	0.74	0.01	2	Not different
	888/719	0.14	0.15	0.14	0.01	5	Not different
	877/719	0.18	0.19	0.18	0.01	4	Not different
	814/719	0.18	0.19	0.19	0.01	5	Not different
	748/719	0.29	0.30	0.30	0.02	5	Not different
	729/719	0.75	0.75	0.75	0.00	0	Not different

Table 4.4: Comparison of peak height ratios between N. American and HFO (d/c) asphaltenes: (a), comparison of peak height ratios data for duplicate N. American asphaltene fractions (b), and comparison of peak height ratios for duplicate HFO (d/c) asphaltene fractions (c). If the relative difference for a single peak height ratio is greater than the threshold of 20%, the peak height ratio is classified as ‘different’; vice versa, the peak height ratio is classified as ‘not different’. A relative difference of 200 is obtained when a peak or shoulder is observed in one IR spectrum, which is not present in the other IR spectrum.

(a)						
Ratio	Peak height ratios		Mean	Absolute difference	Relative difference (%)	Conclusion
	N. American	HFO (d/c)				
1463/1377	1.36	1.11	1.24	0.25	20	Not different
1457/1377	1.51	1.28	1.39	0.24	17	Not different
1437/1377	1.11	1.16	1.14	0.05	5	Not different
1368/1377	0.80	0.88	0.84	0.07	8	Not different
888/719	0.52	0.00	0.26	0.52	200	Different
877/719	0.72	0.00	0.36	0.72	200	Different
867/719	0.68	0.74	0.71	0.06	9	Not different
814/719	0.84	0.00	0.42	0.84	200	Different
809/719	0.00	1.01	0.50	1.01	200	Different
748/719	1.17	1.14	1.15	0.03	3	Not different

(b)						
Ratio	Peak height ratios		Mean	Absolute difference	Relative difference (%)	Conclusion
	N. American	N. American duplicate				
1463/1377	1.36	1.41	1.39	0.04	3	Not different
1457/1377	1.51	1.58	1.55	0.07	4	Not different
1437/1377	1.11	1.06	1.09	0.05	4	Not different
1368/1377	0.80	0.76	0.78	0.05	6	Not different
888/719	0.52	0.45	0.49	0.07	13	Not different
877/719	0.72	0.64	0.68	0.09	13	Not different
867/719	0.68	0.60	0.64	0.08	12	Not different
814/719	0.84	0.79	0.82	0.05	6	Not different
748/719	1.17	1.13	1.15	0.03	3	Not different

(c)						
Ratio	Peak height ratios		Mean	Absolute difference	Relative difference (%)	Conclusion
	HFO (d/c)	HFO (d/c) duplicate				
1463/1377	1.11	1.10	1.11	0.02	1	Not different
1457/1377	1.28	1.28	1.28	0.01	1	Not different
1437/1377	1.16	1.20	1.18	0.04	3	Not different
1368/1377	0.88	0.88	0.88	0.00	0	Not different
867/719	0.74	0.78	0.76	0.04	6	Not different
809/719	1.01	1.06	1.03	0.06	5	Not different
748/719	1.14	1.27	1.20	0.13	11	Not different

The same pairwise ratio comparisons were performed for asphaltenes from the remaining oils. Importantly, peak height ratios for all duplicate asphaltene fractions fell within the 20% threshold; hence were correctly identified as being from the same origin (as the true origins of duplicates were known, identification conclusions could be confirmed). The only oil for which duplicate asphaltenes were not identified as being the same was Aust. 3, but this result is also correct. As previously discussed, the Aust. 3 oil contained a mixture of crystalline or resinous asphaltenes which provided for two different IR spectra. The fact that the method considers the duplicate asphaltene fractions from Aust. 3 to be different is therefore appropriate. Importantly, and despite the variance in Aust. 3 duplicate spectra, both the resinous and crystalline Aust. 3 spectra were differentiated from all other asphaltene spectra. From a casework perspective, it would be necessary to conduct multiple precipitations and analysis on any sample that is identified as having a composite (mixture of resinous and crystalline) visual appearance. This will eliminate any problems during comparison that may arise due to the existence of two different spectra for the same oil.

When comparing all of the studied oils to one another using ratios, all oils from different origins were correctly differentiated. The M. Eastern (w) asphaltenes were also included in this comparison and, interestingly, the M. Eastern (w) asphaltenes were shown to be the same as the M. Eastern (mean) asphaltenes, yet different to all the other asphaltenes. This ratio data further supported the visual similarities observed between the weathered and un-weathered M. Eastern IR spectra.

Through combining peak height ratios with visual interpretation of asphaltene IR spectra, the studied oils were correctly classified. This classification consisted of correct inclusion as well as exclusion of oils. Although further research will need to be conducted, the results demonstrate that the method is potentially also able to discern the geographical origin of oils.

4.4.5. Overall Evaluation of IR Profiling

Firstly, the IR profiling method developed herein met the operational requirements of a forensic method. IR profiling proved to be cost effective, rapid, non-destructive and capable of analysing small sample sizes suited to the asphaltenes yields expected from casework. Furthermore, asphaltenes were successfully analysed in a solid state without chemical alteration prior to analysis.

The developed proof-of-concept spectroscopic method in this study demonstrates significant potential to offer additional information in oil spill investigations through the chemical profiling of asphaltene fractions. All ten crude and heavy fuel oils used in this study (excluding the weathered oil sample) could be differentiated based on IR profiling of asphaltenes. One oil did not yield an asphaltene fraction and was hence considered different to all the other oils in this study. Visual interpretation, combined with peak height ratio analysis of IR spectra, was capable of distinguishing the remaining nine oils from one another. Duplicate asphaltenes were also classified correctly. For one oil sample, the asphaltene fraction appeared to be highly sensitive to precipitation conditions. Further research will be required to determine exactly which conditions are causing this. Interestingly, the developed IR profiling method did not differentiate a non-weathered oil sample from a weathered oil sample, despite originating from the exact same source. This is promising as it suggests that the developed IR method may avoid significant issues associated with the interpretation of weathered oils during oil fingerprinting. Prior to operational application, the method will need to be evaluated by analysing a larger number of crude oils and HFOs as well as more weathered oils.

4.5. Chapter 4 Summary

In regards to UV-Vis, Raman, and fluorescence spectroscopy, fluorescence spectroscopy was the only technique that aligned reasonably well with the requirements of a forensic method. Fluorescence profiling allowed for rapid and cost effective analysis, which produced repeatable asphaltene profiles. Fluorescence spectroscopy also provided a desirable degree of discrimination between asphaltenes from different oils. Fluorescence profiling also allowed for the differentiation of asphaltenes with different size aromatic structures as indicated by blue shifts (smaller aromatics) or red shifts (larger aromatics) in fluorescence spectra (Mullins 2010).

Despite the relatively high probative value of fluorescence spectra, fluorescence profiling could not differentiate all oils from one another. Furthermore, asphaltenes could not be analysed in a solid state as the dissolution of asphaltenes in solvent was required prior to analysis. Dissolving asphaltenes prior to analysis may result in asphaltene aggregation and possible changes in chemical composition of asphaltenes which is not ideal for forensic comparisons. In contrast, IR profiling was capable of analysing solid state asphaltenes and provided greater discrimination of oils when comparing asphaltene spectra. All crude oils of different origin were differentiated successfully using IR profiling and oils from the same origin were correctly grouped together. Additionally, IR profiling was cost effective, rapid, non-destructive and capable of analysing small sample sizes; hence accommodating all of the requirements for a forensic method. Consequently, the developed IR method was deemed the most suitable spectroscopic asphaltene profiling method for oil spill investigations. The IR profiling method is further tested during the blind study in Chapter 7 to determine if the IR profiles of asphaltenes can be interpreted reliably.

It should be reinforced that the IR method is not be considered as a standalone approach to oil spill investigations. As stated previously, the methods developed herein have been

designed to complement the existing CEN or other oil fingerprinting methods. This IR method would be best applied as a pre-screening method for application in the oil fingerprinting process ahead of standard analysis. If two oils cannot be differentiated through IR profiling, the oils should be analysed further using the conventional oil fingerprinting method. Secondary asphaltene profiling is also recommended to support the conclusions derived from IR profiling by providing additional information to assist in drawing conclusions. A range of thermal degradation techniques are explored in Chapter 5 to determine if a suitable secondary profiling method can be developed to support IR asphaltene profiling.

Chapter 5 - Thermal Profiling of Asphaltenes

Similarly to Chapter 4, Chapter 5 addresses Research Questions 1 and 2. To address Research Question 1, each of the thermal asphaltene profiling methods was evaluated against the forensic requirements specified in Chapter 1. To address Research Question 2, each of the asphaltene profiling methods was compared to one another to determine which thermal method was most suitable for oil spill investigations. Comparisons were based on the ability of each method to address the forensic requirements specified for Research Question 1. Asphaltene profiling methods were developed for three thermal degradation techniques: EGA-MS, TGA-DSC, and Py-GC-MS.

Although thermal degradation techniques are destructive, these techniques are advantageous as they allow for the breakdown of asphaltene molecules into smaller, easier to analyse molecules. It makes sense that thermal degradation of asphaltenes would be conducted following non-destructive IR profiling with an aim to provide further discrimination during investigations.

5.1. EGA-MS

EGA-MS uses a high temperature furnace to heat solid samples and generate evolved gases. These gases are then analysed using a mass spectrometer (Dollimore et al. 1984). EGA-MS can be conducted at a single furnace temperature; however, in most applications the temperature is slowly ramped to allow for a slow release of gases (i.e., the most volatile compounds will be released first followed by less volatile compounds at higher temperatures). EGA-MS provides data that can be processed quickly, which is desirable for casework (Frontier Laboratories 2012, Yang et al. 2012). EGA-MS was appealing in this study due to the ability to analyse very small, solid-state asphaltenes as obtained directly from precipitation. Also, the sample size required for EGA-MS analysis was so small, that

the destructive nature of EGA-MS was not detrimental. The data output produced by EGA-MS is easy to interpret, which is desirable.

A technical note provided by Frontier Laboratories (2012) discusses the forensic application of EGA-MS for the analysis and comparison of 21 natural and synthetic fibres. A database was developed using the 21 fibres that catalogued the average mass spectra calculated from each peak in the thermograms generated from EGA-MS. One fibre was selected as an 'unknown' and was searched against the fibre database. A short candidate list of 'suspect' fibres with high percentage matches to the unknown fibre was produced from the database. Percentage matches were based on the similarity of the average mass spectra between the unknown fibre and the suspect fibres. Thermograms were visually compared between the unknown fibre and each of the suspect fibres on the candidate list. If the thermogram of a suspect fibre differed visually to the thermogram of the unknown fibre, the suspect fibre was excluded from the comparison. Identification of the unknown fibre was confirmed when both the average mass spectra and the visual thermogram profiles of the unknown fibre were the same as a suspect fibre. This fibre study was appealing as the ability to produce a library for the forensic comparison of asphaltenes would allow for time efficient and objective exclusions of non-related oil samples during investigations.

As mentioned previously, another key factor that made EGA-MS appealing was the ability to handle small sample sizes. In the Frontier Laboratories Multi-Shot Pyrolyzer Model EGA/Py-3030D Operation Manual, it was suggested to analyse 100 µg of polystyrene standard, which would be of similar weight to the small sample scrapings used by Yang et al. (2012) for the forensic analysis of polystyrene in paints. The technical note by Frontier Laboratories (2012) recommended the analysis of natural and synthetic fibres at a weight of 300 µg per sample. Whilst there was no available literature that specified the sample weight

required for EGA-MS of asphaltenes, it is likely to be a very small weight similar to the weights in the discussed examples.

5.1.1. Method Uncertainty/Comparison of Asphaltene Thermograms

To gauge method uncertainty, thermograms obtained from replicate asphaltene fractions were observed. Seven replicate asphaltene extracts were precipitated from M. Eastern oil and HFO (u/c). Triplicates analysis was feasible on most of the remaining oils due to the considerably smaller sample size required for EGA-MS profiling as compared to other methods tested in this research. Triplicate asphaltene fractions were precipitated from the three Australian oils as well as the two SE Asian oils. As HFO (d/c) thermograms were unlikely to differ from HFO (u/c) thermograms, HFO (d/c) was only analysed in duplicate. M. Eastern (w) was also included in the sample-set however only a single precipitated asphaltene fraction was analysed. Two of the seven HFO (u/c) asphaltenes were analysed at the beginning of the batch analysis followed by the analysis of the five remaining HFO (u/c) asphaltenes at the conclusion of the batch. This process ensured that the performance of the instrument did not deviate throughout the course of the batch analysis.

Asphaltene thermograms were visually interpreted. When interpreting thermograms, all peaks around 260°C were referred to as Peak 1 whilst all peaks at 470°C were referred to as Peak 2. The first consideration when interpreting thermograms was to assess repeatability by observing the replicate results for each of the asphaltenes. Figure 5.1 shows the thermograms for all of the tested asphaltenes. Firstly, the seven replicate HFO (u/c) thermogram profiles were visually repeatable for both Peaks 1 and 2 (Figure 5.1 (b)). The seven M. Eastern profiles were repeatable for Peak 2 however, some variance was observed for Peak 1 (Figure 5.1 (a)). Despite this variability, it is still obvious that both the HFO (u/c) and M. Eastern profiles are Peak 2 dominant; Peak 2 is higher in intensity than Peak 1.

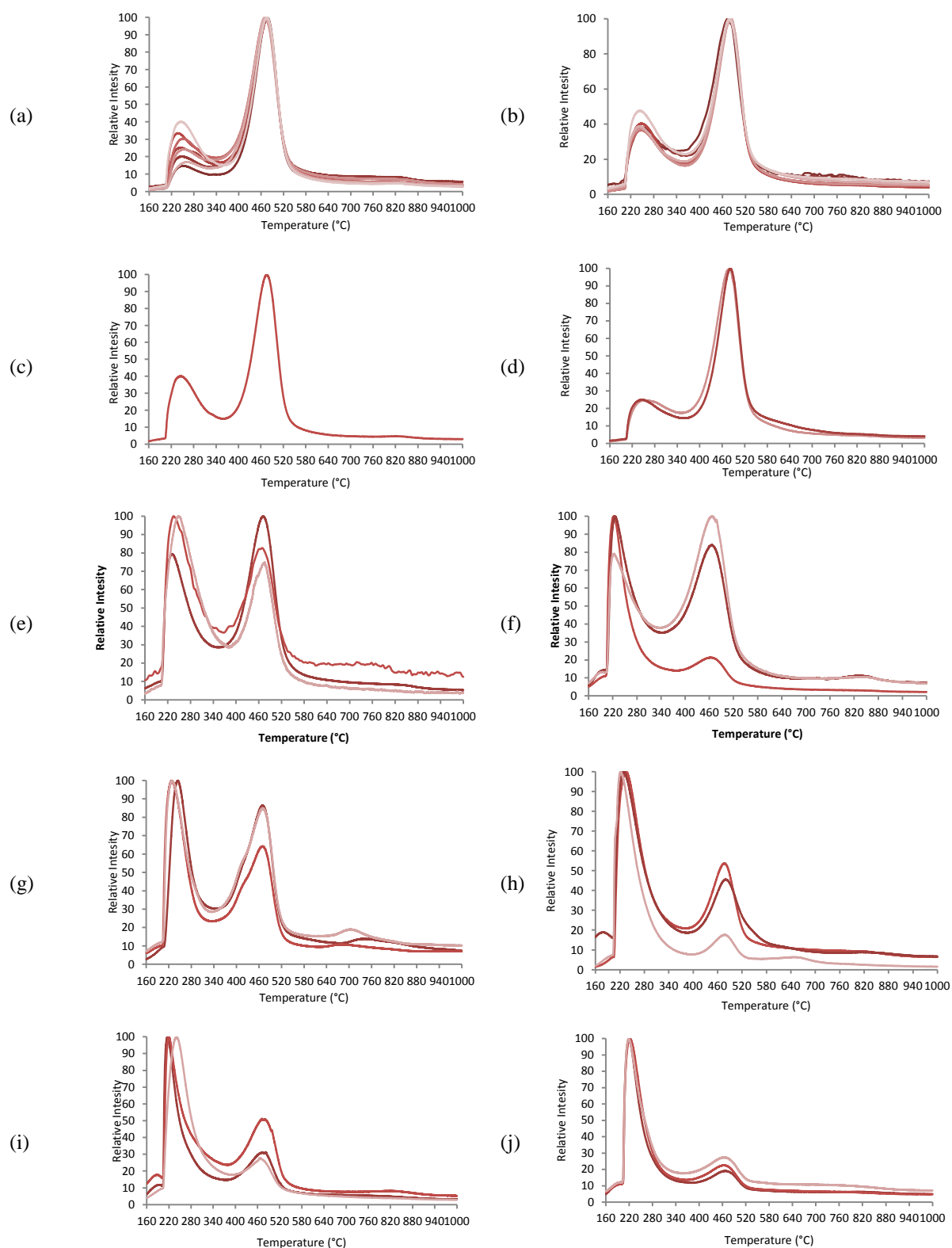


Figure 5.1: Asphaltene thermograms generated from EGA-MS. Asphaltenes exhibiting Peak 2 dominant thermograms included (a) M. Eastern replicates, (b) HFO (u/c) replicates, (c) M. Eastern (w) and (d) HFO (d/c) duplicates.

Asphaltenes exhibited mixed thermogram profiles included (e) N. American triplicates and (f) Aust. 3 triplicates.

Asphaltenes exhibiting Peak 1 dominant thermograms included (g) SE Asian 2 triplicates, (h) SE Asian 1 triplicates, (i) Aust. 1 triplicates and (j) Aust. 2 triplicates.

In regards to triplicates, significant variability was observed for N. American and Aust. 3 profiles (Figure 5.1 (e) and (f)). Mixed profiles were observed for the triplicate asphaltene fractions from both of these oils with both Peak 1 dominant and Peak 2 dominant profiles observed. The triplicate profiles observed for SE Asian 2, SE Asian 1 and Aust. 1 all repeatedly exhibited Peak 1 dominance however variability was still observed in peak intensities across all three oils (Figure 5.1 (g), (h) and (i)). Aust. 2 triplicates were the only triplicate asphaltene fractions to exhibit repeatable thermogram profiles, also with Peak 1 dominance (Figure 5.1 (j)). The duplicate HFO (d/c) profiles were also repeatable, however exhibited Peak 2 dominance (Figure 5.1 (d)). The single M. Eastern (w) profile could not be assessed for repeatability however the weathered profile was consistent with that observed for the unweathered M. Eastern asphaltenes (Figure 5.1 (c)). Both weathered and unweathered asphaltene profiles were Peak 2 dominant which is interesting.

When considering the poor repeatability observed, it is quite difficult to compare asphaltene thermograms. Whilst it may be stated that M. Eastern, M. Eastern (w), HFO (u/c) and HFO (d/c) asphaltene profiles exhibited Peak 2 dominance and SE Asian 2, SE Asian 1, Aust. 1 and Aust. 2 asphaltenes exhibited Peak 1 dominance, this information is of limited probative value. The degree of variation in the mixed profiles obtained for Aust. 3 and N. American asphaltenes also suggests that EGA-MS may not be a feasible approach to asphaltene profiling. It is not possible to ascertain whether this variability is attributed to sample heterogeneity combined with the very small sample size that is being analysed, or if the analysis technique itself is simply not sufficiently repeatable. As a result, EGA-MS thermograms were not considered further for application in this research.

5.1.2. Method Uncertainty/Comparison of Asphaltene Mass Spectra

Despite the variability observed in thermograms, mass spectra for Peak 1 and Peak 2 were generated for comparison as shown in Figure 5.2. The aim was to determine if mass spectra could provide repeatable information that may still be useful for investigations. Mass spectra were generated from the maxima of Peaks 1 and 2 for each asphaltene thermogram. Average mass spectra were initially obtained for comparison (average of Peak 1 and average of Peak 2) however repeatability was observed to be more consistent between mass spectra of the peak maxima.

Whilst mass spectra were repeatable for M. Eastern and HFO (u/c) replicates and also for all other repeated asphaltene extracts (results not shown), mass spectra offered limited information for use in investigations. In fact, Peak 2 mass spectra were not probative at all; hence Peak 2 results are not reported herein. Out of interest however, the differences observed between asphaltenes for Peak 1 mass spectra have been reported. The mass spectra results are in agreement with the previously defined crystalline and resinous groupings, splitting asphaltenes into these two distinct groups. Mass spectra for resinous asphaltenes exhibited dominance in lower hydrocarbon masses including m/z 43, 57, 71 and 85 (Figure 5.2 (e–i)). Asphaltenes defined as resinous based on mass spectra included SE Asian 1, SE Asian 2, Aust. 1, Aust. 2 and Aust. 3. Conversely, the mass spectra for crystalline asphaltenes showed a more comprehensive array of masses, which also included higher masses such as m/z 111, 125 and 137 (Figure 5.2 (a)–(d)). Crystalline asphaltenes as defined by mass spectra included HFO (u/c), HFO (d/c), M. Eastern and N. American. Mass spectra were not generated for M. Eastern (w). Due to the limited suitability of using EGA-MS in asphaltene profiling, the M. Eastern (w) asphaltene fraction was conserved for other analyses

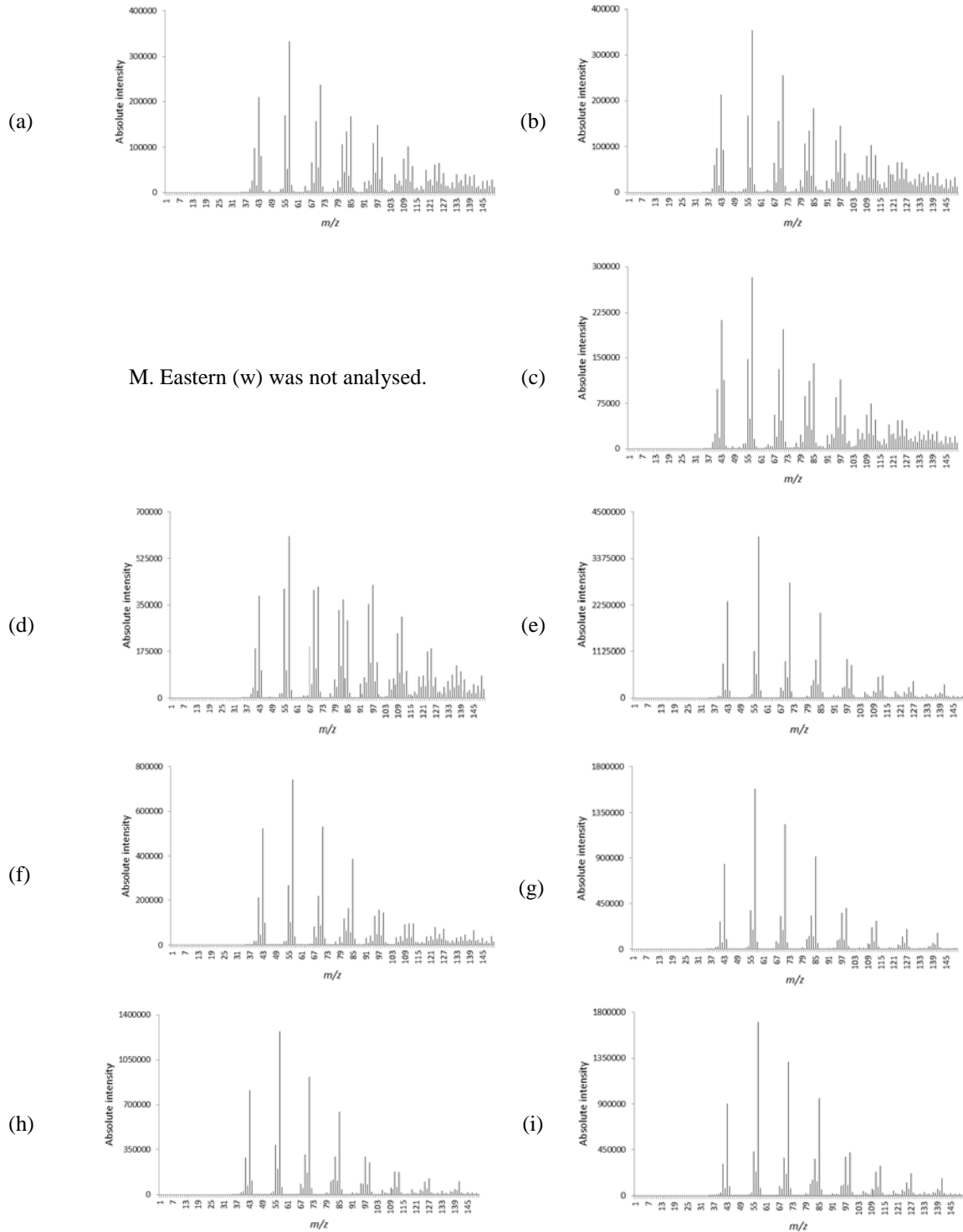


Figure 5.2: MS obtained from asphaltene thermograms using the maxima of Peak 1. Crystalline asphaltenes exhibiting MS dominated with smaller hydrocarbons (m/z 43, 57, 71, 85): (a) M. Eastern; (b) HFO (u/c); (c) HFO (d/c); (d) N. American. Resinous asphaltenes exhibiting a more comprehensive MS distribution including m/z 111, 125 and 137: (e) Aust. 3; (f) SE Asian 2; (g) SE Asian 1; (h) Aust. 1; and (i) Aust. 2.

5.1.3. Overall Evaluation of EGA-MS Profiling

EGA-MS thermograms generated from asphaltenes were not repeatable and did not offer sufficient probative information. Asphaltene mass spectra were repeatable however, offered limited probative information. In conclusion, EGA-MS profiling of asphaltenes was deemed unsuitable for assisting in oil spill investigations and was not further investigated.

5.2. TGA

It is necessary to reinforce that although both TGA and DSC analysis of asphaltenes was conducted (TGA-DSC combined), only the TGA results provided information suitable to oil fingerprinting. The DSC results did not provide probative information hence the results were not discussed herein.

TGA measures the mass change of a sample over a defined temperature range. Thermograms (or TG profiles) allow for the observation of decomposition stages as samples are heated, and also allow for the calculation of percentage mass changes during each decomposition stage. The 1st derivative TG profile (DTG profile) shows the rate of mass change in each decomposition stage and also indicates the temperature at which each mass change occurs most rapidly (Mothé et al. 2008). Although TGA is a specialised instrument that is destructive and requires lengthy analysis, the ability to analyse reasonably small sample sizes of around 1 mg was appealing. The probative value of TGA was also unknown prior to analysis and if the information garnered from TGA was highly probative, the value of the evidence may outweigh the aforementioned limitations.

TGA analysis of asphaltenes in the petroleum science literature is scarce; however, there are some studies such as Mothé et al. (2008) and Sarmah et al. (2010) that have provided preliminary insights into the capabilities of TGA to differentiate asphaltenes. Firstly, Sarmah et al. (2010) analysed and compared asphaltenes from three different oils and

determined that asphaltene decomposition occurred between 375–600°C in the TG profiles. Sarmah et al. (2010) then showed that, although all three asphaltenes exhibited a single stage mass loss, the overall percentage mass loss during this single decomposition stage was different across the three asphaltene fractions. The observations made by Sarmah et al. (2010) were promising for the application of TGA in oil fingerprinting. Secondly, Mothé et al. (2008) analysed a range of Brazilian asphalt samples using TGA and compared the subsequent TG and DTG profiles. Mothé et al. (2008) determined that asphaltene decomposition occurred as a single stage mass loss between 290–590°C as evident in the TG profiles (similarly to Sarmah et al. 2010), and that this thermal decomposition stage indicated the production of petroleum coke from asphaltenes. Using the DTG profile, maximum mass loss rate occurred around 450–460°C. Another interesting observation made by Mothé et al. (2008) was that, in one sample, a two stage mass loss was observed in the DTG profile; a peak at 350°C was observed that indicated the evaporation of asphalt additives prior to the thermal decomposition of asphaltenes at 462°C. The observed two-stage mass loss was very interesting as it suggested that impurities in asphaltenes (or in this case, asphalt) may in fact show a separate mass loss stage that is independent and occurs prior to the thermal decomposition of asphaltenes. It is therefore likely that co-precipitation of resins and waxes alongside asphaltenes may result in a second mass loss stage which would occur prior to asphaltene decomposition.

5.2.1. Method Uncertainty

To gauge method uncertainty, TG profiles were obtained from seven M. Eastern asphaltene replicates for comparison. From the replicate M. Eastern TG profiles, percentage mass losses were calculated. M. Eastern TG and DTG profiles are shown in Figure 5.3. Note,

only six of the seven M. Eastern profiles are shown in Figure 5.3. Due to gas flow malfunctioning, the profile for one of the M. Eastern replicates was not comparable.

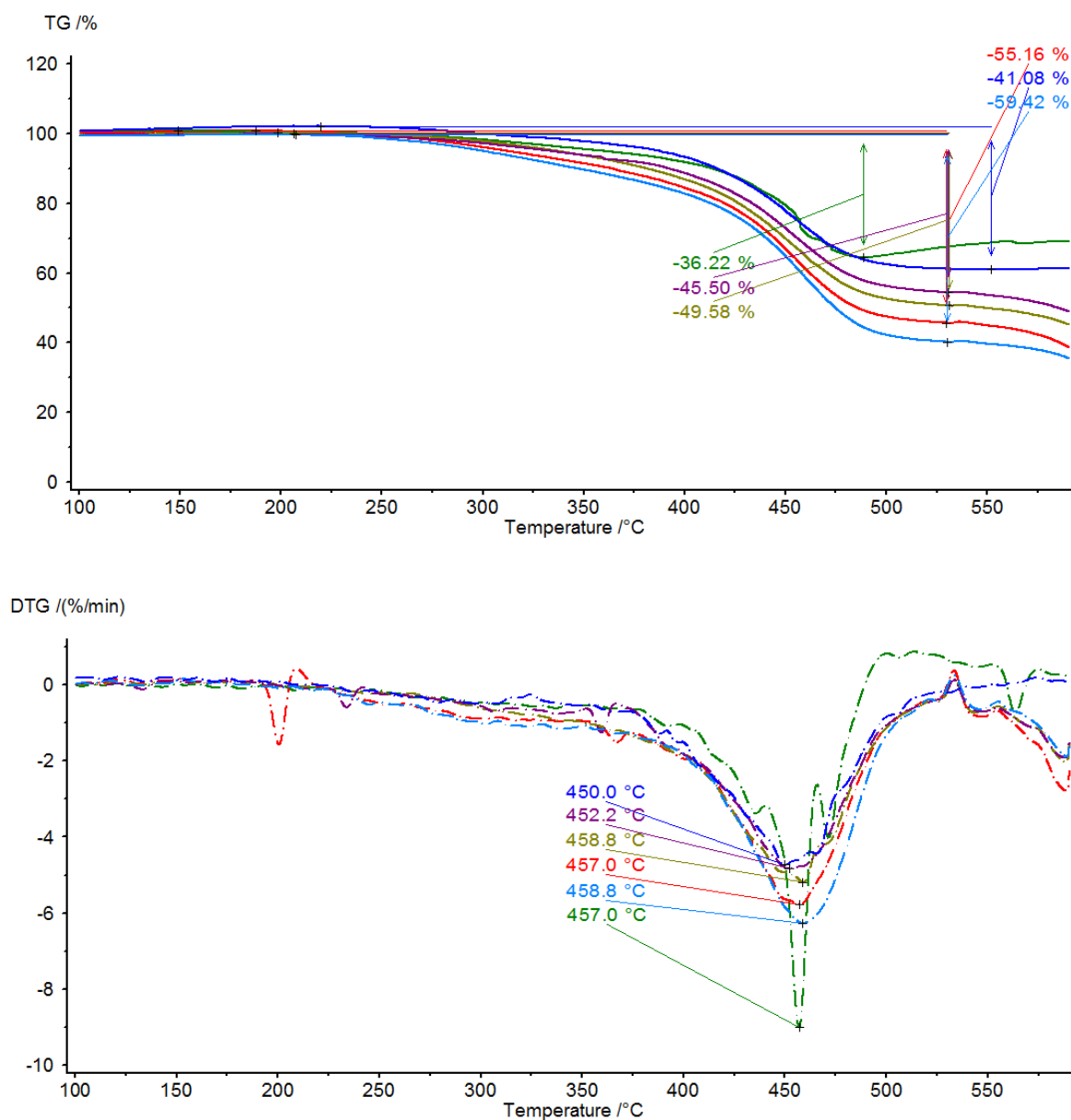


Figure 5.3: TG profiles and DTG profiles of M. Eastern replicate asphaltene fractions (TG profiles are on the top and DTG profiles are on the bottom). Percentage mass loss has been calculated on the TG profile using the DTG profiles. A mass change stage is indicated when the DTG profile deviates positively or negatively from zero; in this case, a negative deviation is observed in the DTG, hence a negative mass loss is observed in the TG profile.

A single-stage mass loss was observed in the TG profiles of M. Eastern asphaltenes. This single-stage mass loss was consistent with the thermal decomposition of asphaltenes to petroleum coke (Mothé et al. 2008). The DTG profile was generated to observe the decomposition stage, which was observed as a negative deviation from zero on the y-axis. The decomposition of M. Eastern asphaltenes started at 175°C and finished between 500°C and 550°C. Using this information from the DTG profiles, the percentage mass losses for the TG profiles were calculated and compared between replicates. Table 5.1 shows the replicate variability observed for the mass loss values. A high %RSD of 18% was calculated for mass loss values which indicated that the quantitative comparison of mass loss values was not a suitable avenue for asphaltene comparison.

As an alternative means of comparison, the temperature at which the maximum rate of mass loss occurred was calculated; this temperature was indicated by the peak maxima in DTG profiles. The maximum of a DTG peak represents the point at which the mass loss rate was greatest during each stage of mass loss. Interestingly, the DTG peak maxima for each replicate were very similar (Figure 5.3). As observed in Table 5.1 a much lower %RSD of 0.8% was calculated for the DTG peak maxima temperatures of replicates. This low %RSD indicated that DTG peak maxima were much less variable than mass loss values; hence better suited for asphaltene comparisons (Table 5.1).

Table 5.1: %RSD calculated from the six replicate M. Eastern asphaltene fractions (labelled 1–6 in the table below).

	1	2	3	4	5	6	Mean	SD	%RSD
Mass Change (%)	-36.22	-45.50	-49.58	-55.16	-41.08	-59.42	-47.83	8.68	18.15
DTG peak (°C)	457.0	452.2	458.2	457.0	450.0	458.8	455.6	3.7	0.8

In light of the replicate observations, it was decided that the best approach to the comparison of asphaltenes using TGA was to: (1) count and compare the number of mass loss stages as observed in TG profiles and DTG peaks; and (2) identify and compare the DTG peak maxima for each mass loss stage observed throughout DTG profiles.

It should be noted that the onset temperatures of each stage of mass loss in DTG profiles is often used as a comparable TGA characteristic. The onset temperature represents the temperature at which a mass loss stage begins. It quickly became evident for the M. Eastern replicates that the DTG profiles were not resolved enough to accurately determine the onset temperatures despite smoothing the DTG profiles prior to comparison. It is worth noting that all TG and DTG profiles shown have been smoothed to the same degree to allow for likewise comparisons. As observed in Figure 5.4, one M. Eastern asphaltene extract (the purple coloured line) generated a poorly resolved DTG baseline.

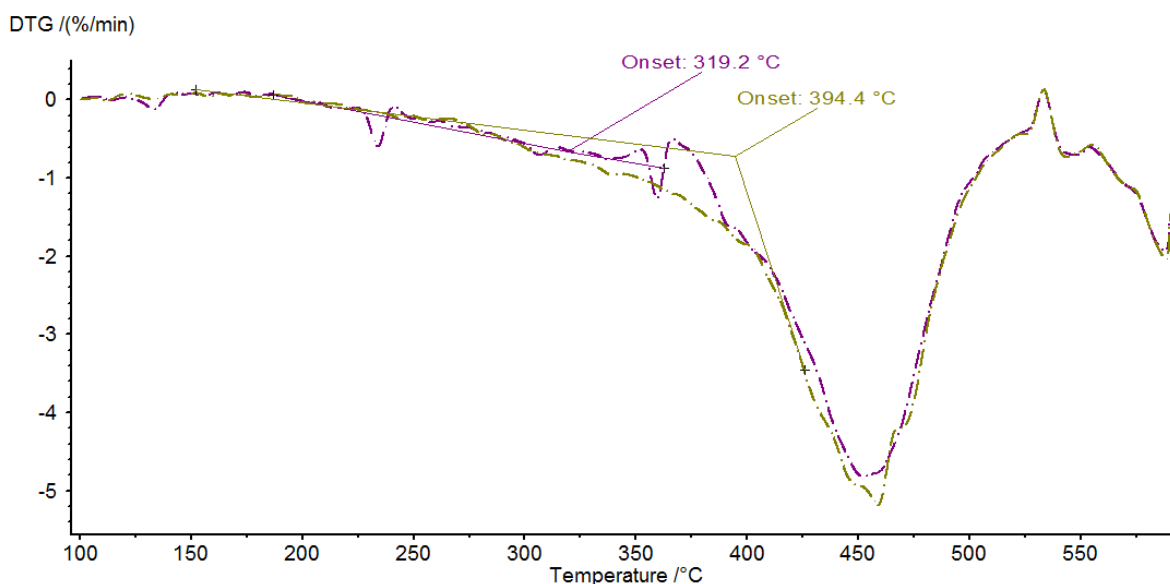


Figure 5.4: Irregularities in the DTG baseline of M. Eastern (purple coloured line) cause problems when calculating onset temperatures as correctly calculated with another M. Eastern extract (mustard coloured line).

The software attempted to calculate the onset temperature; however, due to the irregularities in the baseline, the calculated value was not a true representation of the onset temperature, which is correctly calculated with the mustard coloured line. The poor resolution of TG and DTG profiles was related to the small sample sizes used for analysis. To align with the requirements of oil spill investigations, the sample weight was maintained around 1 mg for TGA analysis. In terms of TGA analysis, this is a very small sample size. For example, Mothé et al. (2008) and Sarmah et al. (2010) used 5 mg and 10 mg of sample for TGA analysis, respectively. Heavier weights such as 5 mg or 10 mg can positively enhance the resolution of TG and DTG profiles by ensuring that there is an even spread of asphaltenes across the Al sample pan during analysis. An even spread of sample in the Al pan is important for maintaining even heating of the asphaltenes, hence producing more repeatable results for mass changes associated with temperature changes.

The calibration range of the TGA-DSC instrument used in this research was between 0.001–5000 mg. Testing a 1 mg sample weight was therefore not unreasonable; however, 1 mg has proven to increase the error for TGA profiling of asphaltenes as evident in the results discussed throughout this section.

5.2.2. Comparison of TG Profiles

To gauge the probative value of TG profiles of asphaltenes, a small selection of asphaltenes were first tested including HFO (d/c), HFO (u/c), N. American, SE Asian 1, SE Asian 2 and Aust. 2 asphaltenes. If TG profiles provided valuable information, the remaining asphaltenes would then also be tested for comparison too. DTG peaks were used to determine when mass loss stages occurred in the TG profiles; three distinct groups of asphaltenes were identified when comparing mass loss stages (Table 5.2).

Table 5.2: Collated data for DTG peak maxima's of asphaltenes. Three different DTG peaks were observed across the analysed asphaltenes.

Asphaltenes	Peak 1 (<340.0°C)	Peak 2 (341.0–439.0°C)	Peak 3 (>440.0°C)
Aust. 2	292.2	412.6	-
	303.1	427.1	-
SE Asian 1	305.3	-	465.5
	316.9	-	466.1
SE Asian 2	310.0	-	477.2
	311.9	-	447.0
N. American	321.0	-	448.0
	326.6	-	456.6
HFO (u/c)	-	-	461.3
	-	-	466.7
HFO (d/c)	-	-	459.1
	-	-	463.2
M. Eastern	-	-	450.0–457.0
	-	-	(replicate range)

Differentiation was based on the presence or absence of peaks in the DTG profiles of the asphaltenes. DTG peak maxima were observed in the studied asphaltenes in three different temperature brackets (or thresholds): Peak 1 was a maximum observed at <340.0°C, Peak 2 was a maximum observed between 341.0–439.0°C, and Peak 3 was a maximum observed at >440.0°C. It should be noted that the three identified temperature brackets (or thresholds) used to differentiate the asphaltenes have been generated as a conservative, qualitative way of comparing DTG profiles. As more asphaltenes are analysed, the temperature thresholds may become more resolved, which will allow for increased probative value. Based on the observed results, however, the distinction of only three temperature thresholds was identified. Asphaltenes that exhibited a single DTG peak were identified as single-stage mass loss asphaltenes, whilst asphaltenes that exhibited two DTG peaks were identified as two-stage mass loss asphaltenes.

The TG and DTG profiles of Aust. 2 asphaltenes were distinct from those of all other asphaltenes analysed in this study (Figure 5.5). The duplicate DTG profiles of Aust. 2 asphaltenes exhibited a two-stage mass loss as indicated by the presence of Peaks 1 and 2,

and the absence of Peak 3. The Peak 2 mass loss temperature aligns with asphaltene decomposition as reported by Sarmah et al. (2010) however the Peak 1 mass loss does not. Instead it is likely that Peak 1 is attributed to the presence of non-asphaltenic compounds (Mothé et al. 2008). Although further research is required to confirm this observation, the Peak 1 mass loss is likely attributed to the decomposition of resin or wax co-precipitates. Aust. 2 also exhibits a maximum rate of mass loss for Peak 2 at a temperature of around 410–430°C, which was different to the remaining asphaltenes. Perhaps this may be explained by Aust. 2 asphaltenes being smaller compounds which decompose at lower temperatures than the remaining studied asphaltene fractions. Despite the observed repeatability of M. Eastern replicates, variability between Aust. 2 duplicates was observed in the DTG profiles. The DTG peak at 224.9°C observed in one duplicate was inconsistent with the generic DTG profile trends observed for all other asphaltenes (Figure 5.5). The inconsistent peak is likely an error attributed to uneven sample coverage in the Al pan as previously discussed. Due to the limited yields achievable from Aust. 2 oil, re-precipitation of additional Aust. 2 asphaltenes for re-analysis was not feasible.

Asphaltenes from SE Asian 1, SE Asian 2, and N. American oils exhibited a two-stage mass loss in the TG and DTG profiles that was attributed to the presence of Peak 1 (300–330°C) and Peak 3 (460–470°C), whilst Peak 2 was absent (Figures 5.6– 5.8). Peak 1 is likely related to non-asphaltenic compounds (as explained previously for Aust. 2), whilst Peak 3 is likely attributed to asphaltene decomposition. The higher decomposition temperature may simply be due to larger asphaltene molecules existing in the precipitated asphaltene fractions as compared to the smaller molecules which may exist in Aust. 2 asphaltenes. Interestingly, all four asphaltenes which showed a two-stage mass loss (Aust. 2, SE Asian 1, SE Asian 2 and N. American) did exhibit resinous/waxy properties when observed under the SEM as discussed in Chapter 3.

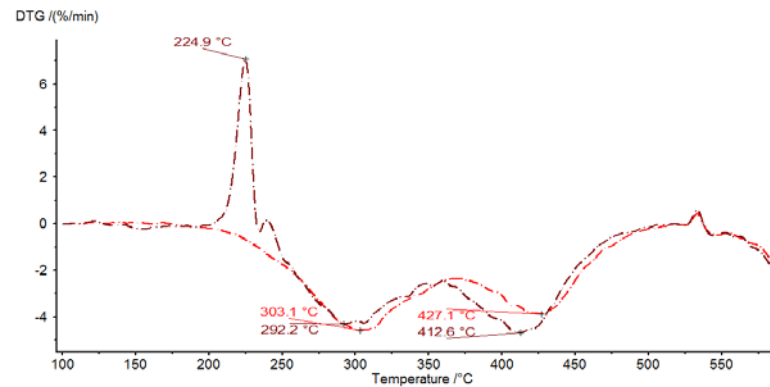
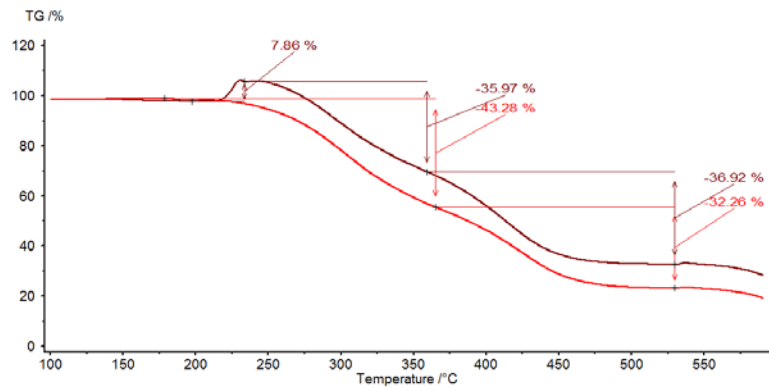


Figure 5.5: TG and DTG profiles for duplicate Aust. 2 asphaltene fractions (TG profiles are on left, DTG profiles are on the right).

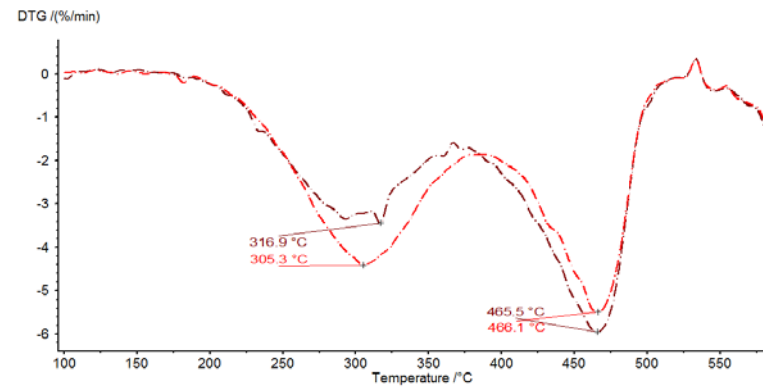
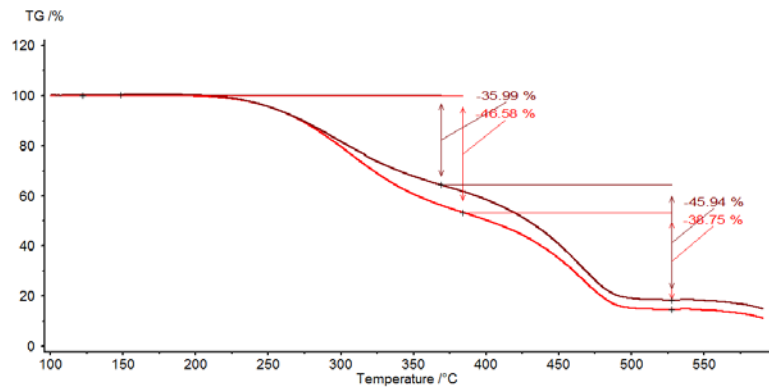


Figure 5.6: TG and DTG profiles for duplicate SE Asian 1 asphaltene fractions (TG profiles are on the left, DTG profiles are on the right).

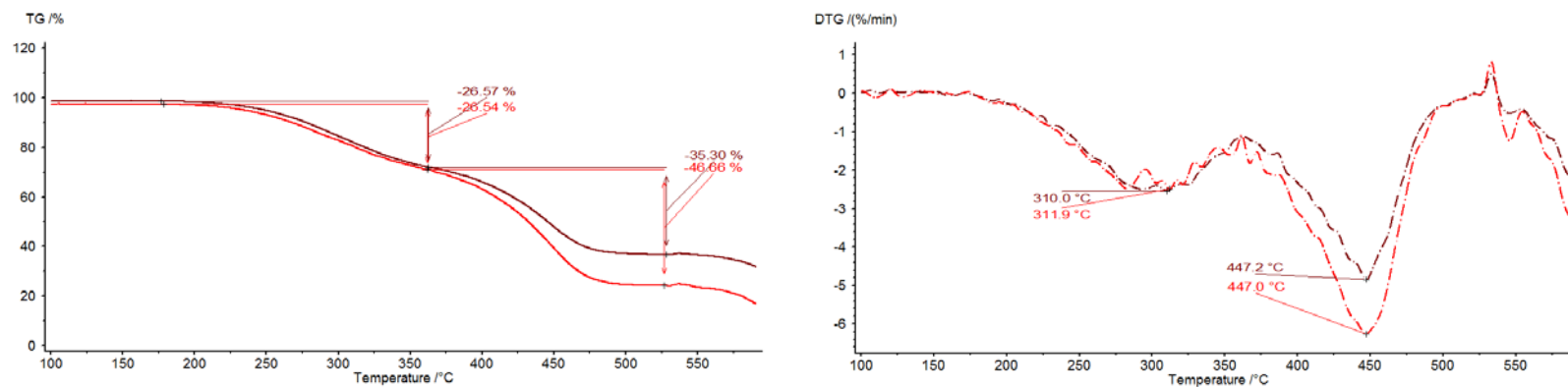


Figure 5.7: TG and DTG profiles for duplicate SE Asian 2 asphaltene fractions (TG profiles are on the left, DTG profiles are on the right).

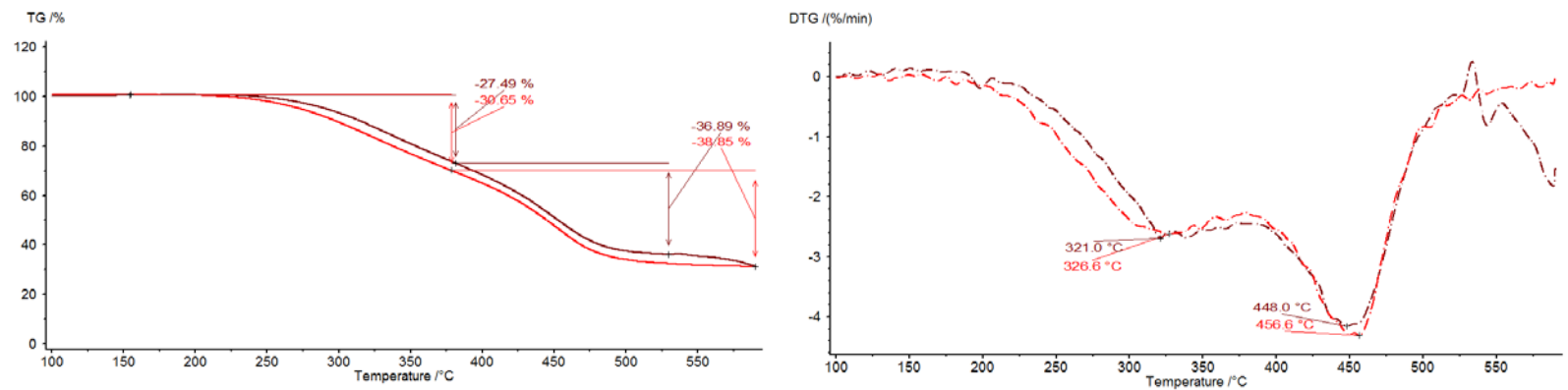


Figure 5.8: TG and DTG profiles for duplicate N. American asphaltene fractions (TG profiles are on the left, DTG profiles are on the right).

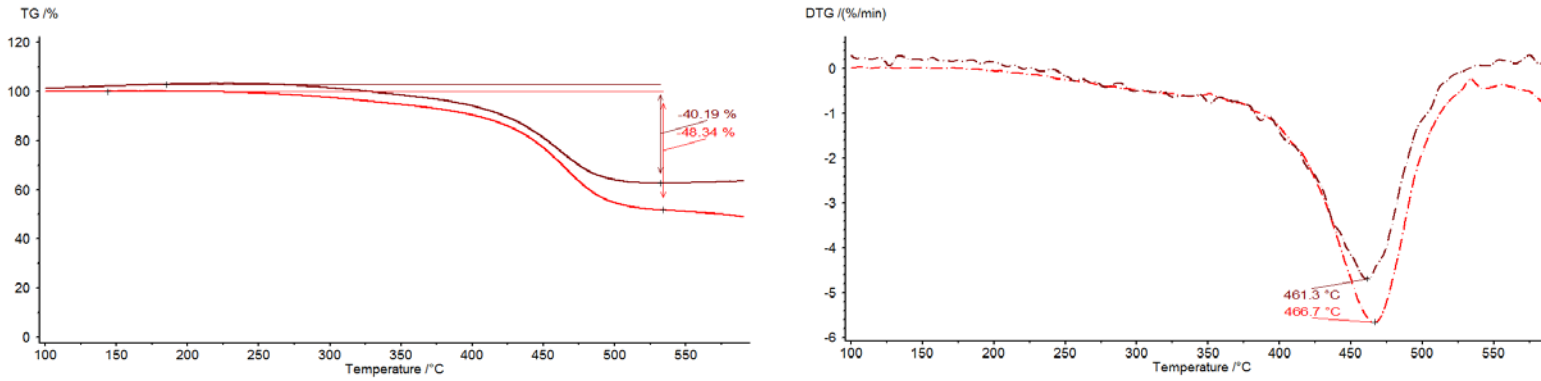


Figure 5.9: TG and DTG profiles for duplicate HFO (u/c) asphaltene fractions (TG profiles are on the left, DTG profiles are on the right).

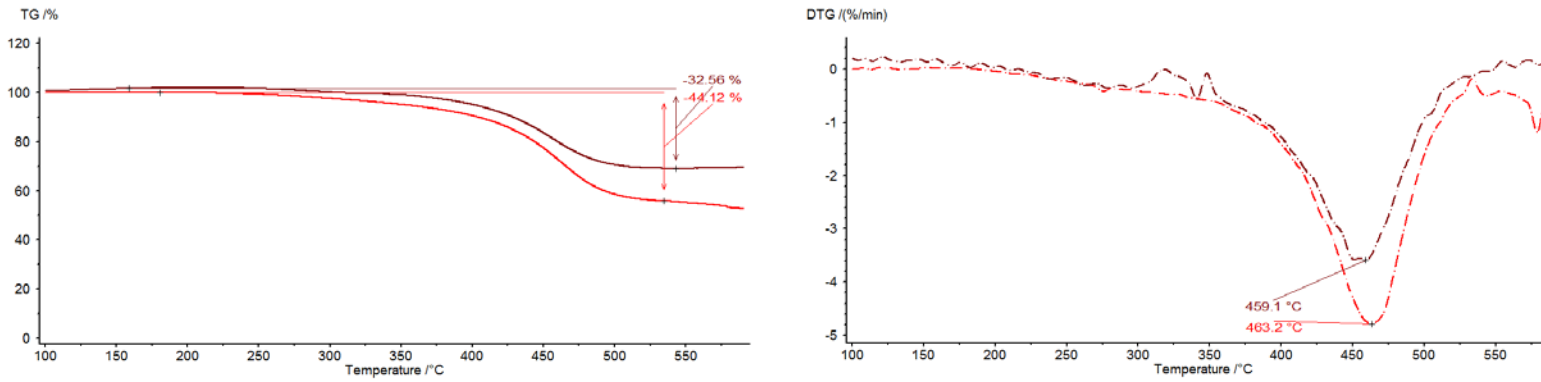


Figure 5.10: TG and DTG profiles for duplicate HFO (d/c) asphaltene fractions (TG profiles are on the left, DTG profiles are on the right).

The M. Eastern, HFO (u/c) and HFO (d/c) asphaltenes were observed to be of crystalline appearance in Chapter 3, which suggested the presence of less co-precipitates and a higher content of asphaltene molecules. The TGA and DTG profiles of M. Eastern, HFO (u/c) and HFO (d/c) asphaltenes support the crystalline observations made in Chapter 3. A single mass loss stage was observed in these crystalline asphaltenes with only Peak 3 present around 450–460°C (Figures 5.3, 5.9, and 5.10). The mass loss temperatures observed for the M. Eastern and HFO asphaltenes aligned with the proposed asphaltene decomposition temperatures observed by Mothé et al. (2008).

5.2.3. Overall Evaluation of TG Profiling

TGA profiling of asphaltenes provided limited probative information: seven oils from different origins were differentiated into three distinct groups. Whilst the findings from TGA profiling were interesting, there were a number of limitations that were detrimental to the requirements of an ideal forensic method. Firstly, the repeatability of TG profiling was limited by the necessary asphaltene sample size required for analysis. Small sample sizes likely introduced error during TGA analysis which resulted in limited profile resolution and decreased repeatability. Another limitation was the duration required for the analysis of each asphaltene sample. Analysis required two hours per asphaltene sample, which allowed for 1 hr acquisition (heating) and 1 hr for cooling of the instrument. Considering the low probative value of TGA profiles, the duration of analysis was not worthwhile. As stated previously, if TG profiles were highly probative, the longer analysis time may have been justified; however, this was not the case. It is likely that there are quicker and more efficient thermal degradation techniques that may provide more probative information. TGA profiling was therefore not deemed suitable for application in oil spill investigations.

5.3. Py-GC-MS

The Py-GC-MS results presented herein have been published (Riley et al. 2018). As mentioned previously, given the large size of asphaltene molecules, it is common to break down asphaltenes into smaller, more volatile compounds for analysis. The molecular breakdown of asphaltenes is commonly conducted using heat, which is a process known as pyrolysis (Eglinton et al. 1990). The combination of pyrolysis and GC-MS allows for the thermal breakdown of solid samples which generate volatile gases that are subsequently analysed using GC-MS. The thermal breakdown of asphaltenes into smaller, volatile compounds is therefore very appealing. As stated in Chapter 1, oil-source rock correlation studies have shown that pyrolysing asphaltenes generates smaller, volatile compounds that are akin to current oil fingerprinting target compounds (Galarraga et al. 2007, Makeen et al. 2015). The ability to target volatile compounds that are currently accepted by oil spill investigators may prove highly beneficial when pyrolysing asphaltenes.

Whilst Py-GC-MS methods for asphaltene analysis are well established in the field of geochemistry, these methods are not immediately suitable for transposition to oil spill investigations. Sample sizes obtained from oil spills may be too small for the current methods as developed by Oudot and Chaillan (2010), Galarraga et al. (2007), Liao et al. (2009) and Van Graas (1985), and reporting timeframes make existing methods impractical for casework application (Stout and Wang 2016, CEN 2012). A desirable Py-GC-MS method would utilise small sample sizes for analysis. Additionally, the sample-sets presented in casework may consist of a range of oils from different origins, or may be different oil types, such as crude oils or HFOs. Some oil types might not be traceable to source rock, particularly in the case of HFOs, which are products of oil refining (Speight 2014). It is for these reasons that a Py-GC-MS method suitable for oil-oil (asphaltene-asphaltene) comparison needed to be investigated and developed.

Py-GC-MS is not a readily available technique in most laboratories, nor is it a fast analytical technique, however the ability to analyse small, solid state asphaltenes is an attractive proposition. It is also acknowledged that Py-GC-MS is a destructive technique; however, as discussed previously for EGA-MS, the very small sample sizes required for analysis outweigh the destructive nature of the technique and a significant portion of precipitated asphaltenes would remain after analysis for most oils.

5.3.1. Interpretation of Py-GC-MS Results

As stated in Chapter 2, a principally visual approach was adopted that is in line with common forensic practice for comparing pyrograms (Zellner and Quarino 2009, Palus et al. 2008, Sarkissian et al. 2004). Ideally, a single standard oil sample could be developed to contain all of the unique pyrolysates for a broad range of different oil types. Such a standard is not currently available, therefore seven replicate asphaltene fractions from both the M. Eastern crude oil and HFO (u/c) oil were precipitated and analysed as a measure of repeatability. The repeatability of the method was also assessed through the analysis of duplicate samples of the remaining oils (except Aust. 3, which was analysed in triplicate). A discussion of the repeatability data is included with the other results.

5.3.1.1. Selection of Representative Asphaltene Pyrolysates

The CEN oil fingerprinting method targets and compares a range of volatile organic compounds including alkanes, PAHs (2 to 6 rings in size), sulfur compounds (2 or 3 rings in size) and biomarkers. It is interesting to observe that many CEN target compounds were also identified in asphaltene pyrograms. There are two possible explanations for observing CEN target compounds in asphaltene pyrolysates: (1) CEN target compounds are moieties in asphaltene molecules that are released upon degradation of these molecules during pyrolysis

(Liao et al. 2009); or (2) CEN target compounds are trapped inside the 3-dimensional space of asphaltene molecules and are released once the asphaltene conformation is broken (Liao et al. 2006). Based on the signal intensities obtained for CEN compounds in pyrograms, it is more likely that the first option is the correct assumption. However, further research should be conducted to confirm the origin of CEN target compounds generated from asphaltene pyrolysis.

In a similar approach to Makeen et al. (2015), the comparison of asphaltene pyrograms was conducted using representative compound groups. However, rather than using the same compounds as Makeen et al. (2015), compounds from a cross-section of alkanes, alkylthiophenes and PAHs were compared (CEN 2012). The CEN target compounds used were: alkanes (aliphatics), C₂-naphthalenes (C₂-N) (2-ring aromatics), benzopyrenes (BPy) (5-ring aromatics), benzo(*g,h,i*)perylene (BPE) (6-ring aromatics), and BT (2-ring sulfur compound). This range of target compounds was chosen for two reasons: (1) they represent the largest compound groups formed upon pyrolysis; and (2) they cover the entire pyrogram RT window. In regards to sulfur compounds, only BT was used. The 3-ring sulfur compound dibenzothiophene (DBT) was also considered; however, DBT did not offer additional information to BT.

5.3.2. Py-GC-MS Optimisation

Prior to the analysis of asphaltenes, the pyrolysis furnace temperature was optimised using HFO (u/c) asphaltenes. HFO (u/c) asphaltenes were flash pyrolysed at 650°C, 750°C and 850°C, and the results compared. Selected ion profiles for alkanes (*m/z* 85), BT (*m/z* 134) and C₂-N (*m/z* 156) were compared for each pyrolysis temperature to determine which furnace temperature was most informative (Figure 5.11).

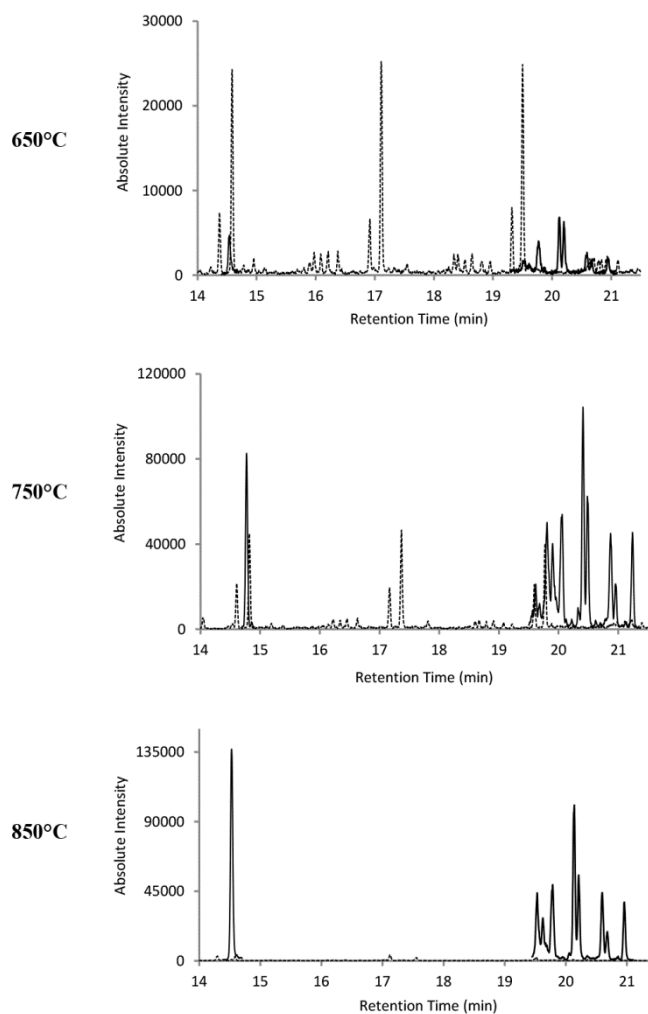


Figure 5.11: Selected ion pyrograms obtained from HFO (u/c) asphaltenes when analysed at three different pyrolysis temperatures showing alkanes (dotted line), BT (unbroken line, RT of 14.5–14.6 min) and C_2 -N (unbroken line, RT of 19.6–21.2 min).

Although 650°C was most consistent with the temperatures reported in geochemical applications (Eglinton et al. 1990, Makeen et al. 2015), the 650°C profile appeared to be dominated by aliphatic content (alkanes), with a reduced presence of sulfur (BT) and aromatic (C_2 -N) content. In addition, the temperature resulted in significant carry-over from one injection to the next. The 850°C profile showed a significant reduction in aliphatic information with mostly aromatic and sulfur compounds present. The 750°C profile contained all three compound classes at similar intensities and, hence, was deemed most informative. Furthermore, flash pyrolysis at 750°C overcame the issue of sample carry-over

that occurred at 650°C. While it is not the purpose of this research to investigate the thermal mechanisms responsible for the observed variations between temperatures, it is interesting to note that the effects of heating on asphaltenes have been shown to increase aromaticity of asphaltene molecules (Chiaberge et al. 2009, Calemma and Rausa 1997, Akmaz et al. 2012).

5.3.3. Comparison of Oils Using Alkane Profiles

Aliphatic pyrograms (or profiles), generated from the pyrolysis of asphaltenes, provide useful information in the geochemical comparison of oils to source rock (Eglinton et al. 1990, Makeen et al. 2015, Galarraga et al. 2007). It was therefore logical to assess the use of aliphatics in oil-to-oil comparisons, specifically the alkane (m/z 85) profiles. The alkane profiles obtained for both M. Eastern and HFO (u/c) replicates were compared to assess repeatability. Representative alkane profiles for asphaltenes from both oils are presented in Figures 5.12 and 5.13, respectively.

The overall alkane profiles for M. Eastern and HFO (u/c) were similar in that the low-boiling alkane intensities were highest, with the intensity tapering off rapidly as RT increased. Although alkane profiles were similar between replicates, minor variations were observed when focusing on the high-boiling, latter regions. Two alkane profiles are shown for both M. Eastern and HFO (u/c) asphaltenes which represent the maximum variance observed in the latter regions of replicate analyses (Figures 5.12 and 5.13). For M. Eastern asphaltenes, Figure 5.12 (a) shows little to no rise in peak intensities between RTs of 37 and 42 min, whilst Figure 5.12 (b) has a minor rise in this same profile region. For HFO (u/c) asphaltenes, Figures 5.13 (a) and (b) both show a rise in peak intensities between 32 and 50 min; however, this rise is more pronounced in (b) than it is in (a).

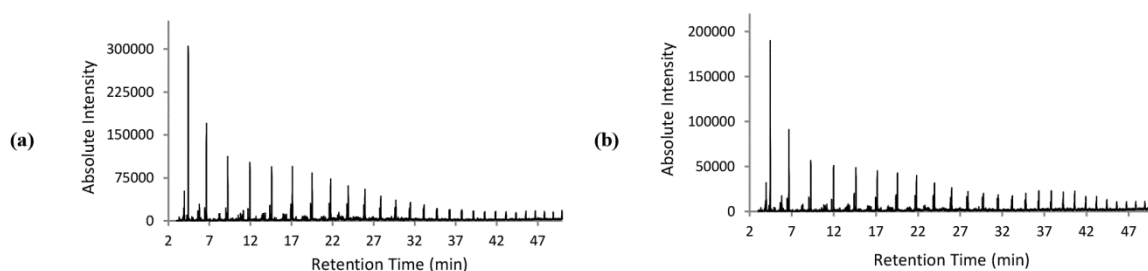


Figure 5.12: Two M. Eastern alkane profiles which represent the maximum variance observed between all seven replicate M. Eastern asphaltene fractions.

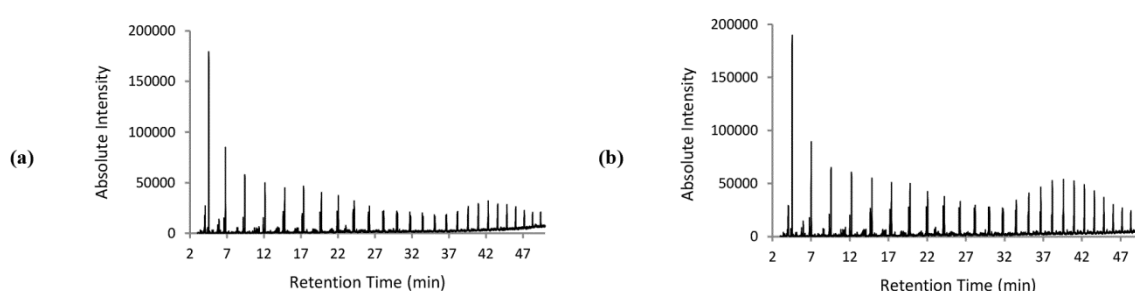


Figure 5.13: Two HFO (u/c) alkane profiles, which represent the maximum variance observed between all seven replicate HFO (u/c) asphaltene fractions.

As a result of these minor replicate variations, it is crucial that the comparison of oils using alkane profiles is conducted conservatively and focuses on comparing overall profiles. Comparisons of oils should only focus on obvious differences in the overall profiles for asphaltene alkanes, rather than relatively small differences in specific regions that do not necessarily change the overall profile. Nevertheless, it is equally important to highlight that probative information can still be obtained from alkane profiles.

To gauge the probative value of asphaltene alkane pyrograms, asphaltenes from ten different oils were analysed including Aust. 1, Aust. 2, Aust. 3, SE Asian 1, SE Asian 2, N. American, HFO (u/c), HFO (d/c), and the un-weathered and weathered M. Eastern oils. The S. Pacific oil did not yield sufficient asphaltenes for Py-GC-MS analysis; hence S. Pacific asphaltenes were not analysed.

The comparison of alkane pyrograms resulted in the differentiation of the ten oils into three distinct groups. The first group contained the M. Eastern, M. Eastern (w), HFO (u/c), HFO (d/c) and N. American oils; representative pyrograms are shown in Figure 5.14. The asphaltene profiles for these oils were dominated by low-boiling alkanes with reduction in alkane intensity towards the latter regions of the pyrograms. M. Eastern, M. Eastern (w), HFO (u/c), HFO (d/c) and N. American oils were grouped together despite some minor differences observed in the latter regions. Based on repeatability data, these minor variations should not be relied upon to differentiate the oils.

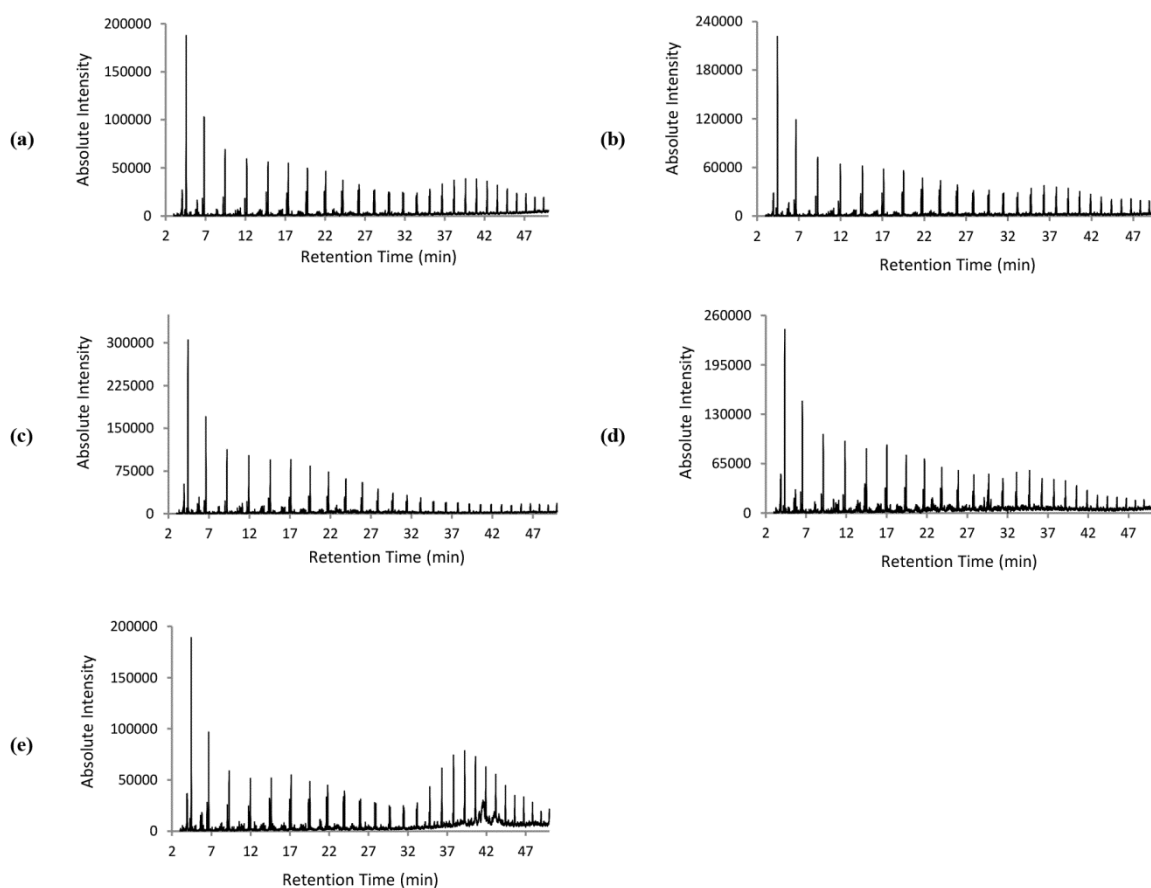


Figure 5.14: The first group of oils classified by alkane profiles: (a) HFO (u/c); (b) HFO (d/c); (c) M. Eastern; (d) M. Eastern (w); and (e) N. American.

The second group consisted of the SE Asian 1 and SE Asian 2 oils, whilst the third group contained the Australian oils (Aust. 1, Aust. 2 and Aust. 3) (Figures 5.15 and 5.16). In contrast to the first group of oils, the SE Asian and Australian alkane profiles were all dominated by high-boiling alkanes. Despite a shared dominance in high-boiling alkanes, the SE Asian and Australian oils can be differentiated based on their overall profiles. All Australian profiles showed defined clusters of peaks between 35 and 45 min, whilst the SE Asian profiles showed wider, less defined clusters of peaks in this same region.

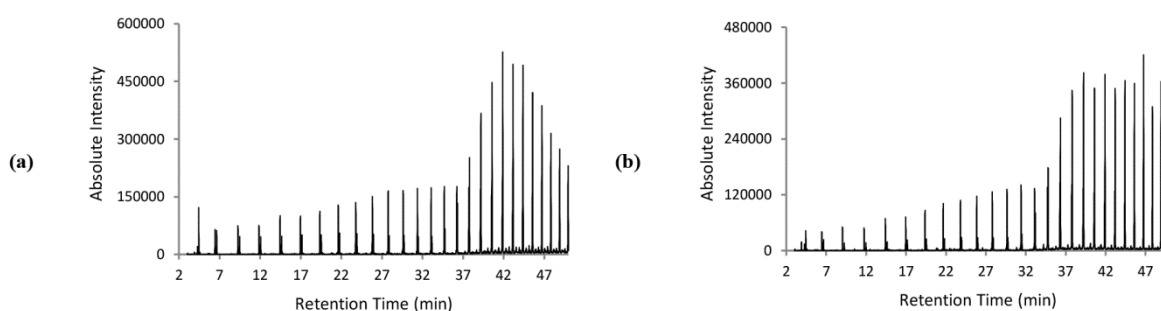


Figure 5.15: The second group of oils classified by alkane profiles: (a) SE Asian 1; and (b) SE Asian 2.

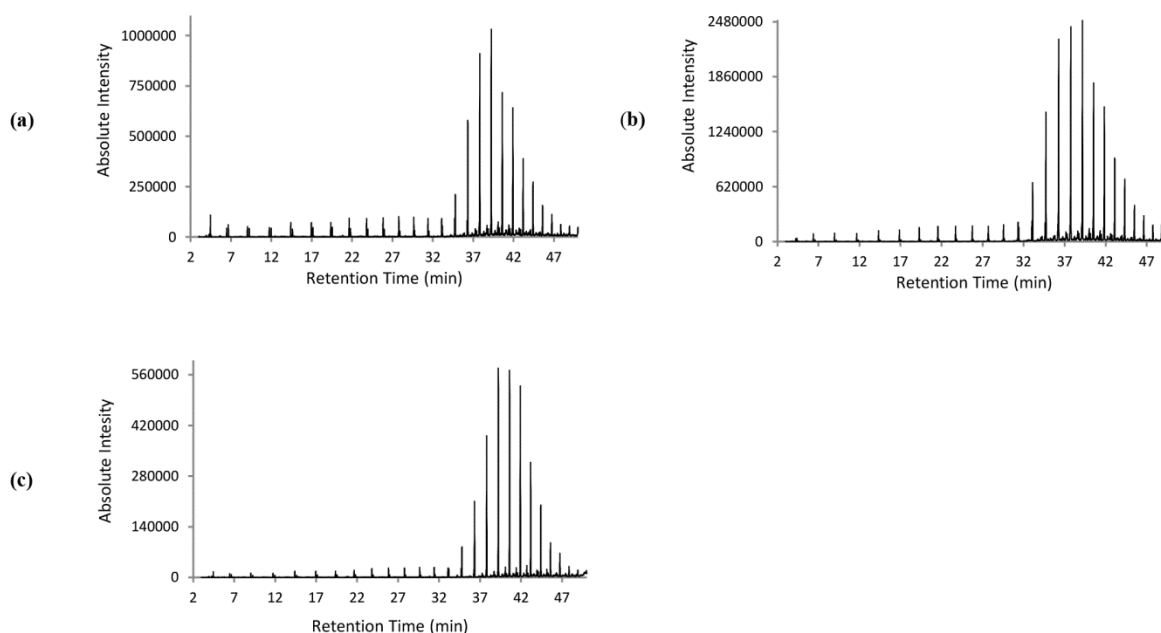


Figure 5.16: The third group of oils classified by alkane profiles: (a) Aust. 1; (b) Aust. 2; and (c) Aust. 3.

5.3.4. Comparison of Oils Using Sulfur/Aromatic Profiles

As discussed previously, BT (m/z 134) was chosen as a representative sulfur compound, whilst C₂-N (m/z 156), BPy (m/z 252) and BPE (m/z 276) were chosen as representative aromatic compounds (of varying sizes). The extracted ion chromatograms for these four sulfur/aromatic compounds were overlaid and the combined sulfur/aromatic profiles were used for the comparison of oils. The RTs of these representative compounds/compound groups were observed as follows: BT (14.5 min), C₂-N (19.5–21.5 min), BPy (44–45 min) and BPE (49.5 min). Some slight RT shifts were observed between asphaltenes due to the nature of manual pyrolysis injection.

The sulfur/aromatic profiles generated from replicate M. Eastern and HFO (u/c) asphaltene extracts were compared to assess repeatability. Representative sulfur/aromatic profiles for replicate M. Eastern and HFO (u/c) asphaltenes are presented in Figures 5.17 and 5.18, respectively. The overall profiles for the M. Eastern replicates were found to be repeatable. High relative intensities of both BT and C₂-N were observed, with an obvious absence (below detection limit) of BPy and BPE. BT had a consistently higher intensity than C₂-N. The peak profile of the C₂-N group (m/z 156) also remained consistent across all M. Eastern replicates. The HFO (u/c) replicates also showed good repeatability. High intensities of both BT and C₂-N were observed, with the intensities of C₂-N consistently higher than BT. Both BPy and BPE were present in all seven HFO (u/c) replicates and although intensities differed slightly between replicates, these minor differences were not relied upon for the differentiation of oils. BPy and BPE were only used for the comparison of oils based on their presence/absence. Overall, the sulfur/aromatic profiles were found to be repeatable when comparing C₂-N and BT profile intensities and when comparing the presence/absence of BPy and BPE.

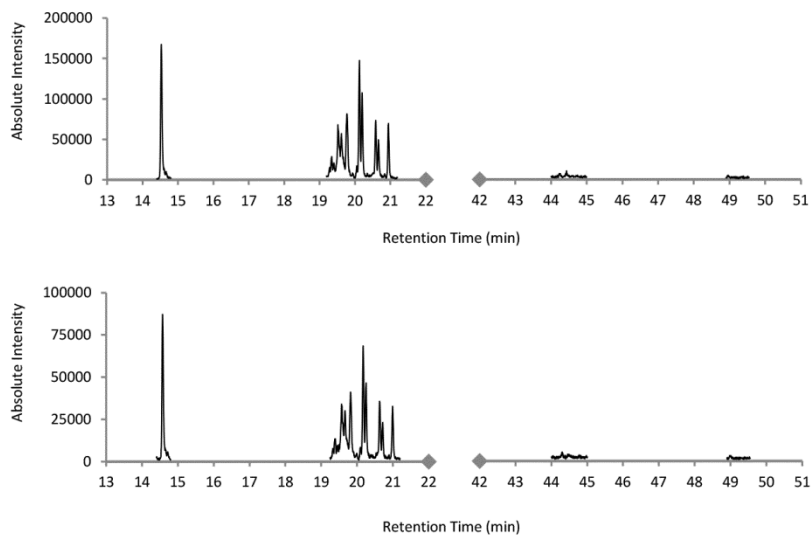


Figure 5.17: Two representative sulfur/aromatic profiles for the replicate M. Eastern asphaltenes

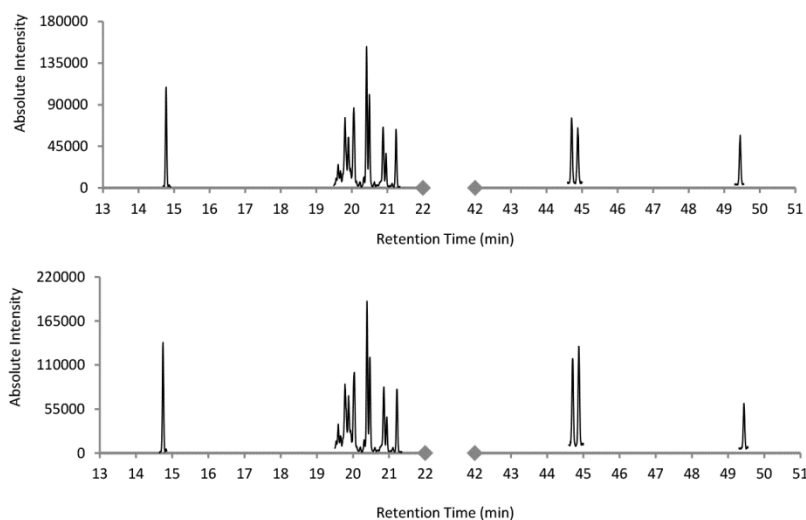


Figure 5.18: Two representative sulfur/aromatic profiles for the replicate HFO (u/c) asphaltenes.

To gauge the probative value of asphaltene sulfur/aromatic pyrograms, the oils within each of the three previously defined groups (based on alkanes) were compared using sulfur/aromatic profiles. Figure 5.19 shows representative sulfur/aromatic profiles generated from the pyrolysis of HFO (d/c), HFO (u/c), M. Eastern, M. Eastern (w) and N. American

asphaltenes. Sulfur/aromatic profiles were found to provide additional probative information that allowed for further differentiation of this group.

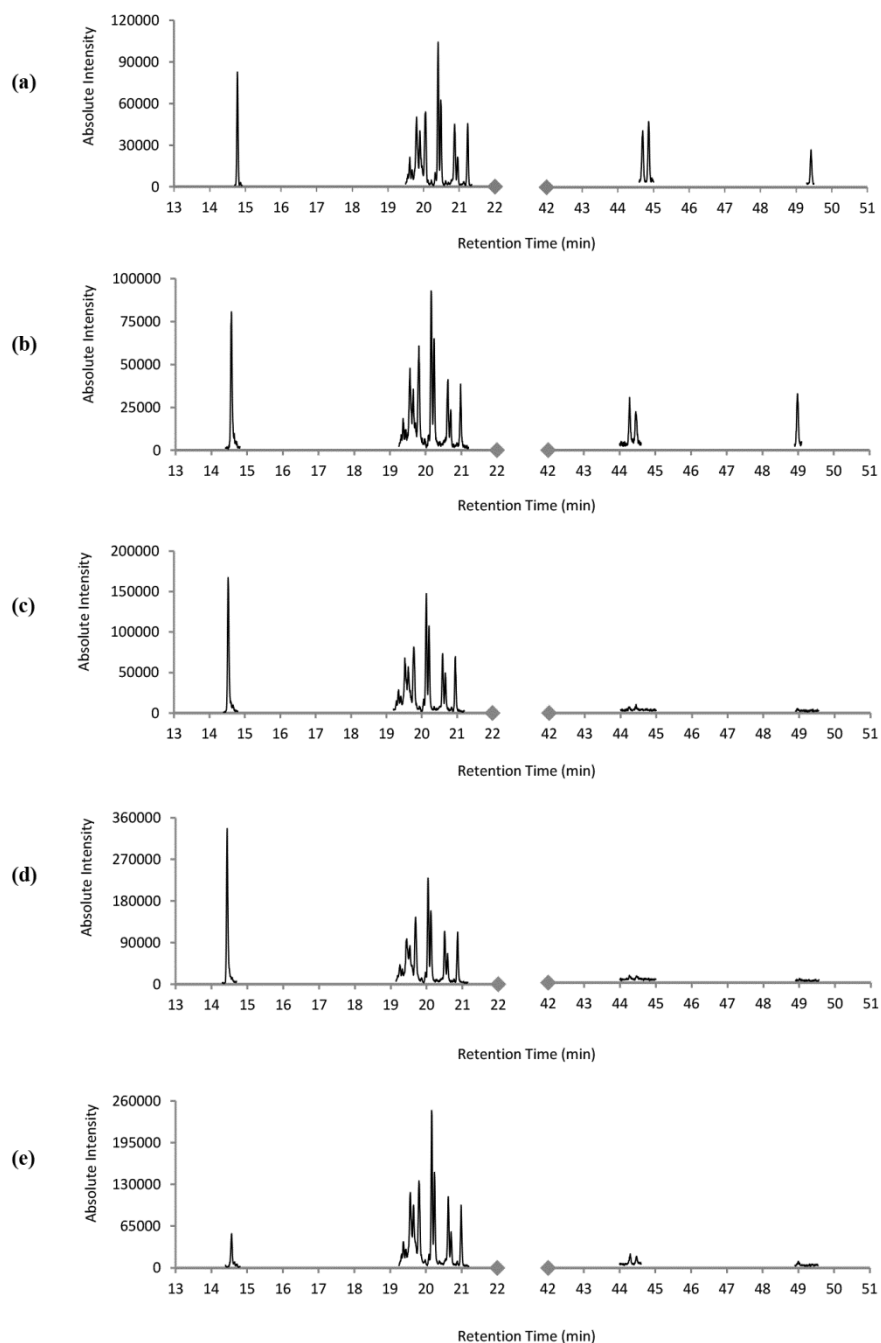


Figure 5.19: Representative sulfur/aromatic profiles of group 1 asphaltenes: (a) HFO (u/c); (b) HFO (d/c); (c) M. Eastern; (d) M. Eastern (w); and (e) N. American.

Firstly, both HFOs were differentiated from the N. American and M. Eastern oils based on the presence/absence of BPy and BPE. BPy and BPE were both present in the HFOs, yet both absent (below the detection limit) in the N. American and M. Eastern sulfur/aromatic profiles. The two HFO oils could not be differentiated, which is consistent with the knowledge that they are both derived from the same oil or oil mixture. Secondly, the M. Eastern and M. Eastern (w) profiles showed a repeatedly higher intensity of BT than C₂-N, as compared to the significantly reduced intensity of BT observed in the N. American profiles. Taking into account the repeatability of pyrograms, the asphaltene profiles obtained from the un-weathered and weathered M. Eastern oils were consistent with one another. It is of great interest to oil fingerprinting to observe such similarities between weathered and un-weathered oils from the same source. As indicated previously, weathering of oil can cause significant chemical variations in volatile profiles; however, the asphaltene pyrograms obtained from the un-weathered and weathered M. Eastern oil did not exhibit such chemical variations. Although the results observed herein should certainly be treated with caution as only one weathered oil sample was analysed, these results are promising and allude to the potential benefits of using asphaltenes in oil fingerprinting when weathered oils are present. It is also interesting to note that while C₂-N profiles generated from asphaltene pyrolysis can differentiate some oils (as will become apparent when discussing the SE Asian C₂-N profiles), the C₂-N profiles for the asphaltenes from both HFOs, the M. Eastern crude oils and the N. American crude oil did not differ from one another.

Figure 5.20 shows representative sulfur/aromatic profiles for SE Asian 1 and SE Asian 2 asphaltenes. The overall sulfur/aromatic profiles were very similar but differences between C₂-N profiles were observed as shown in Figure 5.20 (b) and (d), respectively. The most notable difference within these C₂-N groups was the alternating profiles of the two major peaks in this group at 20.2 and 20.3 min, respectively. The peak at 20.2 min was highest in

intensity in the SE Asian 1 profile, whilst the peak at 20.3 min was marginally lower in comparison. In contrast, the SE Asian 2 profile showed a significantly lower peak at 20.2 min in relation to the peak at 20.3 min. These observations were consistent across both sets of SE Asian duplicates. It must be noted that while C₂-N profiles are not source-specific when analysing volatiles, clear, repeatable differences between C₂-N profiles generated from asphaltene pyrolysis were observed.

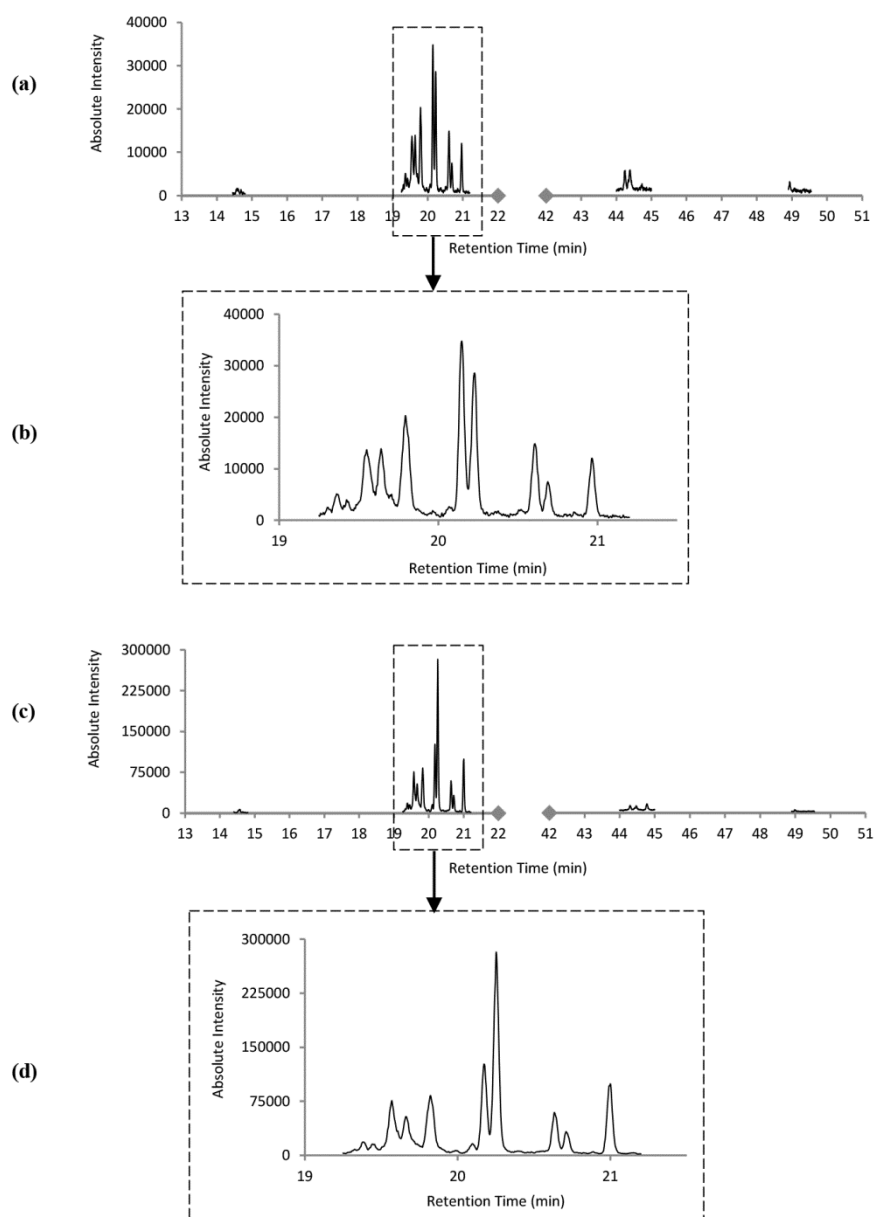


Figure 5.20: Representative sulfur/aromatic profiles of group 2 asphaltenes: (a) SE Asian 1; and (c) SE Asian 2. C₂-N profiles have been enlarged for comparison in (b) and (d).

Figure 5.21 shows representative sulfur/aromatic profiles for Aust. 1 and Aust. 2 asphaltenes as well as two representative profiles obtained for the Aust. 3 asphaltenes. The overall profiles for Aust. 1 and Aust. 2 were similar; however, the signal-to-noise (S/N) ratio of BPE and BPy was found to be consistently higher in Aust. 1 compared to Aust. 2. In the Aust. 2 profiles, these compounds fell around or below a S/N ratio of 5, meaning that identification of these compounds in Aust. 2 was uncertain (CEN 2012). S/N ratios can more easily be observed in Figure 5.22 where the BPy and BPE peak regions have been enlarged for both Aust. 1 and Aust. 2 profiles. It is interesting that differences between Aust. 1 and Aust. 2 oils were observed in the asphaltene pyrograms given that the oils were collected from a common source ten years apart. Although the intensity of the BT peak was slightly variable between Aust. 3 replicates (Figure 5.21 (c) and (d)), BT was clearly present in all Aust. 3 replicates, yet absent from Aust. 1 and Aust. 2 profiles. IR analysis of Aust. 1, Aust. 2 and Aust. 3 asphaltenes also found that these oils could be distinguished based on their respective asphaltene fractions (Riley et al. 2016 and Chapter 4). Although differences were observed between the sulfur/aromatic pyrograms of asphaltenes from the Australian oils, it is advisable to also analyse asphaltene fractions using IR to confirm these differences, in particular for the differentiation of Aust. 1 and Aust. 2. It is also worth noting that, unlike the SE Asian asphaltenes, C₂-N profiles of the Australian oils did not differ from one another.

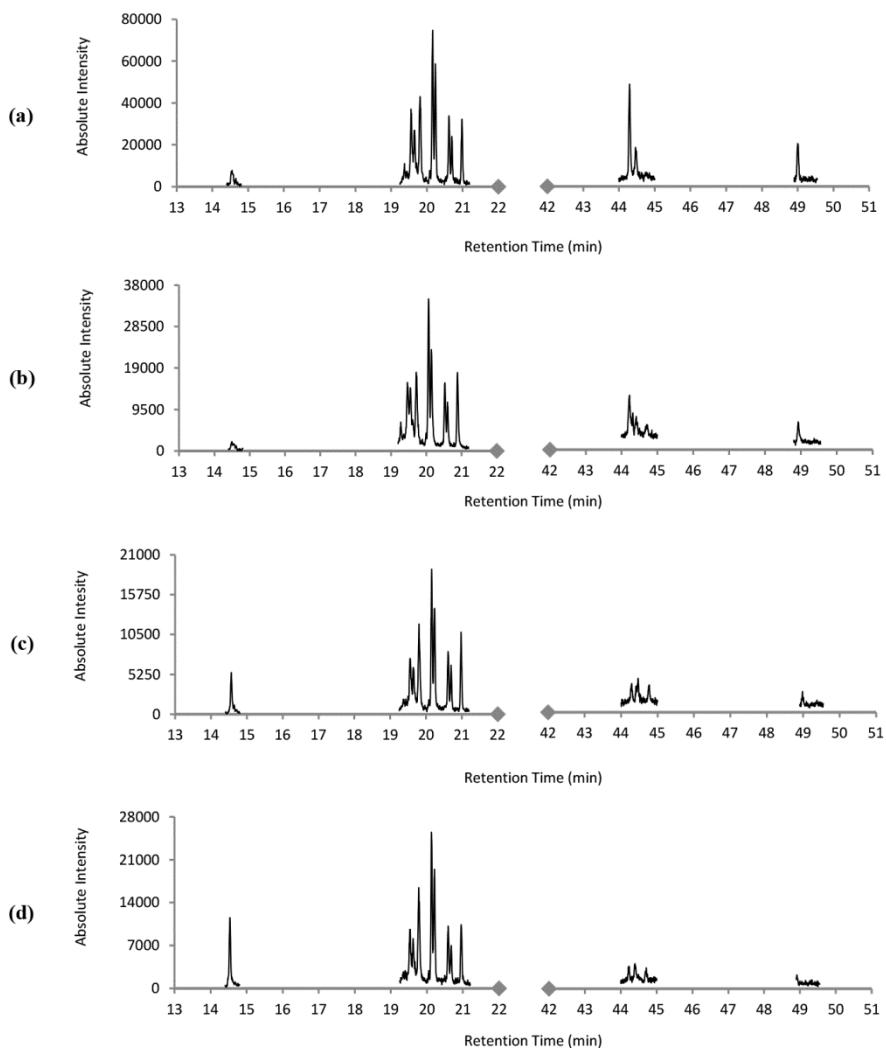


Figure 5.21: Representative sulfur/aromatic profiles of group 3 asphaltenes: (a) Aust. 1; (b) Aust. 2; (c) Aust. 3; and (d) Aust. 3 duplicate.

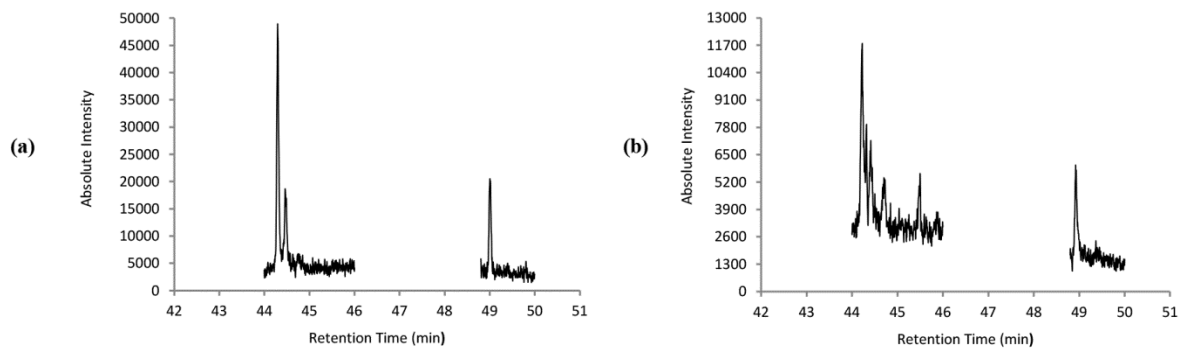


Figure 5.22: Enlarged BPy and BPE regions for (a) Aust. 1 and (b) Aust. 2. The S/N ratio of BPy and BPE peaks is higher for Aust. 1 compared to Aust. 2.

5.3.5. Overall Evaluation of Py-GC-MS Profiling

Whilst Py-GC-MS is a destructive and relatively slow analysis technique, the sample size required for analysis is very small and the interpretation of pyrograms is very quick. Furthermore, asphaltenes were successfully analysed in a solid state without chemical alteration prior to analysis. Asphaltene pyrograms were also repeatable and highly probative as discussed below.

By combining the visual comparison of asphaltene alkane profiles and sulfur/aromatic profiles, the ten studied oils were differentiated into eight distinct groups as shown in Figure 5.23: (1) M. Eastern and M. Eastern (w); (2) HFO (d/c) and HFO (u/c); (3) N. American; (4) SE Asian 1; (5) SE Asian 2; (6) Aust. 1; (7) Aust. 2; and (8) Aust. 3.

It was found that the following step-wise approach provided for the easiest comparison of oils using asphaltene pyrograms:

1. Firstly, the overall shape of the alkane profiles (m/z 85) should be compared. The oils are divided into groups of similar overall profiles.
2. Secondly, oils within each group (from step one) should be compared using sulfur/aromatic profiles. Although this method demonstrates that C₂-N, BT, BPy and BPE can be successfully used for this purpose, expansion of the target compound list could be considered if required.

As a result of the aforementioned approach, all oils from different origins were successfully differentiated, whilst the oils from the same origin were correctly grouped together. Both HFOs were also from the same origin (same oil, different grade) and were hence correctly grouped. Also the M. Eastern and M. Eastern (w) asphaltenes remained unchanged, and these two oils were also correctly grouped together. The inability to differentiate weathered and unweathered asphaltenes supports the weathering results observed during IR profiling. The combined weathering results from IR and Py-GC-MS

further reinforces the hypothesis that asphaltene fractions may exhibit a degree of resistance to weathering which makes them attractive for casework comparisons (Lewan et al., 2014).

Overall, Py-GC-MS profiling of asphaltenes successfully addressed many of the requirements for an ideal forensic method as proposed in Chapter 1.

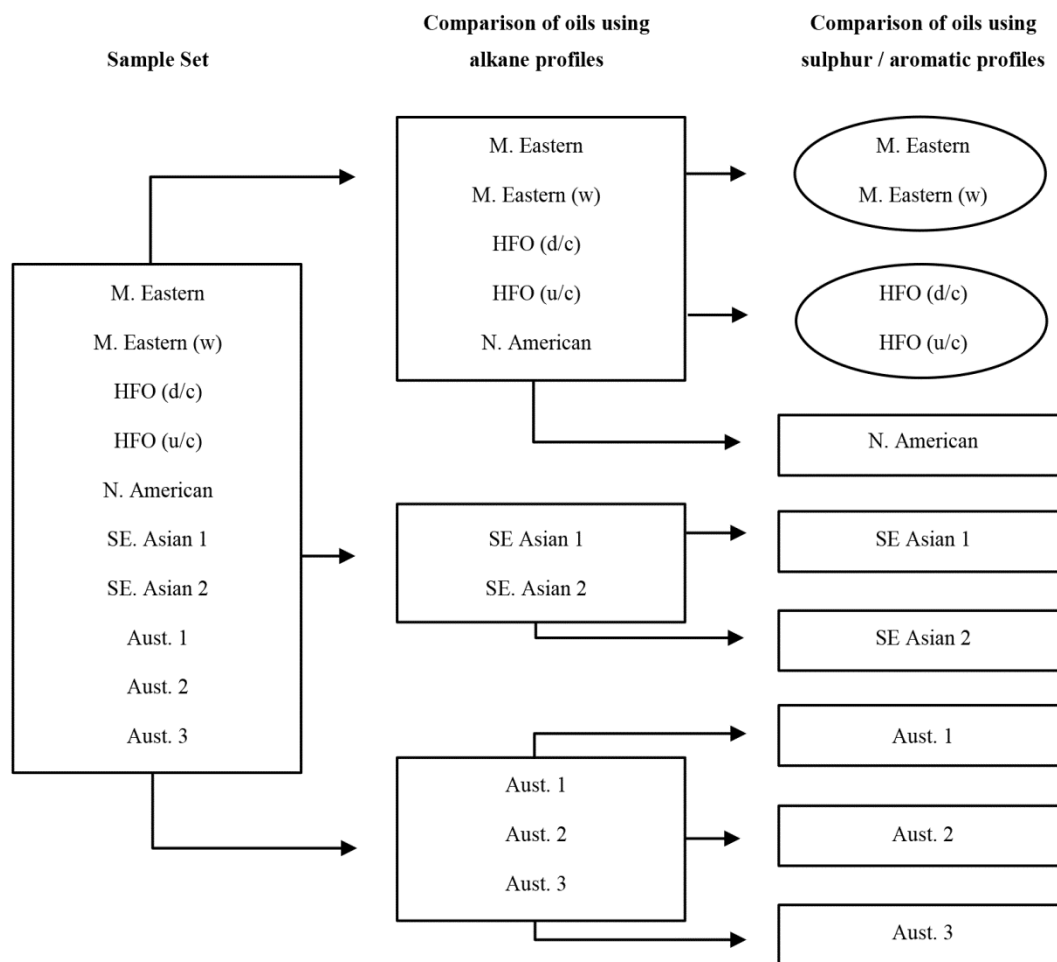


Figure 5.23: Flow chart indicating the differentiation of the ten studied oils into eight groups based on pyrolysis of asphaltenes. The groups that could not be differentiated (circled) were oils from the same source and were classified correctly.

5.4. Chapter 5 Summary

EGA-MS profiling of asphaltenes was deemed unsuitable for application in oil spill investigations. EGA-MS profiling was not sufficiently repeatable to allow for reliable forensic comparison of asphaltenes. EGA-MS was also not probative enough to assist in oil spill investigations. TGA profiling offered an acceptable degree of repeatability for some components of analysis; however, the probative value of TG and DTG profiles was relatively poor when comparing asphaltenes from different oils. Furthermore, TGA was likely limited by the small sample sizes of the studied asphaltenes. TGA required more than a realistic amount of asphaltenes for analysis when considering limited casework sample sizes. TGA analysis also proved to be relatively time consuming. It was determined that TGA profiling was not suitable for application in oil spill investigations. Whilst TGA profiling was deemed unsuitable for oil fingerprinting, TG and DTG profiles did provide interesting information regarding the possible physical morphology of asphaltenes, which was supportive of the visual observations made in Chapter 3.

Of all thermal methods tested herein however, Py-GC-MS profiling of asphaltenes was the most suitable thermal degradation method for oil spill investigations. The previously developed asphaltene precipitation method proved effective for yielding sufficient asphaltenes from small oil samples which allowed for successful Py-GC-MS profiling. For the sample-set evaluated, the developed Py-GC-MS method was able to correctly group oils from the same origin, and differentiate oils from different origins on the basis of asphaltenes. Asphaltene profiles generated from Py-GC-MS were therefore deemed highly probative in comparison to the other tested methods.

The strength of the Py-GC-MS method is in its simplicity. With the addition of a pyrolysis unit attached to an existing GC-MS, oil spill investigators would be sufficiently equipped with instrumentation capable of obtaining chemical fingerprints of not only the

volatile fractions of oil, but also the non-volatile, asphaltene fraction that is currently discarded. Whilst Py-GC-MS profiling has shown promising results thus far, it is acknowledged that further validation is required prior to operational application. The blind study detailed in Chapter 7 tests the reliability of interpreting asphaltene profiles obtained from the developed Py-GC-MS method. The blind study will gauge whether or not the same degree of probative information can be obtained from the Py-GC-MS method without knowledge of the origin of oils which was known throughout method development.

Although Py-GC-MS alone provides a high degree of discrimination, it is common in many forensic disciplines to combine information from multiple techniques before drawing conclusions to ensure the highest degree of discrimination possible (Yang et al. 2012, Palus et al. 2008). The confidence of sample inclusion or exclusion based on Py-GC-MS profiling of asphaltenes may be further strengthened by complementing Py-GC-MS with the previously developed IR method (Chapter 4). IR and Py-GC-MS profiling methods were deemed the most suitable methods for oil fingerprinting. Both methods generated probative information from the same sample-set of oils, and both methods produced conclusions that were supportive of one another. Chapter 6 outlines how the collaboration of IR and Py-GC-MS profiling will function in a casework environment. The dynamics of profiling asphaltenes using both techniques will be discussed as well as the functionality of asphaltene profiling alongside existing volatile oil fingerprinting. Chapter 7 then tests the collaboration of IR and Py-GC-MS profiling through a casework scenario in the form of a blind study.

Chapter 6 - The Asphaltene Profiling Method

As discussed in Chapter 4, of the spectroscopic methods assessed in this study for the profiling of asphaltenes, IR was found to be the most suitable method for oil fingerprinting. IR profiles were capable of differentiating ten oils through the visual comparison of spectra and comparison of peak height ratios. In regards to thermal degradation methods, Py-GC-MS profiling was found to be the most suitable method for oil fingerprinting (Chapter 5). Py-GC-MS was capable of correctly differentiating ten oils through the visual comparison of aliphatic and aromatic/sulfur pyrograms.

Although both the IR and Py-GC-MS methods independently achieved the same degree of discrimination when provided with the same sample-set of oils, it is important to consider combining both methods. Complementary methods provide for a higher level of confidence when determining sample inclusion or exclusion than each of the individual methods alone (Riley et al. 2016). Whilst complementing IR with Py-GC-MS may be very helpful, particularly when comparing chemically similar asphaltene fractions, if obvious differences are observed using either IR or Py-GC-MS alone, it may not be necessary to use both techniques. It is important that the analyst does not invest additional time comparing results from both techniques if one technique can already clearly differentiate two asphaltene fractions.

A proposed asphaltene profiling method that utilises both IR and Py-GC-MS profiling is outlined in Figure 6.1. The suggested asphaltene profiling method is designed to support existing methods for volatile fractions of oil by providing additional information to oil spill investigations. The primary aim of the asphaltene profiling method is to exclude non-related oils from oil spill investigations prior to volatile fingerprinting. Oils that cannot be excluded based on asphaltene profiles should be carried forward for confirmatory analysis via volatile fingerprinting.

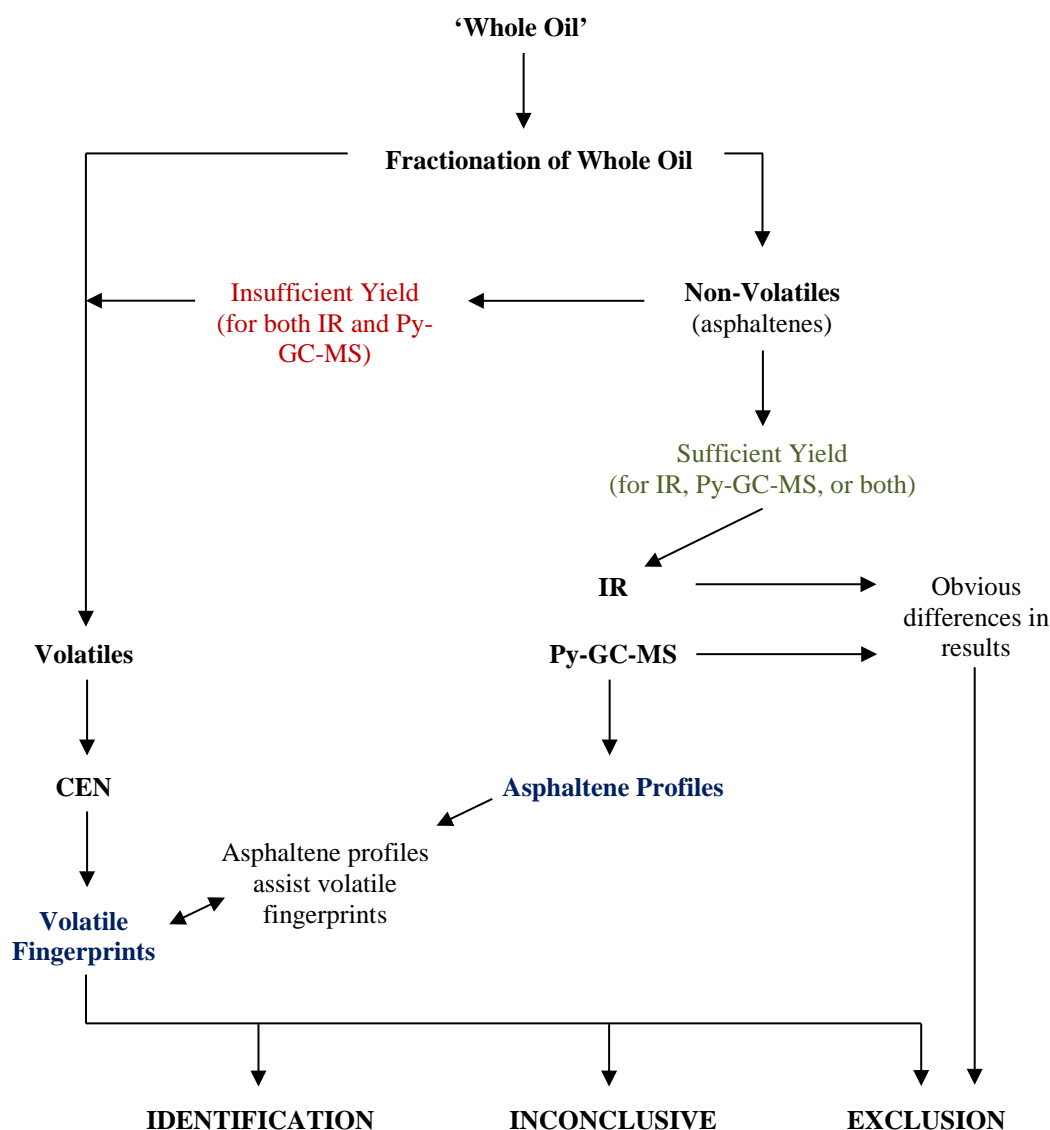


Figure 6.1: A simplified flowchart showing the proposed workflow of asphaltene profiling assisting volatile oil fingerprinting.

The practicality of using asphaltene profiles in oil spill investigations stems from the fact that current oil fingerprinting approaches already separate the asphaltene fraction from the volatile fractions prior to analysis (Figure 6.1). Instead of discarding the asphaltene fraction, it is proposed that asphaltenes are profiled using both IR and Py-GC-MS. Although it is recommended that the analysis sequence for asphaltenes should commence with non-destructive IR analyses followed by destructive Py-GC-MS analyses (Figure 6.1), this

process does not have to be strictly followed if sufficient asphaltene yields are obtained for both IR and Py-GC-MS profiling. Also, there may be circumstances where a sufficient asphaltene yield is obtained for Py-GC-MS but not for IR. In such circumstances, Py-GC-MS profiling would occur first as IR profiling would not be possible.

The inclusion of asphaltene profiles in oil fingerprinting would allow for a more holistic ‘whole oil’ approach than the current volatile-only approach. Whilst volatile fingerprinting is highly robust and widely accepted throughout the oil fingerprinting community, complementary information provided by asphaltenes may allow for easier interpretation of overall results (CEN 2012, Desideri et al. 1985, Wang et al. 2006 [a]). As shown in Figure 6.1, whole oil fingerprints may be generated that combine information from both volatile fingerprints and asphaltene profiles to derive conclusions during oil spill investigations. If however, asphaltene profiles can exclude non-related oils, it would not be necessary to produce a whole oil fingerprint. Non-related oils would simply be excluded based on asphaltene profiles which would negate the need for volatile fingerprinting. Oils that cannot be differentiated based on asphaltene profiles would be analysed using volatile fingerprinting methods and conclusions would be supported by the previously generated asphaltene profiles. Whilst this may appear to create unnecessary additional work, Chapter 7 will discuss that the amount of data obtained for asphaltene profiles is much less than for volatile fingerprints and may be utilised for quicker exclusion of non-related oils.

The preliminary results obtained from IR and Py-GC-MS asphaltene profiling thus far support the hypothesis that asphaltenes are resistant to weathering to some degree. The asphaltene profiles obtained from un-weathered and weathered oil from the same source could not be differentiated. The volatiles currently targeted in oil fingerprinting are susceptible to weathering; therefore, the interpretation of results can rely heavily on the knowledge and experience of investigators. The application of asphaltenes in cases where

weathered oils are encountered may avoid difficulty during interpretation, as asphaltene profiles may alter to a lesser extent than the volatile fraction. Although the observed weathering results are purely proof-of-concept, the observed results do suggest a significant advantage with the inclusion of asphaltene profiles in oil fingerprinting, particularly when weathered oils are present. Even if further research shows that asphaltenes do in fact weather, the asphaltene profiles will still provide additional information to investigations that is otherwise currently overlooked.

The main limitation that will be encountered with asphaltene profiling is when insufficient asphaltene yields are encountered. If oils do not produce a sufficient asphaltene yield, the existing volatile-only approach may be the only feasible fingerprinting approach. Alternatively, and as discussed earlier, there may be a chance that due to small asphaltene yields, Py-GC-MS profiling of asphaltenes can be conducted but IR profiling cannot. In such circumstances, only the Py-GC-MS asphaltene profile would be used to supplement volatile fingerprints.

Chapter 7 - Validation of the Asphaltene Profiling Method - A Blind Study

The asphaltene profiling method outlined in Chapter 6 was evaluated through a blind study herein. The aim of the blind study was to determine whether the interpretation of asphaltene profiles was reliable. Asphaltene profiles were generated from 21 unknown oils through profiling using both IR and Py-GC-MS methods combined. The asphaltene profiles were interpreted with the primary aim of excluding all non-related oils from the data-set. The benefit of the blind study was that any bias associated with prior knowledge of oil origins (prior to analysis and interpretation) was eliminated. During method development in Chapters 4 and 5, the origin of the oils was known; hence the interpretation of the results may have been influenced by cognitive bias. If oils from the same origin can be correctly grouped and asphaltenes from different oils can be correctly differentiated during the blind study, the interpretation of asphaltene profiles can be deemed reliable for the developed methods (at least across the sample-set in question). The blind study was designed as follows, with reference to Person A and Person B (PhD candidate):

1. Person A selected and labelled 21 oils (labelled A–U). The source of the oils was known to Person A.
2. Person B received the 21 oils (A–U) from Person A without knowledge of the oil sources. Person B independently analysed oils A–U firstly using the asphaltene profiling method. The aim was primarily to exclude all non-related oils from each other, and consequently grouping together oils of common origin.
3. Steps 1 and 2 were repeated a second time following asphaltene profiling, however:
 - i. The identical sample-set of 21 oils was re-labelled from A–U in a different order by Person A.
 - ii. Person B independently analysed oils A–U using the CEN method.

4. Person B provided two separate conclusions to Person A:
 - i. Firstly, a conclusion for the asphaltene profiling method; and
 - ii. Secondly, a conclusion for the CEN method.

The conclusions of the asphaltene profiling method were provided to person A prior to commencing the CEN analyses. This meant that the asphaltene conclusions could not be influenced by the interpretation of the CEN results. The sources of the 21 oils were revealed to Person B by Person A following the submission of both the asphaltene and CEN conclusions.

The CEN method (a standard method for oil fingerprinting) has been used during this blind study to assist in the validation of the asphaltene profiling method. This chapter provides the results from asphaltene profiling, and compares asphaltene profiling conclusions to the conclusions derived from the CEN method to help gauge method performance. The CEN method results are reported separately in Appendix C. The reader is referred to the CEN method itself for further details on the method optimisation, analysis conditions and interpretation parameters (CEN, 2012).

7.1. Asphaltene Profiling Method

The asphaltene fractions of oils A–U were extracted using the precipitation method outlined in Chapter 2. The asphaltenes from oils A–U were then analysed following the asphaltene profiling method proposed in Chapter 6. It should be noted that the physical properties of oils and asphaltenes were not assessed during the blind study. Although interesting, the physical properties of asphaltene do not provide evidentiary value to investigations. Additionally, the aim of the blind study was to assess the reliability of interpreting asphaltene chemical profiles.

During the course of the blind study, a single additional compound, Perylene (PER), was identified in asphaltene sulfur/aromatic pyrograms. PER was not previously used for the comparison of asphaltene sulfur/aromatic pyrograms in Chapter 5 (Riley et al. 2018). The presence of PER was repeatable in all of the K triplicates and also in the HFO (u/c) standard during the blind study; hence PER was included in comparisons.

7.1.1. Asphaltene Precipitation of Replicates and Standards

As a measure of repeatability, three separate aliquots of oil were taken from oil K and asphaltene fractions were precipitated from each of these aliquots (K.1, K.2 and K.3). Asphaltenes from aliquots K.1, K.2 and K.3 were then analysed at the beginning of each batch analysis of asphaltenes (A–U), and re-analysed once again at the end of each batch (labelled K.1.2, K.2.2 and K.3.2). Oil K was chosen for replicate precipitations due to the colour of the oil as described below.

A known asphaltene standard (HFO (u/c) asphaltenes) was also analysed as a quality control using both IR and Py-GC-MS. The known standard was analysed every tenth sample to ensure that the IR and Py-GC-MS methods were performing reliably. The results obtained for the HFO (u/c) standard were compared visually to the results obtained for HFO (u/c) asphaltenes in Chapters 4 and 5 (Riley et al. 2016, Riley et al. 2018). The results of the visual comparison between the HFO (u/c) standard and the HFO (u/c) asphaltene from Chapters 4 and 5 are shown and discussed in Section 7.1.2.1.

7.1.2. Asphaltene Profiles

The asphaltene profiles of oils A–U are presented below as well as the repeatability of the profiles for oil K. Alkane pyrograms are presented first to differentiate oils into distinct groups, followed by sulfur/aromatic pyrograms, IR spectra and IR ratios to further

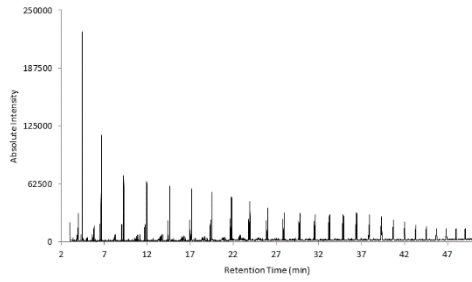
differentiate oils or confirm similarities. IR spectra and IR ratios were only used if the oil sample was not already differentiated based on alkane and/or sulfur/aromatic profiles. Interestingly, asphaltenes were not yielded from oil J; hence an asphaltene profile was not generated for oil J asphaltenes. As a result, oil J was distinguished from the remaining oils in the blind study which all successfully yielded asphaltenes.

7.1.2.1. Method Uncertainty

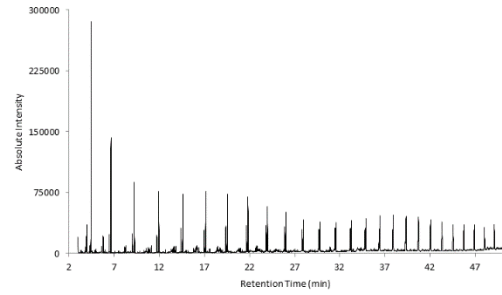
The method uncertainty of asphaltene profiling (including asphaltene precipitation) was gauged by comparing the results from triplicate asphaltene fractions yielded from oil K. K.1, K.2 and K.3 asphaltene fractions were analysed together at the beginning of the sample batch (A-U asphaltenes) using both IR and Py-GC-MS. The oil K triplicates were then re-analysed at the end of the batch (labelled K.1.2, K.2.2, K.3.2). The IR and Py-GC-MS asphaltene profiles for all K analyses were considered repeatable as shown below in Figures 7.1–7.3.

It is worth reinforcing that the slight variations observed between oil K triplicates, such as the slightly differing ratio of BT to C₂-N in the sulfur/aromatic pyrograms (Figure 7.2), are within the degree of repeatability observed when designing the IR and Py-GC-MS methods (refer to Chapters 4 and 5). IR ratios were also calculated for all K analyses, to ensure the repeatability of thresholds. All pairwise comparisons of K analyses were below the previously defined threshold of 20% (Riley et al., 2016 and Chapter 4). Table 7.1 shows an example of IR ratios compared for one of the oil K asphaltene fractions analysed at the beginning and end of the batch (K.1 and K.1.1). Table 7.2 shows an example of K.1 compared to K.2; two completely separate asphaltene fractions yielded from oil K. The repeatability of oil K triplicates ensured that all asphaltenes analysed between the beginning and end of the batch (oils A–U) were suitable for comparison.

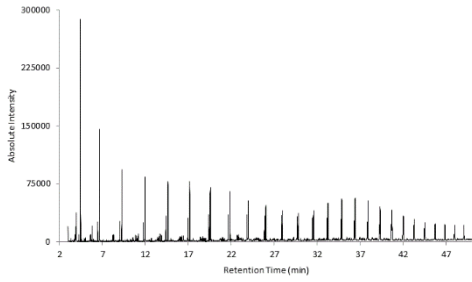
K.1



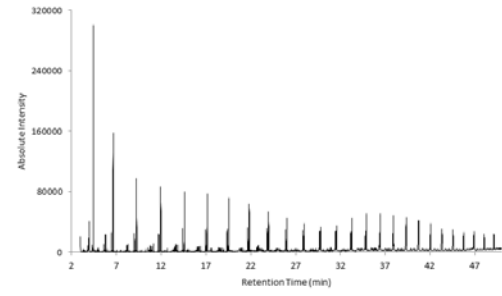
K.1.2



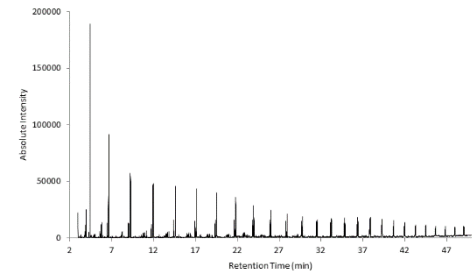
K.2



K.2.2



K.3



K.3.2

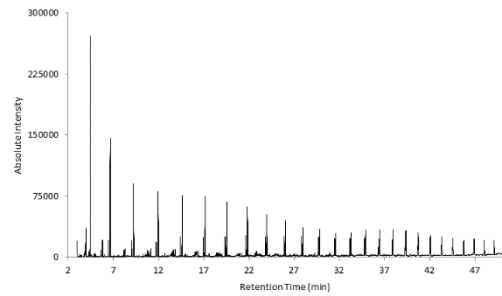


Figure 7.1: Alkane pyrograms of the oil K asphaltene triplicates (K.1, K.2 and K.3) and the re-analysed triplicates (K.1.2, K.2.2, K.3.2).

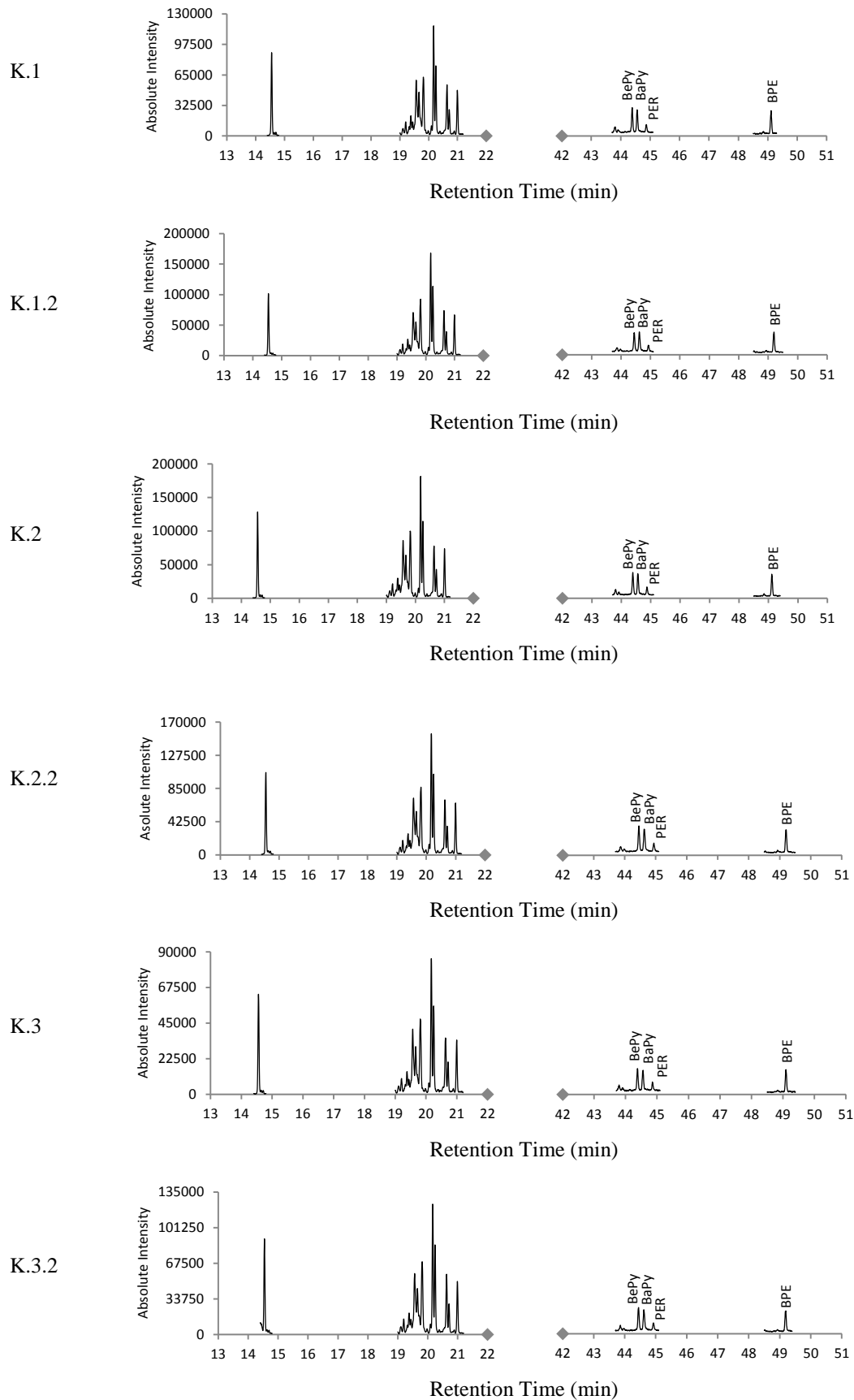


Figure 7.2: Sulfur/aromatic pyrograms of the oil K asphaltene triplicates (K1, K2 and K3) and the re-analysed triplicates (K.1.2, K.2.2, K.3.2).

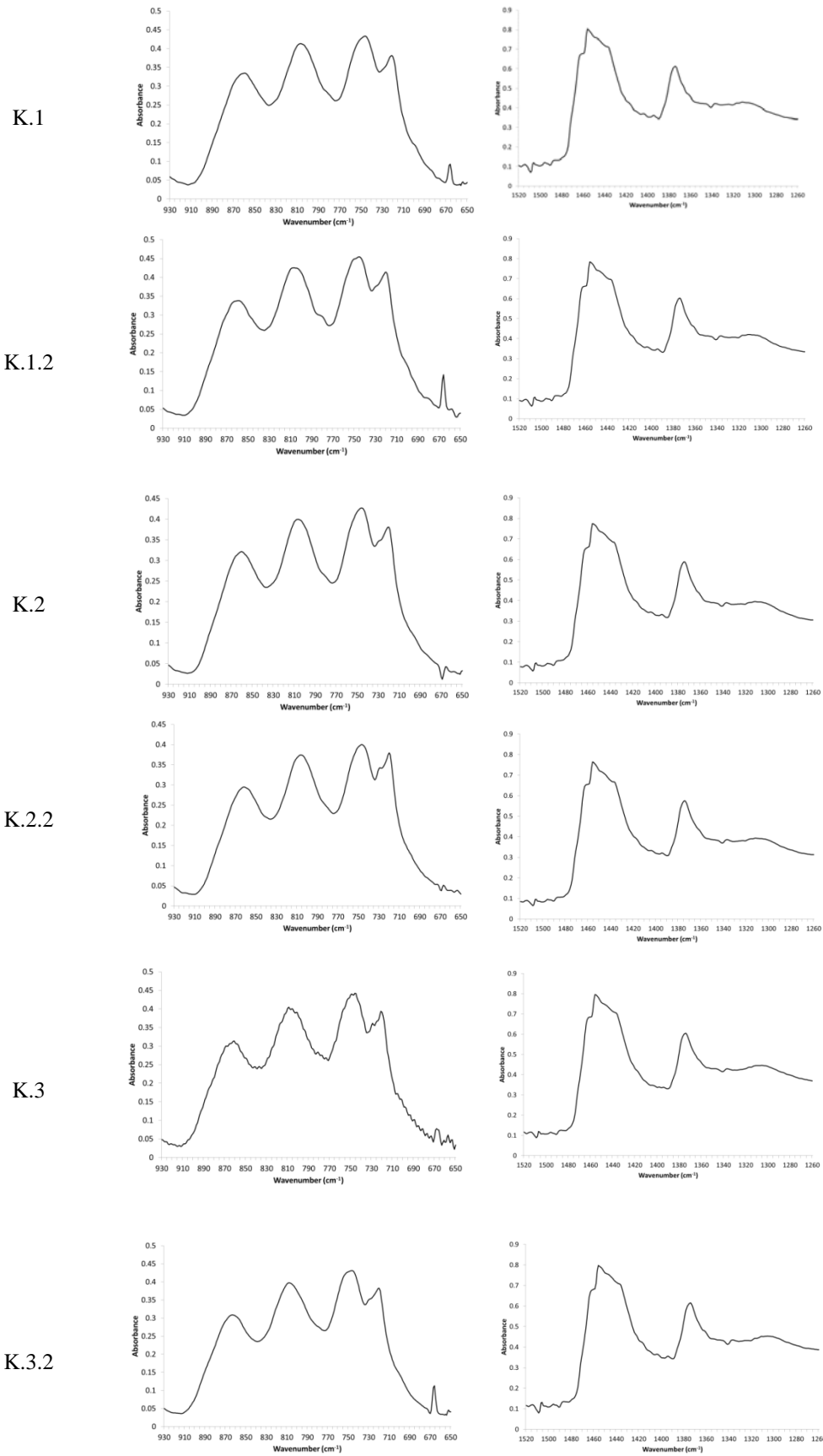


Figure 7.3: IR spectra of the oil K asphaltene triplicates (K.1, K.2 and K.3) and the re-analysed triplicates (K.1.2, K.2.2, K.3.2).

Table 7.1: Peak height ratios compared between K.1 and K.1.2 asphaltenes. K.1 asphaltenes were analysed at the beginning of the batch and again at the end of the batch sequence (K.1.2).

IR Ratio	Peak Height Ratio		Mean	Absolute Difference	Relative Difference (%)	Conclusion
	K.1	K.1.2				
1463/1377	1.13	1.13	1.13	0.00	0	Not Different
1457/1377	1.31	1.30	1.30	0.01	1	Not Different
1437/1377	1.20	1.20	1.20	0.00	0	Not Different
867/719	0.87	0.79	0.83	0.08	10	Not Different
809/719	1.11	1.04	1.08	0.08	7	Not Different
748/719	1.17	1.10	1.14	0.06	6	Not Different

Table 7.2: Peak height ratios compared between K.1 and K.2 asphaltenes. K.1 and K.2 asphaltenes were two separate asphaltene fractions obtained from the same oil.

IR Ratio	Peak Height Ratio		Mean	Absolute Difference	Relative Difference (%)	Conclusion
	K.1	K.2				
1463/1377	1.13	1.13	1.13	0.00	0	Not Different
1457/1377	1.31	1.31	1.31	0.00	0	Not Different
1437/1377	1.20	1.20	1.20	0.00	0	Not Different
867/719	0.87	0.82	0.84	0.05	6	Not Different
809/719	1.11	1.06	1.09	0.05	5	Not Different
748/719	1.17	1.13	1.15	0.03	3	Not Different

As mentioned previously, the performance of the asphaltene profiling method was also gauged by using a known standard (HFO (u/c) asphaltenes) which was sequential analysed after every tenth sample. When visually compared, the IR and Py-GC-MS results for the HFO (u/c) standard were consistent with those previously reported for HFO (u/c) in Chapter 4 and 5 (Figures 7.4–7.6). Slight variability was observed between the HFO (u/c) standard and the HFO (u/c) asphaltenes from Chapter 5 when comparing the intensities of BaPy, BePy and BPE in relation to the intensities of C₂-N and BT. As stated in Chapter 5 however, the intensity of BPy and BPE peaks may vary slightly between replicates therefore

minor differences in intensity were not relied upon for the differentiation of oils. Instead, only very obvious differences in the intensities of BPy and BPE peaks may be relied upon for the differentiation of oils, as well as clear presence/absence differences. It is worth noting too, that PER was not extracted for comparison in Chapter 5; hence PER is not shown in the Chapter 5 pyrograms presented in Figure 7.5.

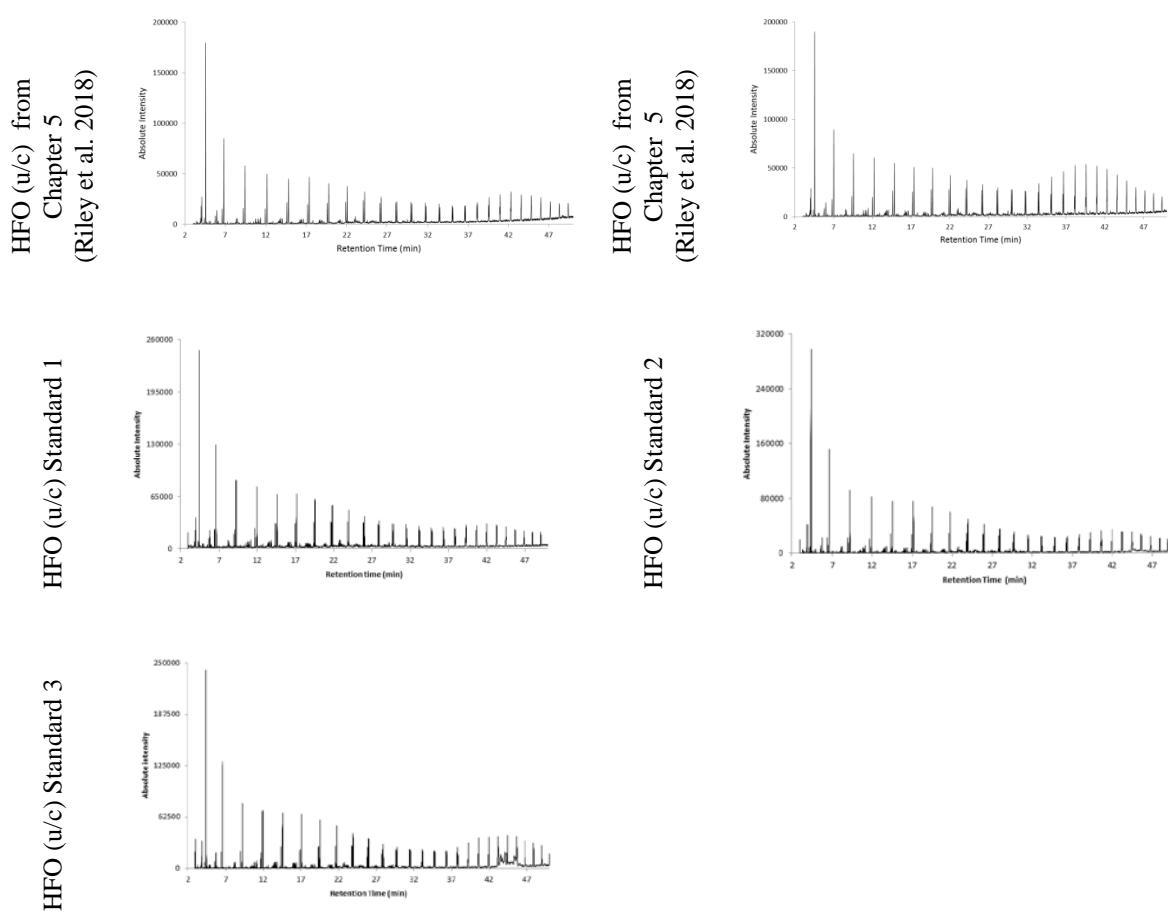


Figure 7.4: Alkane pyrograms of the HFO (u/c) asphaltene standard (analysed 3 times during the blind study) and of 2 separate HFO (u/c) asphaltene samples from Chapter 5, which represent the maximum variance observed between 7 replicates (Riley et al. 2018).

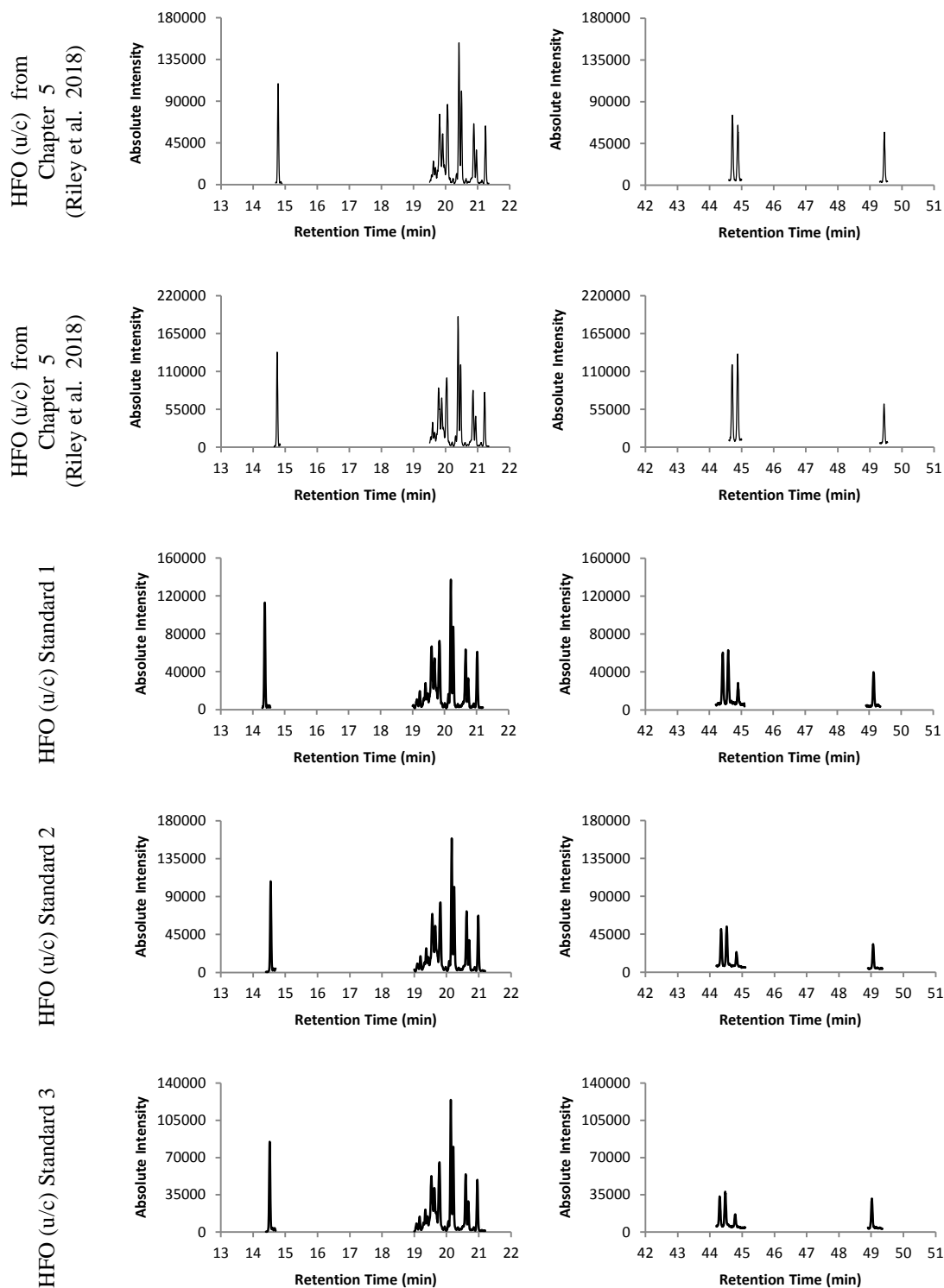


Figure 7.5: Sulfur/aromatic pyrograms of the HFO (u/c) asphaltene standard (analysed 3 times during the blind study) and of 2 separate HFO (u/c) asphaltene samples from Chapter 5, which represent the maximum variance observed between 7 replicates (Riley et al. 2018). PER was not extracted for comparison during Chapter 5; hence PER is not shown in the Chapter 5 pyrograms.

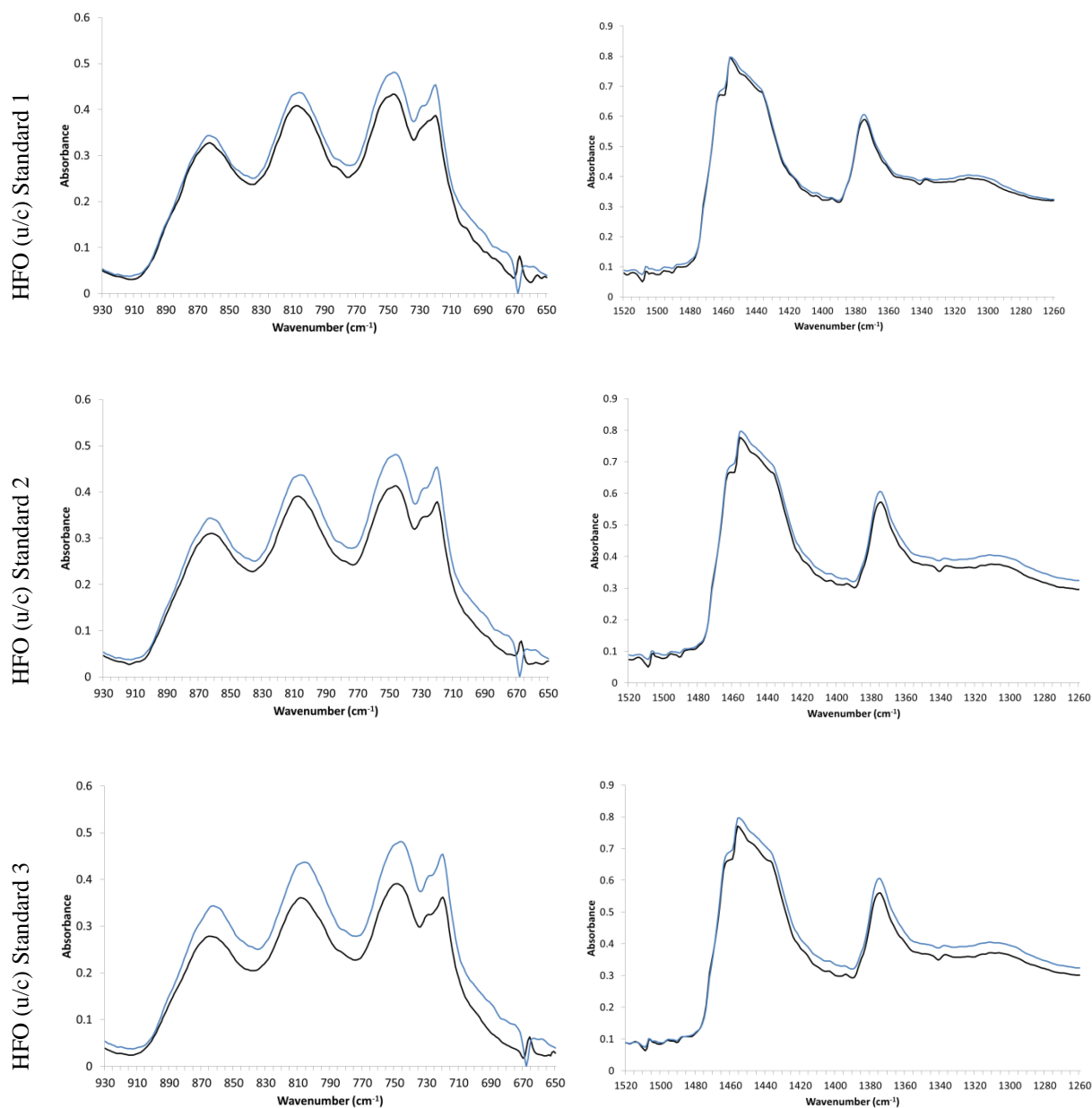


Figure 7.6: IR spectra of HFO (u/c) asphaltenes. Black line: HFO (u/c) standard analysed during the blind study (analysed 3 times); Blue line: HFO (u/c) IR spectra (mean of 7 replicates) as published in Riley et al. (2016).

Re-analysis of each asphaltene fraction (A-U) was also conducted during IR analysis to gauge method error, particularly when calculating and comparing peak height ratios. It should be noted that asphaltenes were re-analysed on a different day to the initial analysis, and following Py-GC-MS. Asphaltenes analysed in the initial batch analysis are indicated as

a black line in all IR spectra presented throughout this chapter, whilst re-analysed asphaltenes are indicated as red lines and are labelled ending in '.2' in all text. Note, not all asphaltene fractions could be re-analysed due to insufficient amounts of asphaltenes available after Py-GC-MS.

7.1.2.2. Alkane Pyrograms

Asphaltenes from oils A–U (excluding J) were first compared using alkane pyrograms. This visual comparison was capable of quickly differentiating oils that were very clearly unrelated. Note, this initial comparison of alkane pyrograms is subjective; hence asphaltenes were only separated based on very obvious differences in profile shapes. The aim of using alkane pyrograms was to quickly break down the sample-set by excluding clearly unrelated asphaltenes, not to definitively exclude all unrelated oils. It may be possible to further separate the three groups presented below based on alkanes; however this is ultimately at the discretion of the analyst's opinion and experience. In this blind study, the analyst decided that if smaller differences were observed in the alkane pyrograms between two asphaltenes, these asphaltenes would be included within the same group to remain conservative. If unrelated asphaltenes were falsely included based on alkane pyrograms, IR spectra and sulfur/aromatic pyrograms should be capable of excluding these unrelated oils as this information is more discriminatory than alkane pyrograms. It is acknowledged that with further research, more definitive exclusions based on alkane pyrograms may be achievable.

The first group of asphaltenes (C, R, E, Q and S) exhibited alkane pyrograms that were dominated by high-boiling compounds (Figure 7.7). The overall profile shape of the C, R, E, Q and S pyrograms was much broader in the high-boiling region than the second group of asphaltenes (I, G, D, N, P and L) which were also dominated by high-boiling compounds (Figures 7.7 and 7.8). The second group exhibited a sharper profile shape in the high boiling

region than the first group. Whilst the alkane profile for S asphaltenes showed a presence of low-boiling compounds, S asphaltenes were grouped alongside the C, R, E and Q asphaltenes due to the similarity of the profile shape in the high-boiling region.

To be certain, S asphaltenes were also compared to F, K, B, T, U, A, H, O and M asphaltenes. These asphaltenes make up the third group and were characterised by low-boiling compounds (refer below). From the IR spectra alone, S asphaltenes were different to F, K, B, T, U, A, H, O and M asphaltenes. Therefore S asphaltenes are better situated alongside C, R, E and Q asphaltenes as previously indicated.

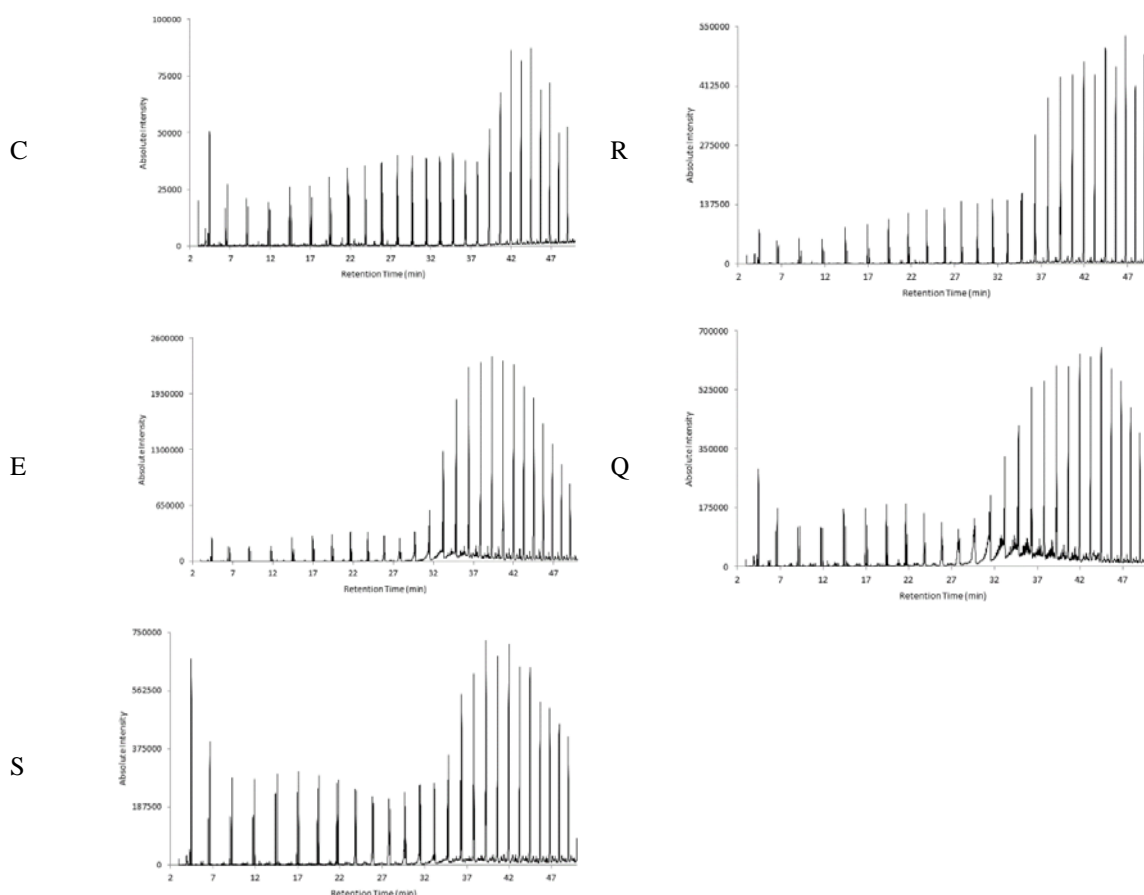


Figure 7.7: C, R, E, Q and S asphaltene alkane pyrograms that were dominated by high-boiling compounds.

The third group of asphaltenes (F, K, B, T, U, A, H, O and M) was defined by alkane pyrograms that were dominant in low-boiling compounds with a reduction in intensity of

alkanes as RT increased (Figure 7.9). It must be noted that the alkane profile for H asphaltenes displayed dominance in low-boiling compounds and also showed a sharp raised profile in the high-boiling region which was consistent with I, G, D, N, P and L asphaltenes. H asphaltenes, however, were grouped with F, K, B, T, U, A, O and M asphaltenes as the pyrograms for I, G, D, N, P and L asphaltenes lacked low-boiling compounds. To be certain, the IR spectra of H asphaltenes were also compared to the IR spectra of I, G, D, N, P and L asphaltenes. The IR spectra of H asphaltenes were different to I, G, D, N, P and L asphaltenes which confirmed that H asphaltenes were indeed better grouped with F, K, B, T, U, A, O and M asphaltenes.

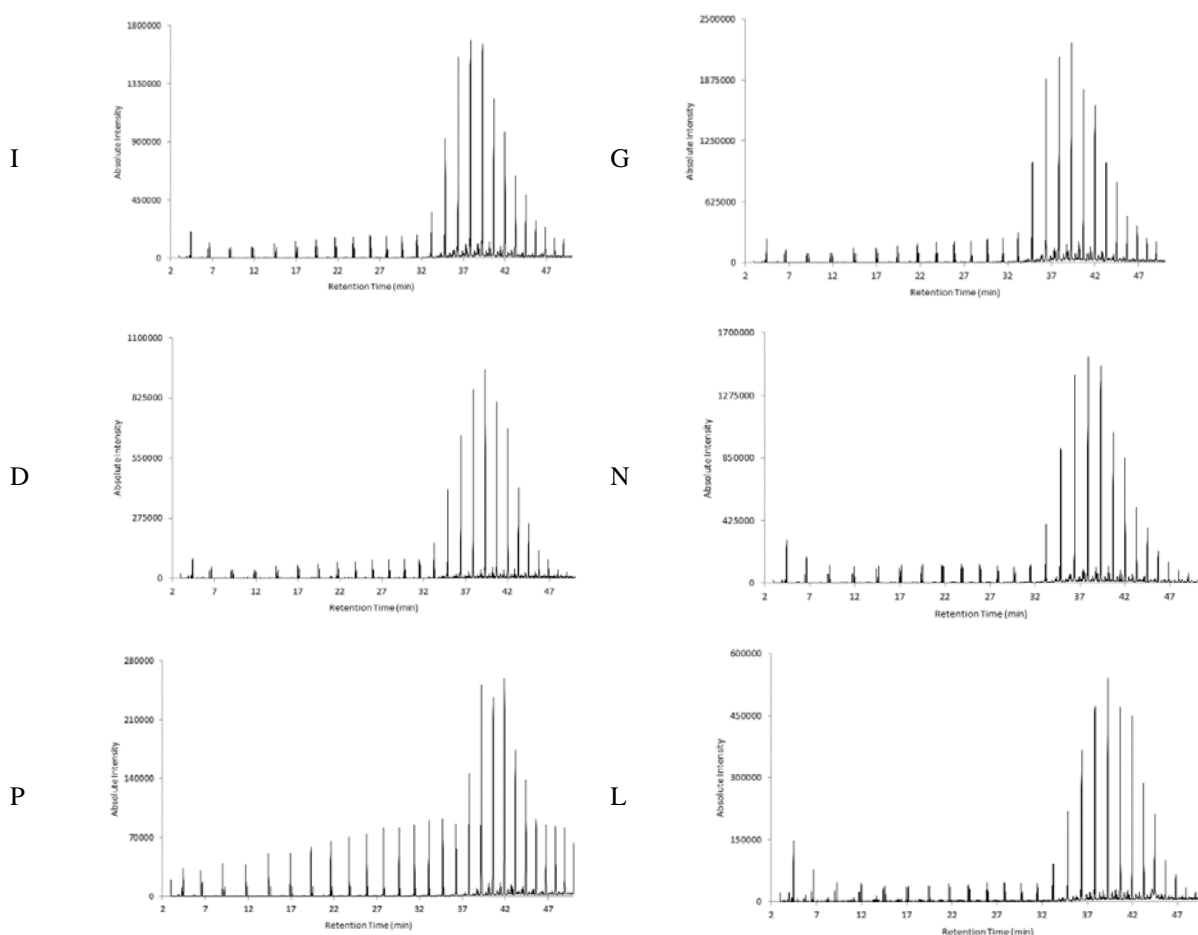


Figure 7.8: I, G, D, N, P and L asphaltene alkane pyrograms with a sharp, defined cluster of peaks between 32 and 47 min.

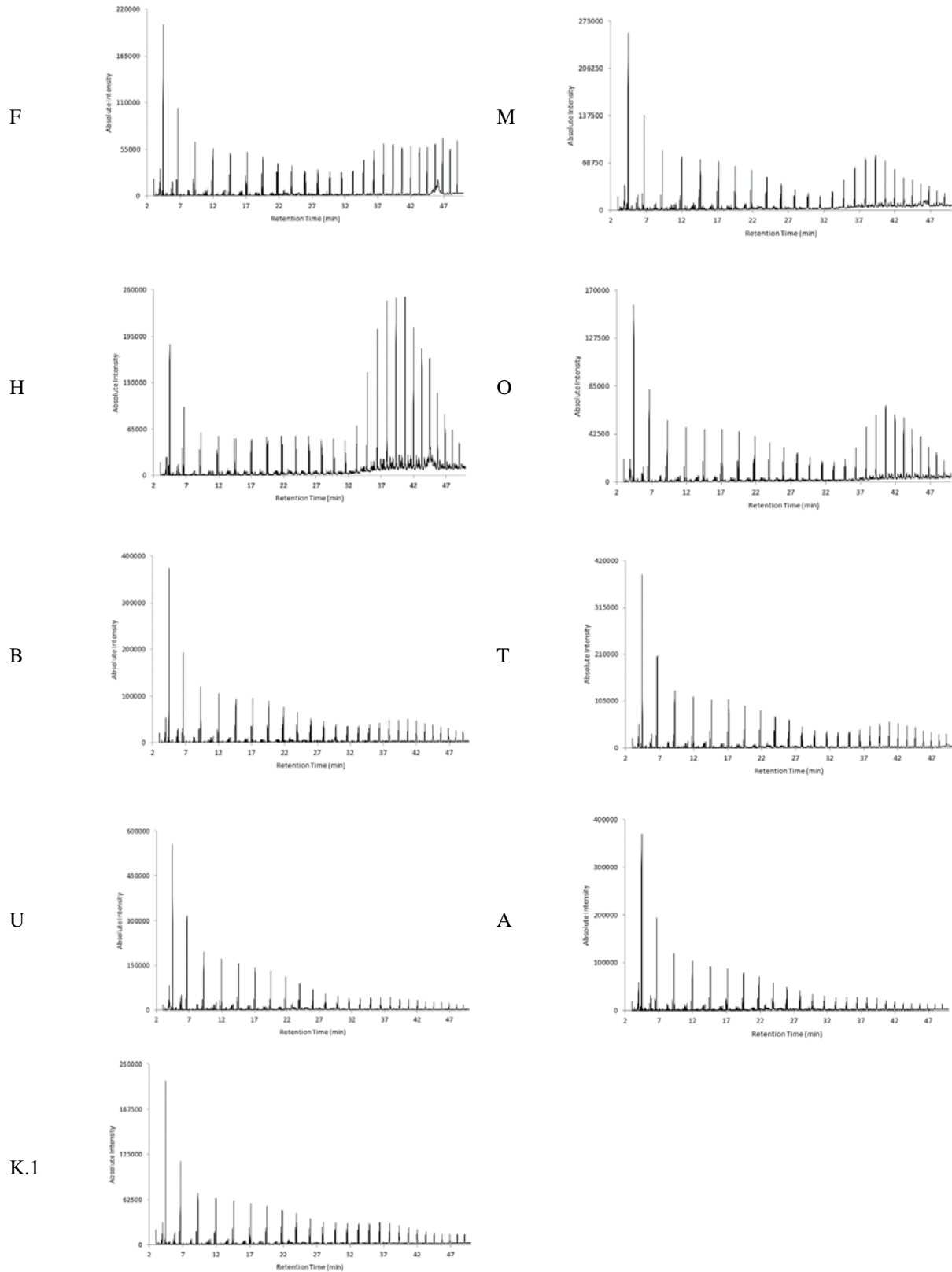


Figure 7.9: F, K, B, T, U, A, H, O and M asphaltene alkane pyrograms dominated by low-boiling compounds with reduced alkane intensity as RT increased.

7.1.2.3. Sulfur/Aromatic Pyrograms and IR Spectra

The three groups of oils, as defined by alkane pyrograms, were further differentiated by comparing sulfur/aromatic pyrograms and IR spectra of asphaltenes. Visual comparisons of pyrograms and IR spectra were first conducted, and any asphaltene fractions that were visually indistinguishable were compared using IR ratios as a final check. The results for each of the three groups are shown below.

Asphaltenes from oils C, R, E, Q and S

Oils C and R were separated from oils E, Q and S on the basis of differences observed in the asphaltene sulfur/aromatic pyrograms. In both C and R pyrograms, benzo(e)pyrene (BePy), benzo(a)pyrene (BaPy) and PER peaks were absent, whereas in E, Q and S pyrograms, one or more of these peaks for BePy, BaPy or PER were present. C and R pyrograms are shown in Figures 7.10 and 7.11 below, whilst E, Q and S pyrograms are shown following the discussion for C and R asphaltenes (Figures 7.12–7.14). BePy, BaPy, and PER peaks have been labelled hereafter when present in asphaltene pyrograms. BPE peaks have also been labelled when present to further help interpret pyrograms.

C and R asphaltenes were compared to one another. It was not feasible to analyse C and R asphaltenes using the IR method due to low asphaltene yields from C and R oils. Oils C and R were the two lowest yielding oils with 0.2 mg and 1.4 mg asphaltene yields, respectively. Although 1.4 mg exceeds the minimal amount of asphaltenes required for IR analysis in most cases (1 mg as specified in Chapter 2), it was not possible in this case to cover the ATR crystal due to the very fine composition of the asphaltenes. Consequently, based solely on asphaltene pyrograms, oils C and R could not be differentiated from one another. CEN analysis would be required for oils C and R to determine a confirmatory conclusion. If C and R cannot be separated based on volatile fingerprinting, the asphaltene

pyrograms may provide useful additional information in support of an identification or inconclusive conclusion.

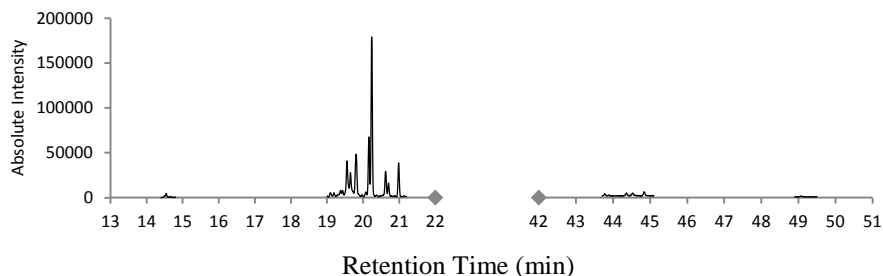


Figure 7.10: Sulfur/aromatic pyrogram obtained from oil C asphaltenes.

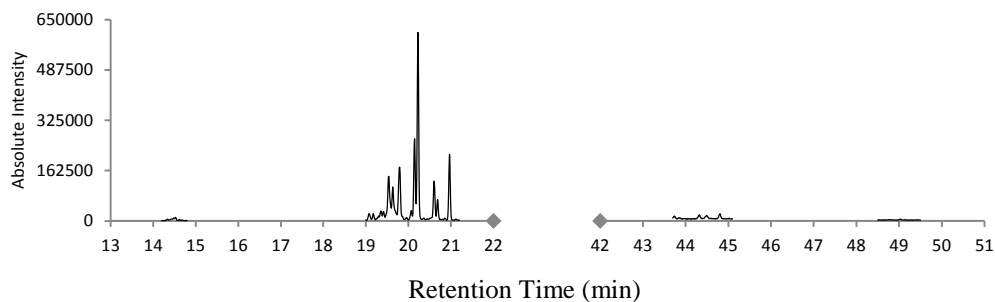


Figure 7.11: Sulfur/aromatic pyrogram obtained from oil R asphaltenes.

E, Q and S asphaltenes were also compared to one another. E asphaltenes were differentiated from Q and S asphaltenes based on a visual comparison of IR spectra. A sharp peak at 1472 cm^{-1} was present in the IR spectra of E asphaltenes as shown in Figure 7.12. In comparison, Q asphaltenes (Figure 7.13) and S asphaltenes (Figure 7.14) did not display a sharp peak at 1472 cm^{-1} in the IR spectra. As a result, Oil E did not originate from the same source as any other oils in the blind study and could be differentiated.

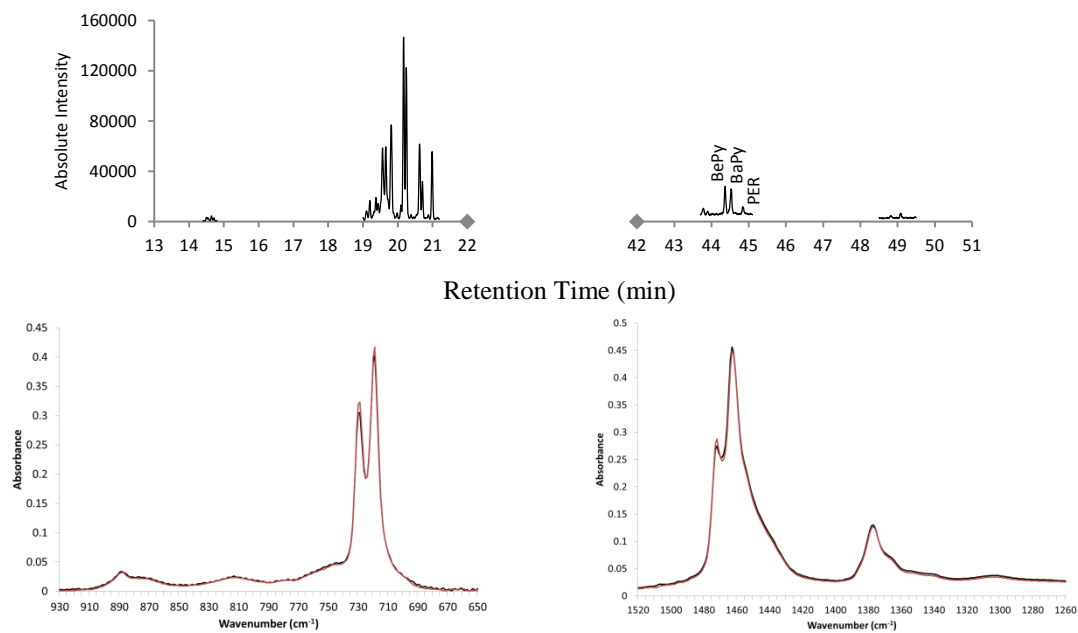


Figure 7.12: Sulfur/aromatic pyrogram and IR spectra from oil E asphaltenes.

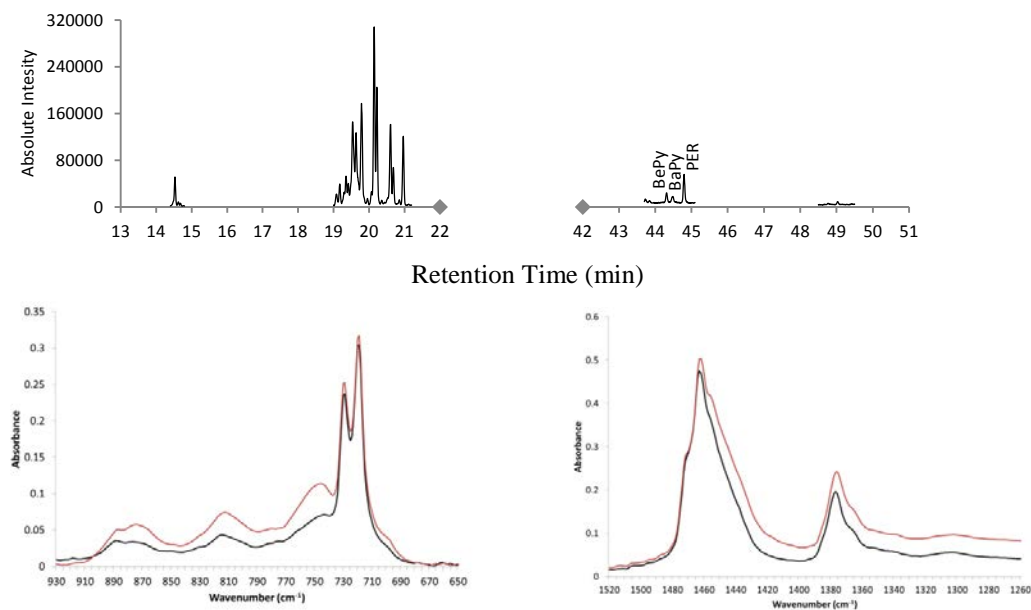


Figure 7.13: Sulfur/aromatic pyrogram and IR spectra from oil Q asphaltenes.

Q and S asphaltenes were differentiated from one another based on the visual comparison of sulfur/aromatic pyrograms. The most obvious difference between Q and S asphaltenes was the presence of PER in Q and absence of PER in S. The presence of PER was repeatable in the K triplicates and also in the HFO (u/c) standard, therefore the

presence/absence difference of PER observed between S and Q was deemed significant. Overall, oils S and Q were differentiated from one another based on asphaltene profiles, and from all other oils in the blind study.

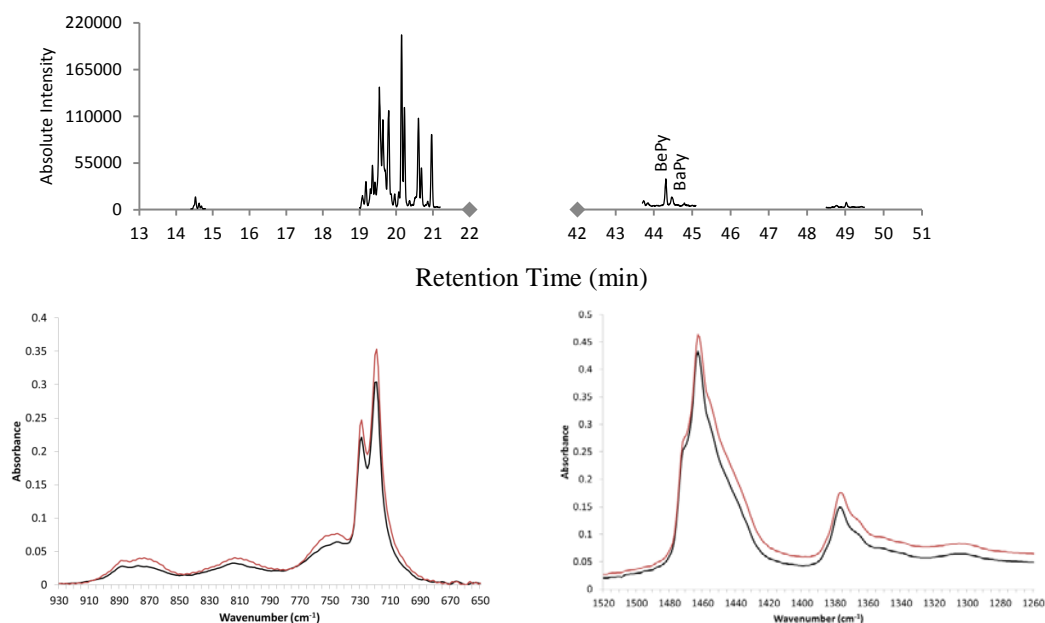


Figure 7.14: Sulfur/aromatic pyrogram and IR spectra from oil S asphaltenes.

Asphaltenes from oils I, G, D, N, P and L

Oils I and G were differentiated from oils D, N, P and L based on the sulfur/aromatic pyrograms of asphaltenes. I and G pyrograms (Figures 7.15 and 7.16, respectively) both exhibited considerably higher intensity BePy peaks in comparison to the very low intensity BePy peaks observed in D, N, P and L pyrograms (figures presented later in this section).

When comparing I and G sulfur/aromatic pyrograms, I and G were indistinguishable. Furthermore, both I and G asphaltenes exhibited resinous IR spectra with very similar profiles when visually observed.

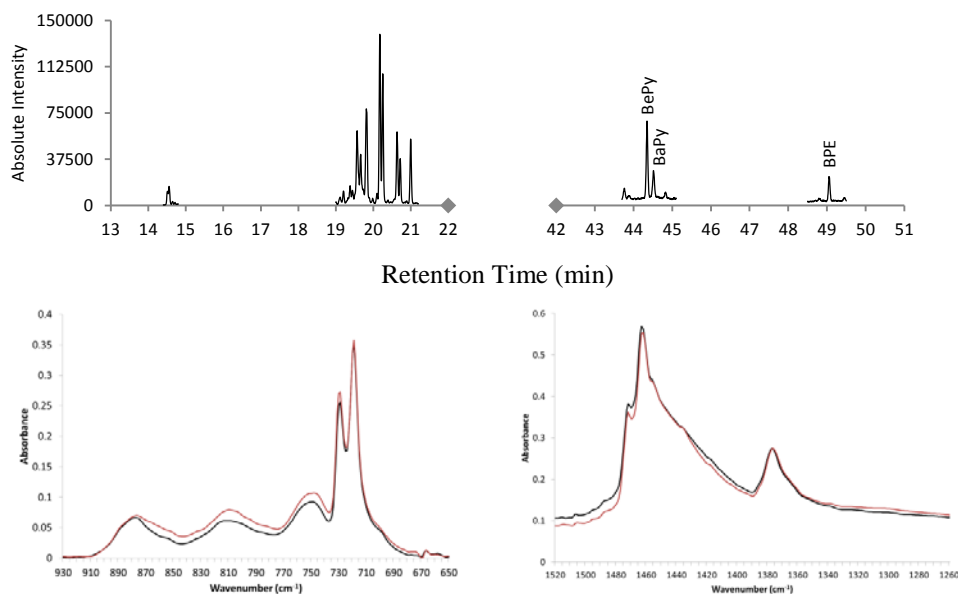


Figure 7.15: Sulfur/aromatic pyrogram and IR spectra from oil I asphaltenes.

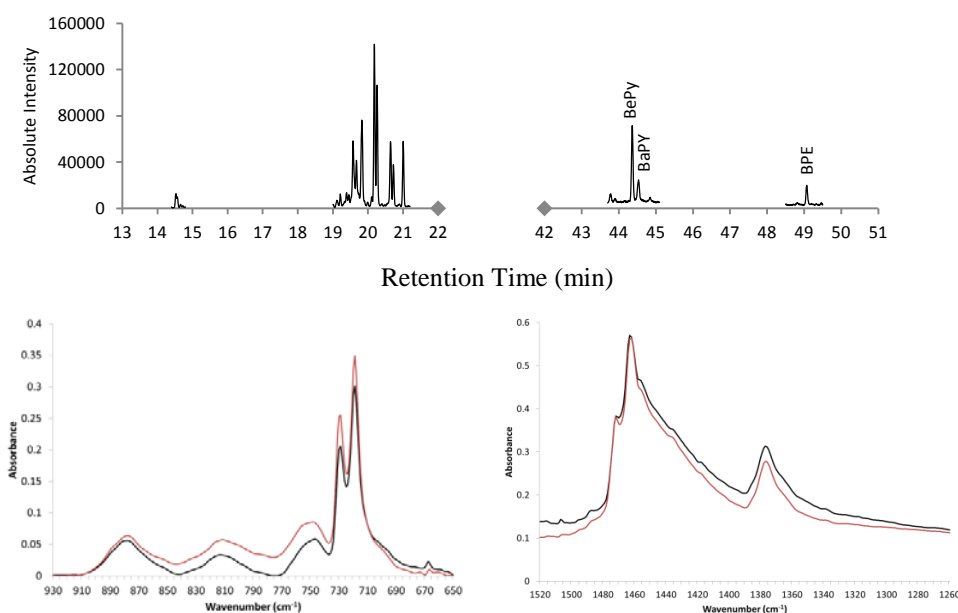


Figure 7.16: Sulfur/aromatic pyrogram and IR spectra from oil G asphaltenes.

IR ratios were calculated for I and G asphaltenes for confirmation. It should be noted that a minor presence/absence difference was observed between G and I spectra. A small peak at 809 cm^{-1} was observed in the I asphaltene spectra and not in the G spectra, whilst a small peak at 814 cm^{-1} was observed in the G spectra and not in the I spectra. This

presence/absence difference was very subtle and was not deemed significant for exclusion at the time of comparison. As such, peak height ratios for peak 809 cm^{-1} and 814 cm^{-1} were not calculated as the result would simply express the presence/absence difference which has already been noted.

Peak height ratios were first calculated and compared between I duplicates (initial analysis and re-analysis) as well as between G duplicates. Whilst all comparable ratios fell below the 20% threshold for the I duplicates as expected, the $748/719\text{ cm}^{-1}$ ratio exceeded the 20% threshold (at 24%) when G duplicates were compared (results not shown). Given the observed variability between G duplicates, the $748/719\text{ cm}^{-1}$ was removed from the comparison of ratios between G and I asphaltenes. This variability must be attributed to changes in instrument conditions in the intervening days between initial analysis and re-analysis.

Pairwise comparisons between all G and I asphaltenes (initial analysis and re-analysis) were conducted using the remaining comparable ratios as shown in Tables 7.3–7.6. All of the compared ratios fell within the 20% threshold for all pairwise comparisons indicating that I and G could not be differentiated on the basis of IR ratios. As a result of comparing asphaltene profiles, oils I and G were not differentiated from one another, however oils I and G were differentiated from all other oils in the blind study. Further analysis using conventional volatile oil fingerprinting would be recommended to determine a confirmatory conclusion between oils I and G.

Table 7.3: Peak height ratios compared between I and G asphaltenes.

IR Ratio	Peak Height Ratio		Mean	Absolute Difference	Relative Difference (%)	Conclusion
	G	I				
1472/1377	1.22	1.39	1.31	0.17	13	Not Different
1463/1377	1.82	2.07	1.95	0.25	13	Not Different
1457/1377	1.49	1.61	1.55	0.12	8	Not Different
1437/1377	1.13	1.19	1.16	0.06	5	Not Different
877/719	0.18	0.19	0.19	0.00	3	Not Different
729/719	0.68	0.73	0.70	0.04	6	Not Different

Table 7.4: Peak height ratios compared between G and I.2 asphaltenes.

IR Ratio	Peak Height Ratio		Mean	Absolute Difference	Relative Difference (%)	Conclusion
	G	I.2				
1472/1377	1.22	1.32	1.27	0.10	8	Not Different
1463/1377	1.82	2.01	1.92	0.19	10	Not Different
1457/1377	1.49	1.59	1.54	0.10	7	Not Different
1437/1377	1.13	1.19	1.16	0.06	5	Not Different
877/719	0.18	0.20	0.19	0.01	7	Not Different
729/719	0.68	0.76	0.72	0.08	11	Not Different

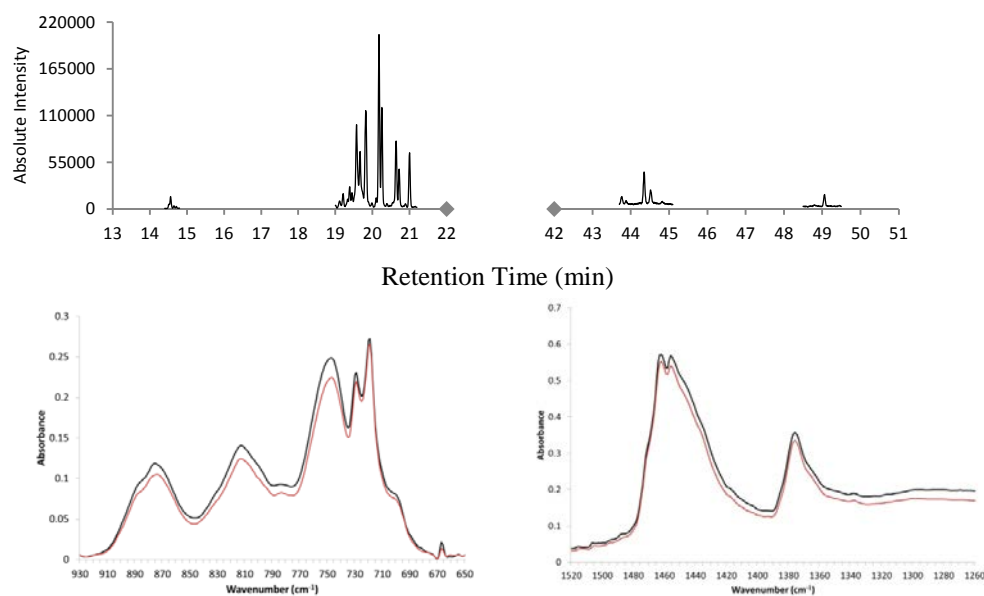
Table 7.5: Peak height ratios compared between I and G.2 asphaltenes.

IR Ratio	Peak Height Ratio		Mean	Absolute Difference	Relative Difference (%)	Conclusion
	I	G.2				
1472/1377	1.39	1.37	1.38	0.02	1	Not Different
1463/1377	2.07	2.02	2.04	0.05	3	Not Different
1457/1377	1.61	1.61	1.61	0.01	1	Not Different
1437/1377	1.19	1.20	1.20	0.02	1	Not Different
1377	1.00	1.00	1.00	0.00	0	Not Different
877/719	0.19	0.18	0.19	0.01	4	Not Different
729/719	0.73	0.73	0.73	0.01	1	Not Different

Table 7.6: Peak height ratios compared between G.2 and I.2 asphaltenes.

IR Ratio	Peak Height Ratio		Mean	Absolute Difference	Relative Difference (%)	Conclusion
	G.2	I.2				
1472/1377	1.37	1.32	1.35	0.05	4	Not Different
1463/1377	2.02	2.01	2.01	0.01	0	Not Different
1457/1377	1.61	1.59	1.60	0.01	1	Not Different
1437/1377	1.20	1.19	1.20	0.01	1	Not Different
877/719	0.18	0.20	0.19	0.02	8	Not Different
729/719	0.73	0.76	0.75	0.03	4	Not Different

Oil L was easily differentiated from oils D, N and P on the basis of asphaltene IR spectra. Asphaltenes from oil L generated a very distinct high intensity peak at 748 cm^{-1} in IR spectra which was unique to L asphaltenes (as observed in Figure 7.17).

**Figure 7.17:** Sulfur/aromatic pyrogram and IR spectra from oil L asphaltenes.

D and N asphaltenes were differentiated from P asphaltenes on the basis of clear differences observed in Region 2 of the IR spectra. A sharp, distinct peak at 1473 cm^{-1} was observed in the IR spectrum of P asphaltenes (Figure 7.18) whereas the peak at 1473 cm^{-1}

was absent in both spectra for D and N asphaltenes (Figures 7.19 and 7.20). Consequently, oil P was differentiated from oils D and N based on asphaltene profiles, as well as being differentiated from all other blind study oils.

D asphaltenes differed slightly from N asphaltenes based on sulfur/aromatic pyrograms; PER was borderline present in D asphaltenes, yet not observed in N asphaltenes. As the PER peak in D was not high intensity (it was not an obvious presence/absence difference), IR ratios for D and N asphaltenes were calculated and compared for confirmation. Prior to comparison of ratios, it should be noted that a very subtle peak at 780 cm^{-1} was observed in the N spectra, however this same peak was absent in the D spectra. Due to the poor resolution of the 780 cm^{-1} peak, this peak was not relied upon solely for exclusion.

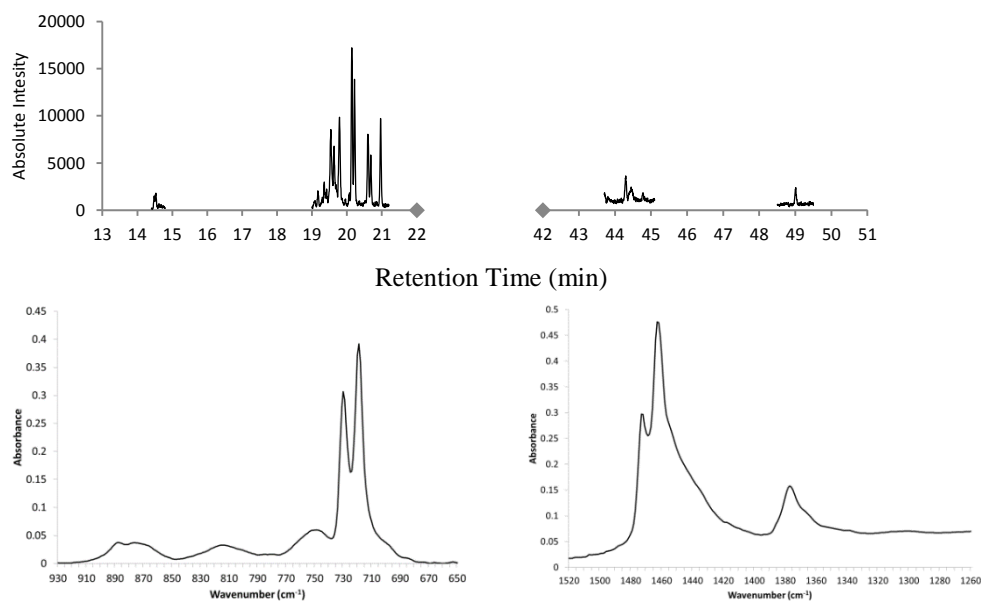


Figure 7.18: Sulfur/aromatic pyrogram and IR spectra from oil P asphaltenes.

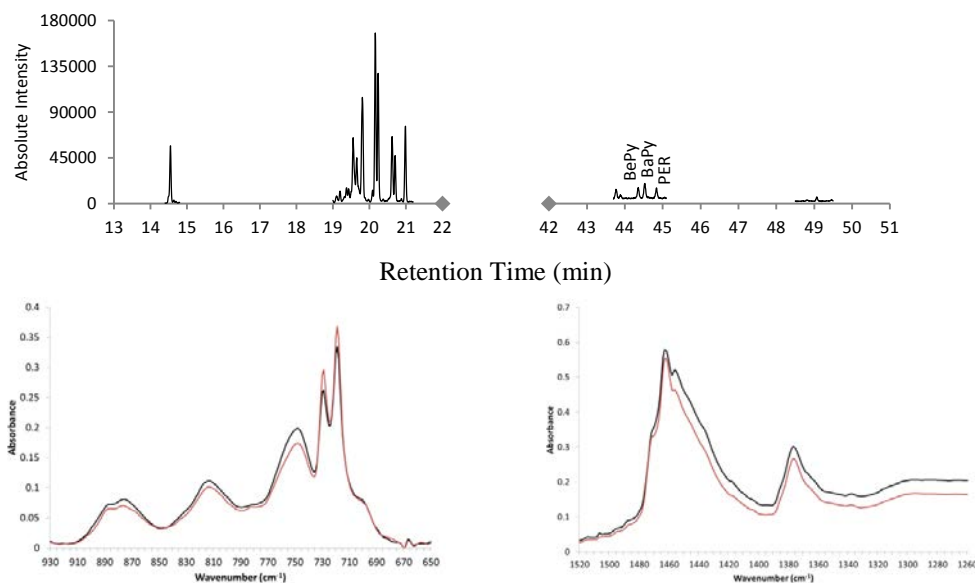


Figure 7.19: Sulfur/aromatic pyrogram and IR spectra from oil D asphaltenes.

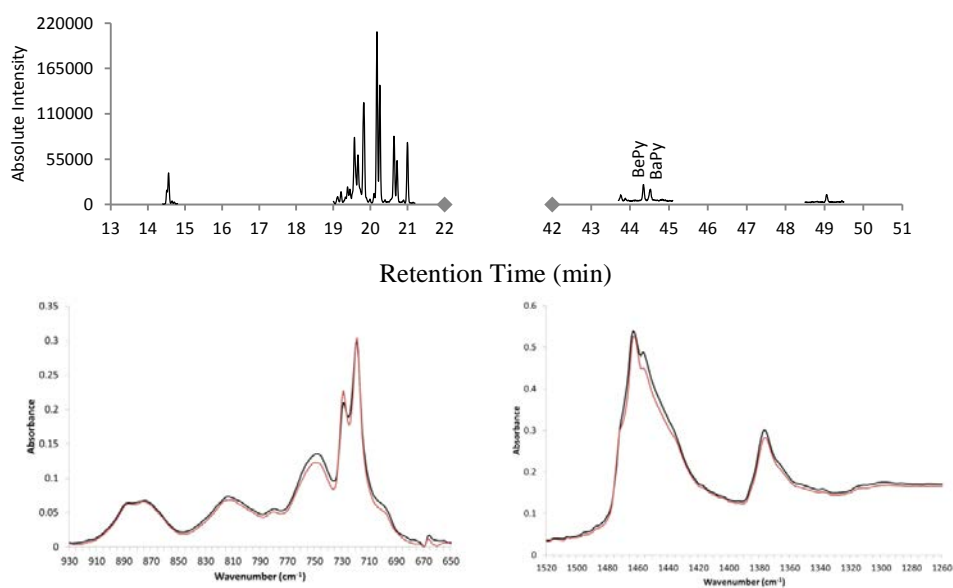


Figure 7.20: Sulfur/aromatic pyrogram and IR spectra from oil N asphaltenes.

Peak height ratios were first calculated and compared between D duplicates (initial analysis and re-analysis) as well as between N duplicates. Whilst all comparable ratios fell below the 20% threshold for the N duplicates as expected, both the $877/719\text{ cm}^{-1}$ and $748/719\text{ cm}^{-1}$ ratios exceeded the 20% threshold (both at 23%) when D duplicates were compared (results not shown). The $877/719\text{ cm}^{-1}$ and $748/719\text{ cm}^{-1}$ ratios could therefore not be relied

upon for the comparison of D to N asphaltenes, hence both ratios were not calculated or compared.

Pairwise comparisons between all D and N asphaltenes (initial analysis and re-analysis) were conducted using the remaining comparable ratios as shown in Tables 7.7–7.10. In the first pairwise comparison (D and N), the 814/719 cm^{-1} ratio exceeded the threshold at 30%. This same ratio (814/719 cm^{-1}) also exceeded the threshold in two other pairwise comparisons; D and N.2 (39%), and D.2 and N.2 (24%). The comparison of D and N.2 also resulted in the 701/719 cm^{-1} ratio exceeding the threshold (29%), whilst the comparison of D.2 and N resulted in the 1472/1377 cm^{-1} ratio marginally exceeding the threshold (21%). Whilst ratio differences were observed across all pairwise comparisons, there was not a single ratio which was different unanimously in all pairwise comparisons; 814/719 cm^{-1} was different in three out of four pairs, whilst 701/719 cm^{-1} and 1472/1377 cm^{-1} were only different in single pairs, respectively. The comparison of D and N asphaltenes alone is not capable of determining if the D and N oils are related or different. Consequently, the results from the comparison of D and N asphaltenes are inconclusive. Based on this observation, volatile fingerprinting is required for oils D and N.

Table 7.7: Peak height ratios compared between D and N asphaltenes.

IR Ratio	Peak Height Ratio		Mean	Absolute Difference	Relative Difference (%)	Conclusion
	D	N				
1472/1377	1.13	1.00	1.07	0.13	12	Not Different
1463/1377	1.92	1.79	1.86	0.13	7	Not Different
1457/1377	1.72	1.62	1.67	0.10	6	Not Different
1437/1377	1.18	1.02	1.10	0.16	15	Not Different
888/719	0.21	0.21	0.21	0.00	0	Not Different
814/719	0.33	0.25	0.29	0.09	30	Different
729/719	0.78	0.70	0.74	0.08	10	Not Different
701/719	0.24	0.21	0.23	0.03	13	Not Different

Table 7.8: Peak height ratios compared between D and N.2 asphaltenes.

IR Ratio	Peak Height Ratio		Mean	Absolute Difference	Relative Difference (%)	Conclusion
	D	N.2				
1472/1377	1.13	1.06	1.10	0.07	6	Not Different
1463/1377	1.92	1.87	1.90	0.05	3	Not Different
1457/1377	1.72	1.59	1.66	0.13	8	Not Different
1437/1377	1.18	1.02	1.10	0.16	15	Not Different
888/719	0.21	0.20	0.21	0.01	5	Not Different
814/719	0.33	0.22	0.28	0.11	39	Different
729/719	0.78	0.75	0.77	0.03	4	Not Different
701/719	0.24	0.18	0.21	0.06	29	Different

Table 7.9: Peak height ratios compared between D.2 and N asphaltenes.

IR Ratio	Peak Height Ratio		Mean	Absolute Difference	Relative Difference (%)	Conclusion
	D.2	N				
1472/1377	1.23	1.00	1.12	0.23	21	Different
1463/1377	2.07	1.79	1.93	0.28	15	Not Different
1457/1377	1.73	1.62	1.68	0.11	7	Not Different
1437/1377	1.11	1.02	1.07	0.09	8	Not Different
888/719	0.18	0.21	0.20	0.03	15	Not Different
814/719	0.28	0.25	0.27	0.03	11	Not Different
729/719	0.80	0.70	0.75	0.10	13	Not Different
701/719	0.21	0.21	0.21	0	0	Not Different

Table 7.10: Peak height ratios compared between D.2 and N.2 asphaltenes.

IR Ratio	Peak Height Ratio		Mean	Absolute Difference	Relative Difference (%)	Conclusion
	D.2	N.2				
1472/1377	1.23	1.06	1.15	0.17	15	Not Different
1463/1377	2.07	1.87	1.97	0.20	10	Not Different
1457/1377	1.73	1.59	1.66	0.14	8	Not Different
1437/1377	1.11	1.02	1.07	0.09	8	Not Different
888/719	0.18	0.20	0.19	0.02	11	Not Different
814/719	0.28	0.22	0.25	0.06	24	Different
729/719	0.80	0.75	0.78	0.05	6	Not Different
701/719	0.21	0.18	0.20	0.03	15	Not Different

Asphaltenes from oils F, K, B, T, U, A, M, H and O

Oil F was quickly differentiated from oils K, B, T, U, A, M, H and O on the basis of asphaltene IR spectra. F asphaltenes generated a typically resinous IR spectrum with sharp double peaks between 710–730 cm^{-1} (Figure 7.21). Sharp double peaks between 710–730 cm^{-1} were not observed in the IR spectra of the other asphaltenes in this group. Oil F was therefore differentiated from all blind study oils. It is also interesting to note that oil F asphaltenes were the only asphaltenes in the blind study to generate a C_2 -N profile with the two central peaks at 20 min showing a higher intensity in the right-hand peak (Figure 7.21).

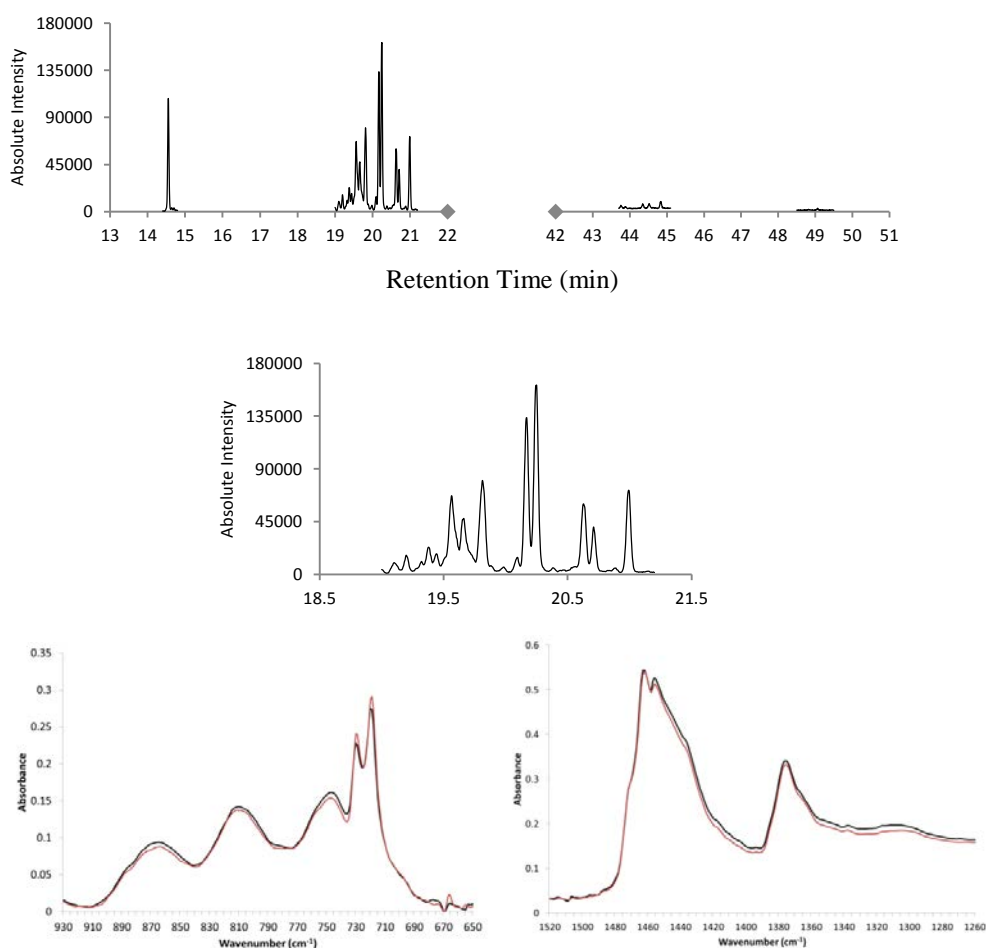


Figure 7.21: Sulfur/aromatic pyrogram and IR spectra from oil F asphaltenes.

Oils A and U were differentiated from oils K, B, T, M, H and O on the basis of sulfur/aromatic pyrograms of asphaltenes. The pyrograms for A and U asphaltenes exhibited BT peaks that clearly exceeded C₂-N intensities (Figures 7.22 and 7.23), which was not observed in the pyrograms for K, B, T, M, H and O asphaltenes (Figures 7.24–7.29).

A was compared to U on the basis of sulfur/aromatic pyrograms and IR spectra, which were both visually consistent with one another (Figures 7.22 and 7.23). IR ratios were also calculated and compared between A and U asphaltenes. Firstly, all of the ratios compared between the A duplicates fell within the 20% threshold (results not shown). The same observations were made when comparing the ratios of the U duplicates (results also not shown). Both A and U duplicates were then compared pairwise to each other as shown in Tables 7.11–7.14. All of the ratios for A and U asphaltenes fell within the 20% threshold for all pairwise comparisons. In conclusion, A and U oils could not be differentiated from one another based on asphaltene profiling, however A and U were differentiated from all other oils in the blind study.

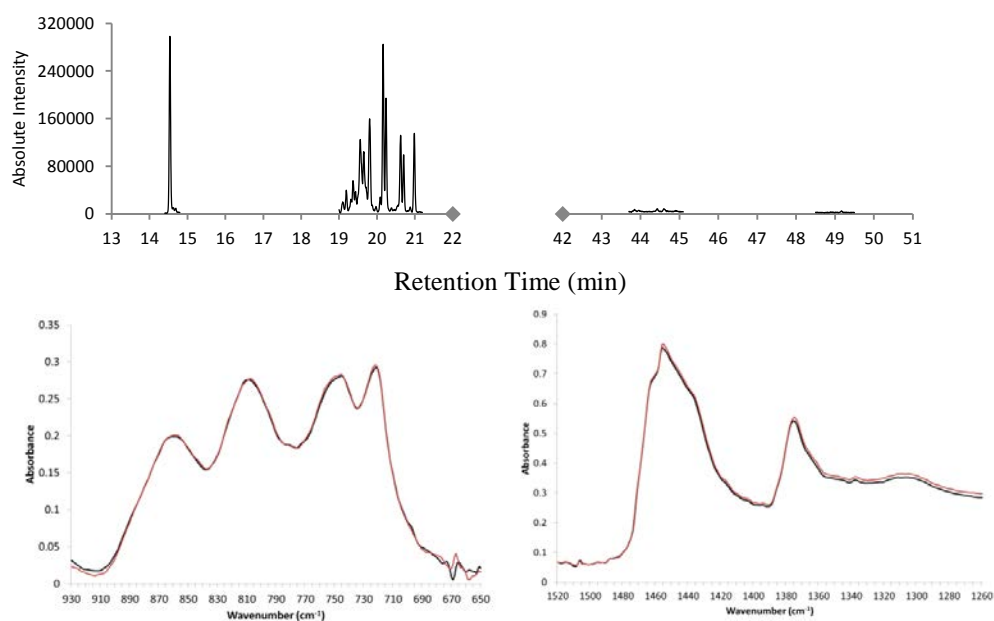


Figure 7.22: Sulfur/aromatic pyrogram and IR spectra from oil U asphaltenes.

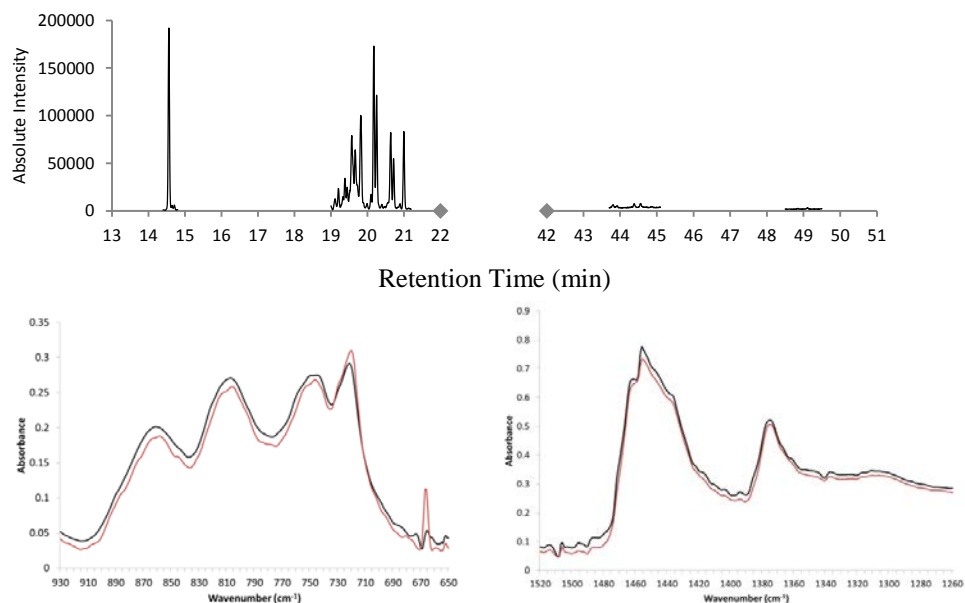


Figure 7.23: Sulfur/aromatic pyrogram and IR spectra from oil A asphaltenes.

Table 7.11: Peak height ratios compared between A and U asphaltenes.

IR Ratio	Peak Height Ratio		Mean	Absolute Difference	Relative Difference (%)	Conclusion
	A	U				
1463/1377	1.28	1.25	1.26	0.03	2	Not Different
1457/1377	1.45	1.44	1.45	0.01	1	Not Different
1437/1377	1.18	1.17	1.18	0.01	1	Not Different
867/719	0.71	0.69	0.70	0.02	3	Not Different
809/719	0.98	1.00	0.99	0.01	1	Not Different
748/719	1.00	1.00	1.00	0.01	1	Not Different

Table 7.12: Peak height ratios compared between A.2 and U asphaltenes.

IR Ratio	Peak Height Ratio		Mean	Absolute Difference	Relative Difference (%)	Conclusion
	A.2	U				
1463/1377	1.28	1.25	1.27	0.03	2	Not Different
1457/1377	1.43	1.44	1.44	0.01	1	Not Different
1437/1377	1.18	1.17	1.18	0.01	1	Not Different
867/719	0.58	0.69	0.64	0.11	17	Not Different
809/719	0.84	1.00	0.92	0.16	17	Not Different
748/719	0.88	1.00	0.92	0.12	13	Not Different

Table 7.13: Peak height ratios compared between A.2 and U asphaltenes.

IR Ratio	Peak Height Ratio		Mean	Absolute Difference	Relative Difference (%)	Conclusion
	U.2	A				
1463/1377	1.25	1.28	1.27	0.03	2	Not Different
1457/1377	1.43	1.45	1.44	0.02	1	Not Different
1437/1377	1.17	1.18	1.18	0.01	1	Not Different
867/719	0.68	0.71	0.70	0.03	4	Not Different
809/719	1.00	0.98	0.99	0.02	2	Not Different
748/719	1.01	1.00	1.01	0.01	1	Not Different

Table 7.14: Peak height ratios compared between A.2 and U.2 asphaltenes.

IR Ratio	Peak Height Ratio		Mean	Absolute Difference	Relative Difference (%)	Conclusion
	A.2	U.2				
1463/1377	1.28	1.25	1.27	0.03	2	Not Different
1457/1377	1.43	1.43	1.43	0.00	0	Not Different
1437/1377	1.18	1.17	1.18	0.01	1	Not Different
867/719	0.58	0.68	0.63	0.10	16	Not Different
809/719	0.84	1.00	0.92	0.16	17	Not Different
748/719	0.88	1.01	0.95	0.13	14	Not Different

Oil M was differentiated from oils K, B, T, H and O on the basis of asphaltene IR spectra and sulfur/aromatic pyrograms. The peak at 810 cm^{-1} was relatively low in intensity in the IR spectra of M asphaltenes, which considerably altered the overall profile of Region 1 (Figure 7.24). In contrast, the peak at 810 cm^{-1} was noticeably higher in intensity in the IR spectra of K, B, T, H and O asphaltenes (Figures 7.25–7.29). In the sulfur/aromatic profiles, BePy, BaPy and PER were present and BPE was absent in M asphaltenes (Figure 7.24). In contrast, BePy, BaPy, PER and BPE were all clearly present in K, B and T asphaltenes (Figures 7.25–7.27). As for H and O asphaltenes, only BePy was present with BaPy near the detection limit; hence deemed absent. PER and BPE were also absent in H and O asphaltenes

(Figures 7.28 and 7.29). Overall, oil M was differentiated from all other blind study oils based on asphaltene profiles. Furthermore, H and O asphaltenes were differentiated from K, B and T asphaltenes due to the aforementioned differences in sulfur/aromatic pyrograms.

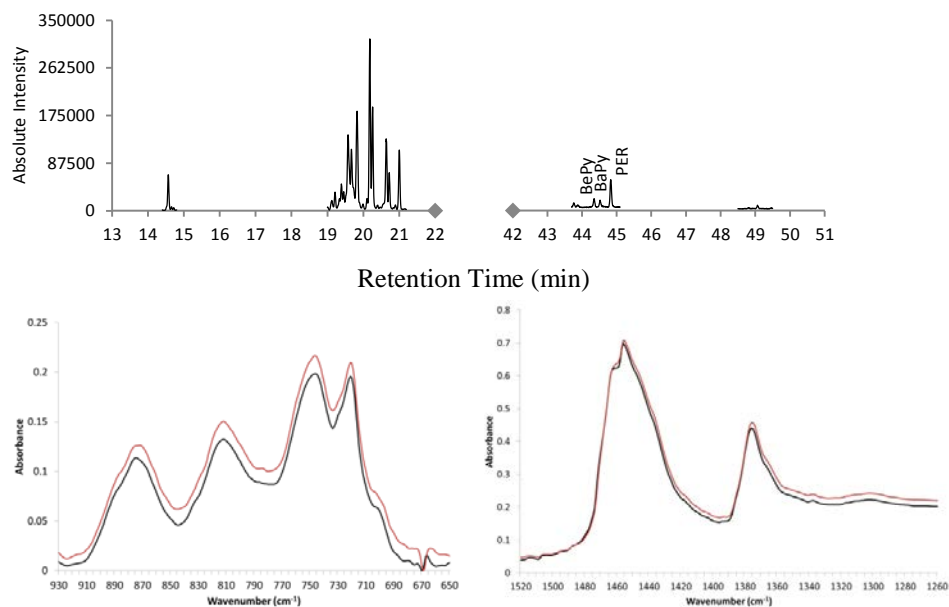


Figure 7.24: Sulfur/aromatic pyrogram and IR spectra from oil M asphaltenes.

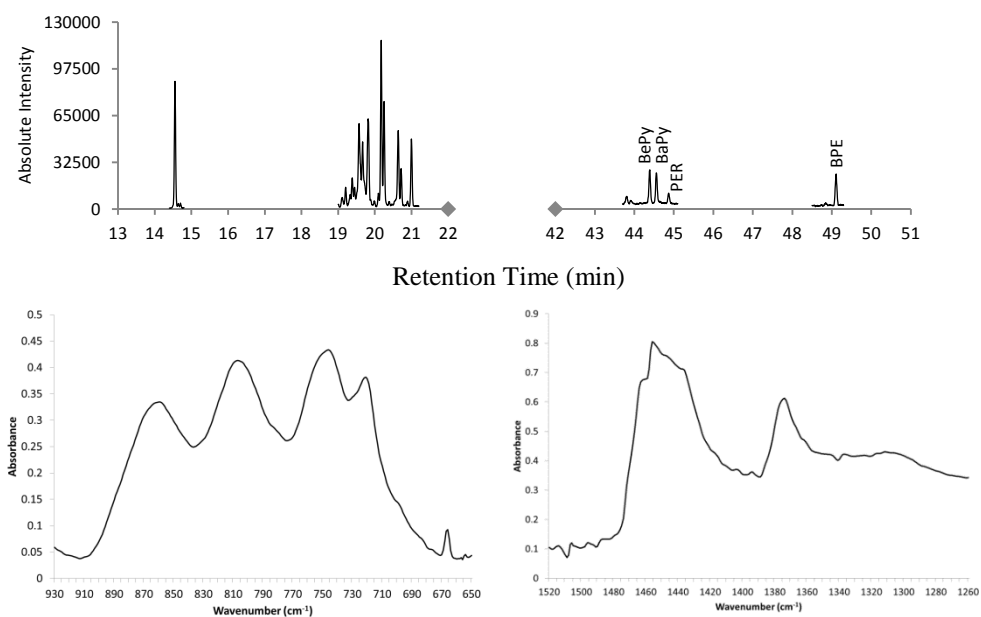


Figure 7.25: Sulfur/aromatic pyrogram and IR spectra from oil K asphaltenes.

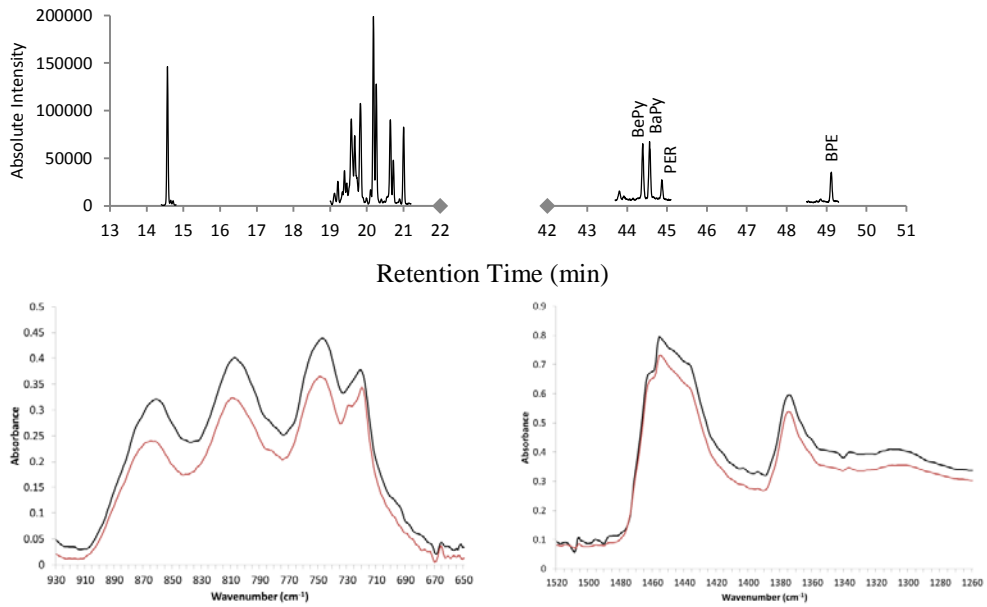


Figure 7.26: Sulfur/aromatic pyrogram and IR spectra from oil B asphaltenes

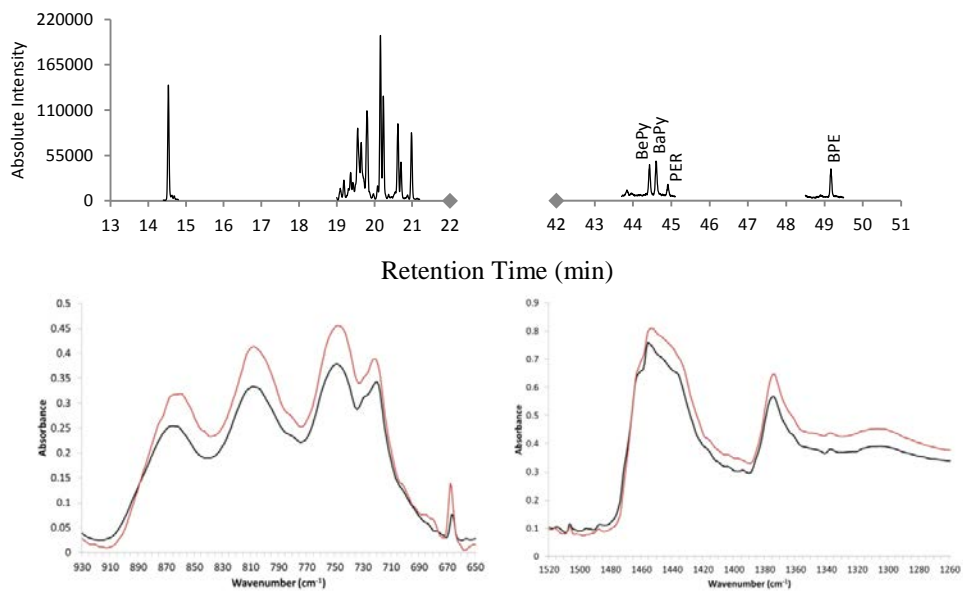


Figure 7.27: Sulfur/aromatic pyrogram and IR spectra from oil T asphaltenes.

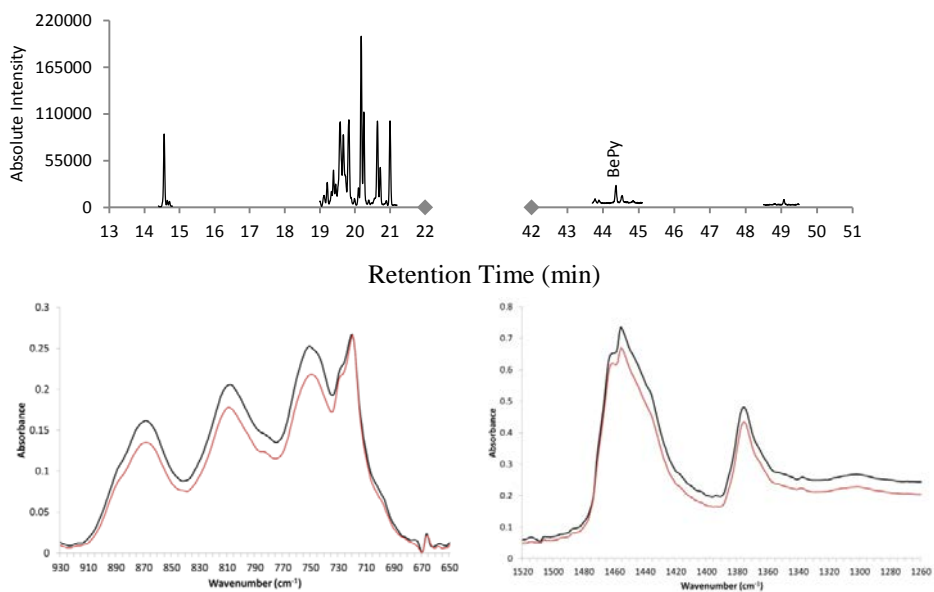


Figure 7.28: Sulfur/aromatic pyrogram and IR spectra from oil H asphaltenes.

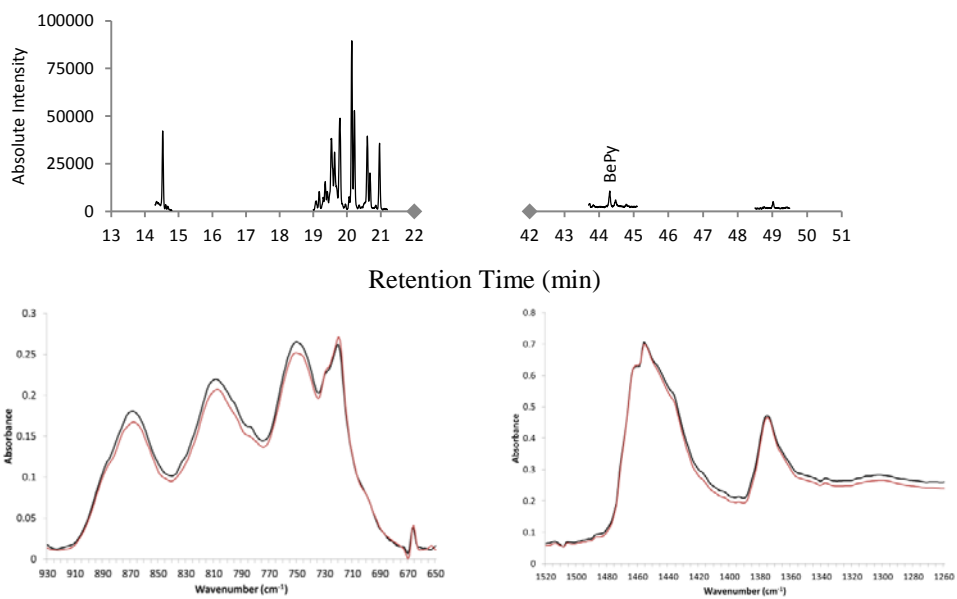


Figure 7.29: Sulfur/aromatic pyrogram and IR spectra from oil O asphaltenes.

K, B and T asphaltenes were compared to each other. IR spectra and sulfur/aromatic pyrograms for K, B and T were all visually consistent (Figures 7.25–7.27).

Peak height ratios were also calculated and compared between K, B and T asphaltenes. Firstly, ratios for the six K replicates (K.1, K.1 (2), K.2, K.2 (2), K.3, K.3 (2)) were compared pairwise to one another (15 pairwise comparisons), the B duplicates were compared to each other, and the T duplicates were compared to one another. The ratios for the K replicates, B duplicates, and T duplicates all fell within the 20% threshold (results not shown).

All of the K replicates and B and T duplicates were then compared pairwise to one another (28 pairwise comparisons). Due to the large number of pairwise comparisons conducted for K, B and T asphaltenes, three representative pairwise comparisons have been shown in Tables 7.15–7.17. Of all pairwise comparisons between K, B and T, only one peak ratio ($867/719\text{ cm}^{-1}$) exceeded the 20% threshold (21%) for a single pairwise comparison (the B duplicate compared to K.1). As the $867/719\text{ cm}^{-1}$ ratio was considerably lower than the 20% threshold for all other pairwise comparisons between K replicates and B duplicates, this difference was not deemed significant for exclusion, especially given that the ratio only just fell outside of the threshold. In conclusion, oils K, B and T were differentiated from all other blind study oils based on asphaltene profiles, but could not be differentiated from one another.

Table 7.15: Peak height ratios compared between B and K.1 asphaltenes.

IR Ratio	Peak Height Ratio		Mean	Absolute Difference	Relative Difference (%)	Conclusion
	B	K.1				
1463/1377	1.14	1.13	1.14	0.01	1	Not Different
1457/1377	1.32	1.31	1.31	0.01	1	Not Different
1437/1377	1.21	1.20	1.21	0.00	0	Not Different
867/719	0.84	0.87	0.86	0.03	3	Not Different
809/719	1.09	1.11	1.10	0.02	2	Not Different
748/719	1.20	1.17	1.18	0.03	2	Not Different

Table 7.16: Peak height ratios compared between K.1 and T asphaltenes.

IR Ratio	Peak Height Ratio		Mean	Absolute Difference	Relative Difference (%)	Conclusion
	K.1	T				
1463/1377	1.13	1.16	1.14	0.03	3	Not Different
1457/1377	1.31	1.33	1.32	0.02	2	Not Different
1437/1377	1.20	1.18	1.19	0.02	2	Not Different
867/719	0.87	0.75	0.81	0.11	14	Not Different
809/719	1.11	0.99	1.05	0.13	12	Not Different
748/719	1.17	1.12	1.14	0.05	4	Not Different

Table 7.17: Peak height ratios compared between B and T asphaltenes.

IR Ratio	Peak Height Ratio		Mean	Absolute Difference	Relative Difference (%)	Conclusion
	B	T				
1463/1377	1.14	1.16	1.15	0.02	1	Not Different
1457/1377	1.32	1.33	1.33	0.01	1	Not Different
1437/1377	1.21	1.18	1.19	0.03	2	Not Different
867/719	0.84	0.75	0.80	0.09	11	Not Different
809/719	1.09	0.99	1.04	0.10	10	Not Different
748/719	1.20	1.12	1.16	0.07	6	Not Different

Oils H and O were both indistinguishable based on the visual comparison of IR spectra and sulfur/aromatic pyrograms (Figures 7.28–7.29). IR ratios were therefore calculated and compared for H and O asphaltenes as a final check. All ratios fell within the 20% threshold when comparing H duplicates to one another, and when comparing O duplicates to one another. All H and O duplicates were then compared pairwise to each other as shown in Tables 7.18–7.21. All ratios fell within the 20% threshold for all pairwise comparisons between H and O asphaltenes, apart from one pair. When O and H.2 were compared to one another, the 867/719 cm^{-1} , 809/719 cm^{-1} and 748/719 cm^{-1} ratios all exceeded the threshold (31%, 23% and 22%, respectively). As these ratio differences were only observed in a single pairwise comparison, and not in all four pairwise comparisons, oils

H and O could not be differentiated from one another. Volatile fingerprinting should be used to confirm if H and O oils are from the same origin or different origins. Asphaltene profiling could confirm however, that oils H and O were different to all other oils in the blind study.

Table 7.18: Peak height ratios compared between H and O asphaltenes.

IR Ratio	Peak Height Ratio		Mean	Absolute Difference	Relative Difference (%)	Conclusion
	H	O				
1463/1377	1.36	1.33	1.34	0.03	2	Not Different
1457/1377	1.50	1.47	1.49	0.03	2	Not Different
1437/1377	1.12	1.17	1.14	0.05	4	Not Different
867/719	0.62	0.71	0.66	0.09	14	Not Different
809/719	0.79	0.86	0.83	0.07	9	Not Different
748/719	0.96	1.04	1.00	0.08	8	Not Different

Table 7.19: Peak height ratios compared between H and O.2 asphaltenes.

IR Ratio	Peak Height Ratio		Mean	Absolute Difference	Relative Difference (%)	Conclusion
	H	O.2				
1463/1377	1.36	1.36	1.36	0	0	Not Different
1457/1377	1.50	1.49	1.50	0.01	1	Not Different
1437/1377	1.12	1.15	1.14	0.03	3	Not Different
867/719	0.62	0.62	0.62	0	0	Not Different
809/719	0.79	0.77	0.78	0.02	3	Not Different
748/719	0.96	0.94	0.95	0.02	2	Not Different

Table 7.20: Peak height ratios compared between H.2 and O asphaltenes.

IR Ratio	Peak Height Ratio		Mean	Absolute Difference	Relative Difference (%)	Conclusion
	H.2	O				
1463/1377	1.43	1.33	1.38	0.10	7	Not Different
1457/1377	1.53	1.47	1.50	0.06	4	Not Different
1437/1377	1.09	1.17	1.13	0.08	7	Not Different
867/719	0.52	0.71	0.62	0.19	31	Different
809/719	0.68	0.86	0.77	0.18	23	Different
748/719	0.83	1.04	0.94	0.21	22	Different

Table 7.21: Peak height ratios compared between H.2 and O.2 asphaltenes.

IR Ratio	Peak Height Ratio		Mean	Absolute Difference	Relative Difference (%)	Conclusion
	H.2	O.2				
1463/1377	1.43	1.36	1.40	0.07	5	Not Different
1457/1377	1.53	1.49	1.51	0.04	3	Not Different
1437/1377	1.09	1.15	1.12	0.06	5	Not Different
867/719	0.52	0.62	0.83	0.10	12	Not Different
809/719	0.68	0.77	0.73	0.09	12	Not Different
748/719	0.83	0.94	0.89	0.11	12	Not Different

7.1.3. Asphaltene Profiling Conclusion

Table 7.22 summarises the blind study results from the asphaltene profiling method. Oils E, S, Q, P, L, F and M were individually differentiated from all other oils in the sample-set based on asphaltene profiles. Oil J was differentiated from all other blind study oils based on unique physical properties; oil J was the only oil not to yield an asphaltene fraction.

Oils K, B and T could not be differentiated based on asphaltene profiles, hence further CEN analysis would be required to confirm if these oils do share a common origin or not. The same conclusion was observed for two other pairs of oils; oils A and U, and oils I and G.

Oils H and O were also not differentiated from one another, however variances in IR ratios were observed for one out of four pairwise comparisons between H and O. To remain conservative, oils H and O were not differentiated as the three remaining pairwise comparisons fell within the variability threshold. CEN analyses would confirm whether or not oils H and O originate from a common origin or not.

A greater degree of variation was observed in the IR ratios during pairwise comparisons of oils D and N. Ratio variations were observed across all four pairwise

comparisons, no single ratio differed across all four pairs. The results for oils D and N were considered inconclusive based on asphaltene profiles.

Oils C and R were not differentiated from one another, however it was only possible to obtain a Py-GC-MS profile for C and R due to low yields. The pyrograms were consistent between C and R therefore these two oils could not be differentiated from one another. CEN analysis would be recommended for confirmatory analysis.

Table 7.22: The blind study conclusion for asphaltene profiling.

Exclusion	Inconclusive	Not Differentiated
E	D, N	G, I
S		K, B, T
Q		U, A
P		H, O
L		C, R
F		
M		
J		

7.2. CEN Method Conclusion

The volatile fractions of oils A–U were isolated from the non-volatile fractions and analysed using the CEN method (CEN, 2012). It should be reinforced that the exact same sample-set of oils was analysed by the CEN method as previously analysed for the asphaltene profiling method; however, this sample-set was re-labelled A–U in a different order. The results of the CEN method have been provided in Appendix C. The overall conclusion for the CEN component of the blind study is shown in Table 7.23. Oils B, I, Q, G, F, J, T, N, C, L, D, U and O were differentiated from all other oils in the sample-set, whilst four pairs of oils were deemed a match: oils S and P; oils E and K; oils M and R; and oils A and H.

Table 7.23: The blind study conclusion for the CEN method.

Exclusion	Identification
B	S, P
I	E, K
Q	M, R
G	A, H
F	
J	
T	
N	
C	
L	
D	
U	
O	

7.3. Discussion

As stated previously in Chapter 6, the primary aim of asphaltene profiling is to exclude non-related oils from oil spill investigations prior to volatile fingerprinting. Oils that cannot be excluded based on asphaltene profiles will be carried forward for confirmatory analysis using volatile fingerprinting. It is important to reinforce this aim so that the discussion below can be correctly interpreted. If non-related oils are differentiated based on asphaltene profiling, the method is successfully achieving its goal. If asphaltene profiling cannot provide enough information to confirm that two oils originate from the same source, this is also fine as the CEN method will confirm this afterwards. The main concern is if asphaltene profiling results in the false exclusion of related oils.

The discussion herein aims to address Research Question 3. The interpretation of asphaltene profiles generated from IR and Py-GC-MS data has been assessed for reliability. To assess the reliability, it was necessary to conduct blind analysis of unknown oils to remove cognitive bias. If the asphaltene profiles generated from unknown oils could be correctly interpreted, the interpretation of asphaltene profiles could be considered reliable.

Once the asphaltene profiling results and CEN results were submitted by the analyst, the origins of the blind study oils were revealed. The geographical origins of the oils and their associated letters for both the asphaltene and CEN analyses are shown in Table 7.24.

Table 7.24: The geographical origin of the oils analysed in this blind study with the corresponding labels provided during asphaltene profiling and CEN analyses.

Origin of Oil	Oil Abbreviation	Oil Type	Label for Asphaltene Profiling	Label for CEN Method
Middle Eastern	M. Eastern 1	Crude	A	D
Heavy Fuel Oil (uncut) - unknown origin	HFO (u/c)	HFO	B	A
South East Asian 2 duplicate	SE Asian 2 dup.	Crude	C	M
Australian 3	Aust. 3	Crude	D	B
South East Asian 1	-	Crude	E	C
South East Asian 2/Middle Eastern ($\pm 3:1$ by volume)	SEA2/ME	Crude blend	F	O
Australian 1	Aust. 1	Crude	G	S
Middle Eastern 3	M. Eastern 3	Crude	H	E
Australian 1 duplicate	Aust. 1 dup.	Crude	I	P
South Pacific	S. Pacific	Crude	J	F
Heavy Fuel Oil (diesel cut) - unknown origin	HFO (d/c)	HFO	K	G
Unknown origin	UKN. 1	Crude	L	T
North American	N. American	Crude	M	Q
Australian 4	Aust. 4	Crude	N	N
M. Eastern 3 duplicate	M. Eastern 3 dup	Crude	O	K
Australian 2	Aust. 2	Crude	P	J
South East Asian 1/North American ($\pm 1:1$ by volume)	SEA1/NA	Crude blend	Q	L
South East Asian 2	SE Asian 2	Crude	R	R
SE Asian 3	SE Asian 3	Crude	S	I
Heavy Fuel Oil (uncut) duplicate - unknown origin	HFO (u/c) dup.	HFO	T	H
Middle Eastern 2	M. Eastern 2	Crude	U	U

The information in Table 7.24 shows how each of the oils in the sample-set was designated a different label for asphaltene profiling and CEN analyses. Five new crude oils were analysed in the blind study which had not previously been analysed by the operator or the developed asphaltene methods. Two of the five new crude oils originated from the Middle

East (labelled M. Eastern 2 and M. Eastern 3), one oil was Australian (labelled Aust. 4), one oil was from south east Asia (labelled SE Asian 3), and the final oil was from an unknown origin (labelled UKN. 1). Interestingly, SE Asian 2, Aust. 1, M. Eastern 3 and HFO (u/c) oils were each included in the blind study as duplicates. Two oil blends were also included: SE Asian 2 crude oil and M. Eastern 1 crude oil were blended (SEA2/ME) as well as SE Asian 1 crude oil and N. American crude oil (SEA1/NA).

Table 7.25 summarises the conclusions for the asphaltene profiling using the geographical origins of oils instead of the previously indicated letter labels.

Table 7.25: The asphaltene profiling conclusion showing the origins of oils.

Exclusion	Inconclusive	Not Differentiated
SE Asian 1	Aust. 3, Aust. 4	Aust. 1, Aust. 1 dup.
SE Asian 3		HFO (d/c), HFO (u/c), HFO (u/c) dup.
SEA1/NA		M. Eastern 1, M. Eastern 2
Aust. 2		M. Eastern 3, M. Eastern 3 dup.
UKN. 1		SE Asian 2, SE Asian 2 dup.
SEA2/ME		
N. American		
S. Pacific		

When observing the asphaltene profiling results in relation to oil origins, the four sets of duplicates were successfully grouped together. The Aust. 1 duplicates could not be differentiated from one another but were differentiated from all other oils in the blind study. The same observations were observed for the M. Eastern 3 duplicates, the SE Asian 2 duplicates, and the HFO (u/c) duplicates. Although SE Asian 2 duplicates were correctly grouped together, both SE Asian 2 duplicates did not yield sufficient asphaltenes for IR analysis. It is therefore important to highlight the limitations associated with asphaltene profiling when provided with low yielding oils. If very small asphaltene yields are obtained such as those from the SE Asian 2 duplicates, it may only be possible to conduct Py-GC-MS profiling and not IR profiling. Py-GC-MS is capable of analysing smaller amounts of

asphaltenes whilst still producing repeatable profiles and may still provide useful information alongside volatile fingerprints. Alternatively, the analyst may decide not to conduct asphaltene profiling at all. Instead, oil fingerprints would be obtained purely based on the volatile fractions as currently practiced. It is worth noting that it was possible to obtain repeatable IR profiles for SE Asian 2 asphaltenes during method development as a slightly greater volume of oil was used for precipitation as compared to the blind study.

Whilst HFO (u/c) and HFO (d/c) asphaltenes were different to all other asphaltenes analysed in the blind study, the analyst was not capable of distinguishing the two different grades of HFO from one another. This result is correct because HFO (u/c) and HFO (d/c) originate from the exact same source. These two HFO grades also could not be distinguished during the development of the IR and Py-GC-MS methods (Chapters 4 and 5).

Two pairs of oils from different origins could not be differentiated from one another using asphaltene profiles. The M. Eastern and M. Eastern 2 oils were not differentiated from one another. Also, the Aust. 3 and Aust. 4 oils could not be differentiated from one another due to an inconclusive result when comparing asphaltenes. It is interesting to observe that both pairs of oils are oils from similar geographical regions. These results may indicate that all asphaltene profiles are not entirely unique. In other words, asphaltene profiles generated from the developed methods may not be unique between oils originating from close proximity sources. Whilst some oils from similar origins could not be differentiated based on asphaltene profiles, it is very important to emphasise that asphaltene profiling could still differentiate the remaining studied oils that originated from similar sources. Firstly, the three different SE Asian oils were successfully differentiated from one another. The M Eastern 3 oil was also differentiated from the M. Eastern and M. Eastern 2 pairing. Furthermore, the Aust. 1 and Aust. 2 oils were differentiated from one another, and also differentiated from the Aust. 3 and Aust. 4 oils.

It is also worth noting that whilst the M. Eastern and M. Eastern 2 oils and the Aust. 3 and Aust. 4 oils were not differentiated, these results would not be detrimental to an investigation. Asphaltene profiling is designed as a pre-screen to the CEN method; hence the CEN method would confirm if the two oils were indeed from the same origin, or if these oils were different. The CEN results for the M. Eastern and M. Eastern 2 oils as well as the Aust. 3 and Aust. 4 oils are discussed and compared to the asphaltene results later in this chapter.

The remaining oils in the blind study were successfully differentiated from all of the other oils in the blind study. The differentiated oils included SE Asian 1, SE Asian 3, SEA1/NA, Aust. 2, UKN. 1, SEA2/ME, N. American, and S. Pacific. All of these oils were from different origins; therefore, these results were as expected. Of particular interest was the ability of asphaltene profiles to differentiate blended oils from unblended oils. Blended oils had not previously been analysed using the developed asphaltene profiling methods, therefore these results were insightful. The SE Asian 1 oil was differentiated from the SE1/NA blend, despite the blend containing ~50% of the SE Asian 1 oil. The N. American oil was also differentiated from the SE1/NA blend, despite the blend containing ~50% of the N. American oil. The asphaltene profiles were even capable of differentiating the SE Asian 2 oil from the SEA2/ME blend which consisted of ~75% SE Asian 2 oil. Asphaltene profiles can not only provide probative information for unblended oils, but also for blended oils.

Also worth noting was the capability of the developed methods to produce asphaltene profiles for five new oils that had not previously been analysed during method development. The asphaltene profiles generated from these additional oils provided reliable results from which oils could be compared.

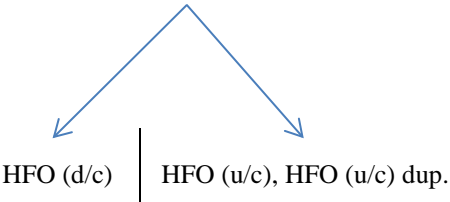
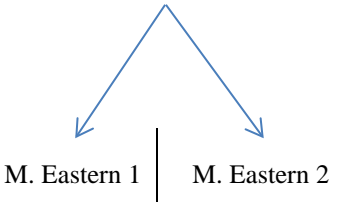
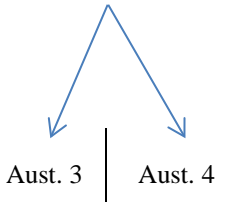
Table 7.26 summarises the CEN method conclusion when provided with the geographical origins of oils instead of the previously indicated letter labels.

Table 7.26: The CEN conclusion showing the origins of oils.

Exclusion	Identification
Aust. 3	Aust. 1, Aust. 1 dup.
SE Asian 3	M. Eastern 3, M. Eastern 3 dup.
N. American	SE Asian 2, SE Asian 2 dup.
HFO (d/c)	HFO (u/c), HFO (u/c) dup.
S. Pacific	
Aust. 2	
UKN. 1	
Aust. 4	
SE Asian 1	
SEA1/NA	
M. Eastern 1	
M. Eastern 2	
SEA2/ME	

The CEN method conclusion was consistent with the asphaltene profiling conclusion apart from three differences. Table 7.27 compares the asphaltene profiling method and CEN method conclusions and highlights observed similarities and differences. Similarities and differences between conclusions are discussed thereafter.

Table 7.27: A comparison of asphaltene profiling and CEN method conclusions derived from the blind study.

Similar Conclusions		Different Conclusions		
Asphaltene Profiling <i>Exclusion</i>	Asphaltene Profiling <i>Not Differentiated</i>	Asphaltene Profiling <i>Not Differentiated</i>	Asphaltene Profiling <i>Not Differentiated</i>	Asphaltene Profiling <i>Inconclusive</i>
CEN Method <i>Exclusion</i>	CEN Method <i>Identification Confirmed</i>	CEN Method <i>Exclusion</i>	CEN Method <i>Exclusion</i>	CEN Method <i>Exclusion</i>
SE Asian 1 SE Asian 3 SEA1/NA Aust. 2 UKN. 1 SEA2/ME N. American S. Pacific	Aust. 1, Aust. 1 dup. M. Eastern 3, M. Eastern 3 dup. SE Asian 2, SE Asian 2 dup.	HFO (d/c), HFO (u/c) , HFO (u/c) dup. 	M. Eastern 1, M. Eastern 2 	Aust. 3, Aust. 4 

The first difference highlighted in Table 7.27 was associated with the two different grades of HFO. The CEN method was capable of distinguishing the two different HFO grades which was not achieved by asphaltene profiling. It is logical, however, that the two different HFO grades were separated based on the volatile fraction, as the only variable between the two grades was the addition of diesel in one grade and not the other.

The second and third differences highlighted in Table 7.27 were that the M. Eastern and M. Eastern 2 oils, and the Aust. 3 and Aust. 4 oils, were differentiated using the CEN method yet not differentiated through asphaltene profiling. As previously discussed, asphaltene profiles may not be capable of resolving differences between oils that originate from close geographical proximities. Whilst asphaltene profiles could not differentiate the M. Eastern oil from the M. Eastern 2 oil, or differentiate the Aust. 3 oil from the Aust. 4 oil, the CEN method was capable of differentiating these four oils. Interestingly however, the M. Eastern and M. Eastern 2 oils were only differentiated from one another in the CEN method by differences in BT and naphthalenes. The biomarker profiles for the two M. Eastern oils were the same indicating that these two oils are likely from close proximity sources. The fact that asphaltene profiles could not distinguish these two closely related M. Eastern oils is not too concerning, particularly when the CEN method had difficulty distinguishing these two oils.

An advantage of asphaltene profiling over the CEN method is the considerably reduced amount of data that is required for interpretation. Despite analysing the exact same sample-set of oils, the amount of data interpreted during the CEN method was more than double the amount interpreted during asphaltene profiling. Non-related oils were quickly eliminated during asphaltene profiling based solely on the visual comparisons of pyrograms and IR spectra. Visual differentiation of oils based on obvious differences in asphaltene profiles eliminated the need to quantify data for comparison and exclusion. IR ratios are more time consuming to compare than visual profiles, however IR ratios were only used in

circumstances when two or more oils could not be visually differentiated. Leaving IR ratios until the end allowed for faster processing of data.

To answer Research Question 3 (*Do the asphaltene profiling methods provide results which allow for reliable interpretation?*), the asphaltene profiles generated from the IR and Py-GC-MS methods were reliably interpreted. Despite not knowing the origins of oils, asphaltene profiles were interpreted to successfully exclude the majority of non-related oils from one another. Although asphaltene profiling could not differentiate two pairs of oils that originated from similar geographical regions, this did not affect the reliability of results. The inability to differentiate these two pairs of oils may simply indicate that the two asphaltene profiles were not unique enough to differentiate these similar oils. The reliability of results would only be affected if oils from the exact same origin were falsely excluded from one another. As false exclusions were not observed in this blind study, the interpretation of asphaltene profiles was deemed sufficiently reliable for screening prior to confirmatory analysis.

Chapter 8 - Conclusions

The results from this research suggest that asphaltene profiling methods can be developed to provide probative information that may assist in oil spill investigations.

The information that has contributed to determining this conclusion is discussed herein. The application of asphaltenes in oil spill investigations was a new endeavour for both asphaltene and oil fingerprinting research. As a consequence, there was a vast array of research avenues to consider. It was therefore very important to identify a realistic scope for this research at the outset of the PhD.

Firstly, it is possible that the asphaltene precipitation method used could be further optimised to improve efficiency and repeatability. It was not possible however, to optimise the precipitation method without first developing asphaltene profiling methods. Asphaltene profiling methods were required to test the efficiency of the precipitation method. Optimisation of the precipitation method was hence reserved for future research pending the outcome of this PhD research.

Another consideration was the amount of probative information that may be available from asphaltenes. Asphaltene fractions contain an abundance of chemical components and therefore characteristics that may provide probative information in oil spill investigations including organic bonds, thermal degradation properties, heteroatomic content, isotopes, and trace metal content. To ensure that the scope of this research was adhered to, only a portion of these chemical components were targeted and tested. The organic components of asphaltenes were targeted, specifically the organic bonds and the thermal degradation properties of asphaltene organics. A number of asphaltene profiling methods were developed using a range of spectroscopic and thermal degradation techniques. The chosen techniques

had shown promise for providing probative information from asphaltenes when consulting previous, non-forensic research.

It was also important to consider the weathering of oils. The decision to investigate the application of asphaltenes in oil fingerprinting stems from two reasons: (1) to allow for a whole of oil approach, where all of the oil is profiled, not just the volatile fraction; and (2) the expectation that asphaltenes are likely more resistant to weathering effects than the currently analysed volatile fractions. Whilst it was acknowledged that weathering must be studied, to determine if asphaltenes are in fact probative, the analysis of asphaltenes from un-weathered oils was first required. By analysing un-weathered oils, there could be certainty in any differences observed as differences would not be attributed to weathering. Instead, differences were attributed to chemical variations in the asphaltenes themselves. Out of interest, a weathered oil sample was included in this research to obtain preliminary information on the performance of weathered asphaltenes when compared to un-weathered asphaltenes from the same oil (M. Eastern crude oil).

The number of oils used for asphaltene profiling was also a consideration for defining the research scope. It was not possible to profile asphaltenes from hundreds of different oils without first having developed the methods to do so. The initial development of asphaltene methods was therefore conducted using a relatively small sample-set of ten oils (excluding the single weathered oil) from a broad range of different geographical regions. This sample size was increased during the blind study, where an additional five oils were analysed; a total of 15 different oils. Of these 15 oils, 13 were crude oils and two were HFOs; the two HFOs were derived from the same oil, but were different grades (HFO180 and HFO380). As mentioned above, one of the crude oils was weathered and included in the analyses. This sample-set was sufficient for gauging the probative value of the developed asphaltene methods, particularly when considering sample sizes encountered during investigations which

are typically small. In an investigation situation, spilt oil is not compared to all other oils in the world, only to a limited number of suspect oils.

8.1. Physical Properties

Basic physical properties of oils and their respective asphaltene fractions were observed for the initial eleven oils used for preliminary method development. Whilst physical properties were certainly interesting, these properties cannot be relied upon for confirming the source of an oil spill. Physical properties were simply observed to correlate with the asphaltene chemical profiles.

The physical properties of asphaltenes, in particular their morphologies, could be linked to the corresponding chemical profiles of asphaltenes. There appeared to be a distinction between crystalline and resinous asphaltenes when observing physical properties. Crystalline asphaltenes were defined by their shiny, crystalline appearance, and their tendency to fracture when pressure was applied. On the contrary, resinous asphaltenes were defined by their matte (non-shiny) appearance, and soft, malleable texture. HFO (u/c), HFO (d/c), M. Eastern and N. American asphaltenes were classified as crystalline whilst SE Asian 1, SE Asian 2, Aust. 1 and Aust. 2 asphaltenes were classified as resinous. Asphaltenes obtained from the Aust. 3 oil could be identified, as they appeared to be a mixture of both resinous and crystalline material. The S. Pacific crude oil did not yield asphaltenes during precipitation; therefore, the S. Pacific oil was readily differentiated from the remaining oils and this sample could not be subjected to asphaltene profiling.

8.2. Addressing the Research Questions

Research Questions 1, 2 and 3 were designed to directly address the aim of this research: to *determine whether asphaltene profiling methods can be developed to provide probative information that may assist in oil spill investigations*. Research Questions 1, 2 and 3 were stated as follows:

1. *Does each asphaltene profiling method meet the requirements for a forensic method?*
2. *Which asphaltene profiling methods are most suitable for oil spill investigations?*
3. *Do the asphaltene profiling methods provide results which allow for reliable interpretation?*

8.2.1. Research Question 1

Research Question 1 was addressed in Chapters 4 and 5. To address Research Question 1, various spectroscopic methods (UV-Vis spectroscopy, Raman spectroscopy, fluorescence spectroscopy, and IR spectroscopy) and thermal degradation techniques (EGA-MS, TGA, and Py-GC-MS) were assessed against the requirements for a forensic method. The aim was to assess each asphaltene profiling method separately, and to determine whether or not each method adhered to the specified forensic requirements.

Firstly, IR profiling was cost effective, non-destructive, fast, and it was suitable for the analysis of small, solid state asphaltene samples. IR spectroscopic analysis of asphaltenes was also widely accepted and readily available throughout the scientific community (Gawel et al. 2014, Asemani and Rabbani 2015). IR profiling of asphaltenes was observed to be repeatable and probative during method development (Chapter 4). Of the nine oils analysed during IR method development, all oils from different origins were correctly differentiated and the two HFOs from the same origin were correctly grouped together. Duplicate asphaltenes from the

same oils were also correctly grouped together using IR. The S. Pacific oil was included in IR method development process however this oil did not yield sufficient asphaltenes for IR profiling. Consequently, the S. Pacific oil was differentiated from all other oils on the basis of yielding insufficient asphaltenes for analysis.

Although it was not the focus of this research, it is interesting to note that the IR profiling of asphaltenes could not differentiate un-weathered oil from weathered oil; both of which originated from the exact same source (M. Eastern). This result suggested that IR profiling of asphaltenes may provide probative information in oil spill investigations when weathered oils are present. Overall, IR profiling addressed all of the requirements for a forensic method.

Fluorescence spectroscopy was also cost effective, fast, and was also suitable for the analysis of small asphaltene samples. A major limitation to fluorescence spectroscopy was that asphaltenes had to be dissolved prior to analysis. The dissolution of asphaltenes can induce asphaltene aggregation; hence it was possible that the chemical structures of asphaltenes may have been altered prior to fluorescence profiling. The possibility of asphaltene aggregation may also complicate the recovery of asphaltenes from the solvent following fluorescence profiling. Whilst fluorescence profiling was observed to be repeatable, the probative value of the fluorescence spectra of asphaltenes was limited. Only five distinct groups could be identified from the same nine oils as analysed by IR.

Raman spectroscopy and UV-Vis spectroscopy were also investigated; however neither technique met the forensic requirements for a method. Raman was incapable of analysing asphaltenes due to fluorescence properties, whilst UV-Vis did not provide probative information from asphaltene fractions.

In regard to thermal degradation techniques, EGA-MS, TGA and Py-GC-MS were tested. Whilst these thermal degradation techniques are destructive, EGA-MS and Py-GC-MS

were advantageous as they both required very small sample sizes for analysis. Consequently, a significant portion of asphaltenes still remaining following analysis provided that a sufficient yield of asphaltenes were obtained from oils. TGA however required more than a realistic amount of asphaltenes for profiling which was not ideal.

Upon testing, EGA-MS profiling was deemed unsuitable for meeting the requirements of a forensic method. EGA-MS was not sufficiently repeatable to allow for the reliable comparison of asphaltene profiles. TGA profiling of asphaltenes provided an acceptable degree of repeatability for most comparison data; however, in order to achieve repeatable results, an unrealistic amount of asphaltenes was required. TGA profiling also proved to be quite time consuming, which was not desirable considering the poor probative value of the TGA profiles. Seven different asphaltene fractions were included in the preliminary TGA tested, and could only be differentiated into three distinct groups.

Py-GC-MS is widely accepted for asphaltene analysis throughout the petroleum sciences, and is capable of solid state analysis of asphaltenes (Galarraga et al. 2007, Douda et al. 2008, Makeen et al. 2015). Although Py-GC-MS was not the most cost effective or readily available technique for asphaltene profiling, and the analysis acquisition was quite long (60 mins as compared to 2 mins for IR profiling), Py-GC-MS was advantageous due to the quick interpretation of asphaltene pyrograms. The asphaltene pyrograms were also observed to be as repeatable and probative as IR profiling when analysing the same sample-set. The same nine oils were analysed during Py-GC-MS method development, and all oils from different origins were correctly differentiated. The two HFOs from the same origin were correctly grouped together. Duplicate asphaltenes from the same oils were also correctly grouped together using Py-GC-MS. The S. Pacific asphaltenes were again differentiated from all of the studied oils due to an insufficient asphaltene yield.

The weathered M. Eastern oil was also included in the Py-GC-MS profiling of asphaltenes for comparison to the unweathered M. Eastern oil. Similarly to IR profiling, the Py-GC-MS profile of the weathered asphaltenes could not be differentiated from the unweathered M. Eastern asphaltene profile.

8.2.2. Research Question 2

Research Question 2 was also addressed in Chapters 4 and 5. Firstly, the spectroscopic methods developed in Chapter 4 were compared to one another to determine which method was most suitable for oil spill investigations. Without doubt, the IR profiling method was the most suitable spectroscopic method. The IR method was more probative than the fluorescence, Raman, and UV-Vis spectroscopy methods. Whilst fluorescence profiling did offer some probative value, asphaltenes had to be dissolved to generate asphaltene profiles. The dissolution of asphaltenes was not ideal as this could induce asphaltene aggregation prior to analysis. IR profiling was therefore superior (in addition to being more probative and reliable) as it allowed for solid state analysis of asphaltenes following precipitation.

In regards to thermal degradation techniques, Py-GC-MS was the most suitable method for oil spill investigations. The Py-GC-MS method was more probative than the TGA and EGA-MS methods. Furthermore, TGA would require in excess of 10 fold more asphaltenes than Py-GC-MS method in order to obtain repeatable results which is not feasible.

8.2.3. Research Question 3

Research Question 3 was addressed in both Chapters 6 and 7. Although both the IR and Py-GC-MS methods independently achieved the same degree of discrimination as each other when provided with the same sample-set of oils, it was important to consider combining both

methods. Complementary methods provide for a higher level of confidence when determining sample inclusion or exclusion than each of the individual methods alone (Riley et al. 2016).

An asphaltene profiling method was therefore proposed in Chapter 6 that involved combining IR and Py-GC-MS profiling of asphaltenes to assist oil fingerprinting. Currently, asphaltenes are already separated from volatiles prior to oil fingerprinting. It therefore makes sense to use asphaltenes instead of discarding them as currently practiced. The inclusion of asphaltenes alongside volatile fingerprinting would allow for a more holistic whole oil approach during oil spill investigations. As observed during method development in Chapters 4 and 5, asphaltene profiling proved sufficiently probative for the exclusion of non-related oils. The inclusion of asphaltene profiling alongside volatile fingerprinting would therefore provide additional information to investigations that would otherwise not be obtained. Furthermore, non-related oils can be quickly differentiated based on obvious visual differences in asphaltene profiles. The ability to exclude non-related oils without requiring the interpretation of large data-sets would be advantageous during investigations.

The blind study in Chapter 7 was designed to assess the reliability of interpreting asphaltene profiles from both IR and Py-GC-MS. A range of unknown oils were provided for asphaltene profiling. The interpretation of asphaltene profiles was free from cognitive bias as the origins of oils were unknown to the analyst (unlike method development where the origins of oils were known during interpretation). By removing bias from the interpretation of results, the reliability of results could be effectively assessed. If the analyst could correctly interpret asphaltene profiles without knowledge of the origins of oils, the interpretation of asphaltene profiles could be considered reliable. Ideally, the analyst would separate all non-related oils from one another, whilst grouping all oils from the same origin together. The CEN method was also conducted as part of the blind study so that the reliability of results

from the developed methods could be compared to the results obtained from the current standard for oil fingerprinting.

In conclusion to the blind study, asphaltene profiles were reliably interpreted to exclude the majority of non-related oils from one another. Two pairs oils that originated from similar geographical regions but not the exact same origin were not excluded from each other. This result did not affect the reliability of the asphaltene profiles, instead it highlighted that the asphaltene profiles were not unique enough to differentiate these similar oils. The aim of the asphaltene profiling methods was to exclude non-related oils prior to volatile fingerprinting. The asphaltene profiles were reliable as only non-related oils were excluded; no false exclusions were observed.

When compared to the CEN method, the results generated from asphaltene profiles were equally as reliable, although not as discriminatory. The two pairs of oils which could not be differentiated by asphaltene profiles were differentiated based on the CEN method. Also, the CEN method successfully differentiated two different HFO grades which were from the same origin. These two HFO grades were inseparable when comparing asphaltene profiles. This result was to be expected however, as the only difference between the two HFO grades was the addition of diesel (volatiles).

8.3. Overall Conclusions

The results from this research suggest that asphaltene profiling methods can be developed to provide probative information that may assist in oil spill investigations. The most probative and reliable asphaltene profiling methods are the IR and Py-GC-MS methods. Both profiling methods are capable of providing useful information during oil spill investigations that would otherwise be overlooked. Asphaltene profiles are particularly useful for the exclusion of non-related oils, as obvious visual differences in profiles may be used to

quickly exclude oils without the need for extensive data processing. It is recommended that asphaltene profiling is conducted as a pre-screening tool prior to volatile fingerprinting. Before asphaltene profiling methods can be considered for casework however, further research is required as discussed in the next chapter.

Chapter 9 - Future Research

As previously indicated, before the developed asphaltene profiling methods can be considered for casework, further research will be required. Now that proof-of-concept asphaltene profiling methods have been developed and tested, further optimisation of these methods is warranted. As new knowledge becomes available through further research, the asphaltene methods presented in this thesis should be continually amended as necessary to remain up to date. This is similar to the CEN method, which is periodically amended as new knowledge is derived from research and casework. Some future avenues for forensic asphaltene profiling research are presented herein.

9.1. Further Investigation of the Variability of Asphaltene Profiles

Whilst it is known from this research that asphaltene profiles can be used to differentiate unrelated oils, it is not yet understood if the information in asphaltene profiles can confirm the identity of individual oils. As evident in the blind study, two pairs of unrelated oils could not be differentiated based on current asphaltene profiling methods. Both pairs of oils did share a common origin however the exact origin of these oils could not be confirmed; only general geographical regions were known upon receiving oil samples for this research. It is not known if these oils were from different oil wells within the same oil field, which would explain the similarity of asphaltene profiles, or whether these oils were simply from different oil fields within the same geographical region. In order to investigate the ability of asphaltene profiles to identify individual oils, the exact origins of oils must be known (specifically the oil well and oil field if possible). It is important to investigate whether asphaltene profiles can identify oils from different oil wells within the same oil field, or whether asphaltene profiles are only capable of distinguishing oils from different oil fields

within the same geographical region. If the information provided by existing asphaltene profiles cannot differentiate closely related oils (for example, oils from different oil wells within the same oil field), further research may be required to improve the discrimination power of asphaltene profiles. Furthermore, statistical approaches should also be considered which may help reveal additional information in data which was not immediately apparent upon visual comparison.

9.1.1. Revision of Asphaltene Pyrograms

Py-GC-MS offers a wealth of information for the comparison of asphaltenes. Whilst asphaltene pyrograms were thoroughly investigated to identify and extract the most probative compounds for comparison, the identification of compounds used for comparison was primarily based on the CEN method. It is possible that additional probative compounds may exist within asphaltene pyrograms that have not yet been discovered. Asphaltene pyrograms could be revised with a focus on identifying compounds not used in the CEN method, to investigate if additional information can be provided for the comparison of asphaltenes.

9.1.2. Statistical Approaches to Asphaltene Profiling

Initially, exploratory data analysis (EDA) would be the most appropriate statistical approach to asphaltene profiling. EDA can help: (1) maximise the understanding of large, complex datasets; and (2) reveal underlying information in data that may otherwise go unnoticed (Hoaglin et al. 1983). Once EDA has been performed, the analyst has a better understanding of the dataset and which aspects of the dataset need to be targeted when comparing asphaltene profiles for source determination. The analyst can then apply statistical approaches that target these specific aspects of the dataset.

Multivariate statistical tools are ideally suited as an EDA approach to asphaltene profiling. Principle Component Analysis (PCA) is an example of a multivariate tool that could be highly suitable for the exploration of asphaltene spectral data.

PCA involves taking large, complex datasets, and expressing the most variable information in the data (the major differences between samples) in a simpler format. To conduct PCA, a number of samples (asphaltenes from different oils) and a number of variables (for example, the IR absorption of asphaltenes at each individual wavenumber in the spectra; from $4000\text{-}650\text{cm}^{-1}$) are required. PCA breaks down data into a number of principle components (ie: PC1, PC2, PC3, etc) and express the percentage of variability in the overall dataset represented by each principle component (these percentages are known as eigenvalues). For example, PC1 may have an eigenvalue of 81% (meaning that PC1 describes 81% of the variance observed in the overall dataset), PC2 may be 12%, and PC3 may be 5%. The remaining principle components would therefore account for only 3% of the overall variance in the dataset; hence, the information represented in PC1, PC2 and PC3 will be most valuable for the discrimination of asphaltene spectra. In order to determine which spectral data is expressed in each principle component, loading plots for each principle component should be observed (Esbensen et al. 2002).

If considering the aforementioned hypothetical eigenvalues, PC1, PC2 and PC3 loading plots would be observed to identify the spectral regions that contribute to the most variability between asphaltene spectra. Loading plots show peaks (either positive or negative peaks) which indicate the spectral regions which contribute most to each principle component. It is worth noting that when using specialised software, loading plots can be expressed as line plots to resemble spectra. The peaks observed in the PC1 loading plot would indicate which spectral regions are contributing to 81% of the variability between all asphaltene spectra. Although it is expected that major spectral regions of variance have been observed visually

during this research, additional variances in spectra may be observed when considering more subtle variations represented by PC2, PC3 or additional principle components (Esbensen et al. 2002).

Another feature of PCA is the ability to view score plots where two principle components are plotted against one another (ie: PC1 vs PC2, PC1 vs PC3, PC2 vs PC3). Each score in a score plot represents the distance of each sample from the mean along each principal component. Score plots can be used to identify relationships between samples and may reveal: (1) similarities between asphaltene spectra (samples would be plotted closely together); or (2) differences between asphaltene spectra (samples would be plotted far away from one another) (Esbensen et al. 2002).

Although score plots may identify groupings, these groupings are inherently subjective; it is still up to the analyst to define whether similarities/differences are significant. It may in fact be easier to differentiate two spectra based on obvious visual differences than to decide whether groupings identified in PCA are significant or not. It is therefore recommended that PCA is considered only for the exploration of asphaltene data; to better understand the data and to work towards identifying statistical models for asphaltene profiling that may offer an objective measure of similarities/differences presented in asphaltene profiles.

9.1.3. Variability of Asphaltene Profiles from Different HFOs

In addition to investigating an increased number of crude oils, it is also necessary to obtain additional HFO samples for asphaltene profiling. Asphaltene profiles were only generated from a single-source HFO; hence, no data currently exists to compare asphaltenes from different HFOs. It is unknown whether asphaltene profiles from different HFOs can be distinguished from one another, and if so, to what extent these asphaltene profiles from different HFOs can be distinguished.

9.2. Further Optimisation of the Asphaltene Precipitation Method

Although the existing precipitation method is fit for purpose, further optimisation may be beneficial to ensure that the fastest and highest yielding method is available. Now that asphaltenes have been confirmed as a probative oil fraction, it will be worthwhile investing further research into the thorough optimisation of the current asphaltene precipitation method.

The following variables may be tested to further optimise precipitation parameters:

1. Increasing the speed of oven drying – future research should be conducted to determine how long asphaltenes are required to remain in the oven after precipitation. The existing precipitation method involves oven-drying asphaltenes overnight to ensure that as much excess C₅ solvent is evaporated as possible prior to profiling. Shorter oven-drying durations were not tested; however, if asphaltenes could be precipitated, dried and analysed in the same day, this would allow for a more time-effective process overall. It would therefore be interesting to analyse and compare a range of asphaltenes after different lengths of time in the oven following precipitation. The aim would be to determine if asphaltene profiles change if the oven drying duration is reduced; is the probative value or reliability of profiles affected?
2. Optimising asphaltene yields – the duration of oil contact (1 hr) with the precipitation solvent was chosen based on a literature review conducted as part of Honours research. It would be worthwhile thoroughly testing a range of shorter and longer contact durations to determine which contact time produces the highest asphaltene yield. This would ultimately require testing across a range of different oils and oil types.

Although it is possible to test the aforementioned variables individually (keeping all precipitation parameters constant and altering each of the variables one at a time to gauge the

best response), it may also be worth considering the development of a statistical experimental design. For example, a 2x2 factorial design could be considered for testing and understanding the effects of both independent variables at the same time in the same experiment. The advantage of doing so over the ‘one at a time’ approach, is that additional information may be gathered based on the relationship between these two variables. Perhaps these two variables are dependent on one another; this would be measurable in a 2x2 factorial design. Additionally, a 2x2 factorial design would likely be more efficient (Hoaglin and Moore 1992).

9.3. Profiling Additional Chemical Compounds in Asphaltenes

As identified in the research scope, not all chemical components of asphaltenes were investigated: only the organic compounds were investigated. In order to obtain holistic asphaltene profiles, future research is necessary to investigate the heteroatomic, trace metal and isotopic content of asphaltenes. There may be a significant amount of probative information that can be obtained from these additional asphaltene characteristics.

9.3.1. Heteroatoms

Heteroatomic composition should be investigated using EA, which is the most commonly applied instrumentation for the determination of S, O, N and C compositions of asphaltenes (Leyva et al. 2013, Gawel et al. 2014, Ancheyta et al. 2002). The wt% of S, O and N should be determined for asphaltenes precipitated from a range of oils from different geographical regions. Calculated wt% values should then be compared between different asphaltenes to determine the probative value of the heteroatomic content. Heteroatomic ratios, such as those calculated by Ancheyta et al. (2002) (O/C, N/C and S/C ratios), should

also be investigated to determine if the probative value can be further improved by calculating such ratios.

9.3.2. Trace Metals

In regards to trace metals, V and Ni are the most commonly targeted metals in asphaltene. Both wt% of V and Ni as well as V/Ni ratios have proven probative when comparing asphaltene from different oils (Yakubov et al. 2016, Leyva et al. 2013). Both Yakubov et al. (2016) and Leyva et al. (2013) utilized AAS for the analysis of Ni and V in asphaltene; however, ICP-MS has also been used successfully (Pillay et al. 2011). Future research could compare both AAS and ICP-MS to determine which technique is most effective for the Ni and V profiling of asphaltene. AAS and ICP-MS could also be compared to assess which technique is quickest, most cost effective and requires the smallest amount of sample for analysis.

Although V and Ni are the most commonly targeted trace metals in asphaltene, it is worth noting that contemporary ICP-MS capabilities allow for forensic profiling of a vast array of elements in addition to V and Ni (Orellana et al. 2013). It would be interesting to investigate the probative value of elemental profiles generated from a range of different asphaltene.

9.3.3. Isotopes

It is known that isotopic analysis is largely limited to use for exclusionary purposes in environmental forensic investigations, unless combined alongside secondary techniques (Philp 2015). As suitable secondary techniques have now been developed (IR and Py-GC-MS), it is worth investigating the isotopic profiling of asphaltene. It is acknowledged that IRMS is not a common instrument that is readily available in all forensic laboratories;

however if interesting information is available from isotopic ratios, IRMS may become a viable option. Studies such as Hartman and Hammond (1980) and Macko and Parker (1983) alluded to the potential probative value of bulk C, N and S asphaltene isotopes. A dedicated research project could be developed to investigate the probative value of bulk C, N and S isotopic ratios generated from a range of different asphaltenes. If bulk (whole sample) isotopic ratios are found to be of low probative value, it would be worth investigating the isotopic ratios of individual compounds separated from asphaltenes through Py-GC-IRMS, as per the study by Xiong and Geng (2000). This of course would not be simple, however could provide useful information for investigations.

To kick-start future research endeavours, proof-of-concept isotopic profiling of asphaltenes was conducted as per the IRMS method outlined in Chapter 2. Preliminary IRMS analysis was conducted to gauge the probative value of bulk C isotope ratios. Bulk isotope profiling of asphaltenes from ten of the studied oils was conducted. Seven replicate asphaltene fractions were analysed from M. Eastern and HFO (u/c) oils to provide a measure of method uncertainty. SE Asian 1, SE Asian 2, Aust. 3, Aust. 1, N. American, and HFO (d/c) asphaltenes were precipitated in duplicate to help gauge the repeatability of isotopic ratios from each individual oils. Only one asphaltene fraction was profiled from the Aust. 2 and M. Eastern (w) oils. The C^{13}/C^{12} isotope ratios of each replicate asphaltene fraction for M. Eastern and HFO (u/c) were calculated. Box-and-whisker plot were generated for M. Eastern and HFO (u/c) by calculating Quartile 1 (Q1), the median, quartile 3 (Q3), as well as the minimum and the maximum values for C^{13}/C^{12} ratios (Tukey, 1977) (Figure 9.1). For duplicates, the minimum and maximum values were plotted to show the absolute difference between duplicates. The single C^{13}/C^{12} ratios generated for asphaltenes from Aust. 2 and M. Eastern (w) oils are also shown in Figure 9.1.

It was observed from the box-and-whisker plots that the variability of C^{13}/C^{12} ratios may differ between oils; a greater variability was observed for the M. Eastern replicates than for the HFO (u/c) replicates. Because duplicate or singular profiling was conducted for the remaining asphaltenes, it was difficult to gauge whether or not observed differences between duplicate or singular asphaltene fractions were significant. Based on the highest variability observed for replicates (M. Eastern), SE Asian 2 asphaltenes were identified as the most depleted asphaltenes as indicated by C^{13}/C^{12} ratios of -28.8‰ to -28.4‰. SE Asian 1 asphaltenes were the only other asphaltenes that were differentiated in the sample-set. The C^{13}/C^{12} ratios for duplicate SE Asian 1 asphaltenes were between -23.0‰ and -22.8‰, indicating that SE Asian 1 asphaltenes were the most enriched asphaltenes.

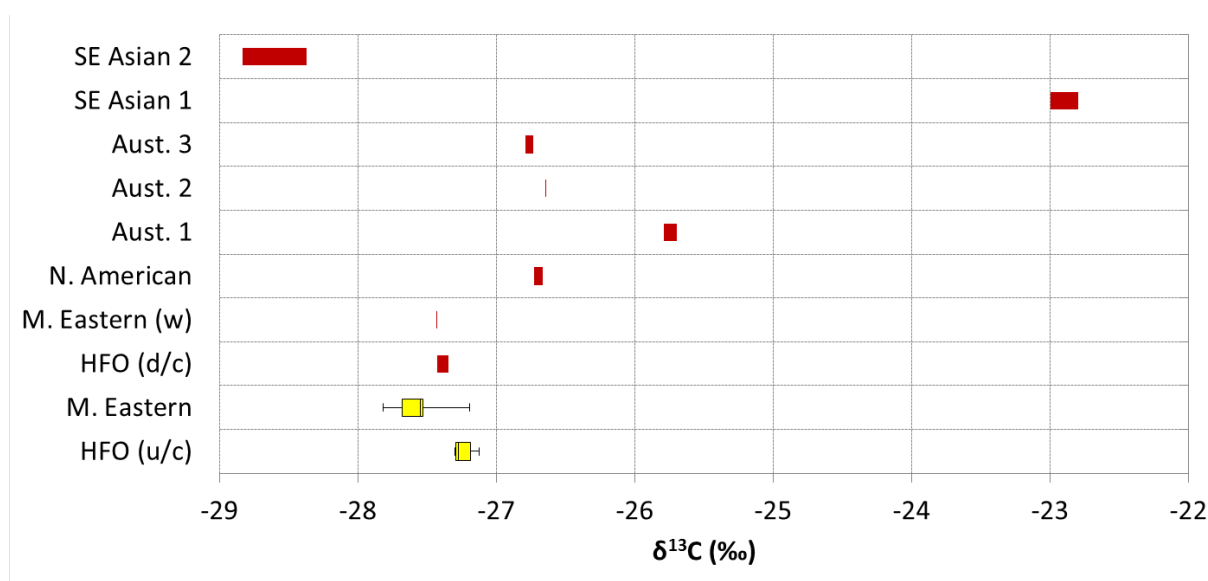


Figure 9.1: C^{13}/C^{12} ratios obtained for the asphaltene fractions of crude and heavy fuel oils. This figure shows the box-and-whisker plots for M. Eastern and HFO (u/c) replicates, and the absolute differences between duplicated asphaltenes (SE Asian 2, SE Asian 1, Aust. 3, Aust. 1, N. American, and HFO (d/c)). The single C^{13}/C^{12} ratios generated for asphaltenes from Aust. 2 and M. Eastern (w) oils are also shown.

It was likely based on the observed replicate variability, that HFO (d/c), HFO (u/c) replicates, and the M. Eastern replicates could not be differentiated from each other. C^{13}/C^{12} ratios for M. Eastern, HFO (d/c) and HFO (u/c) were between -27.8‰ and -27.1‰.

respectively. It was not surprising that the M. Eastern and HFO asphaltenes were very similar based on carbon isotopes, as the M. Eastern and HFO asphaltenes were also very similar when comparing profiles generated from IR and Py-GC-MS. Aust. 3, Aust. 2 and N. American asphaltenes were also indistinguishable from one another, but different to all other oils. C^{13}/C^{12} ratios for Aust. 3, Aust. 2 and N. American asphaltenes were between -26.8‰ and -26.6‰, respectively.

The comparison of C^{13}/C^{12} ratios between the weathered and unweathered M. Eastern asphaltenes was in support of the IR and Py-GC-MS results; the weathered and un-weathered asphaltenes were not differentiated from one another. Whilst this result is certainly worth noting, only a single weathered oil sample was analysed. Future research is therefore required for the analysis of additional weathered oils. Furthermore, it is possible that the isotopic ratio in the weathered oil was not altered as only evaporative and photo-oxidative weathering effects were used for the preparation of the weathered oil. For example, perhaps biodegradation would alter the isotopic ratio of the M. Eastern oil. It will be necessary to consider exposure to additional weathering effects during sample weathering in future research.

The proof-of-concept results presented herein indicate that some probative information was obtainable from bulk C isotope profiling of asphaltenes. Interestingly, as stated in the IRMS method in Chapter 2, only approximately 50 μg (0.05 mg) of asphaltenes were required for bulk C isotope profiling. Isotope ratios appear to be relatively repeatable despite requiring very small sample sizes for analysis. Techniques which allow for the analysis of very small sample sizes are worth investigating further as case-work samples are often very small.

Future research is warranted to determine whether bulk C isotope profiling of asphaltenes can be used to quickly exclude oils. It is worth noting that preliminary bulk N

isotope profiling was also tested. The sample sizes required for N isotope profiling, however, well exceeded realistic sample weights; in excess of 2 mg was required per sample for analysis due to the low N content in asphaltenes as compared to C content. Bulk N isotope profiling is therefore not recommended for asphaltene profiling. Bulk S isotopes were not tested and should be investigated. It is likely that S isotopes will vary between different asphaltenes similarly to the S variations observed in this research between different asphaltene pyrograms.

9.4. Weathering of Asphaltenes

It has been acknowledged throughout this thesis that weathering studies will certainly need to be conducted following this research. The preliminary observations regarding the comparison of asphaltenes from weathered and un-weathered oil supported the current hypothesis stated in the literature; i.e., that asphaltenes are more resistant to weathering than currently targeted volatiles in oil fingerprinting (Lewan et al. 2014; Xiong and Geng 2000). Now that suitable asphaltene profiling methods have been developed, it is necessary to obtain asphaltenes from a large range of weathered and un-weathered oils for profiling. The suitability of IR and Py-GC-MS methods should be gauged when presented with weathered oils for profiling. The benefit of conducting weathering studies using asphaltene profiles from IR and Py-GC-MS is that current oil fingerprinting offers limited or complex information in cases where oils are severely weathered. Asphaltenes may offer an easier form of oil comparison in cases where weathered oils are present.

9.5. Investigating the Robustness of Asphaltene Methods

The blind study validation conducted in Chapter 7 confirmed that asphaltene profiles generated from the developed methods were reliable and suitable for forensic comparison.

Whilst blind study results indicate that the profiling methods are capable of producing comparable forensic results, this blind study did not assess the robustness of the developed methods for casework application. The blind study conducted in Chapter 7 used the same instrumentation on which the asphaltene methods were developed and in the same laboratory. In addition, all of the sample preparation and analyses were performed by the same individual. To consider the application of the developed methods in casework, blind study validation would be required through round-robin testing. Asphaltene profiling using the developed methods would be required on a range of unknown oils across numerous laboratories. If the results obtained from multiple laboratories were consistent with one another, the robustness of the developed asphaltene methods could be confirmed and casework application could potentially be considered. The most effective approach to testing method robustness would be through collaboration of environmental forensic laboratories that are actively involved in oil spill casework. It is likely that further research studies (such as weathering experiments) would be required prior to laboratories considering their participation in a test of method robustness.

9.6. A Standard for Asphaltene Profiling

In this research, an asphaltene standard that contains all of the target IR and Py-GC-MS compounds was not available. As a consequence, method uncertainty was extrapolated from replicate asphaltene fractions obtained from two different oils (M. Eastern and HFO (u/c)). The extrapolation of replicate uncertainty was not ideal as all target compounds were not assessed. The uncertainty of target compounds that were absent from both M. Eastern and HFO (u/c) asphaltenes, yet were present in other asphaltenes, were only gauged through duplicate analysis. Although duplicate analysis of asphaltenes provided reasonable information regarding the repeatability of additional target compounds that were not present

in the replicated asphaltenes, it would be ideal to have a single asphaltene standard that contains all of the necessary target compounds. Future research should therefore be invested into the development of an asphaltene standard that contains all of the possible target compounds compared during the IR and Py-GC-MS profiling of asphaltenes. The asphaltene standard may be produced by blending oils. Oils should be blended so that all of the necessary target compounds are present in a single asphaltene standard (CEN, 2012). Based on the results of this research, a good starting point for a blended oil standard would be a crystalline/resinous asphaltene blend. An example would be a blend between the M. Eastern oil which expressed crystalline asphaltenes, and the Aust. 1 oil which expressed resinous asphaltenes. It would be worthwhile analysing additional oils prior to developing a standard though, as additional target compounds may be identified in asphaltenes from new oils. Consequently, if a standard is produced too early (such as the M. Eastern/Aust. 1 blend) and it does not express newly identified compounds, a new blend would need to be created to include these compounds.

Reference List

- ACD/ChemSketch (Freeware), version 2016 1.1, Advanced Chemistry Development, Inc., Toronto, On, Canada, www.acdlabs.com.
- Adebiyi FM, Thoss V. **2014**. Organic and elemental elucidation of asphaltene fraction of Nigerian crude oils. *Fuel*. 118: 426-31.
- Aeppli C, Nelson RK, Radović JR, Carmichael CA, Valentine DL, and Reddy CM. **2014**. Recalcitrance and degradation of petroleum biomarkers upon abiotic and biotic natural weathering of Deepwater Horizon oil. *Environmental Science and Technology*. 48: 6726-34.
- Akbarzadeh K, Dhillon A, Svrcek WY, Yarranton HW. **2004**. Methodology for the Characterization and Modeling of Asphaltene Precipitation from Heavy Oils Diluted with n-Alkanes. *Energy & Fuels*. 18: 1434-41.
- Akbarzadeh K, Hammami A, Kharrat A, Zhang D, Allenson S, Creek J, Kabir S, Jamaluddin A.J, Marshall A, Rodgers R, Mullins O, Solbakken T. **2007**. Asphaltenes problematic but rich in potential, *Oilfield Review*. 22-43.
- Akmaz S, Gurkaynak MA, Yasar M. **2012**. The effect of temperature on the molecular structure of Ramam asphaltenes during pyrolysis. *Journal of Analytical and Applied Pyrolysis*. 96: 139-45.
- Al Humaidan FS, Hauser A, Rana MS, Lababidi HMS, Behbehani M. **2015**. Changes in asphaltene structure during thermal cracking of residual oils: XRD study. *Fuel*. 150: 558-64.
- Ali HR, El-Gendy NS, Moustafa YM, Roushdy MI, Hashem AI. **2012**. Degradation of Asphaltenic Fraction by Locally Isolated Halotolerant Bacterial Strains. *ISRN Soil Science*. 1-11.
- Ameli F, Hemmati-Sarapardeh A, Dabir B, Mohammadi AH. **2016**. Determination of asphaltene precipitation conditions during natural depletion of oil reservoirs: A robust compositional approach. *Fluid Phase Equilibria*. 412: 235-48.
- Ancheyta J, Centeno G, Trejo F, Marroquín G, García JA, Tenorio E, Torres A. **2002**. Extraction and characterization of asphaltenes from different crude oils and solvents. *Energy Fuels*. 16: 1121-27.
- Andersen SI. **1994**. Effect of precipitation temperature on the composition of n-heptane asphaltenes Part 2. *Fuel Science and Technology International*. 13: 579-604
- Artok L, Su Y, Hirose Y, Hosokawa M, Murata S, Nomura M. **1999**. Structure and Reactivity of Petroleum-Derived Asphaltene. *Energy & Fuels*. 13: 287-96.
- Ascanius BE, Garcia DM, Andersen SI. **2004**. Analysis of Asphaltenes Subfractionated by N Methyl-2-pyrrolidone. *Energy & Fuels*. 18: 1827-31.
- Asemani M, Rabbani AR. **2015**. Oil-Oil correlation by FTIR spectroscopy of asphaltene samples, *Geosciences Journal*. Accessed on ResearchGate 09 November 2015.
- ASTM D2007-**11**. Standard Test Method for Characteristic Groups in Rubber Extender and Processing Oils and Other Petroleum-Derived Oils by the Clay-Gel Absorption Chromatographic Method. ASTM International, West Conshohocken, PA.
- ASTM D3279-**12**. Standard Test Method for n-Heptane Insolubles. ASTM International. West Conshohocken, PA.
- ASTM D3328-**06** (2013). Standard Test Methods for Comparison of Waterborne Petroleum Oils by Gas Chromatography, ASTM International, West Conshohocken, PA.
- ASTM D3414-**98**. Standard Test Method for Comparison of Waterborne Petroleum Oils by Infrared Spectroscopy. ASTM International, West Conshohocken, PA.

- ASTM D893-14. Standard test method for insolubles in used lubricating oils. ASTM International, West Conshohocken, PA.
- ASTM D4124-09. Standard Test Method for Separation of Asphalt into Four Fractions. ASTM International, West Conshohocken, PA.
- Australian Maritime Safety Authority (AMSA). 2000. The Response to the *Laura D'Amato* Oil Spill, Report of the Incident Analysis Team.
- Australian Maritime Safety Authority (AMSA). 2011. DET NORSKE VERITAS Report for Australian Maritime Safety Authority, Appendix IV - Ship Oil Spill Risk Models, Revision 5.
- Australian Maritime Safety Authority (AMSA). 2012. Fact Sheet, Oil spills from ships - who pays?. Canberra, AUS.
- Australian Maritime Safety Authority (AMSA). 2014. National Plan for Maritime Environmental Emergencies.
- Bacosa HP, Erdner DL, Liu Z. 2015. Differentiating the roles of photooxidation and biodegradation in the weathering of Light Louisiana Sweet crude oil in surface water from the Deepwater Horizon site. *Marine Pollution Bulletin*. 95: 265-72.
- Bahrami P, Kharrat R, Mahdavi S, Ahmadi Y, James L. 2015. Asphaltene laboratory assessment of a heavy onshore reservoir during pressure, temperature and composition variations to predict asphaltene onset pressure, *Korean Journal of Chemical Engineering*. 32: 316-22.
- Barakat AO, Mostafa A, El-Gayar MS, Rullkotter J. 1997. Source dependent biomarker properties of five crude oils from the Gulf of Suez, Egypt. *Organic Geochemistry*. 26: 441-50.
- Barakat MK, Shimy T, Mostafa Y. 1999. Mineralogy of Asphaltenes Separated from Crude Oils and Tar Pollutants By X-Ray, Polarizing Microscope, IR and NMR Techniques. *Petroleum Science and Technology*. 17: 667-91.
- Barron M. 2012. Ecological Impacts of the Deepwater Horizon Oil Spill: Implications for Immunotoxicity. *Toxicologic Pathology*. 40: 315-20.
- Béhar F, Pelet R. 1985. Pyrolysis-gas chromatography applied to organic geochemistry, structural similarities between kerogens and asphaltenes from related rock extracts and oil. *Journal of Analytical and Applied Pyrolysis*. 8: 173-87.
- Bjørøy Ø, Fotland P, Gilje E, Høiland H. 2012. Asphaltene Precipitation from Athabasca Bitumen Using an Aromatic Diluent: A Comparison to Standard n-Alkane Liquid Precipitants at Different Temperatures. *Energy Fuels*. 26: 2648-54.
- Bornstein JM, Adams J, Hollebhone B, King T, Hodson PV, Brown RS. 2014. Effects-driven chemical fractionation of heavy fuel oil to isolate compounds toxic to trout embryos. *Environmental Toxicology and Chemistry*. 33: 814-24.
- Boukir A, Guiliano M, Asia L, El Hallaoui A, Mille G. 1998. A fraction to fraction study of photo oxidation of BAL 150 crude oil asphaltenes. *Analysis*. 26: 358-64.
- Bourdet J, Eadington P. 2012. Fluorescence and infrared spectroscopy of inclusion oil. CSIRO internal report EP129625. Australia.
- Bragado GAC, Guzmán ETR, Yacamán MJ. 2001. Preliminary Studies of Asphaltene Aggregates by Low Vacuum Scanning Electron Microscopy. *Petroleum Science and Technology*. 19: 45-53.
- British Petroleum (BP). 2015. BP statistical review of world energy, June 2015 - 64th edn. London, UK.
- Calemma V, Rausa R. 1997. Thermal decomposition behaviour and structural characteristics of asphaltenes. *Journal of Analytical and Applied Pyrolysis*. 40-41: 569-84.

- Chiaberge S, Guglielmetti G, Montanari L, Salvalggio M, Santolini L, Spera S, Cesti P. **2009**. Investigation of asphaltene chemical structural modification induced by thermal treatments. *Energy Fuels*. 23: 4486-95.
- Christensen JH, Tomasi G. **2007**. Practical aspects of chemometrics for oil spill fingerprinting. *Journal of Chromatography A*. 1169: 1-22.
- Coelho RR, Hovell I, Moreno EL, de Souza AL, Rajagopal K. **2007**. Characterization of Functional Groups of Asphaltenes in Vacuum Residues Using Molecular Modelling and FTIR Techniques. *Petroleum Science and Technology*. 25; 41-54.
- Coto B, Martos C, Espada JJ, Robustillo MD, Merino-Garcia D, Pena JL. **2011**. Study of new methods to obtain the n-paraffin distribution of crude oils and its application to the flow assurance. *Energy Fuels*. 25: 487-92.
- Curiale JA. **2008**. Oil-source rock correlations – limitations and recommendations. *Organic Geochemistry*. 39: 1150-61.
- Desideri PG, Lepri L, Heimler D, Checchini L, Giannessi S. **1985**. Fingerprinting of crude oil spills. *Journal of Chromatography A*. 322: 107-16.
- Dollimore D, Gamlen GA, Taylor TJ. **1984**. Mass spectrometric evolved gas analysis-an overview. *Thermochimica Acta*. 75: 59-69.
- Douda J, Alvarez R, Navarrete Bolanos J. **2008**. Characterization of Maya Asphaltene and Maltene by Means of Pyrolysis Application. *Energy & Fuels*. 22: 2619-28.
- Edmonds B, Moorwood R, Szczepanski R, Zhang X. **1999**. Measurement and Prediction of Asphaltene Precipitation from Live Oils', paper presented to the Third International Symposium on Colloid Chemistry in Oil Production (ISCOP). Huatulco, Mexico.
- Eglinton TI, Sinninghe Damsté J.S, Kohnen MEL, de Leeuw JW. **1990**. Rapid estimation of the organic sulphur content of kerogens, coals and asphaltenes by pyrolysis-gas chromatography. *Fuel*. 69: 1394-1404.
- El-Gendy NS, Ali HR, El-Nady MM, Deriase SF, Moustafa YM, and Roushdy MI. **2013**. Effect of different bioremediation techniques on petroleum biomarkers and asphaltene fraction in oil-polluted sea water. *Desalination and Water Treatment*. 52: 7484-94.
- Esbensen KH, Guyot D, Westad F, Houmoller LP. **2002**. *Multivariate Data Analysis: In Practice (4th Edition): An Introduction to Multivariate Data Analysis and Experimental Design*. CAMO Process AS
- European Committee for Standardization (CEN). **2012**. Oil spill identification— waterborne petroleum and petroleum products—part 2: analytical methodology and interpretation of results based on GC-FID and GC-MS low resolution analyses. Brussels, Belgium, no. CEN/TR15522-2:2012.
- Evdokimov I, Losev A. **2011**. On the Nature of of UV-Vis Absorption Spectra of Asphaltenes. *Petroleum Science and Technology*. 25: 55-66.
- ExxonMobil. **2015**. The outlook for energy: A view to 2040. Texas, USA.
- Fahim MA, Alsahhaf TA, Elkilani A. **2010**. *Fundamentals of Petroleum Refining*. Elsevier. Accessed online 13 October 2015:
<http://app.knovel.com/hotlink/toc/id:kpFPR00003/fundamentalspetroleum/fundamentals-petroleum>
- Fan J, Zhang F, Zhao D, Wang J. **2015**. International Oil Spill Response Technical Seminar: Oil Spill Monitoring based on SAR Remote Sensing Imagery, *Aquatic Procedia*. 3: 112-18.
- Filipowski v Fratelli D'Amato SRL; Filipowski v Rosato; Filipowski v Furlan* **2000**, 1, Land and Environment Court of New South Wales, Australia.
- Fossen M, Sjøblom J, Kallevik H, Jakobsson J. **2007**. A new procedure for direct precipitation and fractionation of asphaltenes from crude oil. *Journal of Dispersion Science and Technology*. 28: 193-97.

- Frontier Laboratories. **2012**. Solving Analytical Problems using Multi-functional Pyrolyzer Multi-functional Pyrolyzer® Technical Note (PYA3-012E) Version 1.3.
- Galarraga F, Márquez G, Reategui K, Martínez A. **2007**. Comparative study of crude oils from the Machete area in the Eastern Venezuelan Basin by pyrolysis of asphaltenes. *Journal of Analytical Applied Pyrolysis*. 80: 289-96.
- Ganeeva YM, Yusupova TN, Romanov GV. **2016**. Waxes in asphaltenes of crude oils and wax deposits, *Petroleum Science*. 13: 737-45.
- Gao YY, Shen BX, Liu JC. **2012**. The Structure Identification of Vanadium Porphyrins in Venezuela Crude Oil. *Energy Sources, Part A: Recovery, Utilization, and Environmental Effects*. 34: 2260-67.
- Gawel B, Eftekhardakhah M, Øye G. **2014**. Elemental composition and Fourier Transform infrared spectroscopy analysis of crude oils and their fractions. *Energy & Fuels*. 28: 997-1003.
- GESAMP (IMO/FAO/UNESCO-IOC/UNIDO/WMO/IAEA/UN/UNEP Joint Group of Experts on the Scientific Aspects of Marine Environmental Protection). **1993**. Impact of oil and related chemicals and wastes on the marine environment. *Reports and Studies GESAMP*. No. 50: 180.
- GESAMP (IMO/FAO/UNESCO-IOC/UNIDO/WMO/IAEA/UN/UNEP Joint Group of Experts on the Scientific Aspects of Marine Environmental Protection). **2007**. Estimates of oil entering the marine environment from sea-based activities. *Reports and Studies GESAMP*. No. 75: 96.
- Ghosh AK, Srivastava SK, Bagchi S. **2007**. Study of self-aggregation of coal derived asphaltene in organic solvents: A fluorescence approach. *Fuel*. 86: 2528-34.
- Gill DA, Picou JS, Ritchie LA. **2012**. The Exxon Valdez and BP Oil Spills: A Comparison of Initial Social and Psychological Impacts. *American Behavioural Scientist*. 56: 3–23.
- Gould KA. **1980**. Oxidative demetallization of petroleum asphaltenes and residua. *Fuel*. 59: 733-6.
- Griggs J. **2011**. BP Gulf of Mexico Oil Spill. *Energy Law Journal*. 32: 57-79.
- Groenzin H, Mullins OC. **2000**. Molecular size and structure of asphaltenes from various sources. *Energy & Fuels*. 14: 677-84.
- Gros J, Reddy CM, Aeppli C, Nelson RK, Carmichael CA, Arey JS. **2014**. Resolving biodegradation patterns of persistent saturated hydrocarbons in weathered oil samples from the Deepwater Horizon disaster. *Environmental Science and Technology*. 48: 1628-37.
- Hammer Ø, Harper DAT, Ryan PD. **2001**. PAST: Paleontological statistics software package for education and data analysis. *Palaeontologia Electronica*. 4: 1-9.
- Harayama S, Kishira H, Kasai Y, Shutsubo K. **1999**. Petroleum biodegradation in marine environments. *Journal of Molecular Microbiology and Biotechnology*. 1: 63-70.
- Hartman B, Hammond D. **1980**. The use of carbon and sulfur isotopes as correlation parameters for the source identification of beach tar in the southern California borderland, *Geochimica et Cosmochimica Acta*. 45: 309-19.
- Hoaglin DC, Moore DS. 1992. Perspectives on Contemporary Statistics. MAA Notes and Report Series. USA.
- Hoaglin D, Mosteller F, Tukey JW. **1983**. *Understanding Robust and Exploratory Data Analysis*. Wiley Series in probability and mathematical statistics. New York, USA.
- Independent Statistics & Analysis, U.S. Energy Information Administration. **2014**.
- International Tanker Owners Pollution Federation Limited (ITOPF). **2011**. Fate of marine oil spills: technical information paper. London, UK.
- International Tanker Owners Pollution Federation Limited (ITOPF). **2012**. Sampling and monitoring of marine oil spills: technical information paper. London, UK.

- International Tanker Owners Pollution Federation Limited (ITOPF). **2016**. Oil Tanker Spill Statistics 2015. London, UK.
- Islam A, Cho Y, Yim UH, Shim WJ, Kim YH, Kim S. **2013**. The comparison of naturally weathered oil and artificially photo-degraded oil at the molecular level by combination of SARA fractionation and FT-ICR MS. *Journal of Hazardous Materials*. 263, Part 2: 404-11.
- Jacob J. **1990**. *Sulfur analogues of polycyclic aromatic hydrocarbons (thiaarenes)*. Cambridge University Press. Cambridge, UK.
- Jacobs FS, Filby RH. **1983**. Liquid Chromatographic fractionation of oil-sand and crude oil asphaltenes. *Fuel*. 62:1186-92.
- Jahromi H, Fazaelpoor MH, Ayatollahi S, Niazi A. **2014**. Asphaltenes biodegradation under shaking and static conditions. *Fuel*. 117, Part A: 230-35.
- Jernelov A. **2010**. The Threats from Oil Spills: Now, Then, and in the Future. *AMBIO*. 39: 353-66.
- Karimi A, Qian K, Olmstead WN, Freund H, Yung C, Gray MR. **2011**. Quantitative Evidence for Bridged Structures in Asphaltenes by Thin Film Pyrolysis. *Energy & Fuels*. 25: 3581-9.
- King SM, Leaf PA, Olson AC, Ray PZ, Tarr MA. **2014**. Photolytic and photocatalytic degradation of surface oil from the Deepwater Horizon spill. *Chemosphere*. 95: 415-22.
- Lewan MD, Warden A, Dias RF, Lowry ZK, Hannah TL, Lillis PG, Kokaly RF, Hoefen TM, Swayze GA, Mills CT, Harris SH, Plumlee GS. **2014**. Asphaltene content and composition as a measure of Deepwater Horizon oil spill losses within the first 80 days. *Organic Geochemistry*. 75: 54-60.
- Leyva C, Ancheyta J, Berruoco C, Millán M. **2013**. Chemical characterization of asphaltenes from various crude oils. *Fuel Processing Technology*. 106: 734-8.
- Liao Z, Geng A, Graciaa A, Creux P, Chrostowska A, Zhang Y. **2006**. Saturated hydrocarbons occluded inside asphaltene structures and their geochemical significance, as exemplified by two Venezuelan oils. *Organic Geochemistry*. 37: 291-303.
- Liao Z, Geng A. **2002**. Characterization of nC7-soluble fractions of the products from mild oxidation of asphaltenes. *Organic Geochemistry*. 33:1477-86.
- Liao Z, Zhao J, Creux P, Yang C. **2009**. Discussion on the structural features of asphaltene molecules. *Energy Fuels*. 23: 6272-4.
- Ma A, Zhang S, Zhang D. **2008**. Ruthenium-ion-catalyzed oxidation of asphaltenes of heavy oils in Lunnan and Tahe oilfields in Tarim Basin, NW China. *Organic Geochemistry*. 39: 1502-11.
- Macko SA, Parker PL. **1983**. Stable nitrogen and carbon isotope ratios of beach tars on South Texas barrier islands. *Marine Environmental Research*. 10: 93-103.
- Majumdar RD, Gerken M, Mikula R, Hazendonk P. **2013**. Validation of the Yen–Mullins Model of Athabasca Oil-Sands Asphaltenes using Solution-State 1H NMR Relaxation and 2D HSQC Spectroscopy. *Energy Fuels*. 27: 6528–37.
- Makeen YM, Abdullah WH, Hakimi MH, Hadad YT, Elhassan OM, Mustapha KA. **2015**. Geochemical characteristics of crude oils, their asphaltene and related organic matter source inputs from Fula oilfields in the Muglad Basin, Sudan. *Marine and Petroleum Geology*. 67: 816-28.
- Maqbool T, Balgoa AT, Fogler HS. **2009**. Revisiting Asphaltene Precipitation from Crude Oils: A Case of Neglected Kinetic Effects, *Energy & Fuels*. 23: 3681–6.
- Maqbool T, Srikiratiwong P, Fogler HS. **2011**. Effect of Temperature on the Precipitation Kinetics of Asphaltenes, *Energy Fuels*. 25: 694–700.

- Marine Pollution Act 1987*, Australia.
- McMurry J, Simanek E. **2007**. *Fundamentals of Organic Chemistry*, 6th edn. Thomson Brooks/Cole. Belmont, USA.
- Miller J, Fisher R, van der Eerden A, Koningsberger D. **1999**. Structural Determination by XAFS Spectroscopy of Non-Porphyrin Nickel and Vanadium in Maya Residuum, Hydrocracked residuum and Toluene-Insoluble Solid', *Energy & Fuels*. 13: 719-27.
- Mitchell DL, Speight JG. **1973**. The solubility of asphaltenes in hydrocarbon solvents. *Fuel*. 52: 149-52.
- Mothé MG, Leite LFM Mothé CG. **2008**. Thermal characterization of asphalt mixtures by TG/DTG, DTA and FTIR. *Journal of Thermal Analysis and Calorimetry*. 93: 105–9.
- Muhammad AB, Abbott GD. **2013**. The thermal evolution of asphaltene-bound biomarkers from coals of different rank: A potential information resource during coal biodegradation. *International Journal of Coal Geology*. 107: 90.
- Mullins OC, Sabbah H, Eyssautier J, Pomerantz AE, Barré L, Andrews AB, Ruiz Morales Y, Mostowfi F, McFarlane R, Goual L, Lepkowicz R, Cooper T, Orbulescu J, Leblanc RM, Edwards J, Zare RN. **2012**. Advances in Asphaltene Science and the Yen Mullins Model. *Energy & Fuels*. 26: 3986-4003.
- Mullins OC. **2010**. The modified yen model. *Energy and Fuels*. 24: 2179-207.
- National Association of Testing Authorities (NATA). **2013**. Technical Note 17 - Guidelines for the Validation and Verification of Quantitative and Qualitative Test Methods. Australia.
- National Oceanic and Atmospheric Administration (NOAA). **2012**. Natural Resource Damage Assessment April 2012 - Status Update for the Deepwater Horizon Oil Spill. Accessed on 20 January 2015: www.gulfspillrestoration.noaa.gov
- New South Wales Environment Protection Authority (NSW EPA). **2016**. Incident Response and Recovery. accessed online 15/05/2016: <http://www.epa.nsw.gov.au/pollution/response.htm>
- Nordtest. **2002**. *Nordtest method (NT CHEM 001)*. Nordtest, Finland.
- Oh K, Deo MD. **2007**. Chapter 18: Near Infrared Spectroscopy to Study Asphaltene Aggregation in Solvents, in O Mullins, EY Sheu, A Hammami, AG Marshall (ed.), *Asphaltenes, Heavy Oils and Petroleomics*. Springer Science. New York, USA.
- Orellana FA, Galvez CG, Roldan MT, Garcia-Ruiz C. **2013**. Applications of laser-ablation-inductively-coupled plasma-mass spectrometry in chemical analysis of forensic evidence. *Trends in Analytical Chemistry*. 42: 1-34.
- Ostlund J, Wattana P, Nyden M, Fogler H. **2003**. Characterization of Fractionated Asphaltenes by UV-Vis and NMR Self-diffusion Spectroscopy. *Journal of Colloid and Interface Science*. 271: 372-80.
- Oudot J, Chaillan F. **2010**. Pyrolysis of asphaltenes and biomarkers for the fingerprinting of the Amoco-Cadiz oil spill after 23 years. *C.R. Chimie*. 13: 548-52.
- Oyekunle LO. **2006**. Certain Relationships between Chemical Composition and Properties of Petroleum Asphalts from Different Origin. *Oil & Gas Science and Technology Rev. IFP*. 61:433-41.
- Palus JZ, Zadora G, Milczarek JM, Kościelniak P. **2008**. Pyrolysis-gas chromatography/mass spectrometry analysis as a useful tool in forensic examination of automotive paint traces. *Journal of Chromatography A*. 1179: 41-6.
- Pavia DL, Lampman GM, Kriz GS. **2001**. *Introduction to spectroscopy*, 3rd edn. Brooks/Cole, Thomson Learning, USA.
- Payne JR, Phillips CR. **1985**. Photochemistry of petroleum in water. *Environmental Science and Technology*. 19: 569-79.

- Peng P, Fu J, Sheng G, Morales-izquierdo A, Lown EM, Strausz OP. **1999**. Ruthenium-Ions Catalyzed Oxidation of an Immature Asphaltene: Structural Features and Biomarker Distribution. *Energy & Fuels*. 13: 266-77.
- Peng P, Morales-Izquierdo A, Hogg A, Strausz OP. **1997**. Molecular Structure of Athabasca Asphaltene: Sulfide, Ether, and Ester Linkages. *Energy & Fuels*. 11: 1171-87.
- Pesarini PF, De Souza RGS, Corrêa RJ, Nicodem DE, De Lucas NC. **2010**. Asphaltene concentration and compositional alterations upon solar irradiation of petroleum. *Journal of Photochemistry & Photobiology, A: Chemistry*. 214: 48-53.
- Peterson CH, Rice SD, Short JW, Esler D, Bodkin JL, Ballachey BE, Irons DB. **2003**. Long Term Ecosystem Response to the Exxon Valdez Oil Spill. *Science, New Series*. 302: 2082-86.
- Philp RP. **2015**. Chapter 11 - Application of stable isotopes and radioisotopes in environmental forensics, in BL Murphy, RD Morrison (ed.), *Introduction to Environmental Forensics*, 3rd edn. Academic Press, Oxford, UK.
- Pillay AE, Bassioni G, Stephen S, Kühn FE. **2011**. Depth profiling (ICP-MS) study of trace metal 'grains' in solid asphaltenes. *Journal of the American Society for Mass Spectrometry*. 22: 1403-8.
- Podgorski DC, Corilo YE, Nyadong L, Lobodin VV, Bythell BJ, Robbins WK, McKenna AM, Marshall AG, Rodgers RP. **2013**. Heavy petroleum composition. 5. compositional and structural continuum of petroleum revealed. *Energy and Fuels*. 27: 1268-76.
- Pomerantz AE, Seifert DJ, Bake KD, Craddock PR, Mullins OC, Kodalen BG, Mitra-Kirtley S, Bolin TB. **2013**. Sulfur Chemistry of Asphaltenes from a Highly Compositionally, Graded Oil Column, *Energy Fuels*. 27: 4604-48.
- Prince RC, Garrett RM, Bare RE, Grossman MJ, Townsend T, Suflita JM, Lee K, Owens EH, Sergy GA, Braddock JF, Lindstrom JE, Lessard RR. **2003**. The Roles of Photooxidation and Biodegradation in Long-term Weathering of Crude and Heavy Fuel Oils. *Spill Science & Technology Bulletin*. 8: 145-56.
- Prince RC, Walters CC. **2007**. Chapter 11 - Biodegradation of oil hydrocarbons and its implications for source identification, in Z Wang, SA Stout (ed.), *Oil spill environmental forensics - fingerprinting and source identification*. Elsevier/Academic Press. Boston, USA.
- Riley B. **2013**. Asphaltene Profiling of Crude Oils: A Suitable Addition to the Oil Fingerprinting Arsenal? Honours thesis. University of Western Sydney, Hawkesbury.
- Riley B.J, Lennard C, Fuller S, Spikmans V. **2018**. Pyrolysis-GC-MS analysis of crude and heavy fuel oil asphaltenes for application in oil fingerprinting. *Environmental Forensics*. 19: 14-26.
- Riley BJ, Lennard C, Fuller S, Spikmans V. **2016**. An FTIR method for the analysis of crude and heavy fuel oil asphaltenes to assist in oil fingerprinting. *Forensic Science International*. 266: 555-64.
- Robustillo MD, Coto B, Martos C, Espada JJ. **2012**. Assessment of different methods to determine the total wax content of crude oils. *Energy Fuels*. 26: 6352-57.
- Roehner RM, Hanson FV. **2001**. Determination of wax precipitation temperature and amount of precipitated solid wax versus temperature for crude oils using FT-IR spectroscopy. *Energy & Fuels*. 15: 756-63.
- Roncoroni A, Fusai G, Cummins M. **2015**. *Handbook of Multi-Commodity Markets and Products: Structuring, Trading and Risk Management*. The Wiley Finance Series John Wiley & Sons, West Sussex, UK.
- Ryder AG. **2004**. Time-resolved fluorescence spectroscopic study of crude petroleum oils: Influence of chemical composition, *Applied Spectroscopy*. 58: 613-23.

- Sarkissian G, Keegan J, Du Pasquier E, Depriester JP, Rousselot P. **2004**. The analysis of tires and tire traces using FTIR and Py-GC/MS. *Canadian Society of Forensic Science Journal*. 37: 19-37.
- Sarmah MK, Borthakur A, Dutta A. **2010**. Interfacial and Thermal Characterization of Asphaltenes Separated from Crude Oils Having Different Geological Origins, *Petroleum Science and Technology*. 28: 1068-77.
- Sarmah MK, Borthakur A, Dutta A. **2013**. Pyrolysis of petroleum asphaltenes from different geological origins and use of methyl-naphthalenes and methyl-phenanthrenes as maturity indicators for asphaltenes. *Bulletin of Materials Science*. 36: 311-7.
- Silva TF, Azevedo DA, Rangel MD, Fontes RA, Neto FRA. **2008**. Effect of biodegradation on biomarkers released from asphaltenes. *Organic Geochemistry*. 39: 1249-57.
- Smith E, Dent G. **2005**. *Modern Raman spectroscopy - A practical approach*. John Wiley & Sons. West Sussex, UK.
- Speight JG. **2014**. *The chemistry and technology of petroleum*, 5th edn. Taylor & Francis Group: CRC Press. Florida, USA.
- Stout A, Wang Z. **2016**. *Standard Handbook of Oil Spill Environmental Forensics*, 2nd edn. Academic Press. London, UK.
- Stout SA, Wang Z. **2008**. Chapter 3 - Diagnostic compounds for fingerprinting petroleum in the environment, in RE Hester, RM Harrison (ed.), *Environmental Forensics*, Special publication no. 26. Royal Society of Chemistry. London, UK.
- Tavassoli T, Mousavi SM, Shojaosadati SA, Salehizadeh H. **2012**. Asphaltene biodegradation using microorganisms isolated from oil samples. *Fuel*. 93: 142-8.
- Thanh NX, Hsieh M, Philp RP. **1999**. Waxes and asphaltenes in crude oils. *Organic Geochemistry*. 30: 119-32.
- National Association of Testing Authorities (NATA). **2013**. Technical Note 17 Guidelines for the validation and verification of quantitative and qualitative test methods (2013). Australia.
- Tojima M, Suhara S, Imamura M, Furuta A. **1998**. Effect of heavy asphaltene on stability of residual oil. *Catalysis Today*. 43: 347-51.
- Transport for NSW. **2015**. Response Arrangements for Oil and Chemical Spills in NSW. Accessed on 15 May 2016:
<http://freight.transport.nsw.gov.au/sustainability/marine-pollution.html>
- Trejo F, Centeno G, Ancheyta J. **2004**. Precipitation, fractionation and characterization of asphaltenes from heavy and light crude oils. *Fuel*. 83: 2169-75.
- Tukey JW. **1977**. *Exploratory Data Analysis*. 1st edn. Addison-Wesley, Reading, UK.
- United Nations (UN). **2013**. UN Conference on Trade and Development, Chapter 1 - Review of maritime transport, *Report by the UNCTAD secretariat*. New York, USA. Geneva, Switzerland.
- Van Graas G. **1985**. Biomarker distributions in asphaltenes and kerogens analysed by flash pyrolysis-gas chromatography-mass spectrometry. *Organic Geochemistry*. 10: 1127-35.
- Wang L, He C, Liu Y, Zhao S, Zhang Y, Xu C, Chung KH, Shi Q. **2013**. Effects of experimental conditions on the molecular composition of maltenes and asphaltenes derived from oil sands bitumen: characterized by negative-ion ESI FT-ICR MS. *Science China Chemistry*. 56: 863-73.
- Wang Z, Stout SA, Fingas M. **2006** [a]. Forensic Fingerprinting of Biomarkers for Oil Spill Characterization and Source Identification. *Environmental Forensics*. 7: 105-46.
- Wang Z, Yang C, Fingas M, Hollebhone B, Peng X, Hansen A, Christensen A. **2005**. Characterization, Weathering, and Application of Sesquiterpanes to Source

- Identification of Spilled Lighter Petroleum Products, *Environmental Science & Technology*. 39: 8700-7.
- Wang Z, Yang C, Hollebone B, Fingas M. **2006 [b]**. Forensic Fingerprinting of Diamondoids for Correlation and Differentiation of Spilled Oil and Petroleum Products. *Environmental Science & Technology*. 40, 5636-46.
- Wang, Z., Stout, S.A., Fingas, M. **2007**. Forensic fingerprinting of biomarkers for oil spill characterization and source identification. *Environmental Forensics*. 7: 105-46.
- Xiong Y, Geng A. **2000**. Carbon isotopic composition of individual *n*-alkanes in asphaltene pyrolysates of biodegraded crude oils from the Liaohe Basin, China. *Organic Geochemistry*. 31: 1441-9.
- Yakubov MR, Milordov DV, Yakubova SG, Borisov DN, Ivanov VT, Sinyashin KO. **2016**. Concentrations of Vanadium and Nickel and Their Ratio in Heavy Oil Asphaltenes. *Petroleum Chemistry*. 56: 16-20.
- Yang S. **2017**. *Fundamentals of Petrophysics*. Petroleum Industry Press and Springer-Verlag GmbH. Berlin, Germany.
- Yang S-H, Shen JY, Chang MS, Wu GJ. **2012**. Quantification of vehicle paint components containing polystyrene using pyrolysis-gas chromatography/mass spectrometry. *Analytical Methods*. 4: 1989-95.
- Yang X, Kilpatrick P. **2005**. Asphaltenes and Waxes Do Not Interact Synergistically and Coprecipitate in Solid Organic Deposits. *Energy & Fuels*. 19: 1360-75.
- Yang Z, Chen S, Peng H, Li M, Lin M, Dong Z, Zhang J, Ji Y. **2016**. Effect of precipitating environment on asphaltene precipitation: Precipitant, concentration, and temperature. *Colloids and Surfaces A: Physicochemical and Engineering Aspects*. 497: 327-35.
- Zakaria MP, Bong CW, Vaezzadeh V. **2017**. Chapter 16 - Fingerprinting of petroleum hydrocarbons in Malaysia using environmental forensic techniques: A 20-year field data review, in S Stout, Z Wang (ed.), *Oil Spill Environmental Forensic Case Studies*. Butterworth-Heinemann. Oxford, UK.
- Zellner M, Quarino L. **2009**. Differentiation of twenty-one glitter lip-glosses by pyrolysis gas chromatography/mass spectroscopy. *Journal of Forensic Sciences*. 54
- Zhang L, Yang G, Wang J, Li Y, Li L, Yang C. **2014**. Study on the polarity, solubility, and stacking characteristics of asphaltenes. *Fuel*. 128:366-72.

Appendix A - Precursor Oil Fingerprinting Standards

It should be noted that the term 'precursor' used herein does not refer to the chronological order in which the ASTM and Nordtest methods were developed. Instead, the term precursor refers to the limited degree of forensic discrimination achievable by a method when compared to another. For example, the probative value of the ASTM method is less than the CEN method; hence, the ASTM method is described as a precursor to the CEN method.

A.1. ASTM Method for Oil Fingerprinting

The ASTM method (ASTM D3328-06 (2013)) is essentially Tier 1 of the Nordtest and CEN methods which consists of GC-FID analysis of oils. Chromatograms of spilt oil are overlaid with the chromatograms of suspect oils to ascertain the distribution of *n*-alkanes in oils. GC-FID analyses is limited however, as it cannot identify the specific compounds present in oils unless an alkane standard is used. A second detector known as a flame photometric detector (FPD) can also be used alongside FID. The use of dual detectors (FID/FPD) is not mandatory however it can supply supplementary information regarding the distribution of sulfur-containing compounds in oils. Whether GC-FID or GC-FID/FPD is used, the ASTM method is capable of distinguishing most oils but not all. Further analysis may be required after using the ASTM method in order to identify the source of an oil spill.

A.2. Nordtest Method for Oil Fingerprinting

The Nordtest method is the standard for oil fingerprinting throughout Scandinavia (Finland, Sweden, Norway and Denmark) and was developed by five collaborating Scandinavian laboratories (Nordtest 2002). The Nordtest method uses a two-tiered analysis approach similar to the CEN method: (1) GC-FID screening followed by (2) oil spill identification using GC-MS. GC-FID screening involves the visual comparison of hydrocarbon distributions of oils as observed in chromatograms followed by the calculation and comparison of isoprenoid ratios (Nordtest 2002). The comparison techniques applied in the Nordtest for GC-FID are analogous to Tier 1 of the CEN method. Oil spill identification using GC-MS is also very similar to the CEN method (Tier 2) as selected ion chromatograms for a range of PAHs and biomarkers are generated and compared both visually and statistically (Nordtest 2002). The major difference between the Nordtest and CEN method is that the Nordtest targets less specific PAHs and biomarkers for comparisons than the CEN method.

Appendix B - Development of An Asphaltene Precipitation Method

It is necessary to include the development of the precipitation method used in this research to: (1) better understand the precipitation conditions used to obtain asphaltenes for profiling; and (2) understand why specific precipitation conditions were chosen. As indicated in Chapter 1, this precipitation method was previously developed during past Honours research, and has been applied in this PhD research (Riley 2013). During Honours, the aim was to provide a preliminary insight into the use of asphaltenes in oil fingerprinting. To address this aim, asphaltenes were required for profiling; consequently, an asphaltene precipitation method was also required. A preliminary precipitation method was developed with consideration for the numerous asphaltene precipitation variables observed throughout the literature. Each precipitation variable was considered for forensic suitability. In order to be suitable, the overall precipitation method must be:

- Fast and efficient.
- Repeatable.
- Able to deal with small volumes of oil.
- High yielding.
- Simple, with limited sample handling.

The forensic precipitation method was developed using a range of basic tests as outlined below. The subsequent precipitation method proved suitable for asphaltene profiling during Honours hence was not altered prior to application in this PhD research. While it may be interesting to see if the existing precipitation method may be further optimised, this was reserved for future research as discussed in Chapter 9. During Honours, precipitation parameters including temperature, precipitation solvent, amount of oil required, extraction duration and solvent-to-oil ratio were investigated to determine suitable conditions for each parameter. The discussion presented below has been re-written for this thesis and was not copied directly for the Honours thesis. All figures and tables have also been re-created for the purpose of this thesis.

B.1. Variables Considered during Method Development

Some precipitation conditions were determined based on a literature review. The literature was assessed to make an informed decision regarding specific conditions that would be suitable for oil fingerprinting. Whilst this was possible for assessing some parameters, other parameters endured preliminary testing in the laboratory to determine suitable conditions.

B.1.1. Variables Determined Through a Literature Review

B.1.1.1. Pressure

Controlling pressure during precipitation was beyond the Honours research scope. The experimental setup required in the laboratory to control pressure would unnecessarily complicate the precipitation method.

B.1.1.2. Solvent-to-oil ratio

As discussed in Chapter 1, many studies have been conducted using a vast array of solvent-to-oil ratios for obtaining asphaltenes from oil. The study by Ancheyta et al. (2002) however, tested a range of solvent-to-oil ratios and determined that a 60:1 ratio was most suitable for obtaining a high asphaltene yield and for avoiding error caused by lower ratios (as lower ratios yield much smaller amounts of asphaltenes). This work by Ancheyta et al. (2002) has been acknowledged and applied in other studies such as the study by Trejo et al. (2004). A 60:1 ratio was deemed suitable for use in the developed precipitation method as this ratio aligned with the forensic requirements outlined in Chapter 1: (1) a 60:1 ratio produces a higher asphaltene yield than smaller ratios; and (2) a 60:1 ratio avoids errors associated with lower ratios.

B.1.1.3. Duration of Oil Contact with Solvent

As previously discussed in Chapter 1, the recommended duration of oil contact with solvent for asphaltene precipitation is generally anywhere from 8-10 hr, with some studies challenging this and proposing days or even months for contact (Speight 2014, Maqbool et al. 2009). An overnight solvent to oil contact time is also a commonly used approach (Douda et al. 2008, Sarmah et al. 2010, Silva et al. 2008). These contact durations are not realistic for casework timeframes as a suitable forensic precipitation method should be fast and efficient. The best approach was to trial shorter contact durations than those currently used in the literature. Instead of using a 1 hr agitation period such as that used by Douda et al. (2008), a shorter agitation period of 20 mins was trialled. Instead of 8-10 hrs or overnight solvent to oil contact (prior to extraction of asphaltenes), a much shorter contact time of 1 hr was trialled. The asphaltenes obtained from precipitation using these shorter contact durations were tested for repeatability and were proven to obtain suitable, repeatable asphaltene fractions as discussed throughout this appendix. It is acknowledged that only one contact duration (20 mins agitation followed by 1 hr contact) was tested and accepted as being suitable. Further research may be required to thoroughly investigate a range of different contact durations pending the outcome of this PhD research.

B.1.1.4. Initial Choice of Precipitation Solvent

Prior to beginning laboratory testing it was necessary to consult the literature to determine which precipitation solvents were worth testing. As discussed in Chapter 1, C₇ is a more selective solvent in comparison to C₅ as it only precipitates the highest boiling, heaviest oil compounds. The use of C₇ solvent therefore reduces the chance of co-precipitation of

resins or waxes (Speight 2014, Mullins 2010). C₇ was therefore chosen as the most suitable solvent to begin laboratory testing of precipitation variables.

B.1.2. Precipitation Parameters Tested in the Laboratory

B.1.2.1. Temperature

A basic temperature test was conducted to help determine if heating during precipitation was necessary. Asphaltenes were precipitated from two separate 1 g aliquots of SE Asian 1 oil using C₇ solvent. The two aliquots of oil were exposed to different temperatures (20°C and 50°C) during the agitation (20 min) and rest periods (1 hr). These two temperatures were chosen to remain below the boiling point of C₇, 98°C (NCBI 2016¹). As a result of this basic temperature test, 3.1 mg of asphaltenes were yielded from the 20°C precipitation whilst no asphaltenes were yielded from the 50°C precipitation. Andersen (1994) also observed similar trends in decreased yield with increased temperature when precipitating C₇ asphaltenes from Boscan and Kuwait crude oils at a range of temperatures from -2 to 80°C. It was concluded that precipitation at 20°C (or at room temperature) was therefore most suitable for asphaltene precipitation. The advantage of precipitation at room temperature was that: (1) it requiring less equipment (i.e., thermometers and heating stages were not required for precipitation in a temperature controlled laboratory—controlled at 22 ± 2°C); and (2) it was more cost effective, as heating increased the rate of solvent evaporation which required constant addition of solvent to maintain the desired 60:1 ratio throughout precipitation. From this point onwards all asphaltenes were precipitated at room temperature.

B.1.2.2. Initial Oil Weight Test with C₇ Solvent

Although the amount of oil required for precipitation is not a common concern in mainstream petroleum chemistry, a precipitation method for oil fingerprinting was required to adhere to realistic sample sizes encountered in casework which may only be a gram or two of oil. Small sample sizes such as those observed in forensic casework increase the likelihood of errors during precipitation and as a consequence, chemical variations in subsequent asphaltene fractions may be encountered. It was therefore necessary to precipitate C₇ asphaltenes from the same oil using different initial oil weights to determine if the chemical composition of the C₇ asphaltene fractions were altered due to changes in initial oil weights. IR spectroscopy was used for the chemical analysis of C₇ asphaltenes obtained using different initial oil weights. Two C₇ asphaltene fractions were precipitated from SE Asian 1 oil using approximately 1 g and 2 g initial oil weights and were analysed using IR spectroscopy. The IR spectra were the same for these two C₇ asphaltene fractions which indicated that the spectra for the 1 g fraction could not be differentiated from the spectra of the 2 g fraction (Figure B.1). As a result, although the amount of oil used for precipitation was altered, the bond types of the subsequent asphaltene fractions remained the same as indicated by the consistent IR spectra.

¹ National Center for Biotechnology Information (NCBI 2016). PubChem Compound Database; CID=8900, <https://pubchem.ncbi.nlm.nih.gov/compound/8900> (accessed July 11, 2016).

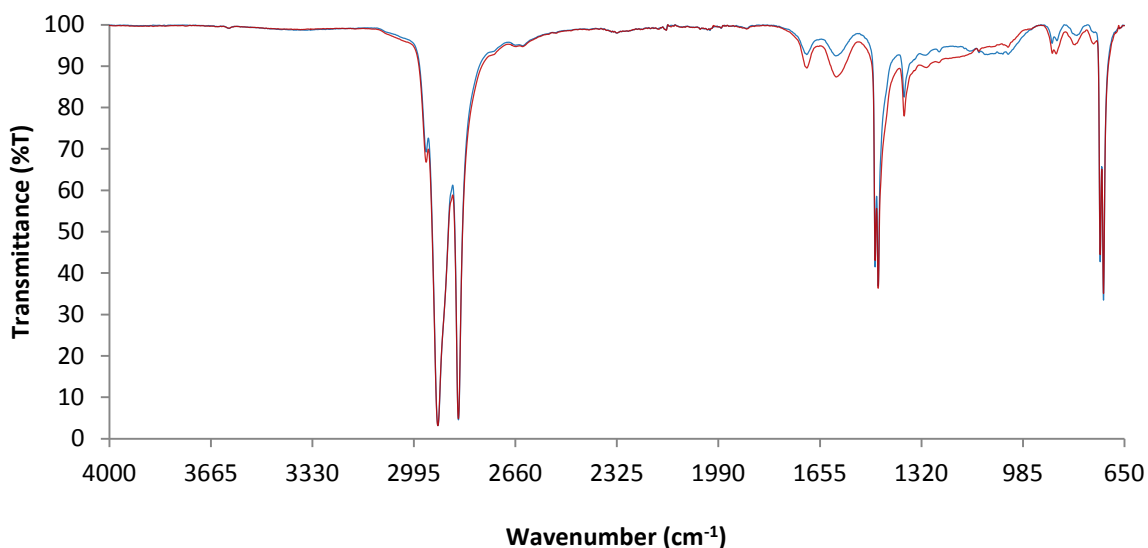


Figure B.1: Two baseline-corrected and normalised IR spectra for SE Asian 1 C₇ asphaltenes are shown. C₇ asphaltenes have been obtained using two different initial oil weights: 1 g (blue line) and 2 g (red line).

Two C₇ asphaltene fractions were also precipitated from M. Eastern oil using approximately 0.25 g and 2 g initial oil weights. The IR spectra obtained for the two M. Eastern C₇ asphaltene fractions also showed no change in the bond types present (Figure B.2). The results observed for the M. Eastern asphaltenes reinforced that a change in initial oil weight does not change the chemical information obtained from IR spectroscopy.

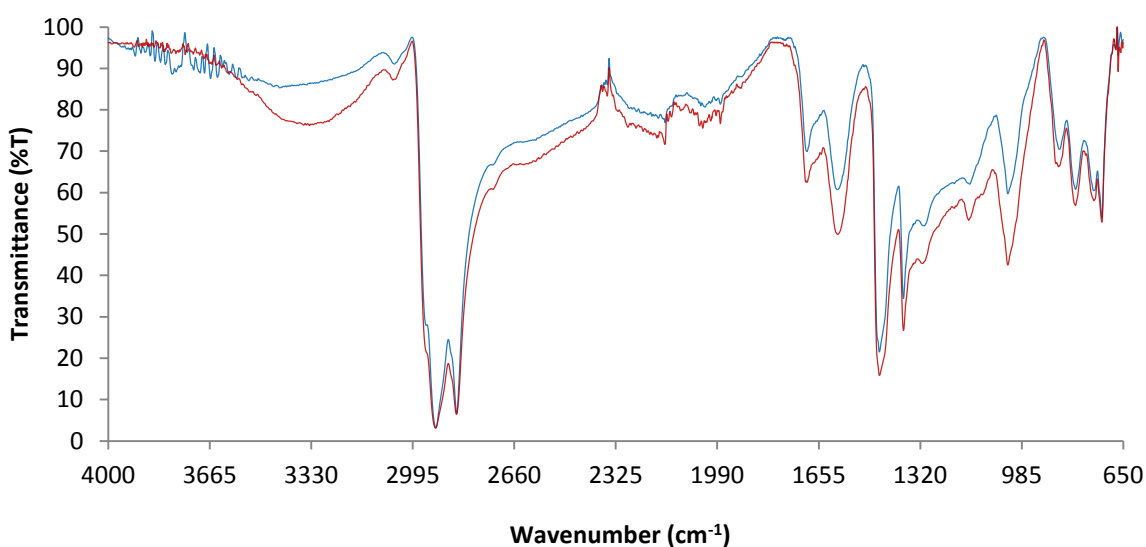


Figure B.2: Two baseline-corrected and normalised IR spectra for M. Eastern C₇ asphaltenes are shown. C₇ asphaltenes have been obtained using two different initial oil weights: 2 g (blue line) and 0.5 g (red line).

As a result of the initial oil weight tests, it was decided that the initial oil weight did not require standardisation for two reasons: (1) IR spectra remained consistent when using different initial oil weights which indicated that bond types in asphaltenes were not changing due to initial oil weights; and (2) different oil weights will be encountered in casework hence the method needs to cater for such variances. Initial oil weights used for precipitation were chosen as a function of the required absolute yield for asphaltene profiling. For example, with SE Asian 1, it was discovered that 1 g of oil yielded around 3 mg of asphaltenes. Initial oil weights used for future precipitations from SE Asian 1 were therefore chosen using these initial yields as a guide to ensure sufficient asphaltene yields were obtained for analysis. Estimation of asphaltene yields allowed for the use of minimal amounts of oil throughout this PhD research for all of the studied oils as suitable initial oil weights could be gauged following preliminary precipitations. Overall, a minimum initial oil weight of 2 g would be used where possible for all oils requiring precipitation.

B.1.2.3. Comparison of Different Precipitation Solvents

As stated previously in Chapter 1, a range of different *n*-alkane solvents have been used throughout the literature for asphaltene precipitation. From an oil fingerprinting perspective, it is not crucial which solvent is used, provided all asphaltenes in a case are treated in the exact same manner to allow for direct comparisons. It is however, crucial that the chosen precipitation solvent is capable of obtaining a suitable asphaltene yield from small amounts of oil. Although C₇ is most likely to reduce co-precipitation, it was necessary to test a range of common *n*-alkane precipitation solvents to compare to C₇. C₅, C₆ and C₇ were therefore tested to determine which solvent was best for obtaining the highest asphaltene yields from five different oils: SE Asian 1, M. Eastern, N. American, Aust. 1 and Aust. 3. Three separate asphaltene fractions were precipitated from each of the oils: C₅, C₆ and C₇ asphaltenes. The initial oil weight was kept constant at 2 g to allow for the most accurate comparison of yields. Precipitation was carried out using the conditions defined thus far (i.e., temperature, solvent-to-oil ratio, duration of contact of solvent-to-oil).

The yields obtained from this experiment revealed that C₅ solvent out-performed both C₆ and C₇ solvents across all five oils (with the exception of Aust. 3 in which C₆ yielded more asphaltene than C₅ by a very minimal amount of 0.4 mg) (Table B.1).

Table B.1: C₅, C₆ and C₇ asphaltene yields obtained from five different oils. The asphaltene yields in red are asphaltenes that could not be analysed using IR spectroscopy with an ATR attachment. All remaining yields (not red) indicated a sufficient yield for IR analysis using and ATR attachment.

Oil	Product Weight (mg) From an Initial Oil Weight of 2 g		
	Yield of C ₅ Fraction	Yield of C ₆ Fraction	Yield of C ₇ Fraction
SE Asian 1	11 mg	8.3 mg	4.1 mg
M. Eastern	81 mg	53 mg	32 mg
N. American	4.9 mg	2.2 mg	0.2 mg
Aust. 1	3.3 mg	1.3 mg	0.5 mg
Aust. 3	1.6 mg	2.0 mg	0.2 mg

The variance observed in Aust. 3 may be explained by the low yielding nature of this particular oil across all three solvents; hence, the increased likelihood of variations in the obtained yields. All asphaltenes were analysed using the IR method outlined in Chapter 2 to test whether the asphaltene yields obtained were sufficient for IR profiling. To be considered a sufficient yield, there had to be enough asphaltene to cover the ATR crystal to generate an IR spectrum. To be considered an insufficient yield, there was not enough asphaltene to cover the ATR crystal; hence, an IR spectrum was not obtained. Insufficient yields were only observed for the N. American C₆ and C₇ fractions, Aust. 1 C₆ and C₇ fractions, and the Aust. 3 C₇ fraction (denoted red in Table B.1). The only two oils to have sufficient yields for all three asphaltene fractions (C₅, C₆ and C₇) were the M. Eastern and SE Asian 1 oils. The IR spectra for C₅, C₆ and C₇ asphaltenes from M. Eastern and SE Asian 1 are shown in Figures B.3 and B.4, respectively. It is interesting to note that the IR spectra remained very consistent for the SE Asian 1 C₅, C₆ and C₇ asphaltenes (Figure B.3). This indicated that the bond types present in the SE Asian 1 C₅, C₆ and C₇ asphaltene fractions did not change. Subsequently, the information gathered using IR spectroscopy was consistent regardless of the precipitation solvent used to obtain SE Asian 1 asphaltenes.

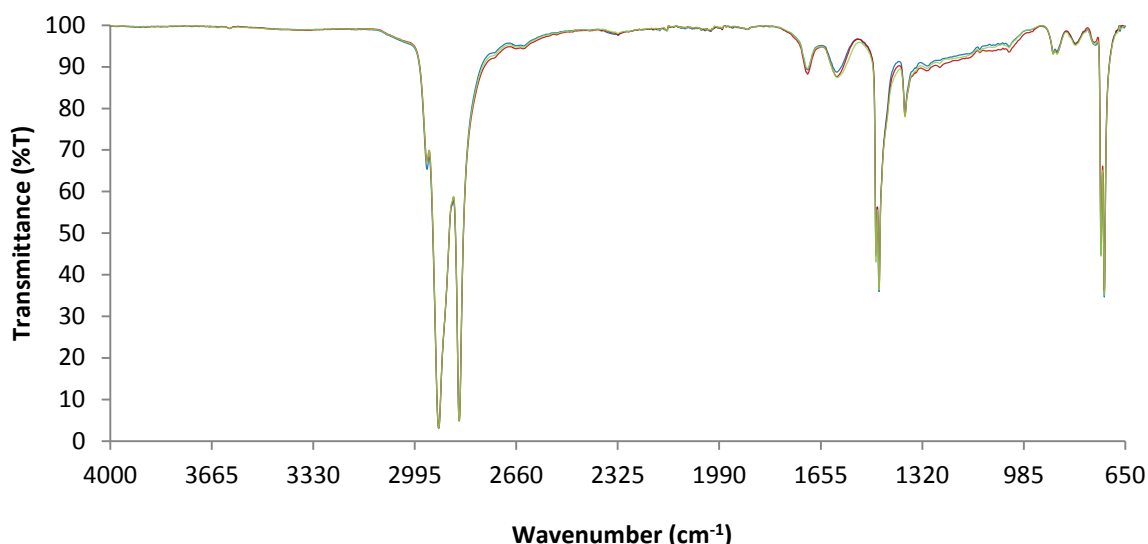


Figure B.3: Three baseline-corrected and normalised IR spectra for three different SE Asian 1 asphaltene fractions, obtained using three different precipitation solvents (C₅, C₆ and C₇): C₅ asphaltenes (blue line), C₆ asphaltenes (red line) and C₇ asphaltenes (green line).

A very similar trend was observed when comparing M. Eastern C₅, C₆ and C₇ asphaltenes, as these three fractions also produced consistent IR spectra (Figure B.4). The only variation between the three spectra was the slightly different peak intensities in the 1600–1700 cm⁻¹ and 1350–1000 cm⁻¹ regions for C₆ asphaltenes, as compared to C₅ and C₇. Overall however, the observations made when comparing M. Eastern C₅, C₆ and C₇ asphaltene fractions supported the results observed for the SE Asian 1 asphaltenes. In light of the preliminary findings presented herein, the high asphaltene yielding nature of C₅ solvent made C₅ the most suitable precipitation solvent for oil fingerprinting.

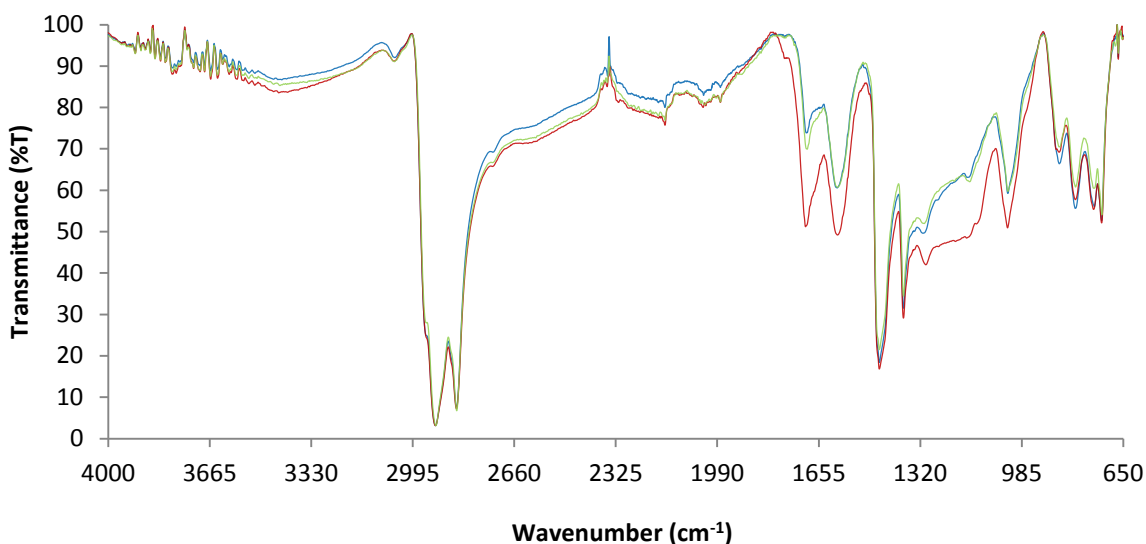


Figure B.4: Three baseline-corrected and normalised IR spectra for three different M. Eastern asphaltene fractions, obtained using three different precipitation solvents (C_5 , C_6 and C_7): C_5 asphaltene (blue line), C_6 asphaltene (red line) and C_7 asphaltene (green line).

It is also worth noting that based on the tested sample-set, the optimum weight required for IR profiling was > 2.2 mg, or 2.5 mg or greater to be conservative. An exception to this was the Aust. 3 C_6 asphaltene, in which 2 mg of asphaltene was successfully analysed. Although the Aust. 3 oil produced a smaller asphaltene yield than the N. American oil, the Aust. 3 asphaltene was more pliable allowing for coverage of the ATR crystal. This was due to the resinous morphology of the Aust. 3 asphaltene; the N. American asphaltene was crystalline and therefore not as pliable. As a consequence, the N. American asphaltene could not cover the ATR crystal, hence the yield was deemed insufficient. Asphaltene morphology is discussed in Chapter 3.

B.1.2.4. Initial Oil Weight Test with C_5 Solvent

Given that C_5 solvent outperformed C_7 thus far, it was necessary to precipitate C_5 asphaltene using different initial oil weights to determine if the chemical composition of the C_5 asphaltene fractions were altered due to changes in initial oil weights (the same test previously conducted using C_7). IR spectroscopy was used again for the profiling of subsequent asphaltene.

Two C_5 asphaltene fractions were precipitated from M. Eastern oil using approximately 0.25 g and 2 g initial oil weights (Table B.2). The two M. Eastern asphaltene fractions were analysed using the IR method specified in Chapter 2. The IR spectra of both M. Eastern asphaltene fractions were the same; the IR spectra of the 0.25 g fraction could not be differentiated from the IR spectra of the 2 g fraction (Figure B.5). This result indicated that the bond types present in M. Eastern C_5 asphaltene were also unaltered with changing initial oil weights. These results further reinforced the suitability of C_5 solvent for oil fingerprinting.

Table B.2: C₅ asphaltene yields from M. Eastern crude oil. The initial oil weights were varied (0.25 g and 2 g) for precipitation.

Solvent	Initial Oil Weight (g)	Product Weight (g)	Product Weight (mg)	% yield
C ₅	0.2520	0.0050	5	2.0
C ₅	2.0060	0.0810	81	4.04

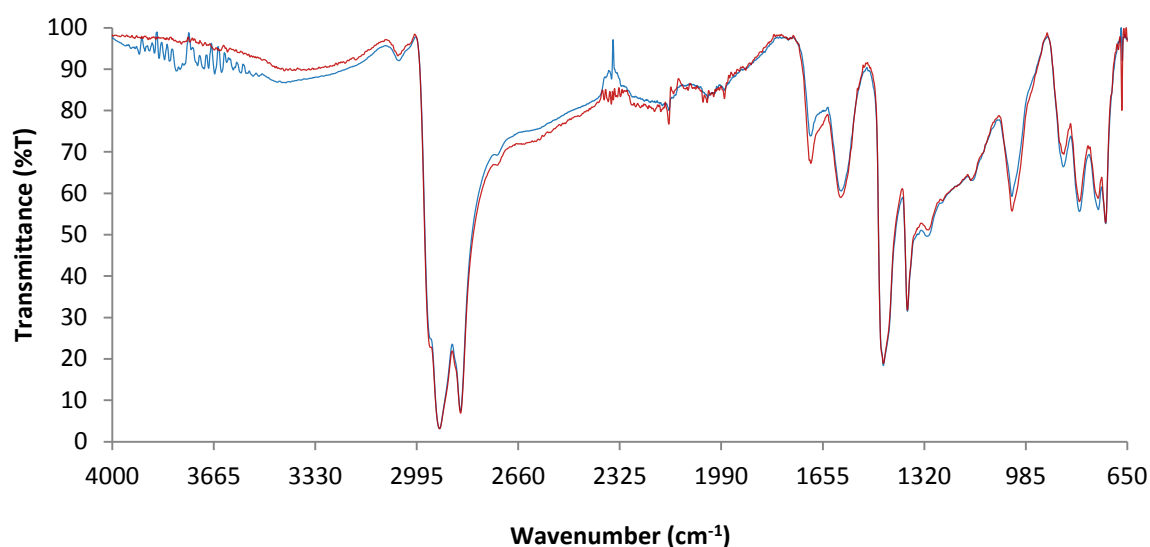


Figure B.5: Two baseline-corrected and normalised IR spectra for M. Eastern C₅ asphaltenes are shown. C₅ asphaltenes have been obtained using two different initial oil weights: 2 g (blue line) and 0.25 g (red line).

B.1.2.5. Co-Precipitation of Non-Asphaltenic Compounds

As discussed previously, resins and waxes often co-precipitate with asphaltenes (Roehner and Hanson 2001). One way to minimise the occurrence of co-precipitation is to choose a solvent such as C₇ that is more selective for isolating only the heaviest oil compounds (Speight 2014, Mullins 2010). It was not possible however, to continue using C₇. In some cases, C₇ did not successfully yield asphaltenes from oils whilst C₅ did yield asphaltenes from the same oils. C₅ was therefore deemed the most suitable solvent for obtaining high yields. It is known however, that C₅ precipitates a broader spectrum of molecular weight compounds than C₇, therefore co-precipitation is more likely with C₅ (Mullins 2010). If C₅ asphaltenes obtained from oils are reproducible, then the presence of co-precipitates in C₅ asphaltene fractions may provide additional information when comparing asphaltenes. As observed in this appendix and also in Chapters 3-7, the precipitation of C₅ asphaltenes was indeed reproducible. Throughout Chapters 3-7, seven replicate C₅ asphaltenes were precipitated from two different oils and duplicate C₅ asphaltenes were precipitated from the remaining oils that were studied. The chemical compositions of replicates and duplicates were found to be reproducible for all of the studied oils. The presence of co-precipitates in C₅ asphaltenes was therefore not concerning; the presence of co-precipitates simply increases the probative value of C₅ asphaltene fractions during comparisons.

Appendix C - CEN Oil Fingerprinting: Blind Study

C.1. Sample Preparation and Analysis Sequencing

Sample preparation for oils A–U involved the extraction of volatile oil fractions from the discarded asphaltene fraction. SPE was used to extract volatiles from non-volatiles. Short Pasteur pipettes were used as SPE columns; each column was packed with a thin layer of glass wool at the bottom (above the neck of the pipette) and then topped up with silica gel with a thin layer of sodium sulfate added on top. Columns were conditioned using HPLC grade DCM prior to extraction. 1 drop of oil was added to 1 mL of HPLC grade DCM. The oil/DCM solution was shaken and added to the SPE column. Asphaltenes were retained in the silica gel, whilst volatiles were eluted from the column and collected for analysis in 4 mL vials (giving approximate concentrations of 20 ppm).

C.2. Tier 1: GC-FID

The conditions defined by the CEN method were followed when obtaining the Tier 1 results (CEN, 2012). Tier 1 analysis may also be conducted using GC-MS instrumentation instead of GC-FID instrumentation. In this blind study, GC-MS was used for Tier 1.

C.2.1. Method Uncertainty

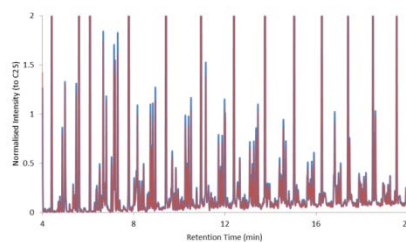
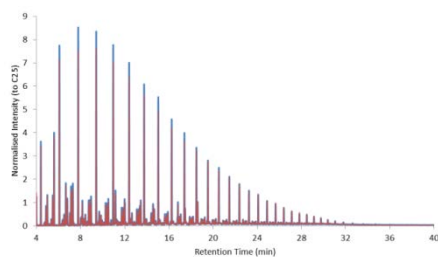
Four separate aliquots of M. Eastern oil were prepared in the same manner as oils A–U and were analysed with the batch of samples.

C.2.1.1. Alkane Chromatograms

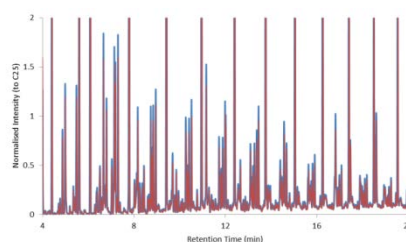
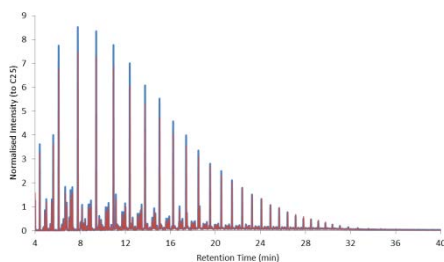
M. Eastern Oil

Alkane chromatograms (m/z 57) were generated. When visually comparing replicate M. Eastern aliquots, both the overall alkane profiles as well as the unresolved complex mixture (UCM) profiles were consistent with one another (Figure C.1). The UCM refers to the mixture of compounds that cannot be fully resolved by GC-MS, hence appearing as a cluster of undefined peaks between alkanes. All alkane chromatograms were normalised to C₂₅ prior to visual comparison.

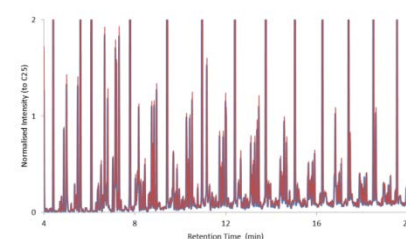
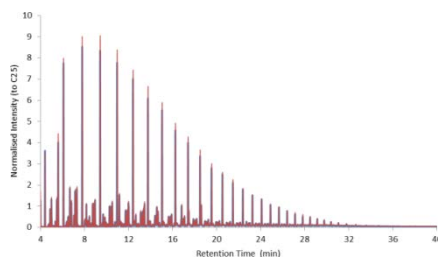
Aliquot 1
versus
Aliquot 2



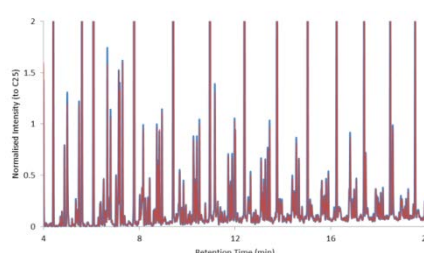
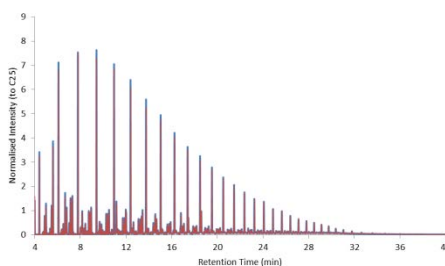
Aliquot 1
versus
Aliquot 3



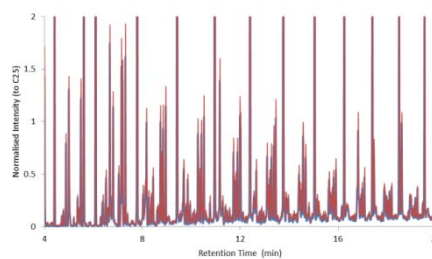
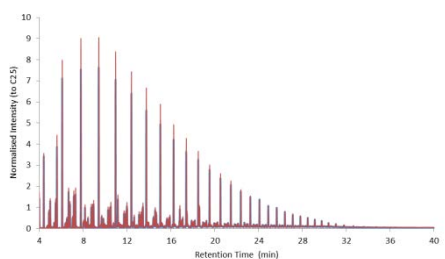
Aliquot 1
versus
Aliquot 4



Aliquot 2
versus
Aliquot 3



Aliquot 2
versus
Aliquot 4



Aliquot 3
versus
Aliquot 4

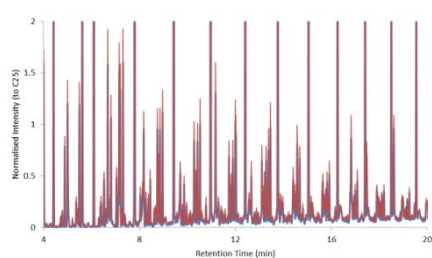
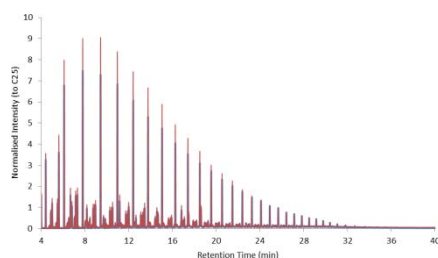


Figure C.1: The alkane chromatograms (m/z 57) from M. Eastern aliquots 1, 2, 3 and 4 normalised to C₂₅. Left hand column: the overall alkane profiles; right hand column: close-up of the UCM profiles.

C.2.1.2. GC-PW-plots and Isoprenoid Ratios

M. Eastern Oil

GC-PW-plots were calculated by normalising the peak height of alkanes to the mean abundance (height) of C₂₀–C₂₄ (refer to CEN method for details). Following normalisation, each M. Eastern aliquot was compared pairwise by dividing the normalised peak height of alkanes from one aliquot against the normalised peak height of alkanes from a second aliquot. The mathematical threshold for which two alkanes must fall within to be considered the same is between 85–118% (CEN, 2012). If the difference between alkanes exceeds these upper or lower thresholds, the difference is deemed significant. Due to the low intensities of C₂₇–C₃₄ peaks in the M. Eastern aliquots and subsequent likelihood of increased error, GC-PW-plots were only produced from C₈–C₂₆. As can be observed in Figure C.2, the C₈–C₂₆ alkanes of all aliquots fell within the desired thresholds indicating that the sample preparation and analysis was repeatable. Low intensity alkane peaks were also removed where necessary when comparing oils A–U using GC-PW-plots.

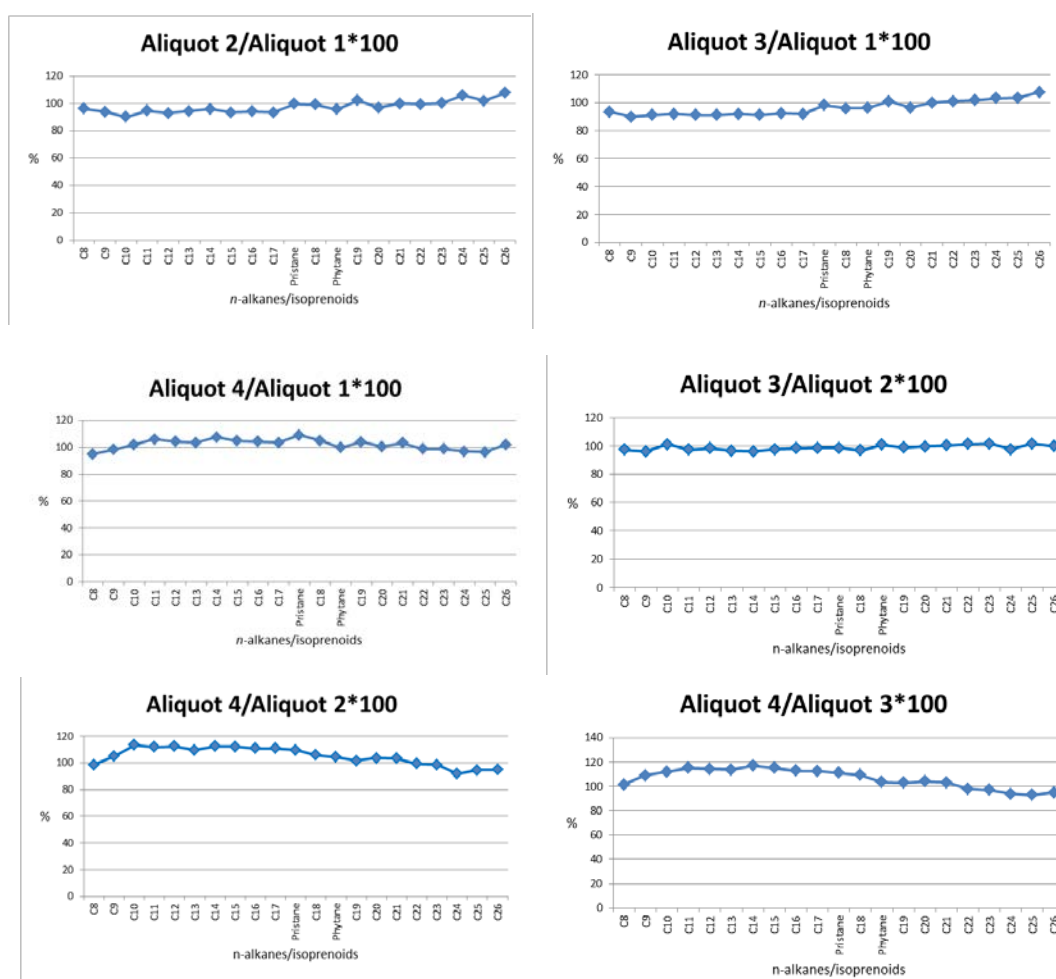


Figure C.2: GC-PW-plots compared pairwise between M. Eastern aliquots 1, 2, 3 and 4.

Table C.1: Pairwise comparison of isoprenoid ratios between M. Eastern aliquots 1, 2, 3 and 4.

Ratio	Peak Height Ratio		Mean	Absolute Difference	Relative Difference (%)	Conclusion
	Aliquot 1	Aliquot 2				
Pri/phy	0.67	0.69	0.68	0.03	4	Not Different
C ₁₈ /phy	3.41	3.53	3.47	0.13	4	Not Different
C ₁₇ /pri	6.12	5.74	5.93	0.39	7	Not Different

Ratio	Peak Height Ratio		Mean	Absolute Difference	Relative Difference (%)	Conclusion
	Aliquot 1	Aliquot 3				
Pri/phy	0.67	0.68	0.67	0.01	2	Not Different
C ₁₈ /phy	3.41	3.39	3.40	0.01	0	Not Different
C ₁₇ /pri	6.12	5.92	6.02	0.20	3	Not Different

Ratio	Peak Height Ratio		Mean	Absolute Difference	Relative Difference (%)	Conclusion
	Aliquot 1	Aliquot 4				
Pri/phy	0.67	0.73	0.70	0.06	9	Not Different
C ₁₈ /phy	3.41	3.59	3.50	0.18	5	Not Different
C ₁₇ /pri	6.12	5.81	5.97	0.32	5	Not Different

Ratio	Peak Height Ratio		Mean	Absolute Difference	Relative Difference (%)	Conclusion
	Aliquot 2	Aliquot 3				
Pri/phy	0.69	0.68	0.69	0.01	2	Not Different
C ₁₈ /phy	3.53	3.39	3.46	0.14	4	Not Different
C ₁₇ /pri	5.74	5.92	5.83	0.19	3	Not Different

Ratio	Peak Height Ratio		Mean	Absolute Difference	Relative Difference (%)	Conclusion
	Aliquot 2	Aliquot 4				
Pri/phy	0.69	0.73	0.71	0.04	5	Not Different
C ₁₈ /phy	3.53	3.59	3.56	0.05	2	Not Different
C ₁₇ /pri	5.74	5.81	5.77	0.07	1	Not Different

Ratio	Peak Height Ratio		Mean	Absolute Difference	Relative Difference (%)	Conclusion
	Aliquot 3	Aliquot 4				
Pri/phy	0.68	0.73	0.70	0.05	7	Not Different
C ₁₈ /phy	3.39	3.59	3.49	0.19	6	Not Different
C ₁₇ /pri	5.92	5.81	5.86	0.11	2	Not Different

Isoprenoid ratios were calculated based on the same normalised peak height values used for the GC-PW-plots. M. Eastern aliquots were also compared pairwise based on ratios (Table C.1), and the relative difference between M. Eastern isoprenoid ratios were below the 14% threshold (as defined in the CEN method) for all aliquots (Figure C.2, CEN 2012).

C.2.2. Oils A–U

C.2.2.1. Alkane Chromatograms

Oils A–U were compared to one another using alkane chromatograms (m/z 57) that were normalised to C₂₅ alkanes. On the basis of alkane profile comparisons, oils B, I, Q, G and F were differentiated from one another and also from all other blind study oils. The remaining oils were differentiated into distinct groups: (1) S, P, J, T and N; (2) E, K, U and D; (3) C and L; (4) M, R and O; and (5) A and H. The distinctions between the individual oils and oil groups are shown below.

Oils B, I, Q, G and F

The alkane chromatograms of oils B, I, Q, G and F were differentiated from each other and also from the remaining blind study oils. Alkane profiles for oils B and I were differentiated due to their relatively even distribution of low-boiling and high-boiling alkanes which was not observed in any other oils. B and I also differed from one another in the high-boiling region of the alkanes, as well as in the UCM profiles (Figure C.3). Oil F was unlike any other oil due to the high abundance of low-boiling alkanes and rapid decline in abundance of alkanes in the mid to high-boiling range (Figure C.3). Oils G and Q displayed alkane profiles that were dominant in mid-boiling alkanes, however the maximum peak in the alkane profiles for G and Q differed between one another and also from all other oils. The UCM profiles of G and Q were also different between one another and from all other oils (Figure C.3). It was therefore concluded that oils B, I, Q, G and F were not related to any other oils in the blind study, hence these oils were not compared further during the CEN method.

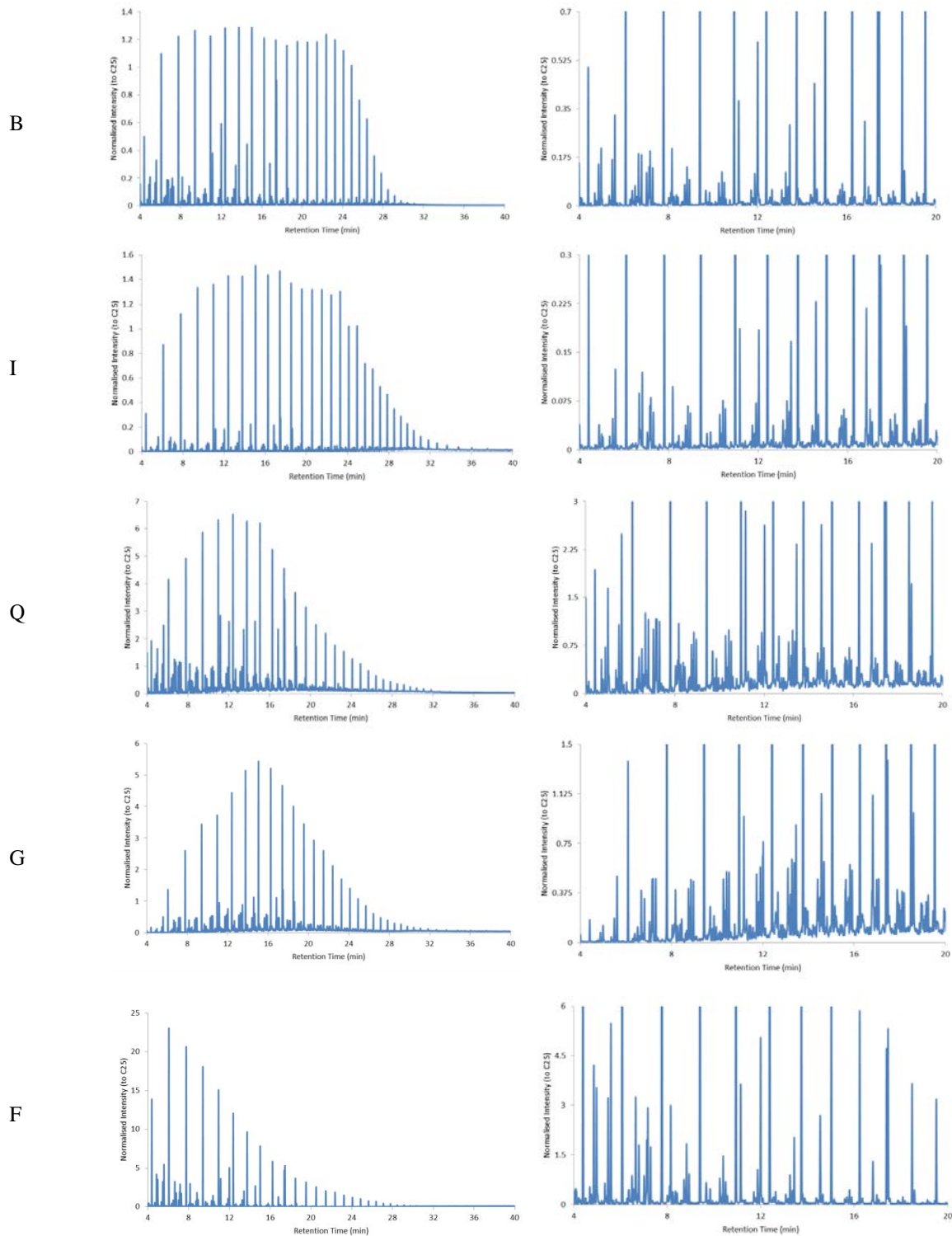


Figure C.3: The alkane chromatograms (m/z 57) from oils B, I, Q, G and F normalised to C₂₅. Left hand column: the overall alkane profiles; right hand column: close-up of the UCM profiles.

Oils S, P, J, T and N

The visual profile of the alkane chromatograms for oils S and P (S vs P) were similar; hence S was used as a representative profile for both oil S and P (Figure C.4). The visual alkane profile of oils T and J (T vs J) were also similar; hence oil J was used as a representative profile for both oil J and T (Figure C.4).

Oil N was grouped with oils S, P, J and T as the visual alkane profile of N indicated that it may have been heavily weathered oil from the same source as oil S, P, J and/or T. The comparison of profiles N vs J and N vs S (Figure C.4) showed that the high-boiling region of the alkane profile for N aligned with both J and S. The low-boiling alkanes of N however, did not align with the profiles of J or S; these compounds were absent in the profile of N, potentially due to severe evaporation. Although this degree of weathering was unlikely, N was still grouped with oils S, P, J and T to be conservative.

Oils S and P may have also been weathered oils from the same source as oil J and/or T. The comparison of alkane profiles S and J (S vs J) in Figure C.4 showed that the low-boiling alkanes and also the low-boiling UCM were absent from the profile of S in comparison to the profile of J where these compounds were present. This may have also been the result of weathering, and these oils were therefore compared more thoroughly prior to differentiating from one another.

Oils E, K, U and D

The visual profiles of alkane chromatograms generated from oils E, K, U and D were all similar to one another as indicated in Figure C.5. Oil E was therefore used as a representative profile for oils E, K, U and D in Figure C.5. It is worth noting that whilst oils E, K, U and D shared very similar alkane and UCM profiles, the abundance of alkanes (peak heights) of oils D and U had a higher abundance overall than oil E (and therefore K). Whilst these were visual differences, further evidence was required to confirm that oils E and K were different to oils D and U; hence oils E, K, U and D were grouped together for further comparison.

Oils C and L

The visual profiles of alkane chromatograms for oils C and L were similar, however some minor variability was observed when comparing the UCM profiles (Figure C.6). The observed differences were not significant enough to differentiate oils C and L; hence further comparison between these oils was required.

Oils M, R and O

The visual profiles of alkane chromatograms for oils M and R were similar; hence oil M was used as a representative profile for both oil M and R (Figure C.7). Oil O did differ slightly to both oils M and R when comparing the profiles of low-boiling alkanes as well as the low-boiling UCM profile (Figure C.7). The alkanes and UCM of oil O appeared to be of a higher abundance than those observed for oils M and R, which could be due to evaporative weathering of the M and R profiles. To remain conservative, oil O remained grouped together with oils M and R for further comparison to confirm if the observed visual differences were significant.

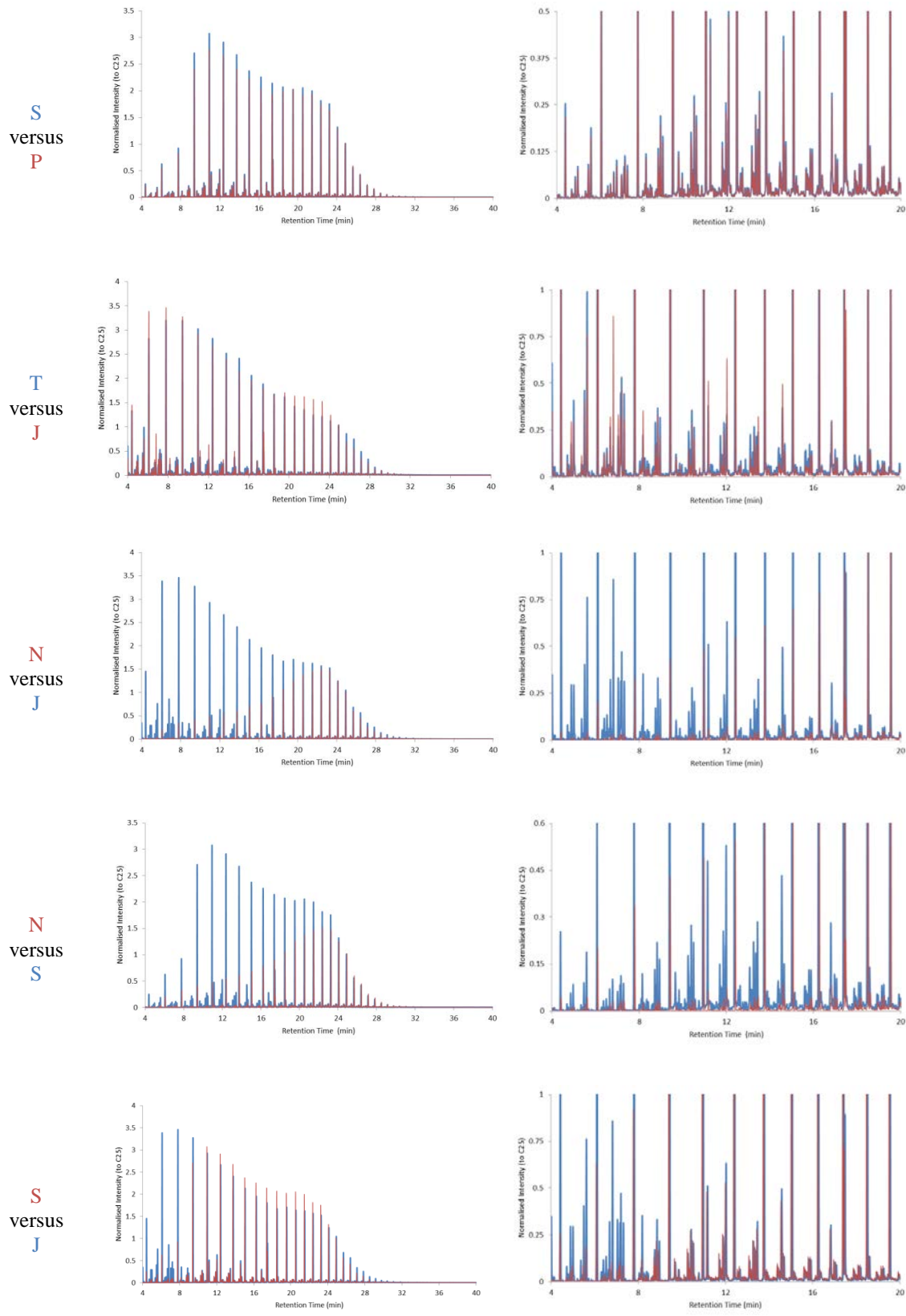
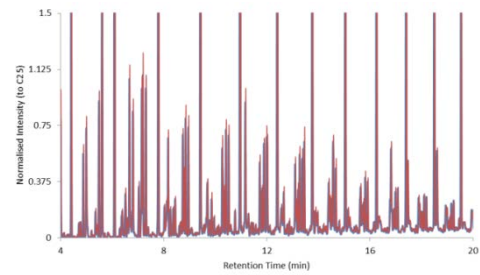
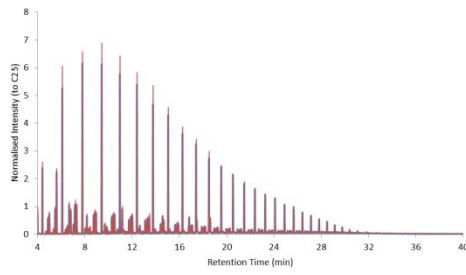
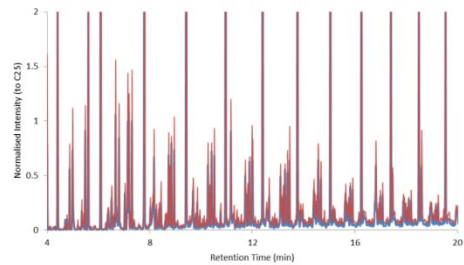
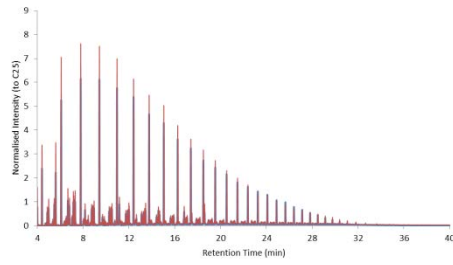


Figure C.4: The alkane chromatograms (m/z 57) from oils S, P, J, T and N normalised to C₂₅. Left hand column: the overall alkane profiles; right hand column: close-up of the UCM profiles.

E
versus
K



E
versus
U



E
versus
D

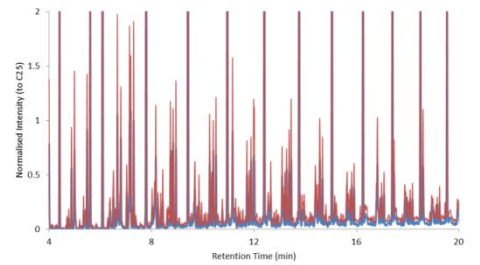
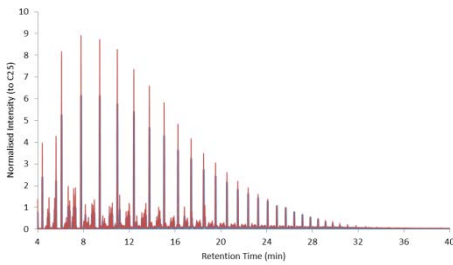


Figure C.5: The alkane chromatograms (m/z 57) from oils E, K, U and D normalised to C₂₅. Left hand column: the overall alkane profiles; right hand column: close-up of the UCM profiles.

C
versus
L

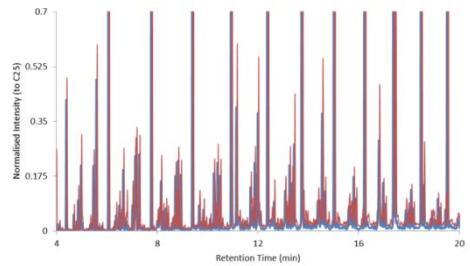
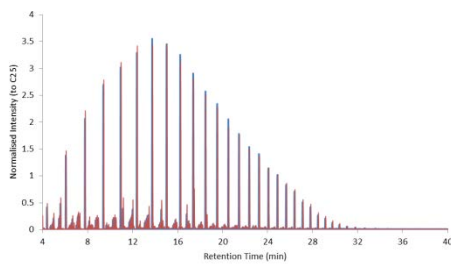


Figure C.6: The alkane chromatograms (m/z 57) from oils C and L normalised to C₂₅. Left hand column: the overall alkane profiles; right hand column: close-up of the UCM profiles.

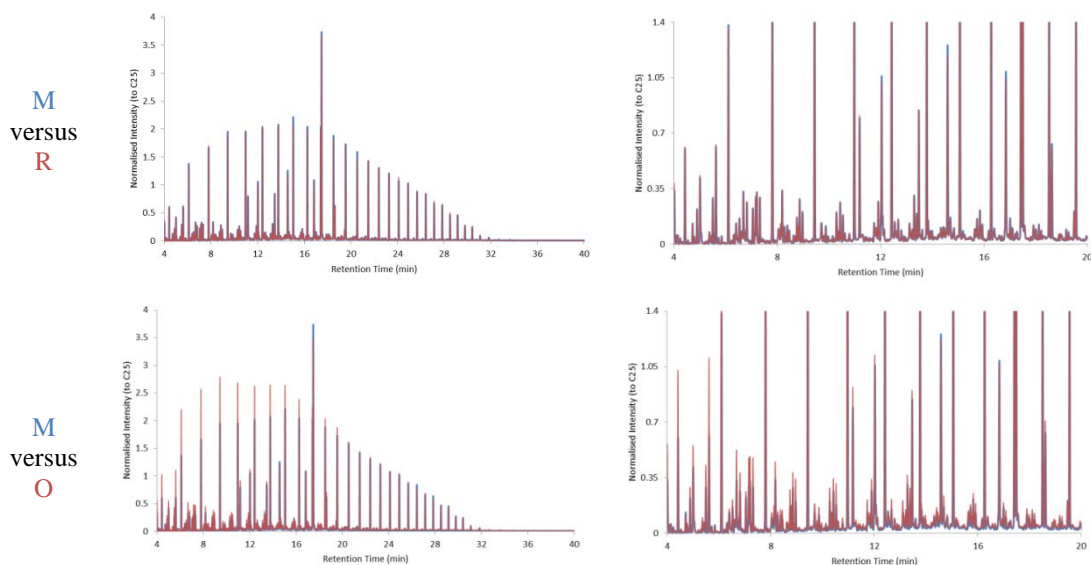


Figure C.7: The alkane chromatograms (m/z 57) from oils M, R and O normalised to C_{25} . Left hand column: the overall alkane profiles; right hand column: close-up of the UCM profiles.

Oils A and H

The visual profiles of alkane chromatograms for oils A and H were similar, however some variability was observed when comparing the UCM profiles (Figure C.8). The observed differences were not significant enough to differentiate oils A and H; hence further comparison between these oils was required.

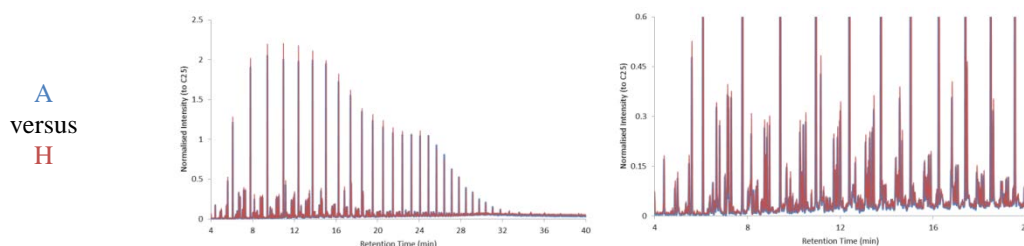


Figure C.8: The alkane chromatograms (m/z 57) from oils A and H normalised to C_{25} . Left hand column: the overall alkane profiles; right hand column: close-up of the UCM profiles.

C.2.2.2. GC-PW-plots and Isoprenoid Ratios

GC-PW-plots and isoprenoid ratios were used to compare oils that could not be differentiated based on the visual comparison of alkane chromatograms. The following groups of oils could not be differentiated based on these visual comparisons: (1) S, P, J, T and N; (2) E, K, U and D; (3) C and L; (4) M, R and O; and (5) A and H. The GC-PW-plots and

isoprenoid ratios were calculated using the same process as previously defined for the M. Eastern aliquots.

Oils S, P, J, T and N

The GC-PW-plot for oils S and P indicated that the alkanes were within the threshold of 85–118% (Figure C.9). Low intensity alkanes were observed in S and P profiles from C₂₆–C₃₄. These alkanes were therefore removed from comparison to avoid errors associated with comparing low intensity peaks. The isoprenoid ratios for oils S and P also fell below the 14% threshold (Table C.2). The collective results observed during Tier 1 indicated that oils S and P could not be differentiated from one another. Oils S and P were therefore carried through for Tier 2 comparison.

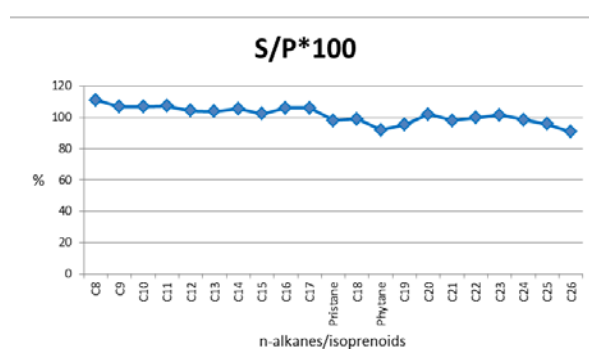


Figure C.9: The GC-PW-plot comparing oils S and P.

Table C.2: Pairwise comparison of isoprenoid ratios between oils S and P.

Ratio	Peak Height Ratio		Mean	Absolute Difference	Relative Difference (%)	Conclusion
	S	P				
Pri/phy	5.62	5.27	5.45	0.35	6	Not Different
C ₁₈ /phy	17.14	15.93	16.54	1.21	7	Not Different
C ₁₇ /pri	3.16	2.92	3.04	0.24	8	Not Different

Whilst the alkane profiles of oils J and T were visually similar to one another, the GC-PW-plot and isoprenoid ratios of oils J and T indicated that these two oils were in fact different. There was a significant variation in alkane abundances across the boiling range as observed in Figure C.10, whilst the ratios of pristane/phytane (pri/phy) and C₁₇/pristane (C₁₇/pri) exceeded the 14% threshold considerably (Table C.3). It was therefore concluded that oils J and T originated from different sources to one another.

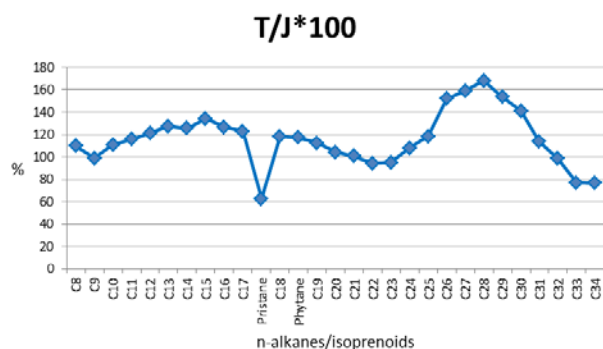


Figure C.10: The GC-PW-plot comparing oils T and J.

Table C.3: Pairwise comparison of isoprenoid ratios between oils T and J.

Ratio	Peak Height Ratio		Mean	Absolute Difference	Relative Difference (%)	Conclusion
	T	J				
Pri/phy	3.69	6.93	5.31	3.24	61	Different
C ₁₈ /phy	13.51	13.40	13.46	0.11	1	Not Different
C ₁₇ /pri	4.09	2.08	3.09	2.01	65	Different

Oil N was compared pairwise to oil J, T, P and S to determine if it was possible that oil N was heavily weathered oil from the same source as oil J, T, P and/or S. The GC-PW-plots for N vs J, N vs T, N vs P and N vs S are shown in Figure C.11; all of which indicated significant variations in alkane abundances across the boiling range.

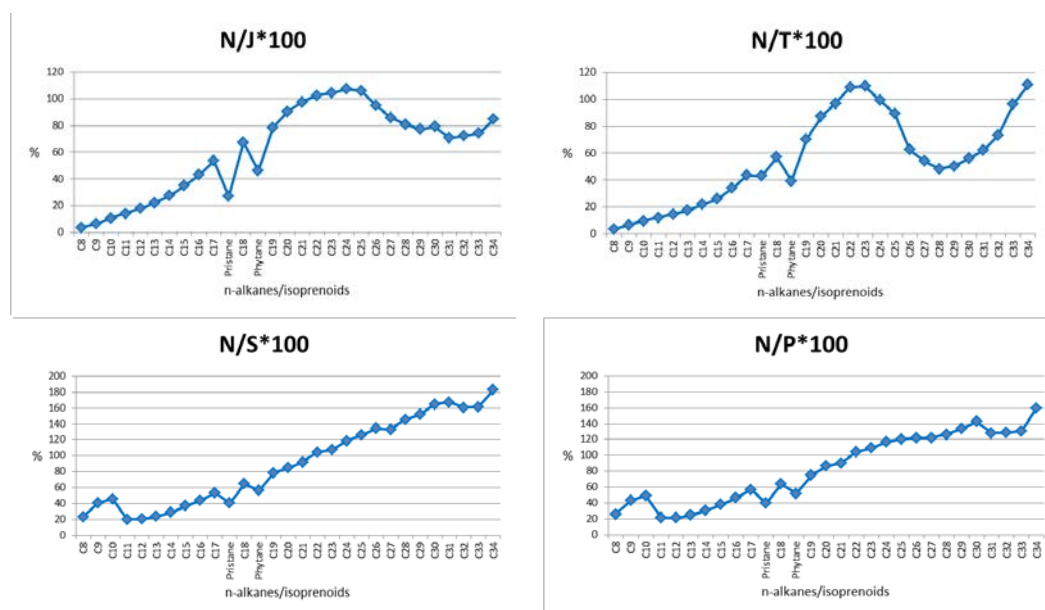


Figure C.11: The pairwise comparison of GC-PW-plots for oils N versus J, T, S and P.

The isoprenoid ratios of the aforementioned pairwise comparisons are shown in Table C.4. All three isoprenoid ratios exceeded the 14% threshold for pairwise comparisons N vs P (Table C.4 (a)) and N vs J (Table C.4 (c)). Two of the three ratios exceeded the 14% threshold for N vs S (Table C.4 (d)), whilst one of the three ratios exceeded the threshold for N vs T (Table C.4 (b)). The GC-PW-plots and isoprenoid ratios therefore did not indicate the presence of weathering. It was concluded that oil N did not originate from the same source as oils T, J, S or P. Oil N was deemed to have originated from a different source to all other blind study oils. No further comparison of oil N was conducted during the CEN method blind study.

Table C.4: Pairwise comparison of isoprenoid ratios between oils: (a) N and J; (b) N and T; (c) N and P; and (d) N and S.

(a)						
Ratio	Peak Height Ratio		Mean	Absolute Difference	Relative Difference (%)	Conclusion
	N	J				
Pri/phy	4.05	6.93	5.49	2.88	52	Different
C ₁₈ /phy	19.68	13.40	16.54	6.27	38	Different
C ₁₇ /pri	4.15	2.08	3.12	2.06	66	Different
(b)						
Ratio	Peak Height Ratio		Mean	Absolute Difference	Relative Difference (%)	Conclusion
	N	T				
Pri/phy	4.05	3.69	3.87	0.36	9	Not Different
C ₁₈ /phy	19.68	13.51	16.59	6.17	37	Different
C ₁₇ /pri	4.15	4.09	4.12	0.05	1	Not Different
(c)						
Ratio	Peak Height Ratio		Mean	Absolute Difference	Relative Difference (%)	Conclusion
	N	P				
Pri/phy	4.05	5.27	4.66	1.22	26	Different
C ₁₈ /phy	19.68	15.93	17.80	3.74	21	Different
C ₁₇ /pri	4.15	2.92	3.53	1.23	35	Different
(d)						
Ratio	Peak Height Ratio		Mean	Absolute Difference	Relative Difference (%)	Conclusion
	N	S				
Pri/phy	4.05	5.62	4.84	1.57	32	Different
C ₁₈ /phy	19.68	17.14	18.41	2.53	14	Not Different
C ₁₇ /pri	4.15	3.16	3.65	0.99	27	Different

Oils S and P were compared pairwise to oil J and T to determine if oils S and P shared a common source to oils J and/or T. The GC-PW-plots for P vs J, P vs T, S vs J and S vs T are shown in Figure C.12; all of which indicated significant variations in alkane abundances across the boiling range. The isoprenoid ratios of the aforementioned pairwise comparisons are shown in Table C.5.

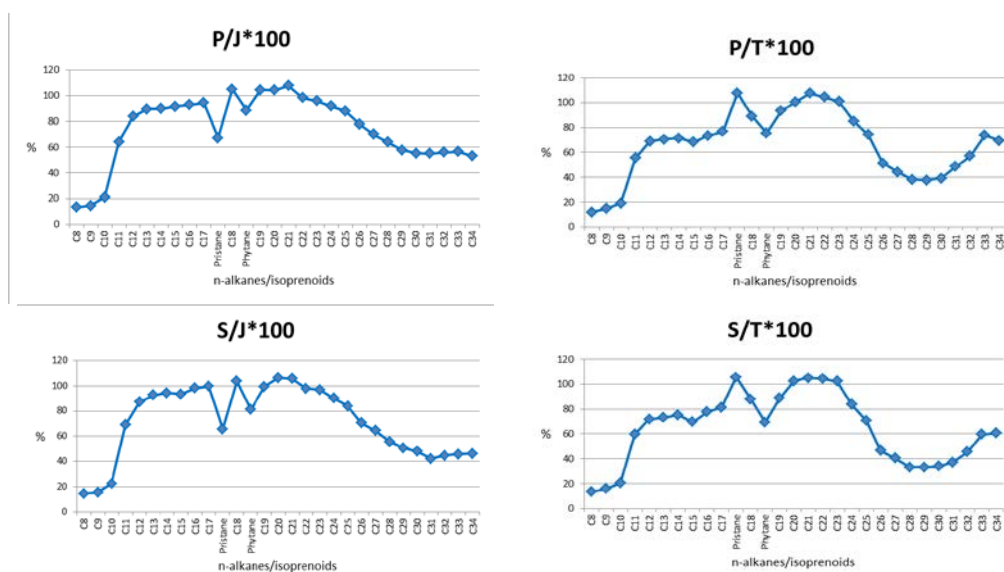


Figure C.12: The pairwise comparison of GC-PW-plots for oils P versus J and T, and S versus J and T.

Table C.5: Pairwise comparison of isoprenoid ratios between oils: (a) P and J; (b) P and T; (c) S and J; and (d) S and T.

(a)	Ratio	Peak Height Ratio		Mean	Absolute Difference	Relative Difference (%)	Conclusion
		P	J				
	Pri/phy	5.27	6.93	3.37	3.79	112	Different
	C ₁₈ /phy	15.93	13.40	11.71	8.45	72	Different
	C ₁₇ /pri	2.92	2.08	4.18	2.53	61	Different
(b)	Ratio	Peak Height Ratio		Mean	Absolute Difference	Relative Difference (%)	Conclusion
		P	T				
	Pri/phy	5.27	3.69	4.48	1.58	35	Different
	C ₁₈ /phy	15.93	13.51	14.72	2.42	16	Different
	C ₁₇ /pri	2.92	4.09	3.51	1.18	34	Different
(c)	Ratio	Peak Height Ratio		Mean	Absolute Difference	Relative Difference (%)	Conclusion
		S	J				
	Pri/phy	5.62	6.93	6.27	1.31	21	Different
	C ₁₈ /phy	17.14	13.40	15.27	3.74	25	Different
	C ₁₇ /pri	3.16	2.08	2.62	1.08	41	Different
(d)	Ratio	Peak Height Ratio		Mean	Absolute Difference	Relative Difference (%)	Conclusion
		S	T				
	Pri/phy	5.62	3.69	4.65	1.93	41	Different
	C ₁₈ /phy	17.14	13.51	15.33	3.63	24	Different
	C ₁₇ /pri	3.16	4.09	3.63	0.94	26	Different

All three isoprenoid ratios exceeded the 14% threshold for all pairwise comparisons: P vs J (Table C.5 (a)); P vs T (Table C.5 (b)); S vs J ((Table C.5 (c)); and S vs T (Table C.5 (d)). The resulting GC-PW-plots and isoprenoid ratios did not indicate the presence of weathering; therefore, it was concluded that oils S and P did not originate from the same source as oils T or J. Oils S and P were therefore deemed to originate from a different source to oils T and J.

Oils E, K, U and D

Oils E, K, U and D were compared pairwise based on GC-PW-plots as shown in Figure C.13, and isoprenoid ratios as shown in Table C.6. For oils D vs E and D vs K, variations in alkane abundances were observed across the entire boiling range in the GC-PW-plots, whilst significant ratio differences were also observed (Table C.6 (a) and (b)). The variations observed in GC-PW-plots and ratios supported the visual differences previously observed in Tier 1 when comparing oil D to both oils E and K. In conclusion, oil D was differentiated from both oils E and K.

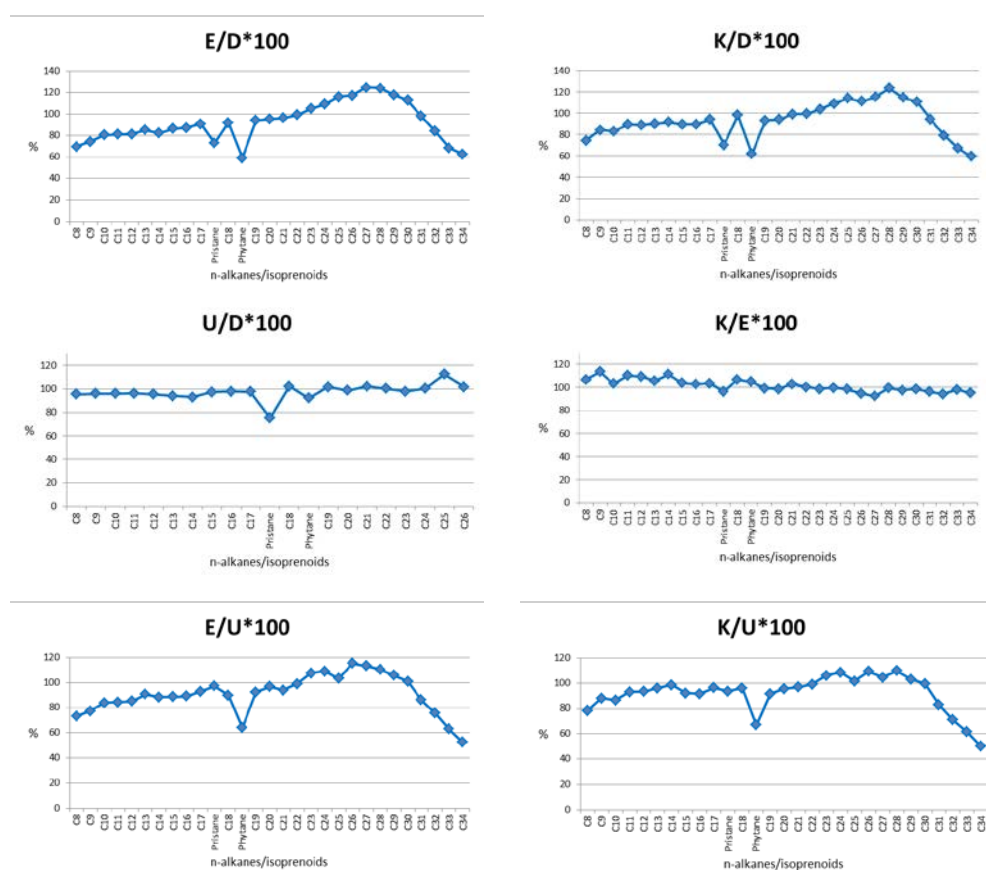


Figure C.13: The pairwise comparison of GC-PW-plots for oils E, K, U and D.

Table C.6: Pairwise comparison of isoprenoid ratios between oils: (a) D and E; (b) D and K; (c) D and U; (d) E and K; (e) E and U; and (f) K and U.

(a)						
Ratio	Peak Height Ratio		Mean	Absolute Difference	Relative Difference (%)	Conclusion
	D	E				
Pri/phy	0.71	0.88	0.80	0.17	21	Different
C ₁₈ /phy	3.40	5.30	4.35	1.90	44	Different
C ₁₇ /pri	5.75	7.16	6.45	1.41	22	Different
(b)						
Ratio	Peak Height Ratio		Mean	Absolute Difference	Relative Difference (%)	Conclusion
	D	K				
Pri/phy	0.71	0.81	0.76	0.10	13	Not Different
C ₁₈ /phy	3.40	5.40	4.40	1.99	45	Different
C ₁₇ /pri	5.75	7.70	6.73	1.95	29	Different
(c)						
Ratio	Peak Height Ratio		Mean	Absolute Difference	Relative Difference (%)	Conclusion
	D	U				
Pri/phy	0.71	0.58	0.65	0.13	20	Different
C ₁₈ /phy	3.40	3.77	3.59	0.37	10	Not Different
C ₁₇ /pri	5.75	7.47	6.61	1.72	26	Different
(d)						
Ratio	Peak Height Ratio		Mean	Absolute Difference	Relative Difference (%)	Conclusion
	E	K				
Pri/phy	0.88	0.81	0.84	0.07	9	Not Different
C ₁₈ /phy	5.30	5.40	5.35	0.09	2	Not Different
C ₁₇ /pri	7.16	7.70	7.43	0.55	7	Not Different
(e)						
Ratio	Peak Height Ratio		Mean	Absolute Difference	Relative Difference (%)	Conclusion
	E	U				
Pri/phy	0.88	0.58	0.73	0.30	41	Different
C ₁₈ /phy	5.30	3.77	4.54	1.53	34	Different
C ₁₇ /pri	7.16	7.47	7.32	0.32	4	Not Different
(f)						
Ratio	Peak Height Ratio		Mean	Absolute Difference	Relative Difference (%)	Conclusion
	K	U				
Pri/phy	0.81	0.58	0.69	0.23	33	Not Different
C ₁₈ /phy	5.40	3.77	4.58	1.63	35	Not Different
C ₁₇ /pri	7.70	7.47	7.59	0.23	3	Different

Oil D was also compared to oil U. Low intensity alkanes were observed in U and D profiles from C₂₆–C₃₄. These alkanes were therefore removed from comparison to avoid errors associated with comparing low intensity peaks. As indicated by the GC-PW-plot, the abundance of pristane exceeded the lower threshold of 85% when comparing U to D, whilst the remaining alkanes fell within the acceptable threshold (Figure C.13). The GC-PW-plot of U vs D did not show evidence of biodegradation therefore the observed difference in pristane suggested that oils U and D were different. The variance in pristane also caused variation in the isoprenoid ratios that rely on pristane (pri/phy and C₁₇/pri) (Table C.6 (c)). The differentiation of oils U and D based solely on the variation of a single compound (pristane) was not ideal. Further evidence was required before oils D and U could be confirmed as being different from one another. Oils U and D were therefore carried through for Tier 2 analysis to confirm if these two oils are indeed different or not.

Oil U was also compared to oils E and K. The GC-PW-plot for oils U and E showed that phytane exceeded the lower threshold of 85% which was not explainable by weathering (Figure C.13). While the lower abundance of alkanes C₈–C₁₇ in oil E (as compared to oil U) may have been explained by evaporative weathering, the lower threshold was exceeded substantially from alkane C₂₇ onwards. The ratios pri/phy and C₁₈/phy for oils U and E also exceeded the 14% threshold substantially (Table C.6 (e)). When considering both the variations in phytane and also in alkanes as observed in the GC-PW-plot, it was concluded that oils E and U were different to one another. Very similar observations for GC-PW-plots and isoprenoid ratios were also recorded for the comparison of oils U and K (Figure C.13, Table C.6 (f)). In conclusion, oils U and K were also differentiated from one another.

Oils E and K could not be differentiated from one another on the basis of GC-PW-plots and isoprenoid ratios. All *n*-alkanes/isoprenoids fell within the minimum or maximum thresholds in the GC-PW-plot and all three isoprenoid ratios also fell within the defined threshold. Oils E and K were therefore continued through for Tier 2 comparison.

Oils C and L

The major differences observed between oils C and L were those of pristane and phytane. Pristane and phytane both exceeded the lower threshold considerably in the GC-PW-plot as indicated in Figure C.14 (c). Consequently, significant variations in all three isoprenoid ratios were also observed (Table C.7). The observed differences between C and L did not follow biodegradation trends which could otherwise explain variations between isoprenoids (CEN 2012). It was concluded that oils C and L were not from the same source as each other. Consequently, oils C and L were found to originate from different sources to all other blind study oils. Oils C and L were not further analysed in Tier 2.

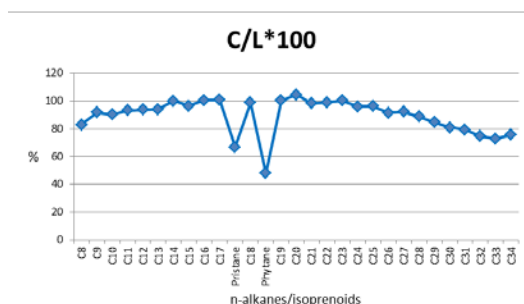


Figure C.14: The GC-PW-plot comparing oils C and L.

Table C.7: Pairwise comparison of isoprenoid ratios between oils C and L.

Ratio	Peak Height Ratio		Mean	Absolute Difference	Relative Difference (%)	Conclusion
	C	L				
Pri/phy	3.79	2.72	3.25	1.06	33	Different
C ₁₈ /phy	19.50	9.49	14.50	10.01	69	Different
C ₁₇ /pri	5.86	3.88	4.87	1.97	41	Different

Oils M, R and O

The GC-PW-plot for oils M and R indicated that the alkanes were within the threshold of 85–118% (Figure C.15). The isoprenoid ratios for oils M and R also fell well below the 14% threshold (Table C.8 (a)). The collective results observed during Tier 1 indicated that oils M and R could not be differentiated from one another. Oils M and R were therefore carried through for Tier 2 comparisons.

Oil O was also compared to oils M and R. The results of these two comparisons were both very similar and were reported as follows. The GC-PW-plots for both O and M, and O and R, showed a gradual decline in the abundance of low-boiling alkanes (C₈–C₁₆) for both M and R in comparison to O (Figure C.15). Whilst the abundance of C₈–C₁₆ exceeded the lower threshold of 85%, it was possible that this was due to evaporative weathering which affects the low-boiling alkanes most rapidly. The isoprenoid ratios however, indicated that the pri/phy ratios of M and O (Table C.8 (b)) and R and O (Table C.8 (c)) were in fact different. These ratio differences were not explainable by evaporative weathering. Considering the difference of pri/phy between O and both M and R, and also the visual differences in alkane chromatograms, it was concluded that oil O was different to oils M and R. Oil O was therefore deemed to originate from a different source to all other blind study oils. Oil O was not analysed further in Tier 2.

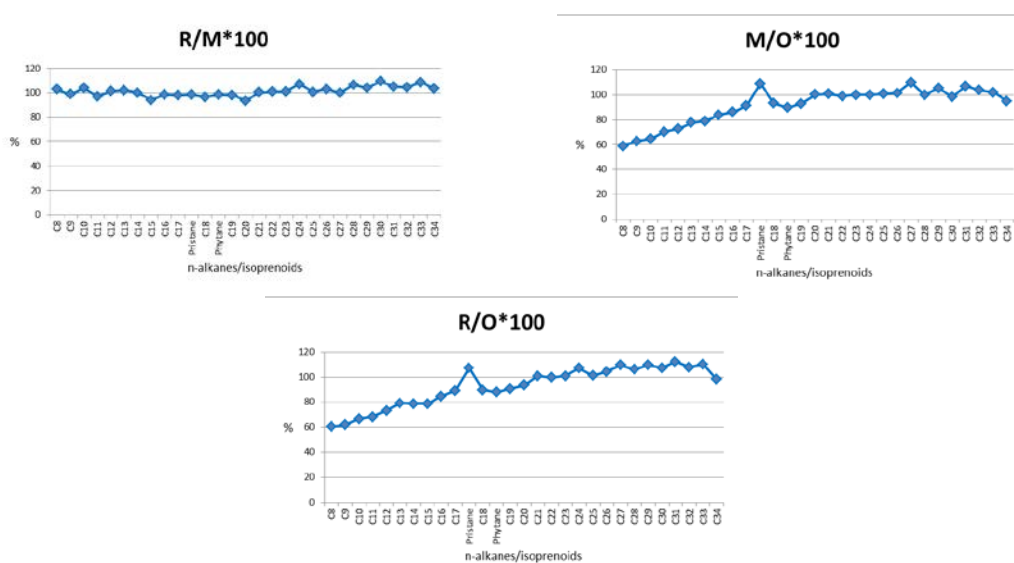


Figure C.15: The pairwise comparison of GC-PW-plot for oils M, R and O.

Table C.8: Pairwise comparison of isoprenoid ratios between oils: (a) M and R; (b) M and O; and (c) R and O.

(a) Ratio	Peak Height Ratio		Mean	Absolute Difference	Relative Difference (%)	Conclusion
	M	R				
Pri/phy	6.19	6.20	6.20	0.00	0	Not Different
C ₁₈ /phy	3.12	3.06	3.09	0.06	2	Not Different
C ₁₇ /pri	0.54	0.54	0.54	0.00	0	Not Different

(b) Ratio	Peak Height Ratio		Mean	Absolute Difference	Relative Difference (%)	Conclusion
	M	O				
Pri/phy	6.19	5.09	5.64	1.10	20	Different
C ₁₈ /phy	3.12	3.00	3.06	0.12	4	Not Different
C ₁₇ /pri	0.54	0.65	0.60	0.11	18	Different

(c) Ratio	Peak Height Ratio		Mean	Absolute Difference	Relative Difference (%)	Conclusion
	R	O				
Pri/phy	6.20	5.09	5.65	1.11	20	Different
C ₁₈ /phy	3.06	3.00	3.03	0.06	2	Not Different
C ₁₇ /pri	0.54	0.65	0.60	0.11	18	Different

Oils A and H

Oil A was compared to oil H using GC-PW-plots and isoprenoid ratios. Low intensity alkanes were observed in A and H profiles from C₂₆–C₃₄. These alkanes were therefore removed from comparison to avoid errors associated with comparing low intensity peaks. The GC-PW-plot for oils A and H indicated that the comparable alkanes were within the threshold of 85–118% (Figure C.16). The isoprenoid ratios for oils A and H also fell below the 14% threshold (Table C.9). The collective results observed during Tier 1 indicated that oils A and H cannot be differentiated from one another. Oils A and H were therefore carried through for Tier 2 comparison.

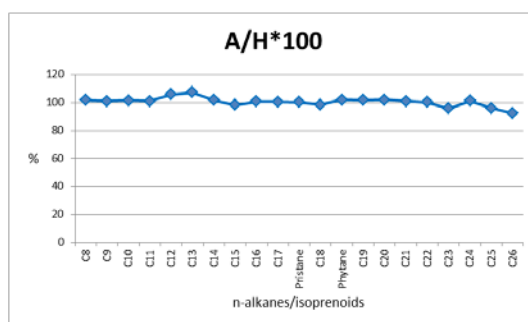


Figure C.16: The GC-PW-plot comparing oils A and H.

Table C.9: Pairwise comparison of isoprenoid ratios between oils A and H.

Ratio	Peak Height Ratio		Mean	Absolute Difference	Relative Difference (%)	Conclusion
	A	H				
Pri/phy	1.43	1.40	1.41	0.02	2	Not Different
C ₁₈ /phy	4.68	4.51	4.60	0.17	4	Not Different
C ₁₇ /pri	3.79	3.79	3.79	0.00	0	Not Different

C.2.3. Tier 1 Conclusions

The overall conclusions for Tier 1 are outlined in Figure C.17. Oils C, L, P, J, N and M were all differentiated from each other based on Tier 1 comparisons. Consequently, the sources of oils C, L, P, J, N and M were different to the sources of other blind study oils. Oils C, L, P, J, N and M were therefore not required for Tier 2 comparisons. The following oils could not be differentiated from one another at the conclusion of Tier 1: (1) S and P; (2) E and K; (3) U and D; (4) M and R; and (5) A and H. Each group of oils were compared internally (to oils within the same group) during Tier 2 to either confirm if oils were from the same source or not.

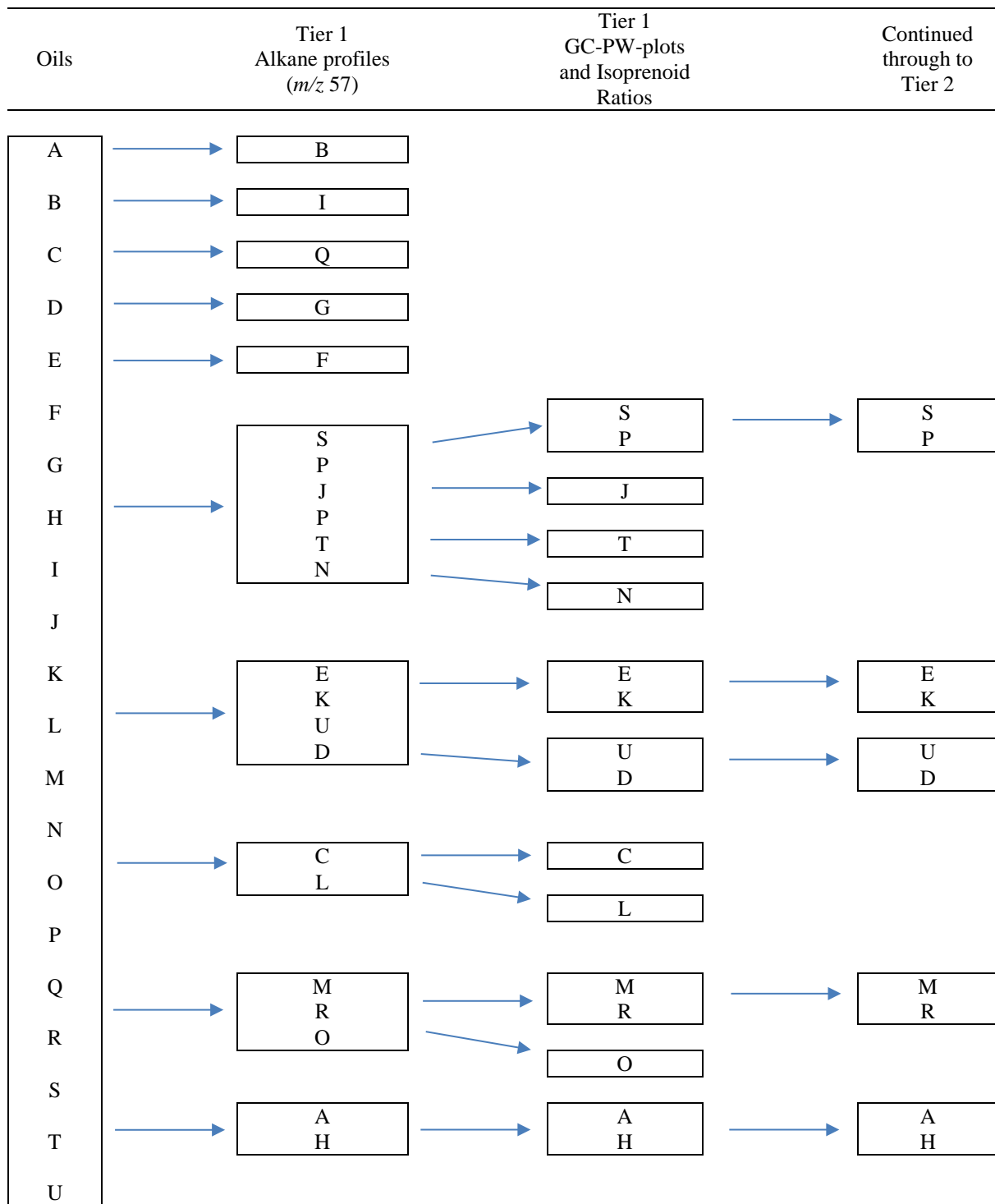


Figure C.17: The separation of oils A-U at the conclusion of Tier 1 of the CEN method blind study.

C.3. Tier 2: GC-MS

C.3.1. Method Uncertainty

M. Eastern aliquots 2, 3 and 4 were analysed and compared to assess the repeatability of Tier 2. Aliquot 1 was not comparable due to an instrument malfunction.

C.3.1.1. Bar Charts and Chromatograms of PAHs and Biomarkers

Tier 2 was also conducted using the CEN method (CEN, 2012). Abbreviations used throughout this appendix are defined by the CEN method. For information regarding these abbreviations, the reader should refer to CEN (2012).

The PAHs and biomarkers of each aliquot were compared pairwise using a bar chart. The bar charts for PAHs and biomarkers allowed for simple visual comparison of normalised peak heights from one aliquot to another aliquot. All peak heights were normalised to the peak height of 30ab hopane as per the CEN method. PAHs and biomarkers were also visually compared by overlaying selected ion chromatograms and comparing aliquots pairwise. The selected ion chromatograms chosen for visual comparison in the blind study were based on the recommended diagnostic PAHs and biomarkers listed by the CEN method (CEN 2012). The specific diagnostic PAHs and biomarkers that were selected for comparison in this blind study are listed in Table C.10.

Table C.10: The diagnostic PAH and biomarker compounds used for visual comparison (selected ion chromatograms) and also used for the calculation of DRs.

PAHs	Selected Ion (<i>m/z</i>)
C ₁ -phe	192
C ₁ -dbt	198
C ₂ -dbt	212
C ₂ -phe	206
C ₁ -fl	216
Retene	219
C ₃ -phe	220
C ₃ -dbt	226
C ₄ -phe	234
C ₃ -chr	270
Biomarkers	Selected Ion (<i>m/z</i>)
Hopanes	191
Steranes	217
Diasteranes	218
Triaromatic steranes	231

The PAHs for aliquots 2, 3 and 4 were all visually consistent when comparing the bar charts (Figure C.18) and the selected ion chromatograms (Figure C. 19). Due to the large number of chromatograms compared between the three aliquots, only a single representative pairwise comparison between aliquots 3 and 4 has been shown in Figure C.19.

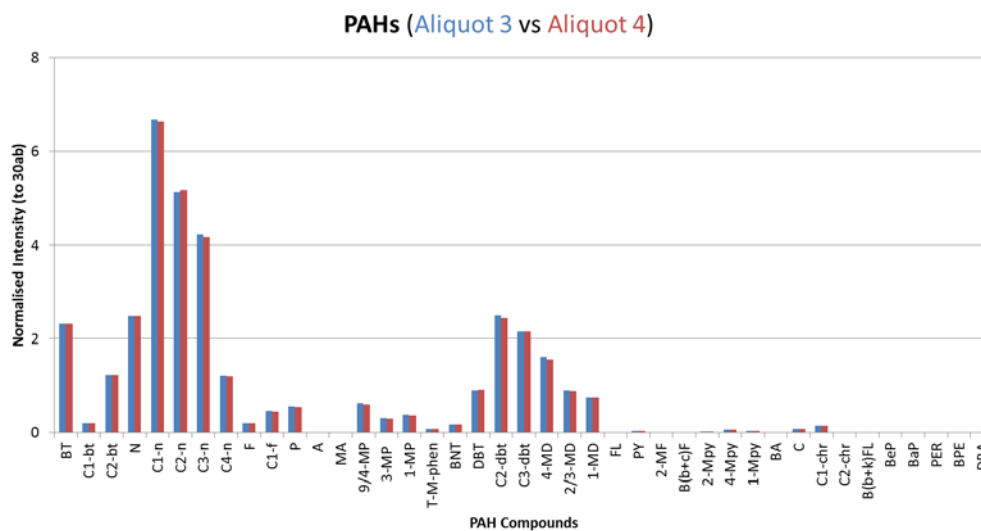
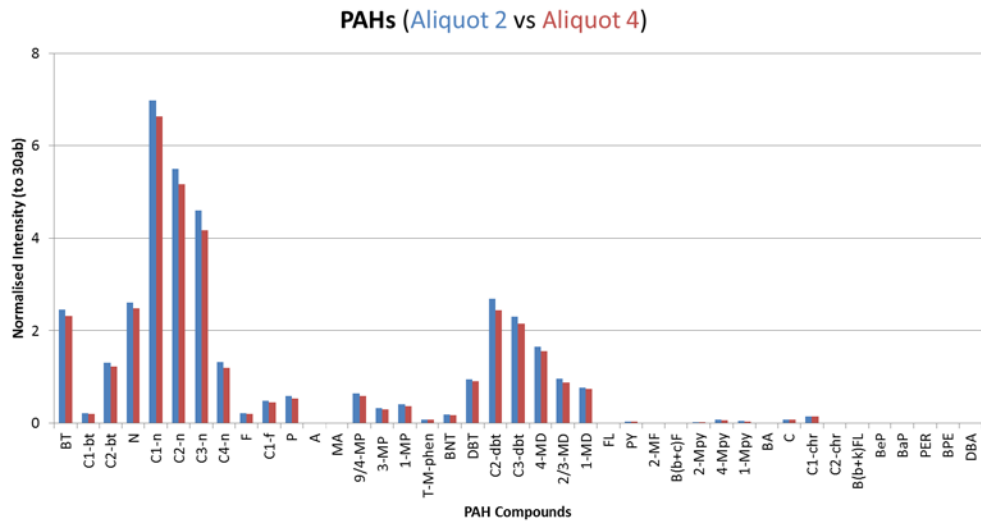
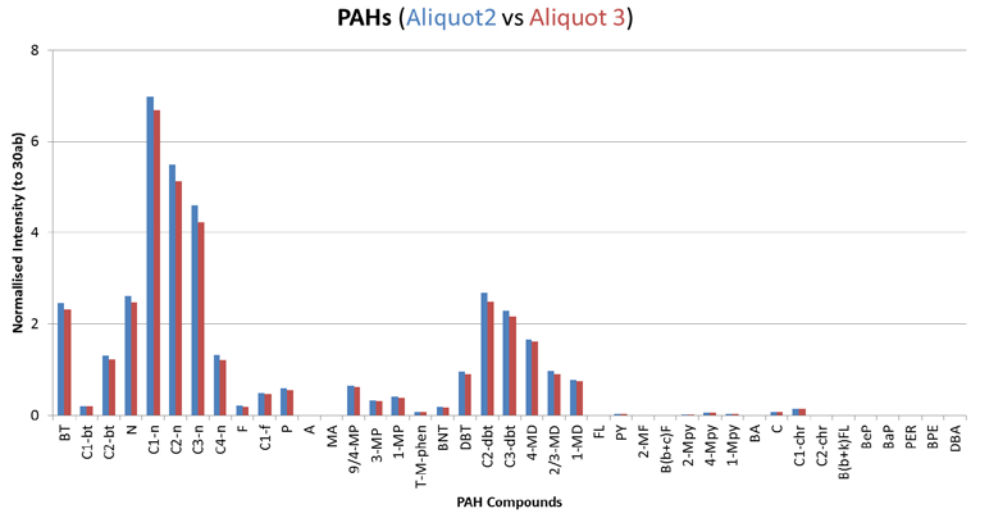


Figure C.18: Bar chart showing the pairwise comparison of normalised PAH intensities for aliquots 2, 3 and 4 from the M. Eastern oil.

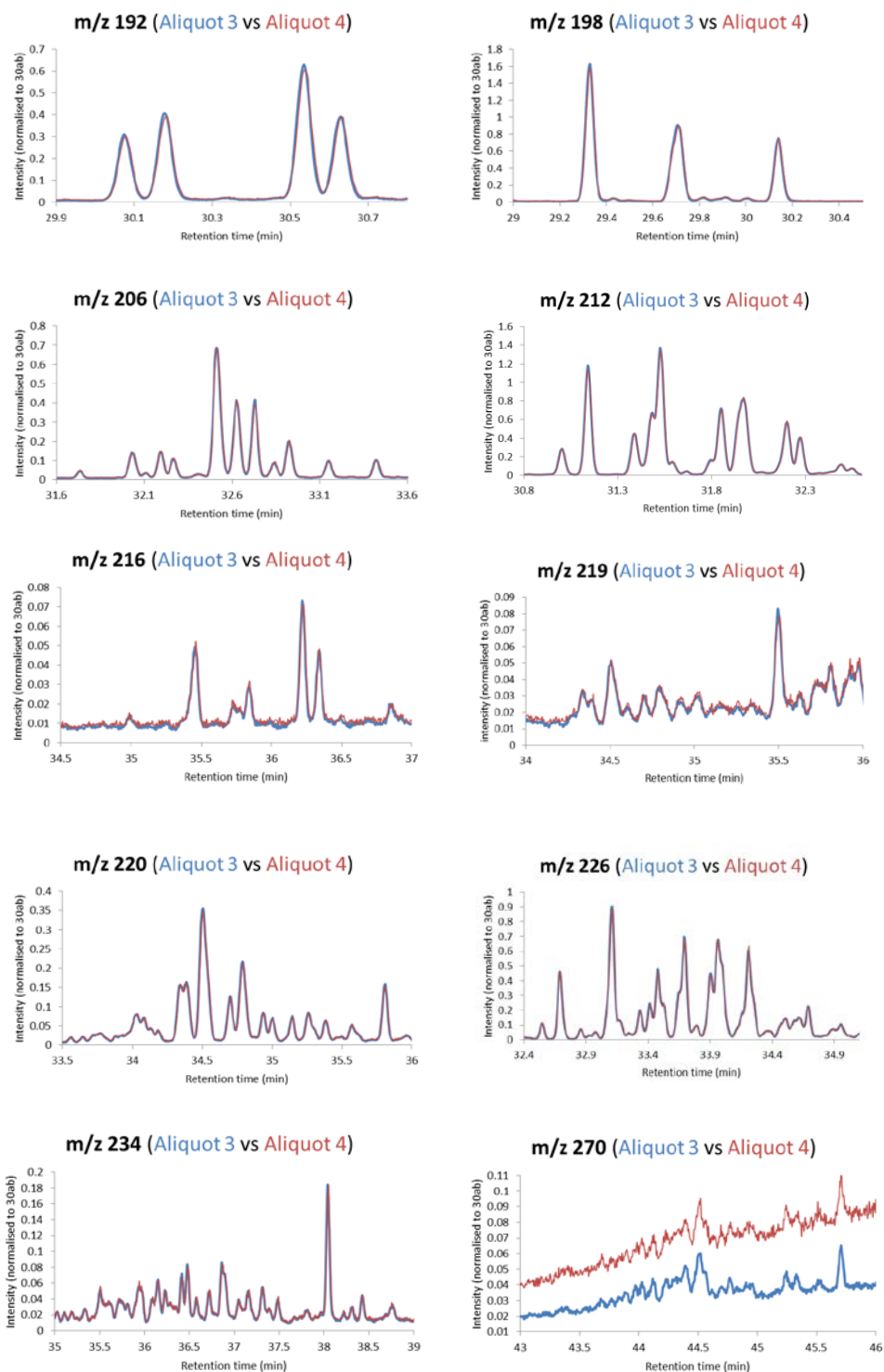


Figure C.19: Representative comparison of diagnostic PAHs between M. Eastern replicates: Aliquot 3 selected ion chromatograms have been overlaid with aliquot 4 chromatograms for pairwise comparison.

The bar charts for the biomarkers (Figure C.20) and the selected ion chromatograms (Figure C.21) were also visually consistent between aliquots 2, 3 and 4. Similarly to the PAHs, only a single representative pairwise comparison has been shown for biomarker chromatograms; aliquot 3 is compared to aliquot 4 (Figure C.21).

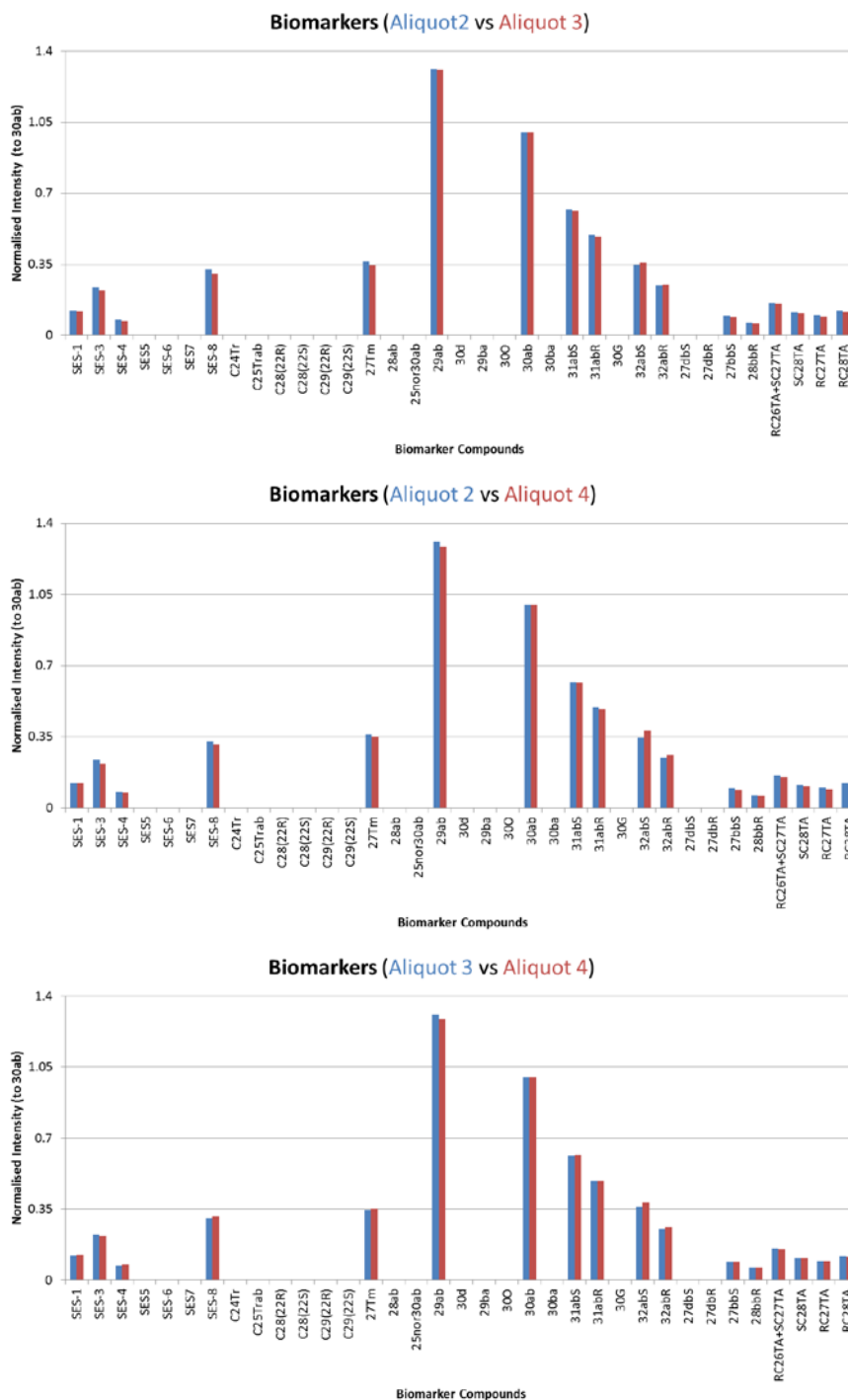


Figure C.20: Bar chart showing the pairwise comparison of normalised biomarker intensities for aliquots 2, 3 and 4 from the M. Eastern oil.

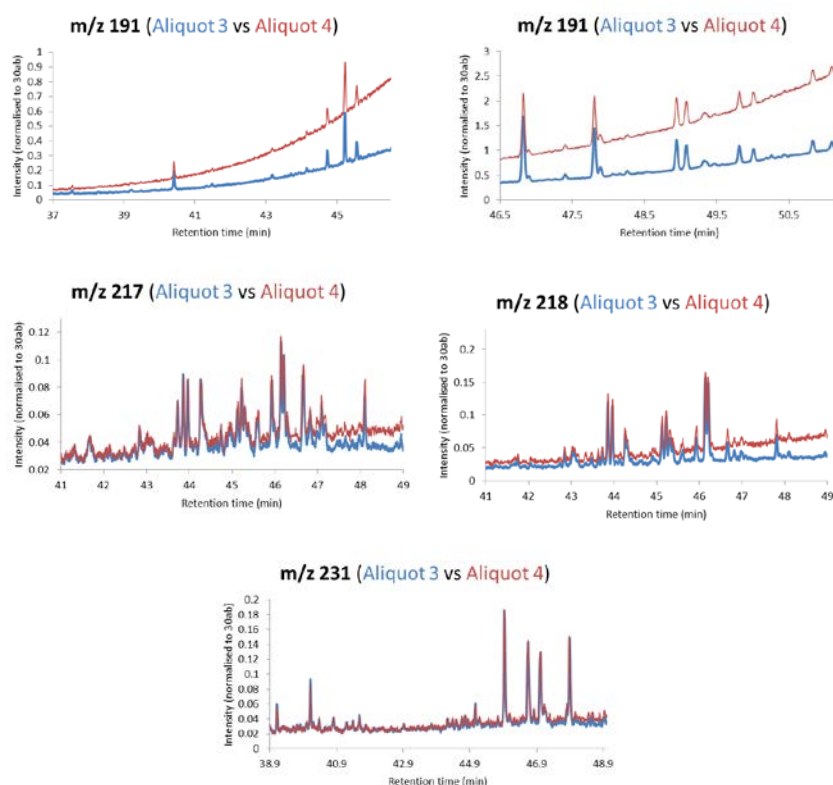


Figure C.21: Selected ion chromatograms for diagnostic biomarkers: chromatograms for aliquots 2, 3 and 4 from the M. Eastern oil have been overlaid pairwise for comparison.

It is important to note that a RT shift was observed in the selected ion chromatograms when comparing aliquot 2 to both aliquots 3 and 4 (results not shown). Aliquot 2 was analysed prior to oils A–U, whilst aliquot 3 and 4 were analysed after oils A–U. The observed RT shift was therefore due to uncontrollable column changes over the course of the analysis sequence. As all peaks were manually integrated during the blind study prior to ratio calculations, the RT shift was not of concern. The main concern when visually comparing selected ion chromatograms was that the relative intensity of peaks and the shape of profiles were consistent.

C.3.1.2. MS-PW-Plot and Diagnostic Ratios

MS-PW-plots were produced for the pairwise comparison of aliquots 2, 3 and 4. MS-PW-plots were calculated by dividing the normalised value of each PAH or biomarker compound (normalised to 30ab) from one aliquot with the normalised value from another aliquot. The values of each compound should fall within the 85–118% threshold as defined in the CEN method (CEN 2012). The MS-PW-plots for all PAH and biomarker compounds fell within the acceptable threshold for each pairwise comparison: aliquot 3/aliquot 2, aliquot 4/aliquot 2, and aliquot 4/aliquot 3. As no differences were observed between all three pairwise comparisons for MS-PW-plots, only a single representative pairwise comparison has been shown between Aliquots 3 and 4 (Figure C.22).

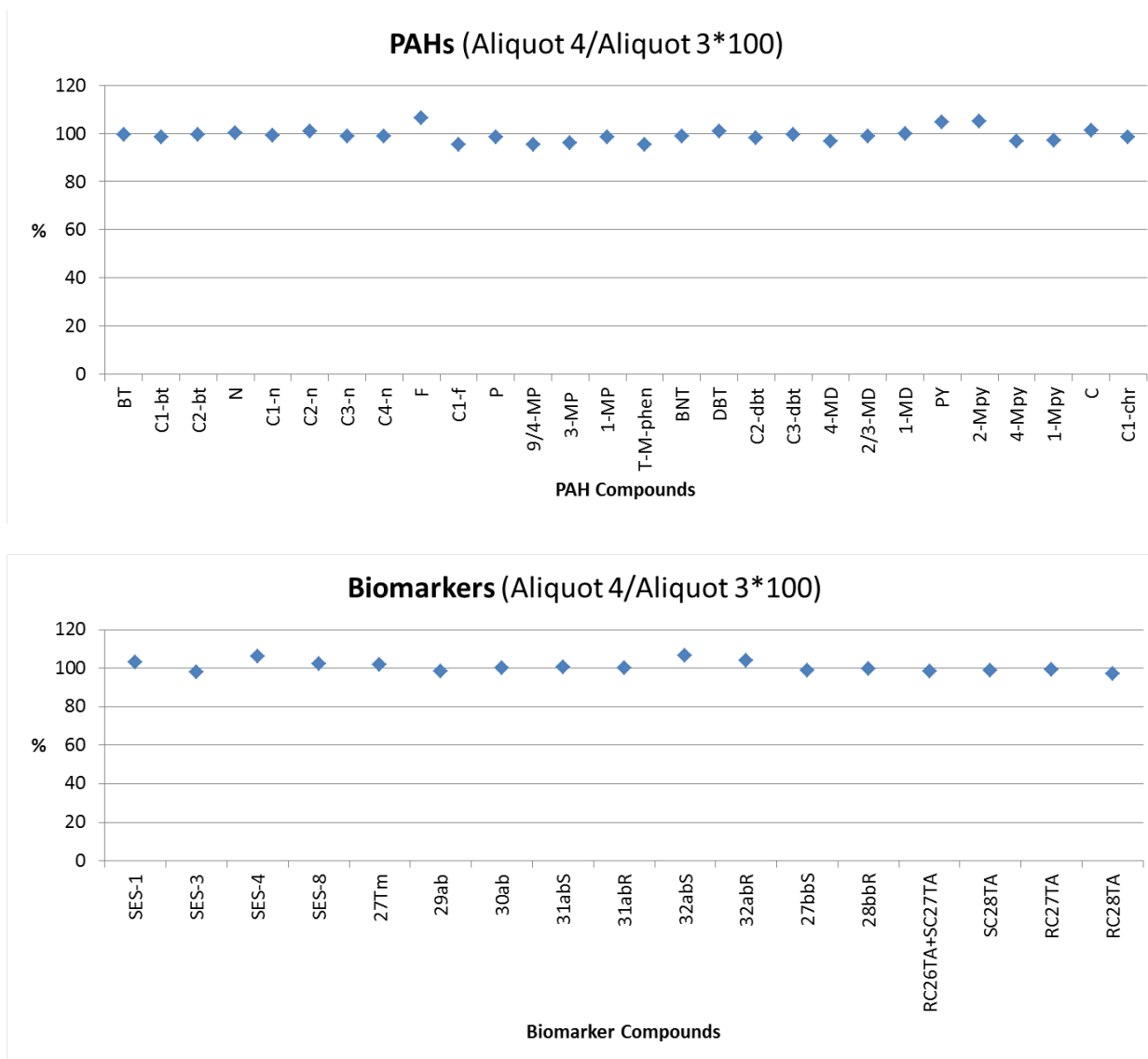


Figure C.22: MS-PW-plots for PAHs and biomarkers for aliquots 3 and 4 from the M. Eastern oil.

DRs were also calculated for suitable PAHs and biomarkers present within the M. Eastern oil aliquots. The suitability of PAHs and biomarkers for DR calculation was gauged by calculating the relative difference of each compound when comparing aliquot 2, aliquot 3 and aliquot 4. Compounds with a relative difference greater than 14% were deemed unsuitable for DR calculation. The majority of compounds that exceeded 14% were found to have peak areas less than 10,000 intensity; therefore, all compounds in oils A–U with a peak area of less than an intensity of 10,000 were compared visually, but were not deemed suitable for DR calculation. The relative differences of suitable DRs were within the acceptable threshold of 14% for all three pairwise comparisons: aliquot 3/aliquot 2; aliquot 4/aliquot 2; and aliquot 4/aliquot 3. As no differences were observed between the three pairwise comparisons, only a single representative pairwise comparison between aliquots 3 and 4 has been shown in Table C.11,

Table C.11: Diagnostic PAH and biomarker ratios for aliquots 2 and 3 from the M. Eastern oil.

PAH Ratio	Peak Height Ratio		Mean	Absolute Difference	Relative Difference (%)	Conclusion
	Aliquot 2	Aliquot 3				
4-MD/1-MD	2.15	2.17	2.16	0.02	1	Not Different
2-Mpy/4-Mpy	0.32	0.32	0.32	0.00	1	Not Different
1-Mpy/4-Mpy	0.61	0.59	0.60	0.01	2	Not Different

Biomarker Ratio	Peak Height Ratio		Mean	Absolute Difference	Relative Difference (%)	Conclusion
	Aliquot 2	Aliquot 3				
SES 1/3	0.51	0.54	0.52	0.03	6	Not Different
SES 2/3	0.30	0.29	0.29	0.01	5	Not Different
SES 4/3	0.33	0.32	0.33	0.01	2	Not Different
SES 8/3	1.38	1.37	1.38	0.00	0	Not Different
27Tm/30ab	0.36	0.35	0.35	0.02	5	Not Different
29ab/30ab	1.31	1.31	1.31	0.00	0	Not Different
31abS/30ab	0.62	0.61	0.62	0.00	1	Not Different
SC28TA/ RC26TA+SC27TA	0.72	0.70	0.71	0.02	3	Not Different
RC28TA/ RC26TA+SC27TA	0.77	0.75	0.76	0.02	2	Not Different
RC27TA/ RC26TA+SC27TA	0.63	0.60	0.62	0.03	5	Not Different
RC27TA/RC28TA	0.83	0.80	0.81	0.03	3	Not Different

C.3.2. Remaining Oils from A–U

Groups of oils that could not be differentiated at the conclusion of Tier 1 were compared during Tier 2. As stated previously, these groups include: (1) M and R; (2) A and H; (3) S and P; (4) E and K; and (5) D and U.

C.3.2.1. Bar Charts and Chromatograms of PAHs and Biomarkers

The bar charts and selected ion chromatograms used for the comparison of PAHs and biomarkers were produced in the same manner as previously described for M. Eastern aliquots.

Oils M and R

The PAHs for oils M and R were visually similar when comparing the selected ion chromatograms (Figure C.23) and the bar chart (Figure C.24).

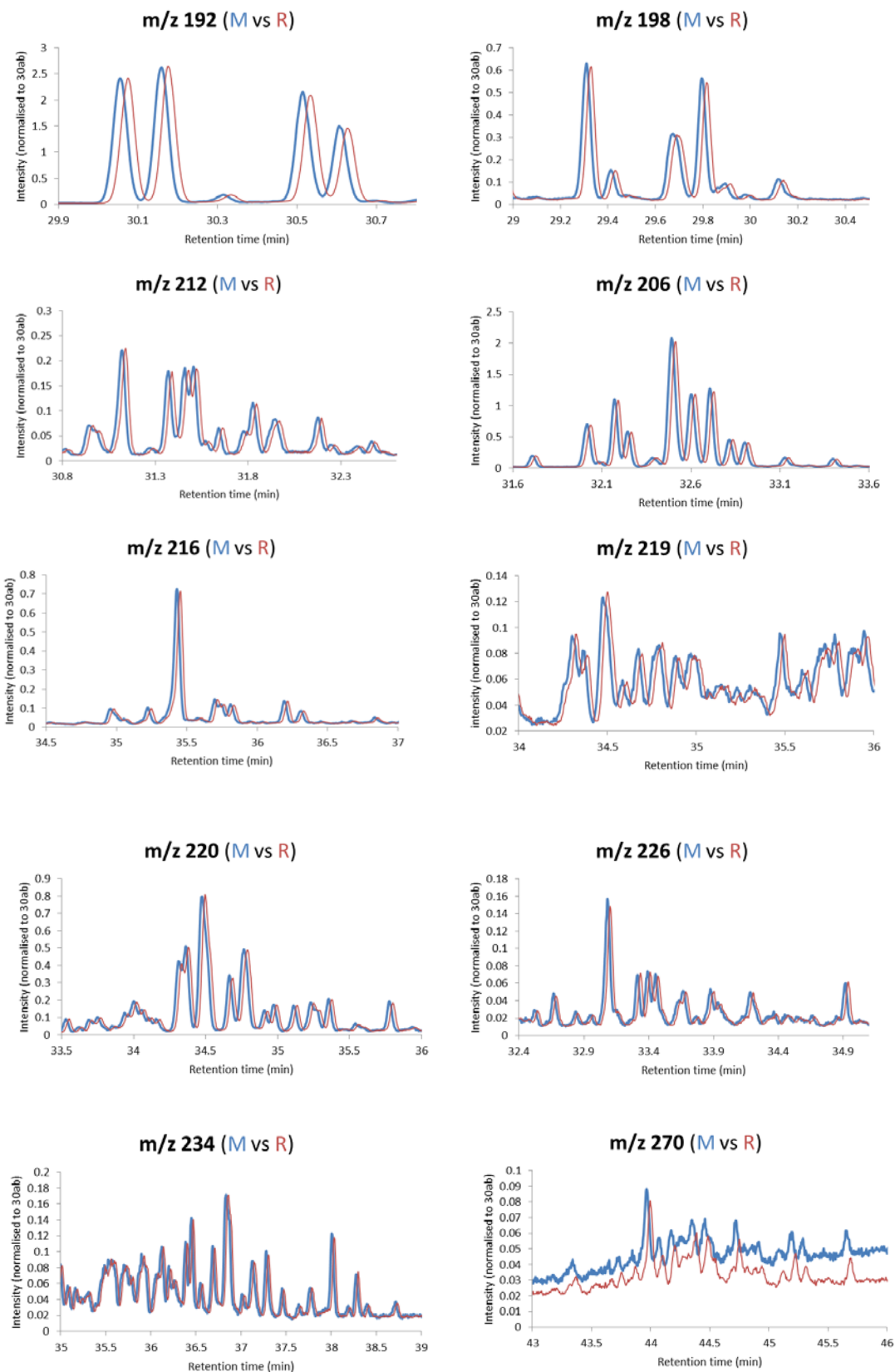


Figure C.23: Selected ion chromatograms for diagnostic PAHs: chromatograms for oils M and R have been overlaid for comparison.

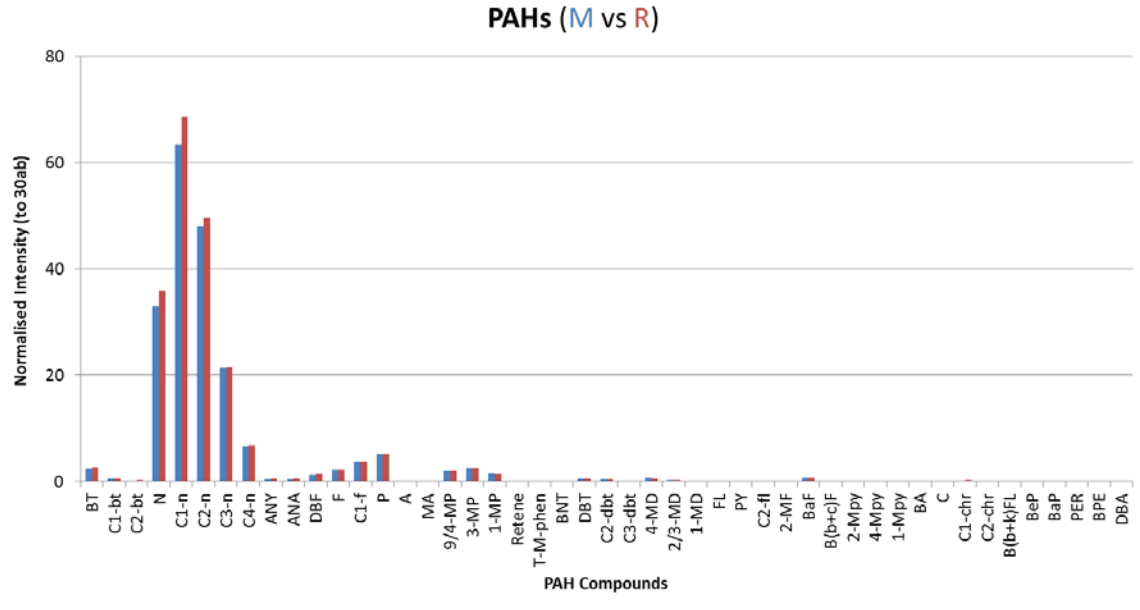


Figure C.24: Bar chart showing the pairwise comparison of normalised PAH intensities for oils M and R.

The bar chart for the biomarkers (Figure C.25) and selected ion chromatograms (Figure C.26) were also visually similar. Some presence/absence differences were observed when comparing biomarkers in Figure C.25 (i.e., presence of 30G hopane in R and absence of 30G in M) however these differences were not deemed significant due to the very small intensities of peaks that differed. Oils M and R could not be differentiated based on visual comparison of PAHs and biomarkers. MS-PW-plots and DRs were therefore compared between oils M and R.

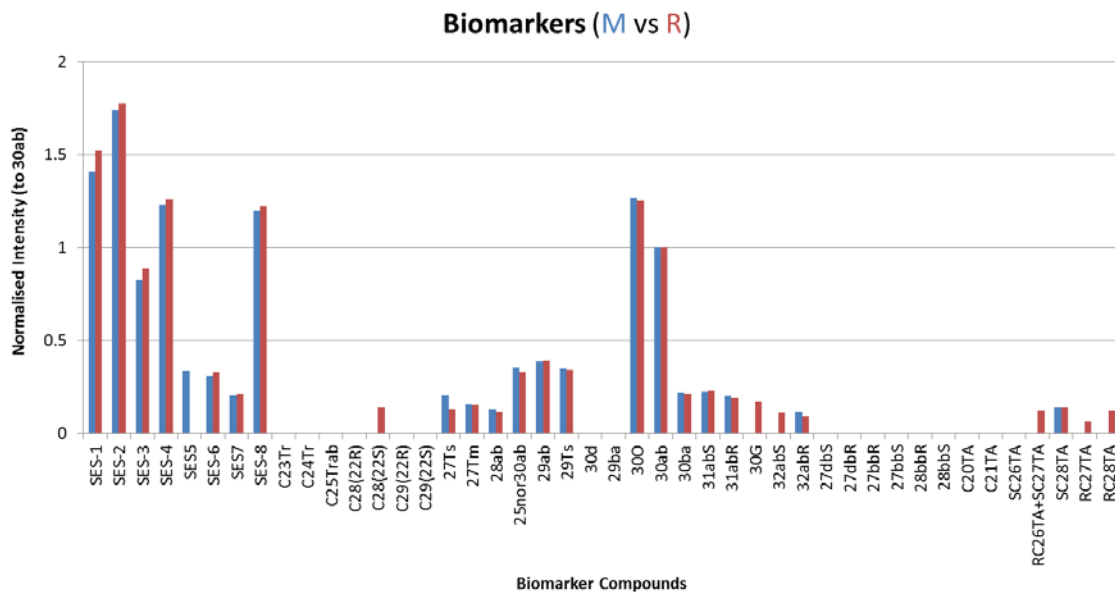


Figure C.25: Bar chart showing the pairwise comparison of normalised biomarker intensities for oils M and R.

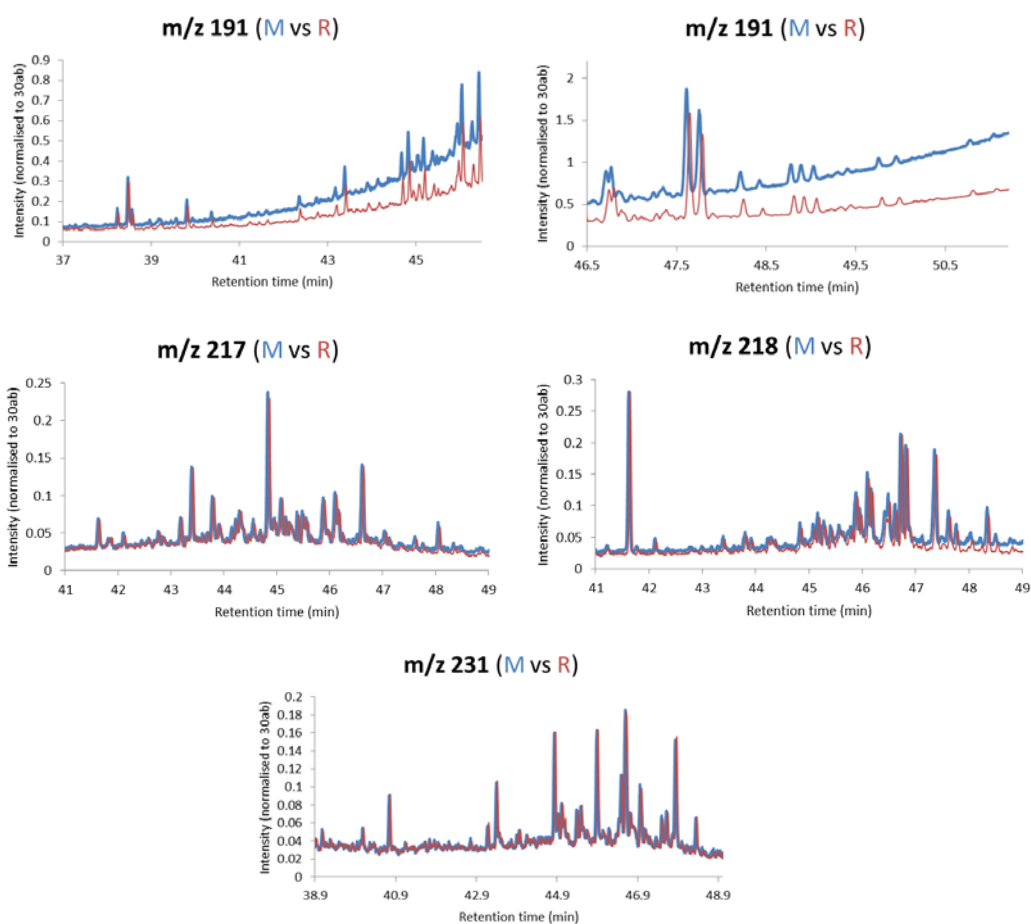


Figure C.26: Selected ion chromatograms for diagnostic biomarkers: chromatograms for oils M and R have been overlaid for comparison.

Oils A and H

The PAHs for oils A and H were visually similar when comparing the selected ion chromatograms (Figure C.27) and the bar chart (Figure C.28). The biomarker bar chart for oils A and H did show obvious presence/absence differences, however all of the biomarker peaks observed in both A and H were very small peaks (Figure C.29). As a consequence, the presence/absence of these small biomarker peaks could not be relied upon for the differentiation of oils A and H. The selected ion chromatograms for oils A and H (Figure C.30) were also visually similar to one another. Oils A and H could not be differentiated based on visual comparison of PAHs and biomarkers; hence oils A and U were carried through for comparison using MS-PW-plots and DRs.

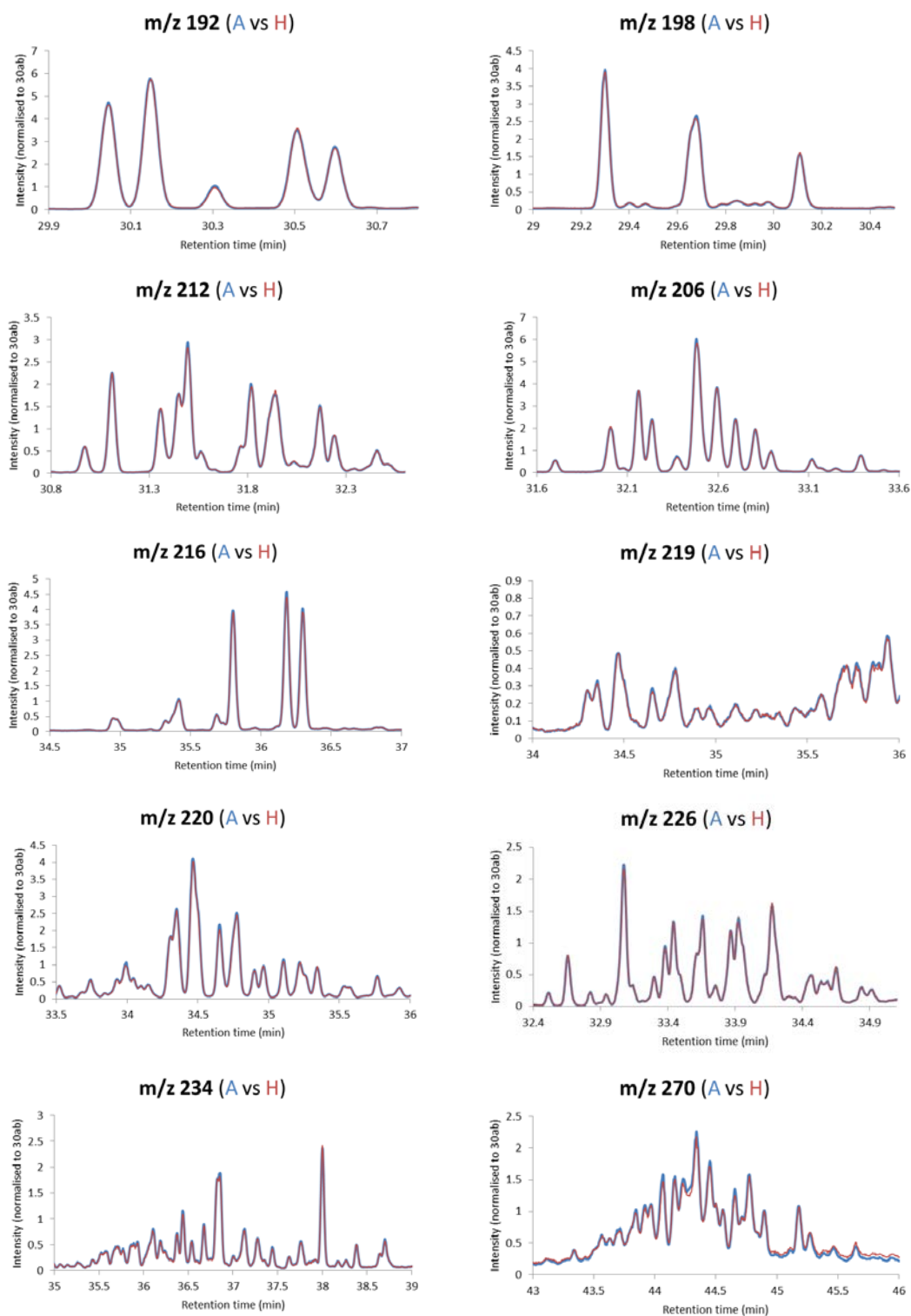


Figure C.27: Selected ion chromatograms for diagnostic PAHs: chromatograms for oils A and H have been overlaid for comparison.

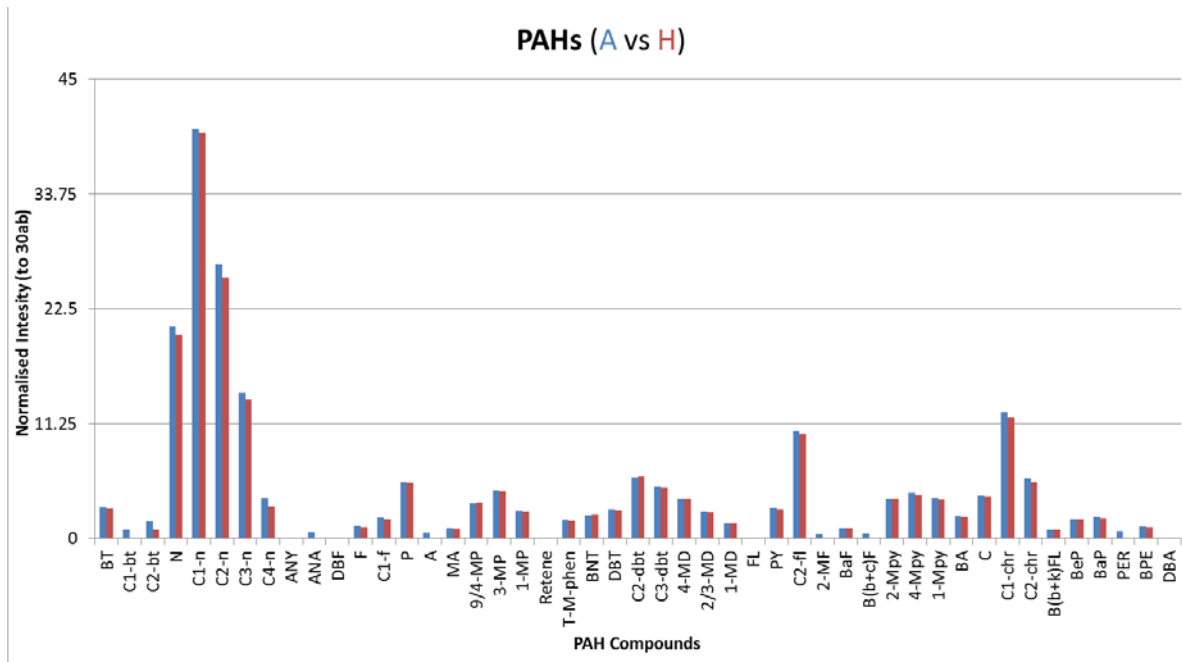


Figure C.28: Bar chart showing the pairwise comparison of normalised PAH intensities for oils A and H.

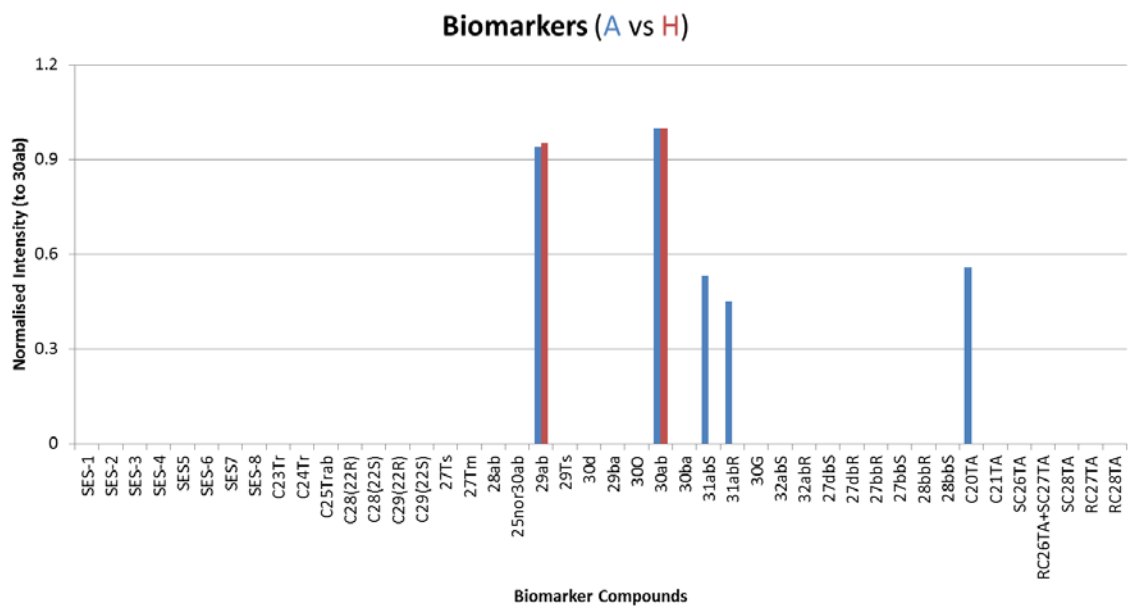


Figure C.29: Bar chart showing the pairwise comparison of normalised biomarker intensities for oils A and H.

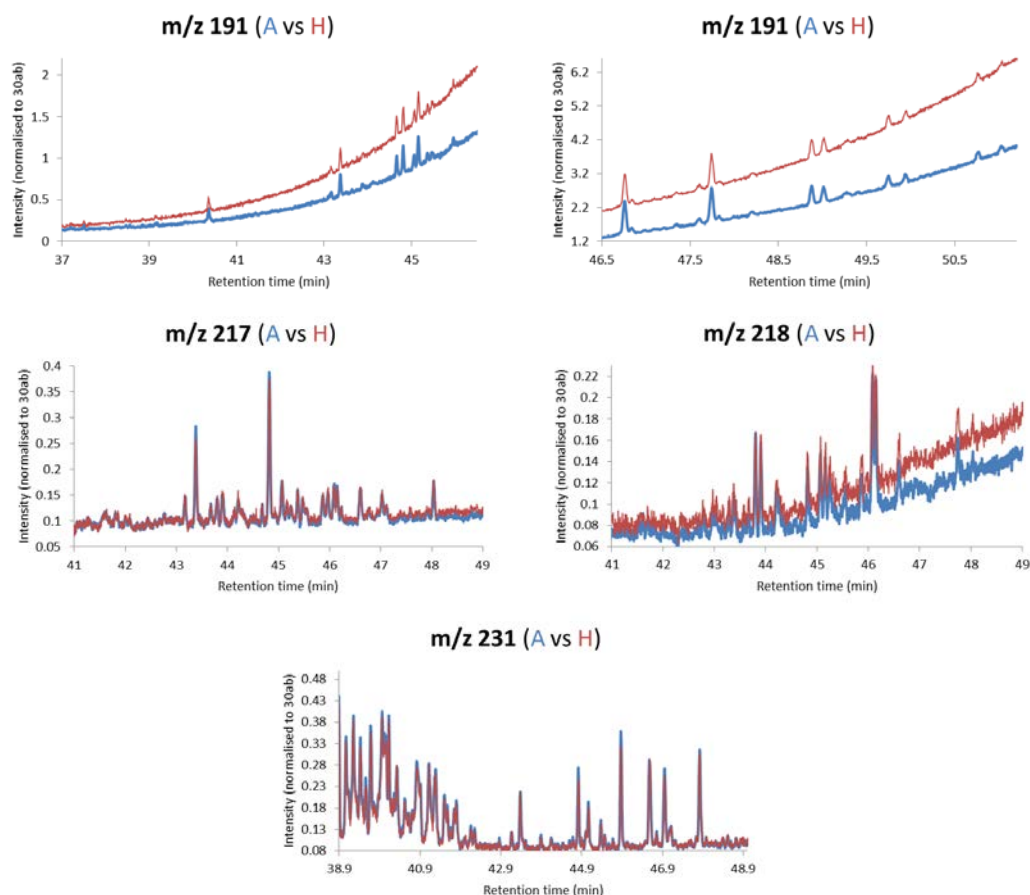


Figure C.30: Selected ion chromatograms for diagnostic biomarkers: chromatograms for oils A and H have been overlaid for comparison.

Oils S and P

The PAH selected ion chromatograms for oils P and S were visually similar (Figure C.31) and so too were the bar chart (Figure C.32). The biomarker bar chart (Figure C.33) and biomarker selected ion chromatograms (Figure C.34) were also visually similar. It is interesting to note that oils S and P exhibited low intensities of biomarkers which were not observed in the other groups in which biomarkers were compared. Oils S and P could not be differentiated based on visual comparison of PAHs and biomarkers; hence MS-PW-plots and DRs were compared between oils S and P.

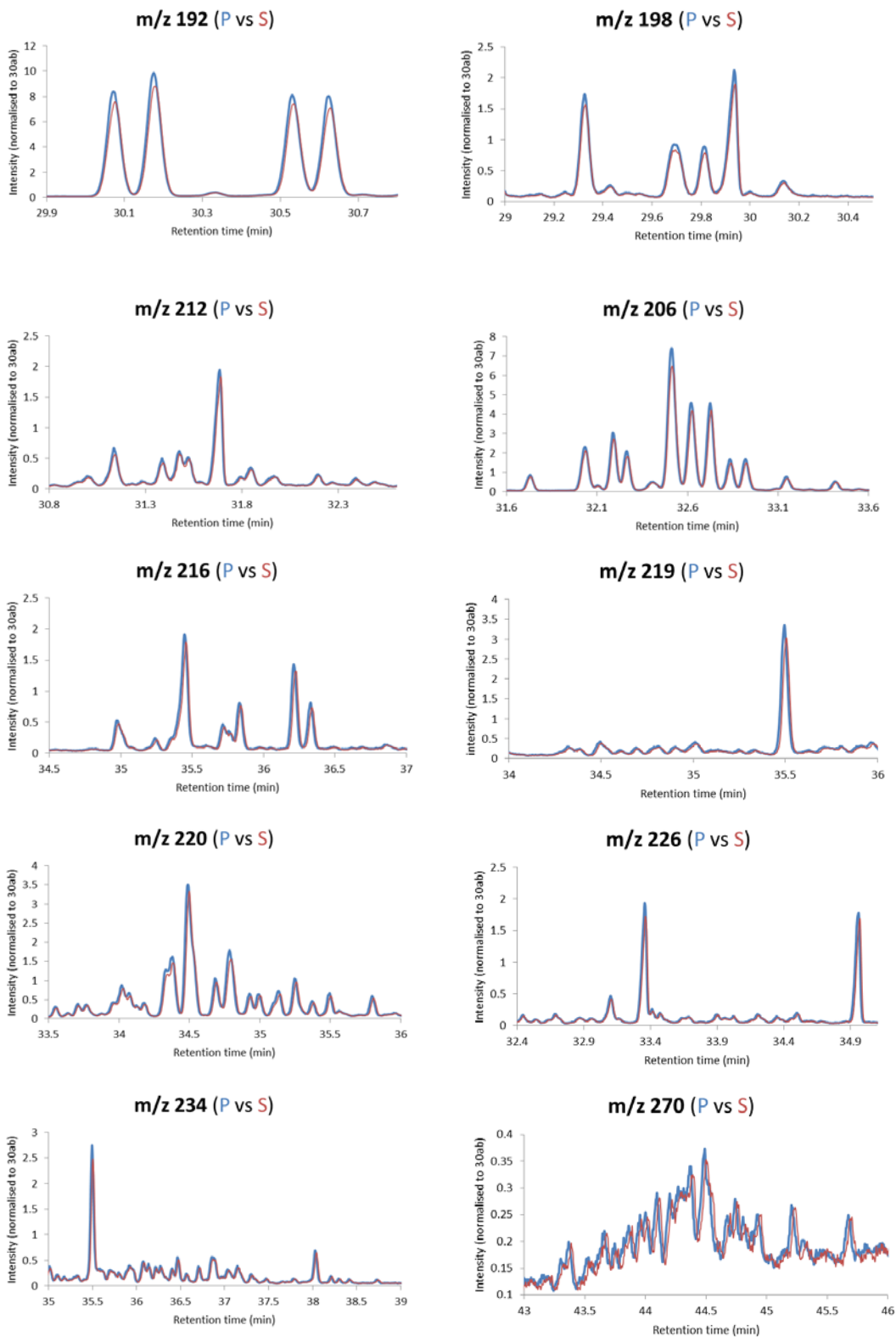


Figure C.31: Selected ion chromatograms for diagnostic PAHs: chromatograms for oils S and P have been overlaid for comparison.

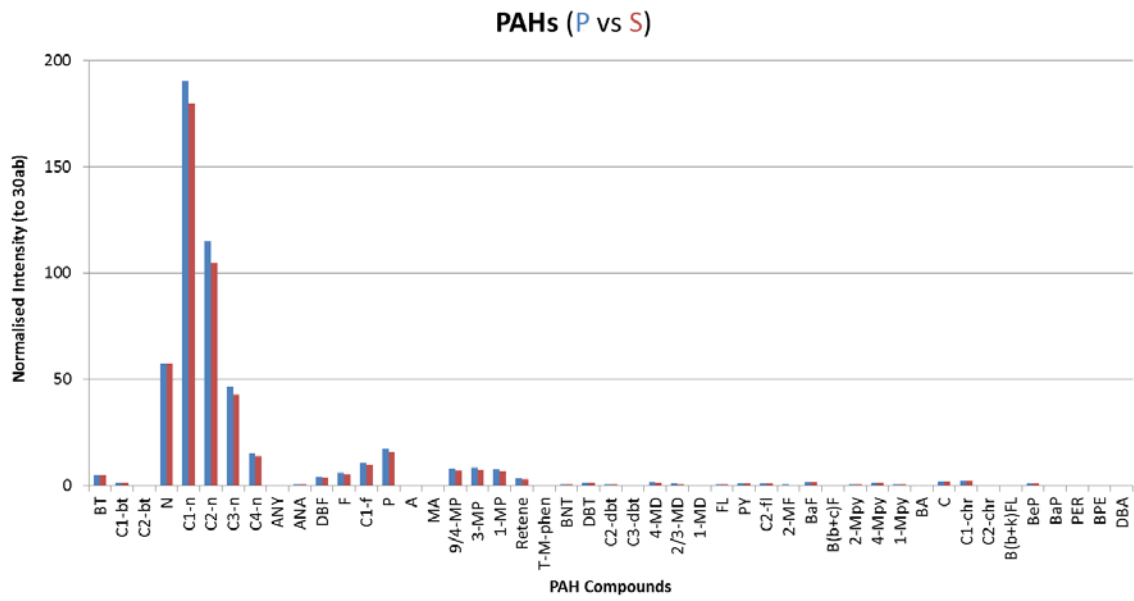


Figure C.32: Bar chart showing the pairwise comparison of normalised PAH intensities for oils S and P.

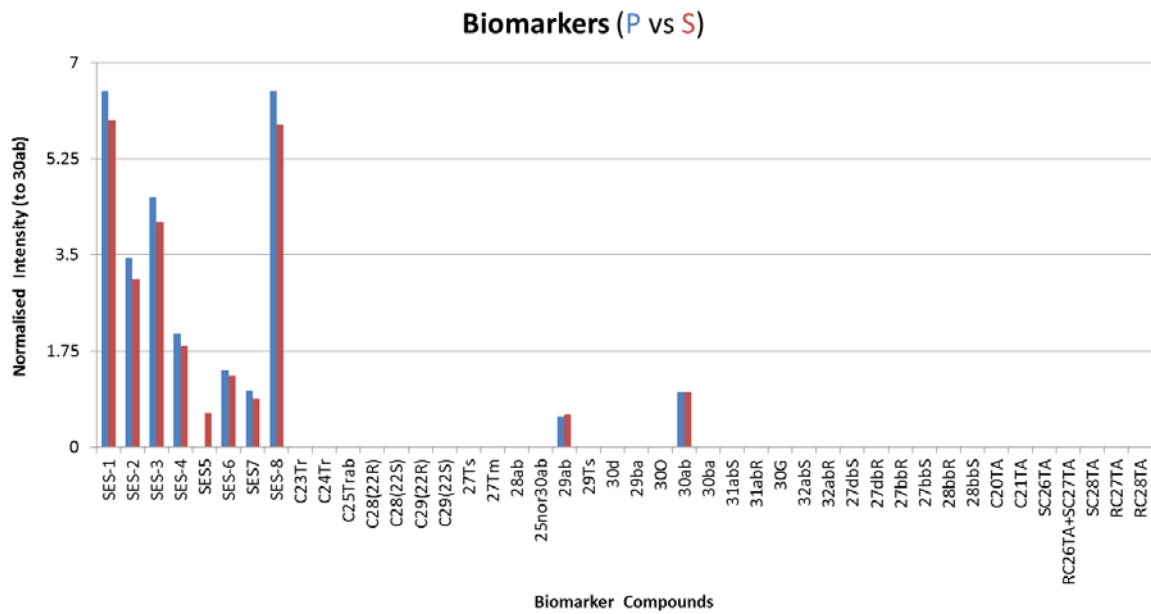


Figure C.33: Bar chart showing the pairwise comparison of normalised biomarker intensities for oils S and P.

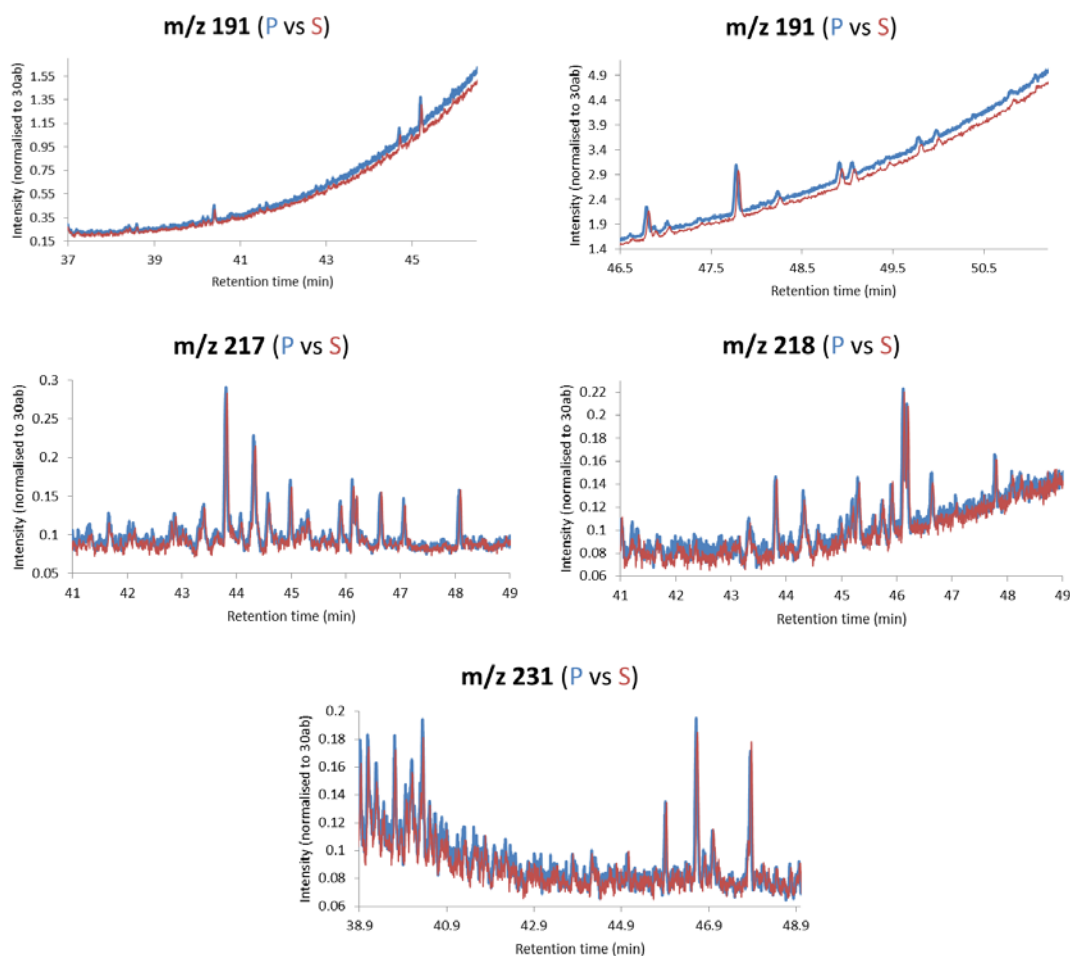


Figure C.34: Selected ion chromatograms for diagnostic biomarkers: chromatograms for oils S and P have been overlaid for comparison.

Oils E and K

The PAHs for oils E and K were visually similar when comparing the selected ion chromatograms (Figure C.35) and the bar chart (Figure C.36). The biomarker bar chart for oils E and K did show presence/absence differences, however all of the biomarker peaks observed in both E and K were very small peaks (Figure C.37). As a result, the presence/absence of these small biomarker peaks could not be relied upon for the differentiation of oils E and K. The selected ion chromatograms of biomarkers (Figure C.38) were also visually similar to one another. Oils E and K therefore could not be differentiated based on visual comparison of PAHs and biomarkers; hence MS-PW-plots and DRs were compared between oils E and K.

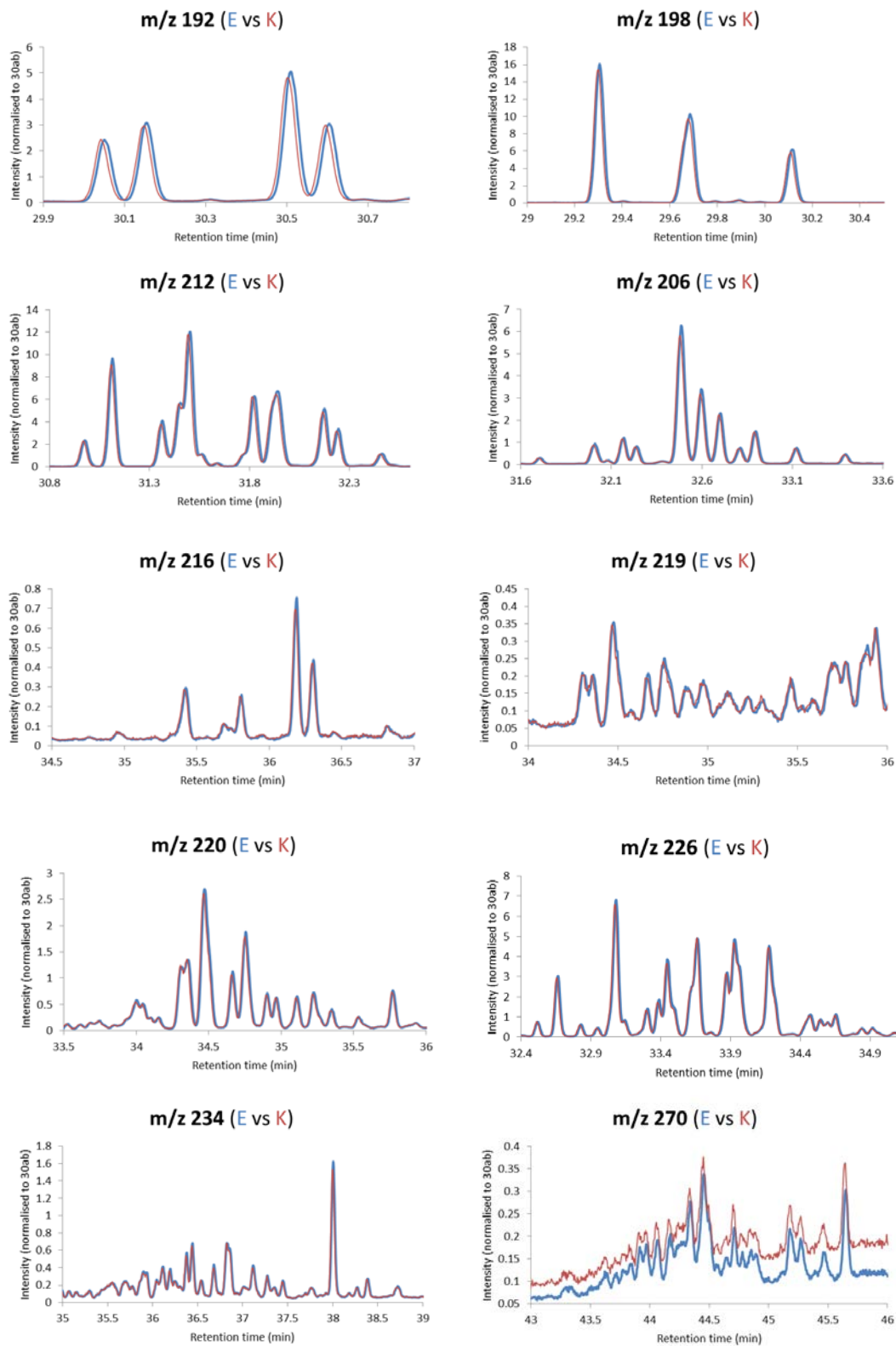


Figure C.35: Selected ion chromatograms for diagnostic PAHs: chromatograms for oils E and K have been overlaid for comparison.

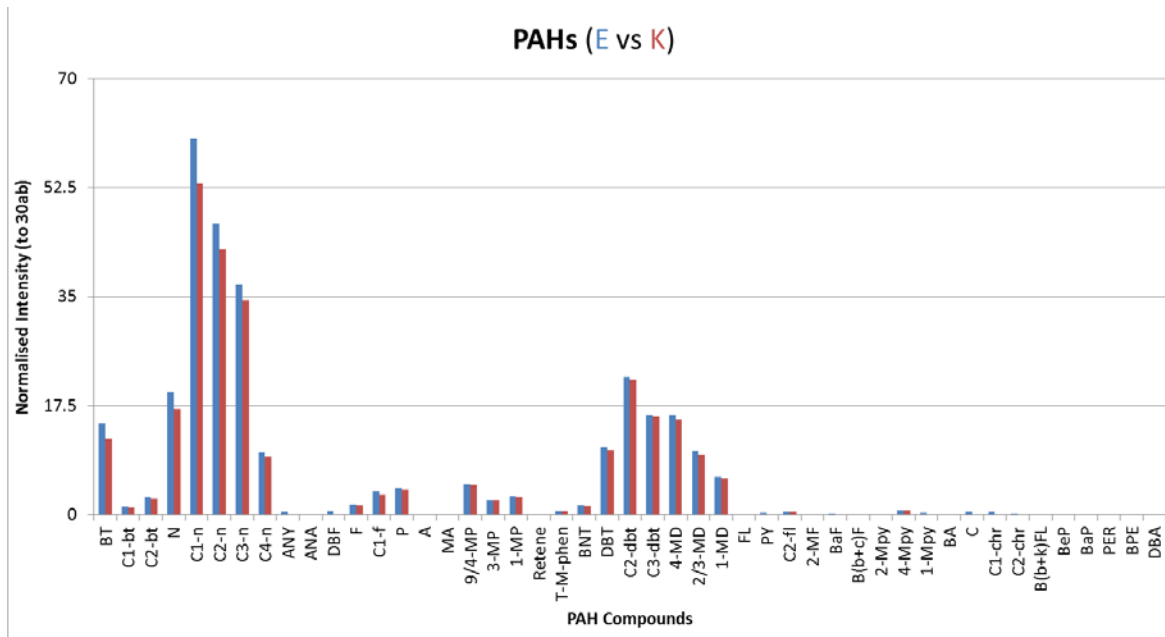


Figure C.36: Bar chart showing the pairwise comparison of normalised PAH intensities for oils E and K.

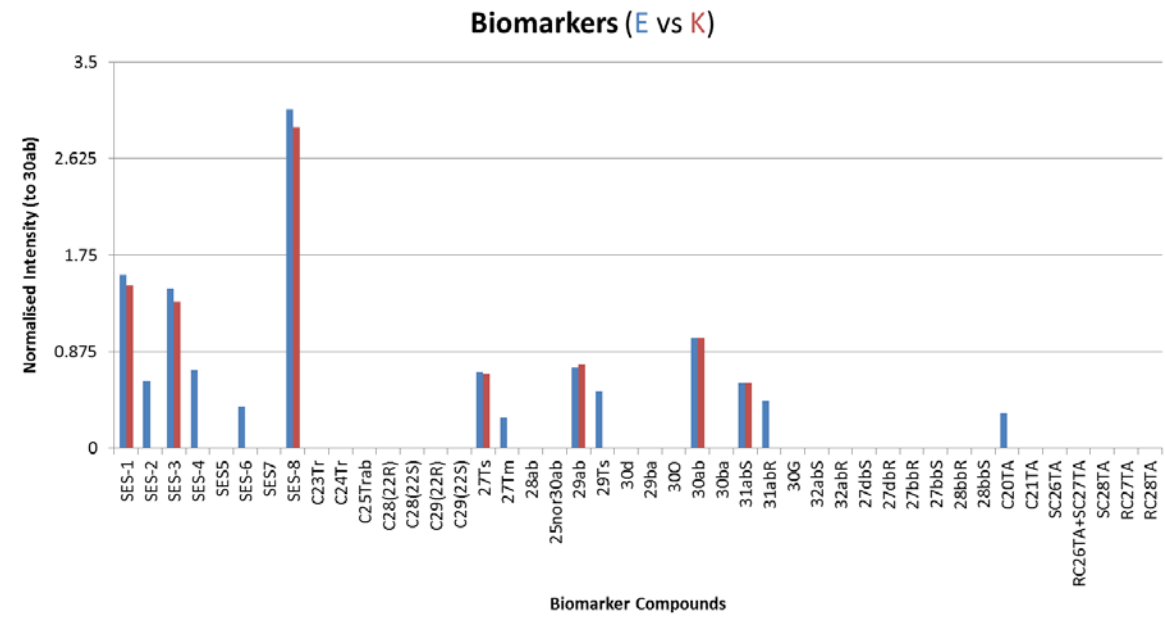


Figure C.37: Bar chart showing the pairwise comparison of normalised biomarker intensities for oils E and K.

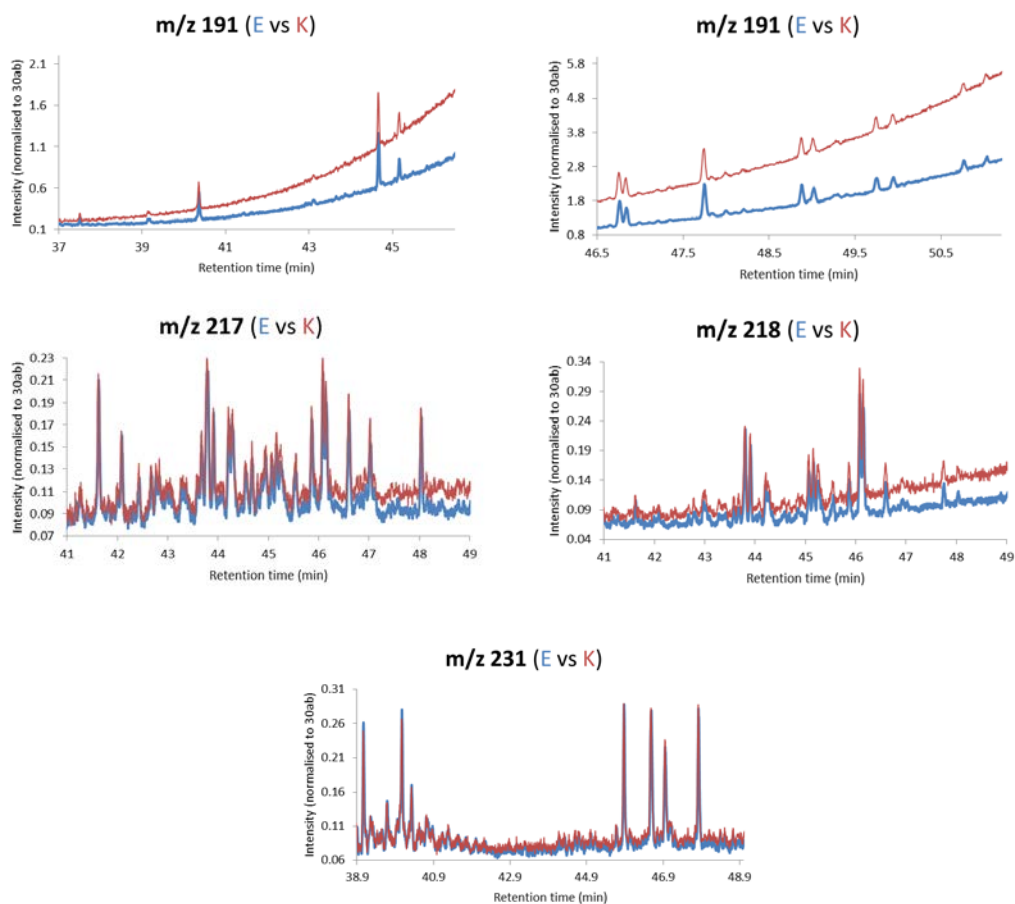


Figure C.38: Selected ion chromatograms for diagnostic biomarkers: chromatograms for oils E and K have been overlaid for comparison.

Oils D and U

Variations in pristane abundances were observed in Tier 1 between oils D and U. Tier 2 was therefore conducted to confirm or disprove these differences. Firstly, the peaks in some selected ion chromatograms for PAHs differed slightly in intensity including m/z 212, 226 and 234 (Figure C.39). Also, notable differences were observed in the normalised intensities of BT and naphthalene when comparing the PAH bar chart of oils D and U (Figure C.40). The biomarker bar chart did show obvious presence/absence differences, however all of the biomarker peaks observed in both D and U that differed were very small peaks (Figure C.41). As a result, the presence/absence of these small biomarker peaks was not deemed significant for exclusion. When comparing the selected ion chromatograms of biomarkers for D and U, no differences were observed (Figure C.42). In conclusion, the notable differences in the intensities of BT and naphthalene between D and U are not explainable by weathering. These Tier 2 differences support the observed pristane variations in Tier 1 providing sufficient evidence to differentiate oils D and U from one another. Oil D and oil U were deemed to originate from different sources to one another, and also from all other blind study oils. Oils D and U were not compared further during Tier 2.

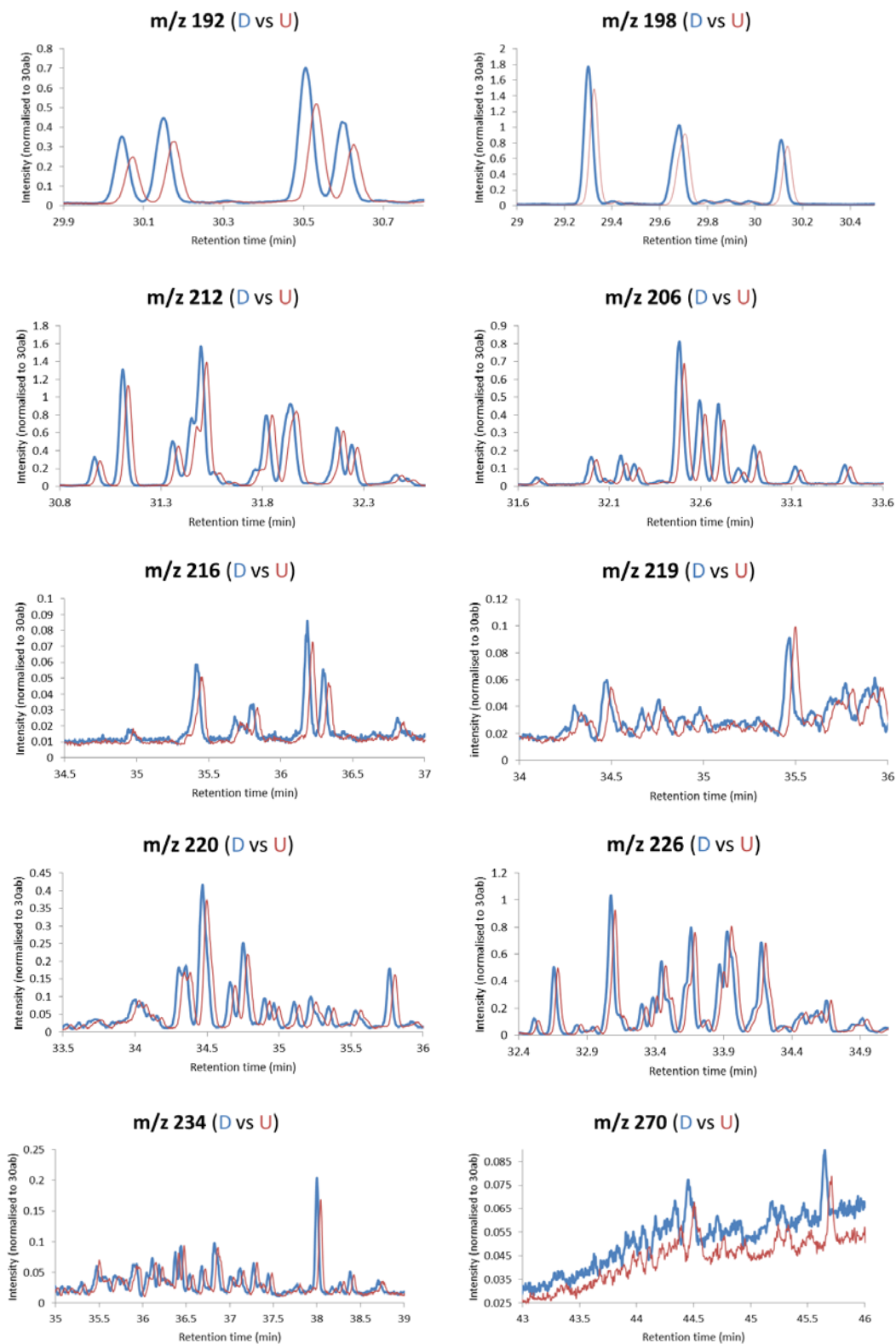


Figure C.39: Selected ion chromatograms for diagnostic PAHs: chromatograms for oils D and U have been overlaid for comparison.

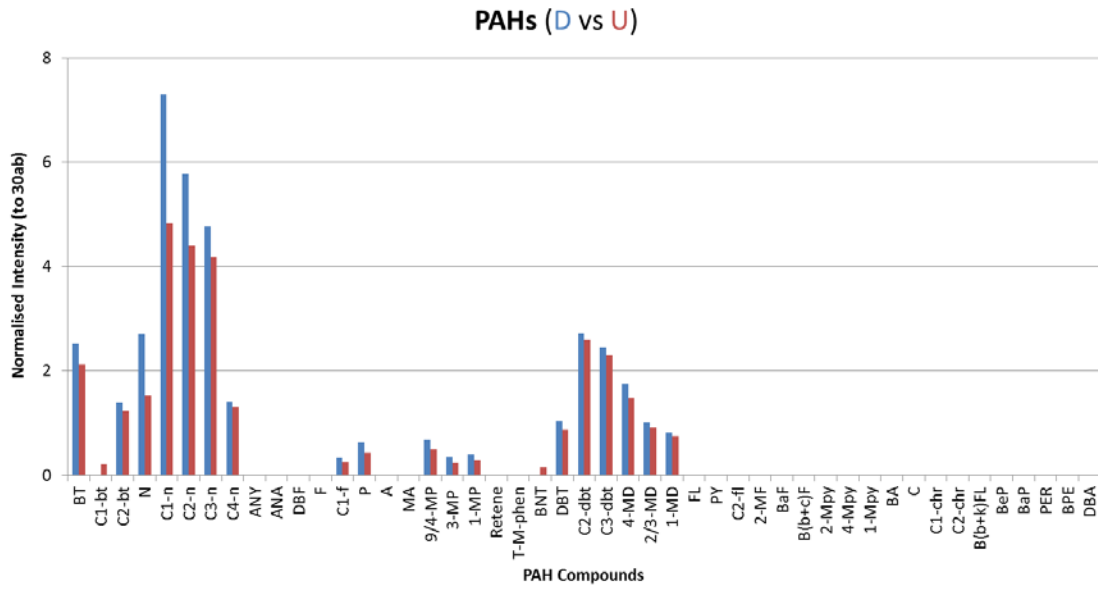


Figure C.40: Bar chart showing the pairwise comparison of normalised PAH intensities for oils D and U.

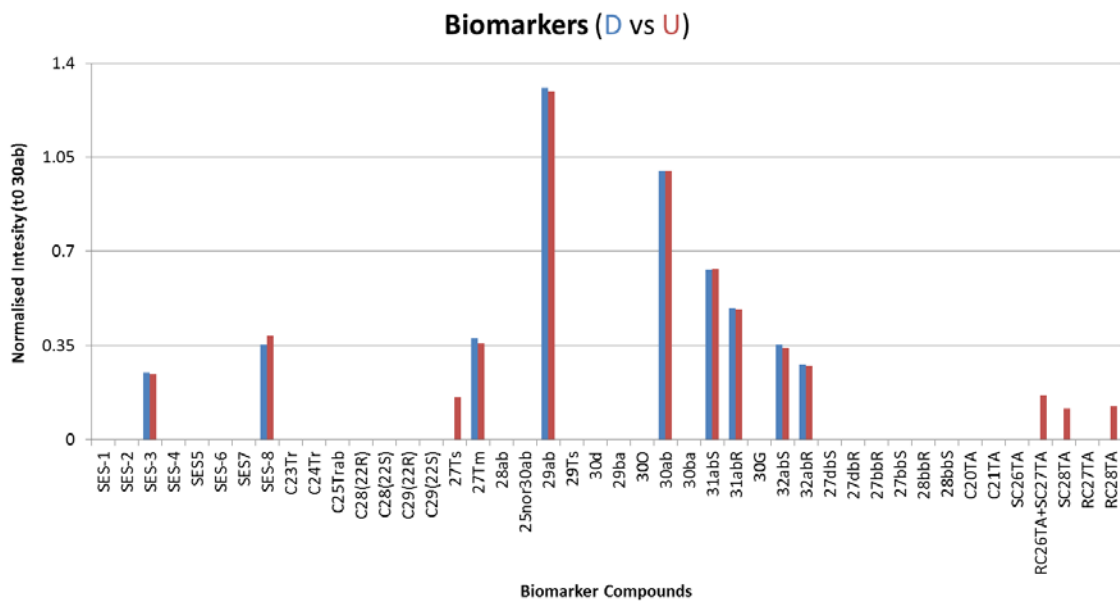


Figure C.41: Bar chart showing the pairwise comparison of normalised biomarker intensities for oils D and U.

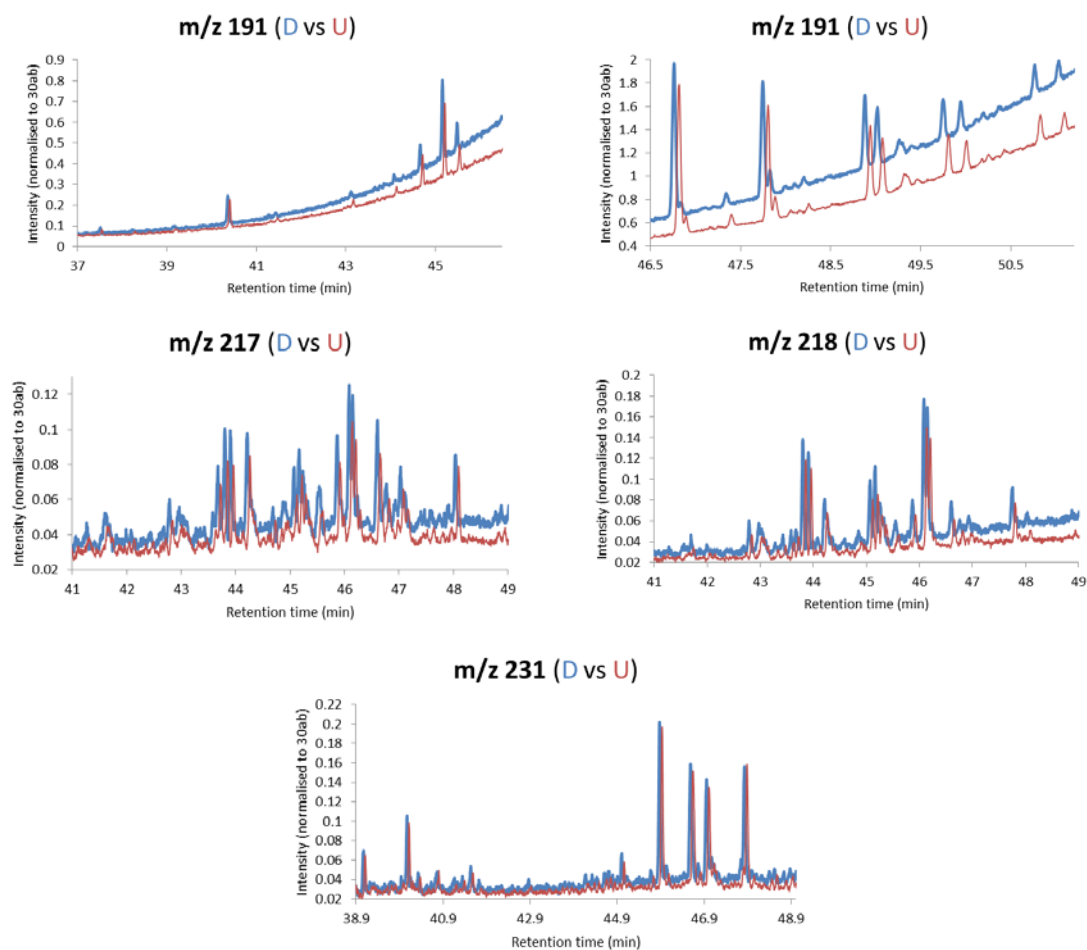


Figure C.42: Selected ion chromatograms for diagnostic biomarkers: chromatograms for oils D and U have been overlaid for comparison.

C.3.2.2. MS-PW-Plot and Diagnostic Ratios

MS-PW-plots and DRs were compared between groups of oils that were not differentiated by Tier 1, or the visual comparison of PAHs and biomarkers in Tier 2. These groups of oils included: S and P; E and K; M and R; and A and H. MS-PW-plots were calculated for comparison as previously outlined for the M. Eastern aliquots. DRs were only calculated for suitable PAHs and biomarkers. Compounds with a peak area of less than 10,000 in intensity were not deemed suitable, and were not used for comparison.

Oils S and P

MS-PW-plots for PAH and biomarker compounds were compared between oils S and P; all of which fell within the acceptable threshold of 85–118% (Figure C.43). The relative differences of PAH and biomarker DRs between oils S and P were also within the acceptable threshold of 14% (Table C.12). In conclusion, oils S and P could not be differentiated from one another, but were different to all other blind study oils.

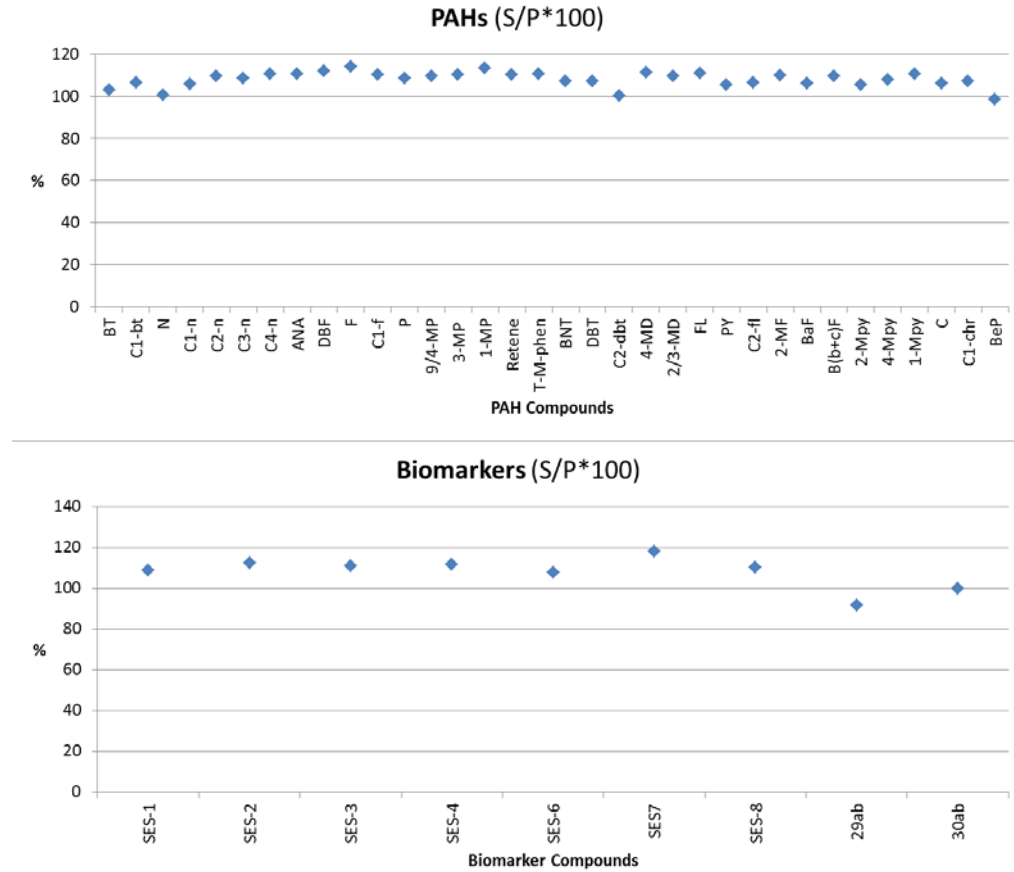


Figure C.43: MS-PW-plots for PAHs and biomarkers for oils S and P.

Table C.12: Diagnostic PAH and biomarker ratios for oils S and P.

PAH Ratio	Peak Height Ratio		Mean	Absolute Difference	Relative Difference (%)	Conclusion
	S	P				
retene/T-M-phe	7.17	7.14	7.16	0.03	0	Not Different
2-MF/4-Mpy	0.35	0.35	0.35	0.01	2	Not Different
BaF/4-Mpy	1.37	1.34	1.35	0.02	2	Not Different
B(b+c)F/4-Mpy	0.29	0.29	0.29	0.00	1	Not Different
2-Mpy/4-Mpy	0.57	0.55	0.56	0.01	2	Not Different
1-Mpy/4-Mpy	0.54	0.55	0.54	0.01	2	Not Different

Biomarker Ratio	Peak Height Ratio		Mean	Absolute Difference	Relative Difference (%)	Conclusion
	S	P				
SES 1/3	1.45	1.42	1.44	0.03	2	Not Different
SES 2/3	0.75	0.76	0.75	0.01	1	Not Different
SES 4/3	0.45	0.45	0.45	0.00	1	Not Different
SES 8/3	1.43	1.42	1.43	0.01	1	Not Different
29ab/30ab	0.60	0.55	0.57	0.05	9	Not Different

Oils E and K

MS-PW-plots for PAH and biomarker compounds were compared between oils E and K; all of which fell within the acceptable threshold of 85–118% except for two PAHs (BT, C₁-f) (Figure C.44). The differences observed between BT and C₁-f were borderline differences, only just in excess of the 118% upper threshold. These differences alone were not significant enough to differentiate oil E from oil K. The relative differences of PAH and biomarker DRs between oils E and K were also within the acceptable threshold of 14% (Table C.13). In conclusion, oils E and K could not be differentiated from one another, but were different to all other blind study oils.

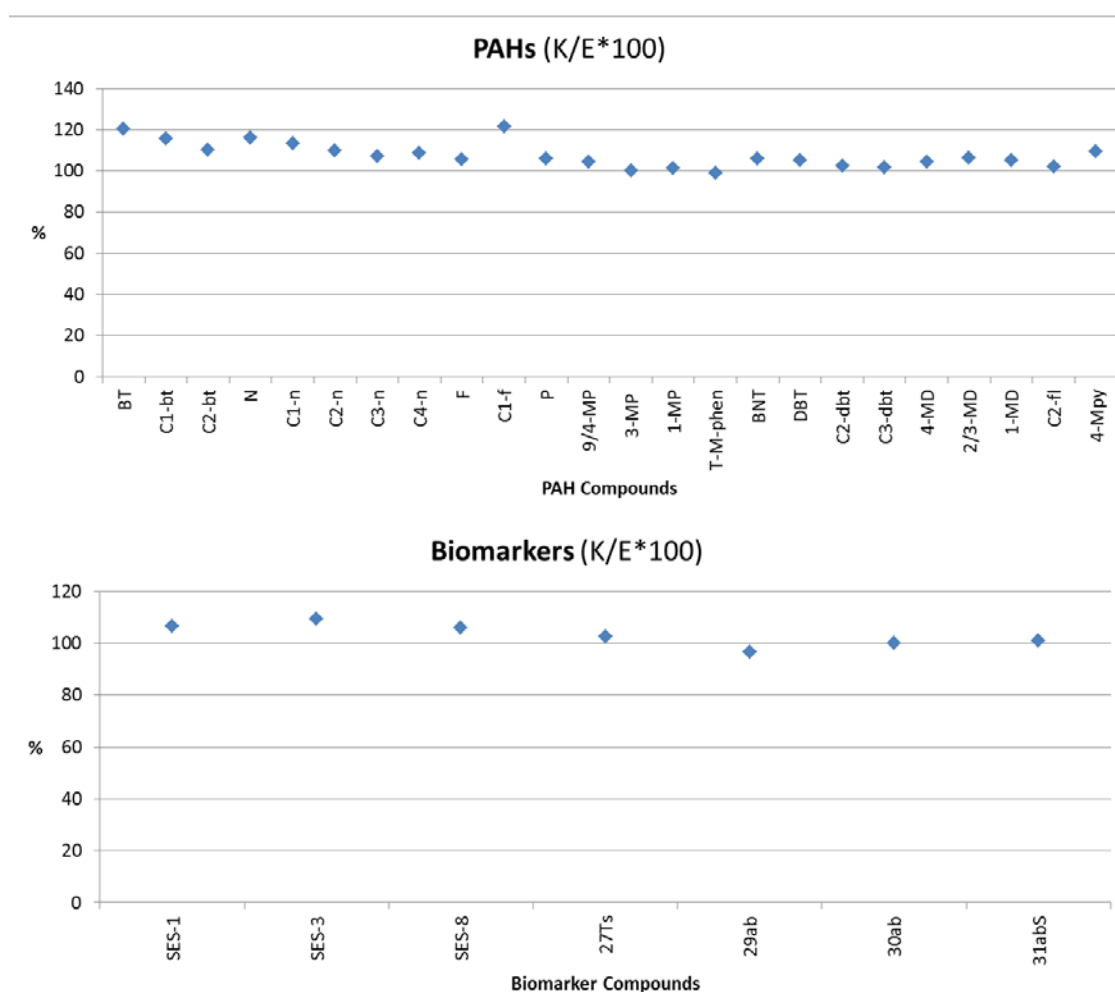


Figure C.44: MS-PW-plots for PAHs and biomarkers for oils E and K.

Table C.13: Diagnostic PAH and biomarker ratios for oils E and K.

PAH Ratio	Peak Height Ratio		Mean	Absolute Difference	Relative Difference (%)	Conclusion
	E	K				
4-MD/1-MD	2.62	2.64	2.63	0.02	1	Not Different

Biomarker Ratio	Peak Height Ratio		Mean	Absolute Difference	Relative Difference (%)	Conclusion
	E	K				
SES 1/3	1.08	1.11	1.10	0.03	2	Not Different
SES 8/3	2.12	2.19	2.15	0.07	3	Not Different
27Ts/30ab	0.69	0.67	0.68	0.02	2	Not Different
29ab/30ab	0.74	0.76	0.75	0.03	3	Not Different
31abS/30ab	0.59	0.59	0.59	0.01	1	Not Different

Oils M and R

Oils M and R were not comparable using DRs for PAHs. Peak areas for either one or both of the diagnostic PAHs required for each ratio calculation for oil M were below an intensity of 10,000 hence calculation of ratios was not possible. The relative differences of biomarker DRs between oils M and R were within the acceptable threshold of 14% (Table C.14). MS-PW-plots for PAH and biomarker compounds were compared between oils M and R, all of which fell within the acceptable threshold of 85–118% except for two PAHs (C₂-bt, C₁-chr) and two biomarkers (27Ts, 32abR) (Figure C.45). The source of these variations is not clearly evident. Given that all other PAHs and biomarkers are very similar, it is unusual that only these four compounds exceeded the threshold. For example, if C₂-bt exceeded the threshold, it would also be reasonable to expect BT and C₁-bt to exceed the threshold; however BT and C₁-bt were both well within the threshold. These differences in MS-PW-plots were therefore not relied upon as sole evidence for the differentiation of oils M and R. In conclusion, there was not enough evidence overall to differentiate M and R oils. M and R oils were however differentiated from all other blind study oils.

Table C.14: Diagnostic biomarker ratios for oils M and R.

Biomarker Ratio	Peak Height Ratio		Mean	Absolute Difference	Relative Difference (%)	Conclusion
	M	R				
SES 1/3	1.70	1.71	1.71	0.01	1	Not Different
SES 2/3	2.10	2.00	2.05	0.11	5	Not Different
SES 4/3	1.49	1.42	1.45	0.07	5	Not Different
SES 8/3	1.45	1.37	1.41	0.08	5	Not Different
27Tm/30ab	0.16	0.15	0.16	0.01	4	Not Different
28ab/30ab	0.13	0.12	0.12	0.01	11	Not Different
25nor30ab/30ab	0.35	0.33	0.34	0.02	7	Not Different
29ab/30ab	0.39	0.39	0.39	0.00	1	Not Different
(27)Ts/(27)Tm	0.35	0.34	0.34	0.01	3	Not Different
29Ts/30ab	0.35	0.34	0.34	0.01	3	Not Different
30O/30ab	1.27	1.25	1.26	0.01	1	Not Different
30ba/30ab	0.22	0.21	0.22	0.01	4	Not Different
31abS/30ab	0.22	0.23	0.23	0.00	1	Not Different

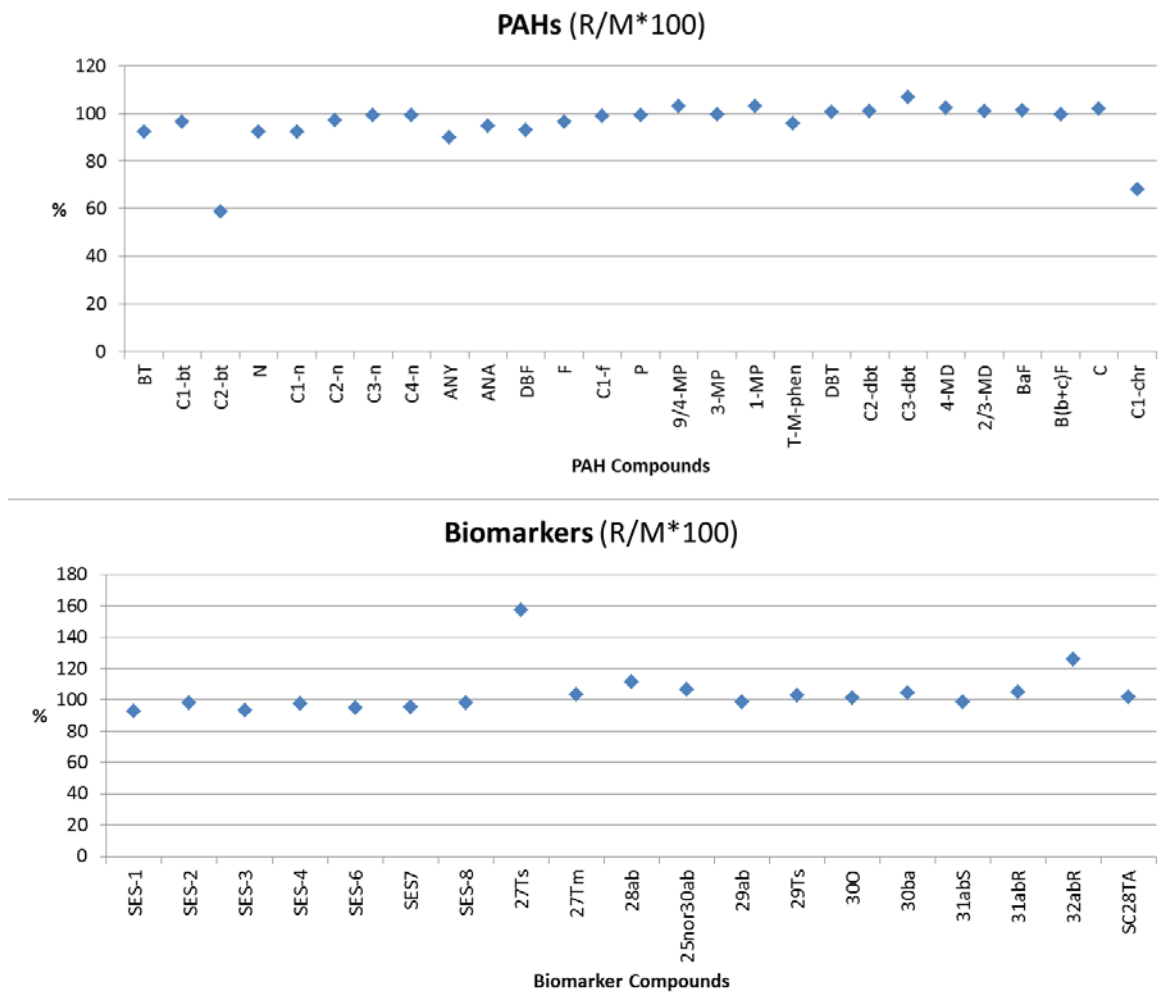


Figure C.45: MS-PW-plots for PAHs and biomarkers for oils M and R.

Oils A and H

A MS-PW-plot for PAH compounds was compared between oils A and H; all PAHs fell within the acceptable threshold of 85–118% except for two PAHs; C₂-bt and C₄-n (Figure C.46). The source of these variations between the two aforementioned PAHs is not clearly evident. Given that all other PAHs are very similar, it is unusual that only C₂-bt and C₄-n exceeded the threshold considerably. As previously stated, if C₂-bt exceeds the threshold it would be reasonable to expect BT and C₁-bt to also exceed the threshold; this however, was not observed. Minimal weighting was therefore placed on these two PAH variations when determining the conclusion between oils A and H. Only one biomarker (hopane 29ab) was comparable between oils A and H using a MS-PW-plot; all remaining biomarkers had peak areas intensities less than 10,000 and were not deemed suitable for comparison. When calculated, 29ab fell within the comparable threshold (result not shown). The relative differences of PAH and biomarker DRs between oils A and H were also within the acceptable threshold of 14% (Table C.15). In conclusion, oils A and H could not be differentiated from one another, but were different to all other blind study oils.

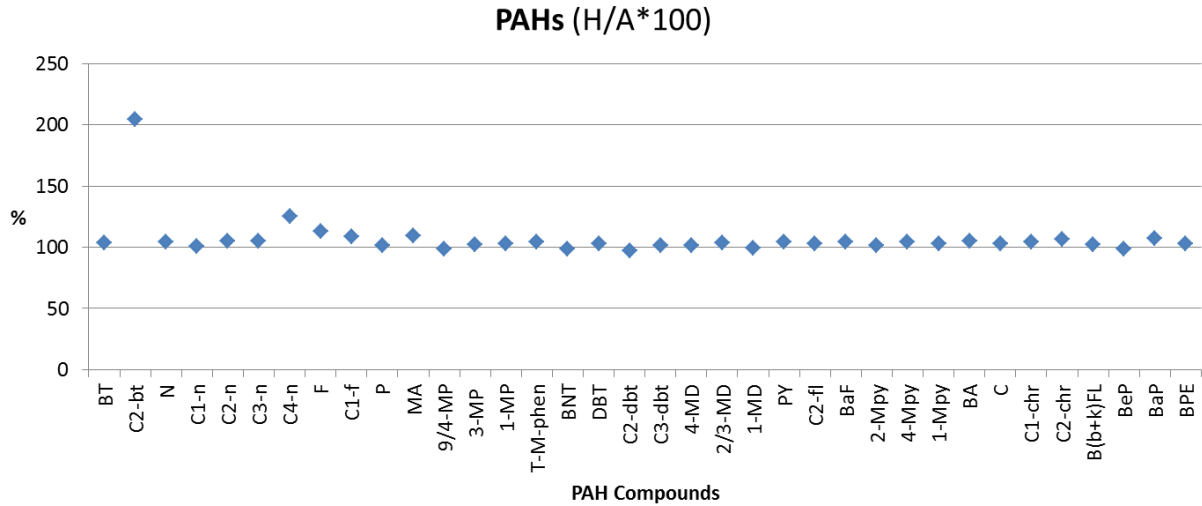


Figure C.46: MS-PW-plots for PAHs for oils A and H.

Table C.15: Diagnostic PAH and biomarker ratios for oils A and H.

PAH Ratio	Peak Height Ratio		Mean	Absolute Difference	Relative Difference (%)	Conclusion
	A	H				
MA/1-MP	0.37	0.35	0.36	0.02	6	Not Different
4-MD/1-MD	2.54	2.48	2.51	0.06	2	Not Different
BaF/4-Mpy	0.23	0.23	0.23	0.00	0	Not Different
2-Mpy/4-Mpy	0.88	0.90	0.89	0.02	3	Not Different
1-Mpy/4-Mpy	0.89	0.90	0.89	0.01	1	Not Different

Biomarker Ratio	Peak Height Ratio		Mean	Absolute Difference	Relative Difference (%)	Conclusion
	A	H				
29ab/30ab	0.94	0.95	0.95	0.01	1	Not Different

C.3.3. Tier 2 Conclusion

In conclusion to Tier 2, oils D and U were differentiated from one another and also from all other oils in the blind study. Oils S and P could not be differentiated from one another but were differentiated from all other blind study oils; this conclusion was also true for oils E and K, oils M and R, and oils A and H. The Tier 2 conclusions as well as the overall CEN method conclusions for the blind study are outlined in Figure C.47.

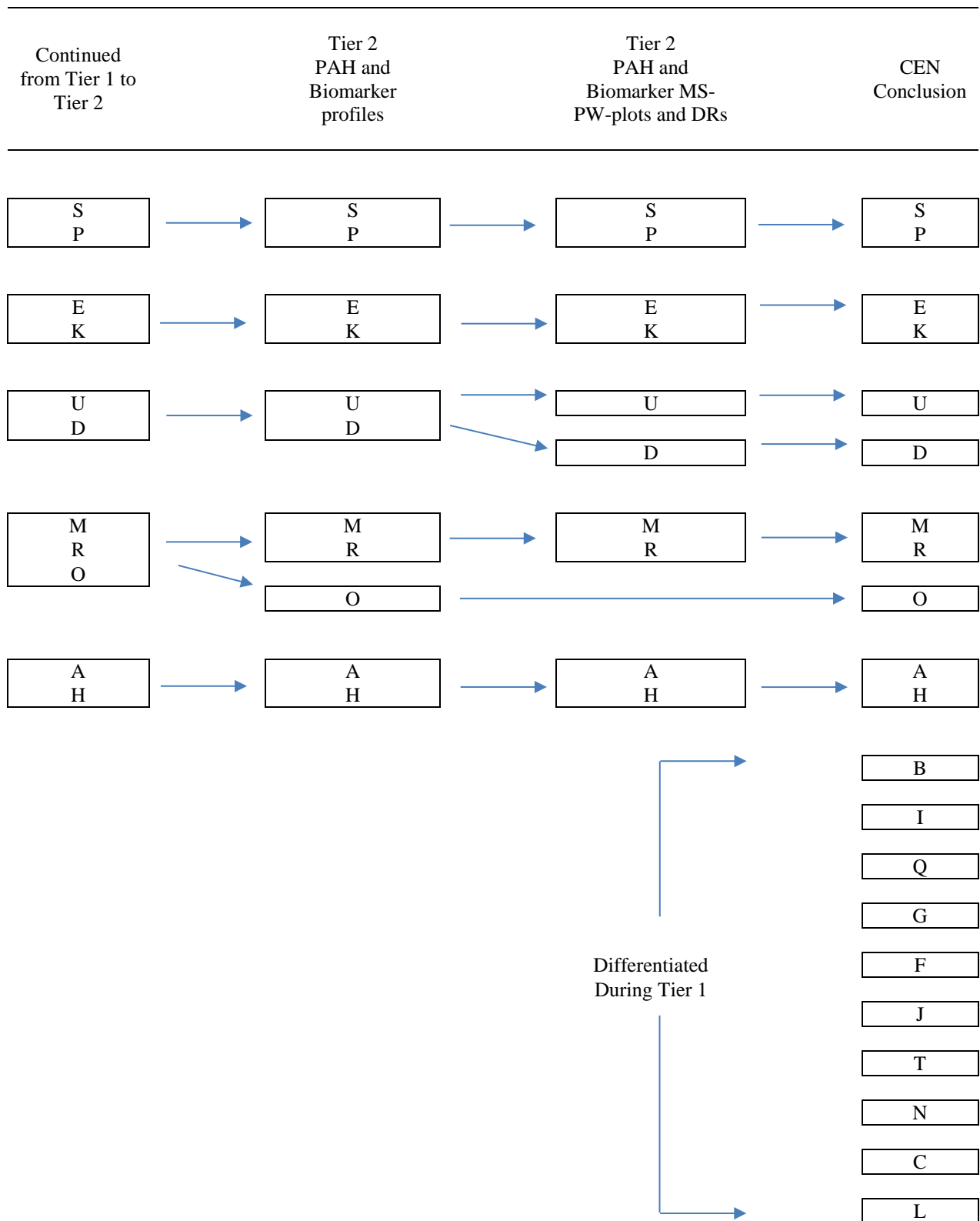


Figure C.47: The overall differentiation of oils carried through for Tier 2 analysis. The overall result of the entire CEN method is also outlined.